TRANSPORTATION RESEARCH RECORD 821

# Bituminous Mixes, Concrete Pavements and Structures, Testing, and Construction Prices

TRANSPORTATION RESEARCH BOARD

COMMISSION ON SOCIOTECHNICAL SYSTEMS
NATIONAL RESEARCH COUNCIL

NATIONAL ACADEMY OF SCIENCES
WASHINGTON, D.C. 1981

**Transportation Research Record 821**
Price $11.60
Edited for TRB by Mary McLaughlin

modes
1 highway transportation
2 public transit
3 rail transportation
4 air transportation

subject areas
24 pavement design and performance
31 bituminous materials and mixes
32 cement and concrete
33 construction
34 general materials

**Library of Congress Cataloging in Publication Data**
National Research Council (U.S.). Transportation Research Board. Meeting (60th: 1981: Washington, D.C.)
Bituminous mixes, concrete pavements, testing and construction prices.

(Transportation research record; 821)
Reports presented at the 60th annual meeting of the Transportation Research Board.
1. Pavements—Addresses, essays, lectures. 2. Building materials—Addresses, essays, lectures. I. Title. II. Series.
TE7.H5 no. 821 [TE250] 380.5s [625.8'5] 82-2150
ISBN 0-309-03263-6 ISSN 0361-1981 AACR2

**Sponsorship of the Papers in This Transportation Research Record**

**GROUP 2—DESIGN AND CONSTRUCTION OF TRANSPORTATION FACILITIES**
*R. V. LeClerc, Washington State Department of Transportation, chairman*

**Bituminous Section**
*J. York Welborn, consultant, Rockville, Maryland, chairman*

Committee on Characteristics of Nonbituminous Components of Bituminous Paving Mixtures
*Gene R. Morris, Arizona State University, chairman*
*John E. Huffman, Sahuaro Petroleum and Asphalt Company, secretary*
*Oliver E. Briscoe, John J. Emery, Richard H. Howe, Bobby J. Huff, L. C. Krchma, Bobby D. Lagrone, Dah-Yinn Lee, Donald W. Lewis, Robert P. Lottman, Charles R. Marek, Charles F. Potts, Vytautas P. Puzinauskas, Donald Saylak, Russell H. Schnormeier, Garland W. Steele, Egons Tons, Richard D. Walker, Leonard E. Wood*

Committee on Characteristics of Bituminous-Aggregate Combinations to Meet Surface Requirements
*Leonard E. Wood, Purdue University, chairman*
*Sabir H. Dahir, Richard L. Davis, John J. Emery, Moreland Herrin, Rudolf A. Jimenez, Bernard F. Kallas, Nabil Kamel, Prithvi S. Kandhal, Larry L. Kole, Dah-Yinn Lee, G.W. Maupin, Jr., James A. Scherocman, Peggy L. Simpson, Stewart R. Spelman, E.A. Whitehurst, L.M. Womack*

Committee on Characteristics of Bituminous Paving Mixtures to Meet Structural Requirements
*Bernard F. Kallas, The Asphalt Institute, chairman*
*Grant J. Allen, Oliver E. Briscoe, R. N. Doty, Jon A. Epps, William O. Hadley, R. G. Hicks, Rudolf A. Jimenez, Ignat V. Kalcheff, Thomas W. Kennedy, Narendra P. Khosla, C. A. Pagen, Richard D. Pavlovich, David W. Rand, Donald R. Schwartz, Jack E. Stephens, Ronald L. Terrel, David G. Tunnicliff, James D. Zubiena*

**Construction Section**
*David S. Gedney, DeLeuw Cather and Company, chairman*

Committee on Rigid Pavement Construction
*M. Lee Powell III, Ballenger Corporation, chairman*
*John J. Carroll, Federal Highway Administration, secretary*
*Woodrow J. Anderson, Luther H. Berrier, Jr., Kenneth J. Boedecker, Jr., Martin L. Cawley, Robert F. Chapin, H. E. Cowger, John E. Eisenhour, Jr., G. L. Godbersen, Harold J. Halm, Michael P. Jones, M. J. Knutson, Robert L. Lucas, Issam Minkarah, Samuel P. Olson, William G. Prince, William J. Ramsey, Bruce L. Ratterree, Gordon K. Ray, Carlton L. Rone, Robert D. Schmidt, Charles F. Scholer, Earl R. Scyoc, Hugh L. Tyner*

Committee on Earthwork Construction
*Charles M. Higgins, Louisiana Department of Transportation and Development, chairman*
*Mehmet C. Anday, Marvin L. Byington, Joseph D'Angelo, Robert C. Deen, William Bryan Greene, Wilbur M. Haas, William P. Hofmann, J. M. Hoover, Eugene Y. Huang, James E. Kelly, Clyde N. Laughter, C. William Lovell, Willard G. Puffer, John R. Sallberg, J. Chris Schwarzhoff, Walter C. Waidelich*

Committee on Construction Management
*Earl R. Scyoc, West Virginia Department of Highways, chairman*
*Donald S. Barrie, H. E. Cowger, John R. Cropper, Warren B. Diederich, Donn E. Hancher, James E. Kelly, William F. Land, RR. Levitt, Robert B. Newman, Harold Rothbart, Robert D. Schmidt, Richard R. Stander, Jr., H. Randolph Thomas, Jr., Alan E. Trotter, Jonathan R. Van Daveer, Charles H. Vandeusen*

**General Materials Section**
*Dale E. Peterson, consultant, Evanston, Wyoming, chairman*

Committee on Sealants and Fillers for Joints and Cracks
*William T. Burt III, Louisiana Department of Transportation and Development, chairman*
*Chris Seibel, Jr., consultant, Norwood, New Jersey, secretary*
*Grant J. Allen, Martin P. Burke, Jr., Terry Church, John P. Cook, Gary L. Fordyce, Frank D. Gaus, C. W. Heckathorn, Arthur Hockman, Richard C. Ingberg, Earl W. Loucks, Richard D. Nourot, Thomas J. Pasko, Jr., Dale E. Peterson, William G. Prince, Guy S. Puccio, Gordon K. Ray, William T. Stapler, Egons Tons, Stewart C. Watson, Richard J. Worch*

Committee on Adhesives, Bonding Agents, and Their Uses
*W. T. McKeel, Jr., Virginia Highway and Transportation Research Council, chairman*
*Gino J. Bastanza, Brian J. Carr, Brian H. Chollar, John P. Cook, Richard H. Frederick, Lawrence I. Knab, Eugene R. Lewis, Robert K. Robson, L. F. Schaefer, Jr., Raymond J. Schutz, Salvatore S. Stivala, Donald W. Vannoy*

**Evaluations, Systems, and Procedures Section**
*Charles S. Hughes III, Virginia Highway and Transportation Research Council, chairman*

Committee on Instrumentation Principles and Applications
*Terry M. Mitchell, Federal Highway Administration, chairman*
*Roy E. Benner, William Bowlby, Theodore R. Cantor, Gerardo G. Clemena, John C. Cook, Robert L. Davidson, Wilbur J. Dunphy, Jr., C. Page Fisher, Thomas A. Fuca, Richard L. Grey, David N. Keast, Donald R. Lamb, James L. Melancon, Ronald J. Piracci, Albert F. Sanborn, Charles H. Shepard, Earl C. Shirley, Marvin P. Strong, Larry G. Walker, David C. Wyant*

Committee on Quality Assurance and Acceptance Procedures
*Garland W. Steele, West Virginia Department of Highways, chairman*
*Robert M. Nicotera, Pennsylvania Department of Transportation, secretary*
*Edward A. Abdun-Nur, Kenneth C. Afferton, Kenneth J. Boedecker, Jr., Frank J. Bowery, Jr., E. J. Breckwoldt, James L. Burati, Jr., James Daves, Richard L. Davis, Francis H. Fee, Jr., Charles S. Hughes, Roy D. McQueen, John T. Molnar, Frank.P. Nichols, Jr., Roger Northwood, Byron E. Ruth, Nathan L. Smith, Jr., Jesse A. Story, Buford D. Stroud, David G. Tunnicliff, Jack H. Willenbrock, William A. Yrjanson*

William G. Gunderman, Transportation Research Board staff

Sponsorship is indicated by a footnote at the end of each report. The organizational units, officers, and members are as of December 31, 1980.

# Contents

# Authors of the Papers in This Record


Allen, G.J., Materials Services, Arizona Department of Transportation, 1745 West Madison Street, Phoenix, AZ 85007

Carpenter, Samuel H., Department of Civil Engineering, Talbot Laboratory, University of Illinois at Urbana-Champaign, 104 South Wright Street, Urbana, IL 61801

Chae, Yong S., Department of Civil and Environmental Engineering, Rutgers–The State University of New Jersey, P.O. Box 909, Piscataway, NJ 08854

Champion, Frank C., California Department of Transportation, P.O. Box 19128, 5900 Folsom Boulevard, Sacramento, CA 95819

Cook, John P., Department of Civil Engineering, University of Cincinnati, Mail Location 71, Cincinnati, OH 45221

Dooley, Thomas, Transportation Systems Center, U.S. Department of Transportation, Kendall Square, Cambridge, MA 02142

Forsyth, Raymond A., California Department of Transportation, P.O. Box 19128, 5900 Folsom Boulevard, Sacramento, CA 95819

Fuchs, F., Centre de Recherches Routières, Boulevard de la Woluwe, 42, Brussels 1200, Belgium

Hannon, Joseph B., California Department of Transportation, P.O. Box 19128, 5900 Folsom Boulevard, Sacramento, CA 95819

Hicks, R.G., Transportation Research Institute, Oregon State University, 201 Apperson Hall, Corvallis, OR 97331

Huff, B.J., Arizona Refining Company, 1935 West McDowell, Phoenix, AZ 85009

Kandhal, Prithvi S., Pennsylvania Department of Transportation, P.O. Box 2926, Harrisburg, PA 17120

Kennedy, Thomas W., Center for Transportation Research, University of Texas at Austin, Austin, TX 78712

Machemehl, Randy B., Center for Transportation Research, University of Texas at Austin, Austin, TX 78712

Mahoney, Joe P., University of Washington, Seattle, WA 98195

Mamlouk, Michael S., Department of Civil Engineering, State University of New York at Buffalo, Parker Engineering Building, Buffalo, NY 14214

Maupin, G.W., Jr., Virginia Highway and Transportation Research Council, Box 3817, University Station, Charlottesville, VA 22903

McDonough, J.F., Department of Civil Engineering, University of Cincinnati, Mail Location 71, Cincinnati, OH 45221

Mellott, Dale B., Pennsylvania Department of Transportation, P.O. Box 2926, Harrisburg, PA 17120

Minkarah, I., Department of Civil and Environmental Engineering, University of Cincinnati, Mail Location 71, Cincinnati, OH 45221

Moore, Richard M., Oregon Institute of Technology, Klamath Falls, OR 97601

Oliver, John W.H., Australian Road Research Board, P.O. Box 156 (Bag 4), Nunawading 3131, Victoria, Australia

Peters, R.J., Materials Services, Arizona Department of Transportation, 1745 West Madison Street, Phoenix, AZ 85007

Rhodes, J.R., Columbia Scientific Industries, P.O. Box 9908, Austin, TX 78766

Ringo, B.C., Department of Civil and Environmental Engineering, University of Cincinnati, Mail Location 71, Cincinnati, OH 45221

Toensmeyer, Michael R., Hazelet and Erdal Consulting Engineers, Dixie Terminal Building, Cincinnati, OH 45202

Vallerga, B.A., B.A. Vallerga, Inc., 2811 Adeline Street, Oakland, CA 94623

Wilson, James E., Oregon Department of Transportation, Transportation Building, Salem, OR 97309

Wood, Leonard E., School of Civil Engineering, Purdue University, West Lafayette, IN 47907

# Performance of Open-Graded Asphaltic Concrete Friction Courses in Arizona

G.J. ALLEN AND R.J. PETERS

There has been a growing emphasis, particularly in the past seven to eight years, on the placement of what have become known as open-graded asphaltic concrete friction courses (ACFCs). Such placement is as a final, or wearing, course for asphaltic concrete pavements and is used not only for highways but for airport runways as well. It was reported in July 1976 that 47 states have now tried some type of open-graded mix and that 20 or 25 states are continuing this type of surfacing on a regular basis. The following performance aspects of proper ACFC design, construction, and maintenance, based on observations made over the past 25 years, are discussed: (a) Although the film coatings on particles in an open-graded ACFC are larger than those in dense-graded designs, a planned maintenance program that requires a fog seal of rejuvenators and/or combined asphalt rejuvenators every two or three years is essential (service life is affected by the lack of such a program); (b) an open-graded ACFC has the ability to hide surface reflective cracking, and it also provides space for subsequent fog seals of rejuvenating agents to retard cracking; (c) since an open-graded ACFC is sensitive to bitumen quantity, temperatures, and hauling distances, consideration should be given to control of the construction season; (d) adequate sealing of the existing pavement surface prior to placement of an open-graded ACFC is essential; and (e) under high traffic volumes and speeds, an open-graded ACFC facilitates the handling of traffic during construction and reduces the splashing effects of surface water.

To the motoring public, the only important component of the entire pavement structure is the surface course. The public is concerned that this surface is pleasing in appearance, promotes a smooth ride with directional stability, and provides adequate frictional characteristics for both vehicle acceleration and subsequent braking. In search of this "ultimate surfacing", varied combinations and gradations of asphalts and aggregates have been used over the past several years.

Particularly within the past seven to eight years, there has been a growing emphasis on the placement of what has become known as the open-graded asphaltic concrete friction course (ACFC). Such placement is as a final, or wearing, course for asphaltic concrete pavements and is used not only for highways but for airport runways as well. It was reported in July 1976 that 47 states have now tried some type of open-graded mix and that 20 or 25 states are continuing this type of surfacing on a regular basis (1). Although it is true that the sudden interest has been generated primarily from a safety standpoint--that is, higher frictional characteristics--this type of surfacing has many other benefits.

The following benefits are generally cited but not necessarily in the order given here (1,2):

1. Improved skid resistance at high speeds during wet weather,
2. Minimization of hydroplaning effects during wet weather,
3. Improved surface smoothness (present serviceability index),
4. Minimization of splash and spray during wet weather,
5. Improved visibility of painted traffic markings,
6. Improved night visibility during wet weather (less glare),
7. Lower tire noise levels,
8. Retardation of ice formation on the surface,
9. Tough and durable wearing surface,
10. Most economical use of high-quality skid-resistance aggregates, and
11. The fact that traffic can use the surface almost immediately after placement.

Notwithstanding this long list of attributes, there are also legitimate concerns and problems, which can be summarized as follows:

1. The use of chemicals for ice control is increased,
2. Spills of petroleum products cause deterioration,
3. Patching is more difficult,
4. Early preventive maintenance is necessary,
5. Handwork in placement creates a different surface texture, and
6. Provision must be made in the shoulder area to allow free flow of water collected in the open-graded mix.

There may be other problems, but these are the ones most often cited. These problems should not be considered completely insurmountable. For instance, spills of petroleum products at intersections can be minimized by densification of the mixture, by sand applications, or by flush applications of coal-tar products.

Successful patching can be accomplished by use of a chip-emulsion technique. As more experience with this technique is gained, problems of patching can be minimized.

## SERVICE LIFE

At this point in the program, it is probably too early to determine a national life expectancy for friction courses, since only a few states had used this type of design prior to encouragement by the Federal Highway Administration (FHWA) through their Notice of May 28, 1973 (3). Current estimates of the service life of such courses range from 7 to 20 years.

It is quite obvious that the extent of service rendered by such friction courses depends on several things. The quality of the materials and the construction methods used are certainly prime factors in performance; of equal importance, however, is the attention given the material after placement. This is to say that preventive maintenance plays a big role in prolonging the life and capability of a friction course. All too often, a surfacing is placed with the assumption that it comes with a 10-year warranty and is then neglected to the degree that the only remedy is extensive patching or total removal and replacement. There are current maintenance sequences for periodic applications of rejuvenating agents or extender oils (every two or three years) that will indeed help to sustain these pavements for 20 years or more. Products are also available today that not only provide rejuvenating qualities but also add asphalt cement to the ACFC at the same time. This eliminates the need to apply dual fog seals (one to add bitumen and one to rejuvenate). It is expected that, depending on the level of maintenance rendered by any particular agency, service life, as reported nationally, will vary considerably.

## ARIZONA EXPERIENCE

In Arizona, we look back at our experience with the use of the ACFC with some pride. ACFCs were first used in Arizona in 1954. These early finishing courses, called plant-mix seal coats, used an open-graded 1-cm (3/8 in) aggregate with 20-25 percent maximum passing the 2-mm (no. 10) sieve. Plant-mix seals were tried in a search for higher-quality seals that would provide a better friction surface and overcome the weaknesses of a chip seal.

To indicate the evolution in design from the first application attempts in 1954, the following table compares the original grading requirements with those finally approved in 1972 and in use today (4,5). It should be noted that the current grading is identical to that recommended by FHWA (1 mm = 0.039 in):

| Item | Percentage Passing 1954 | 1976 |
|---|---|---|
| Sieve size (mm) | | |
| 9.5 | 100 | 100 |
| 6.3 | 65-100 | |
| 4.75 | | 30-60 |
| 2.36 | | 7-15 |
| 2.00 | 10-25 | |
| 0.425 | 0-10 | |
| 0.075 | 0-3 | 0-4 |
| Paving asphalt | | |
| 150-200 penetration | 5.0 | |
| AR 2000 or AR 4000 | | 6.5 |

### Design Considerations

#### Levels of Traffic

The question often arises as to when to specify an ACFC or when to resort to another type of strategy, such as a chip seal, for the surface course. Needless to say, this is a difficult question to handle unless one knows the conditions peculiar to a given project, such as (a) the location and the need for plant setup, (b) local levels of performance with ACFCs and alternate strategies, and (c) the volume and type of traffic to be handled during and after construction.

Previous performance often overshadows other considerations, but it has generally been found advantageous to apply ACFCs when average daily traffic volumes exceed 5000. This results in coverage of the Interstate system and major primary projects with an ACFC. It must be emphasized that the decision may be influenced by local economic situations and other extenuating circumstances. Handling high volumes of traffic during construction is greatly aided by use of an ACFC; this is not meant to infer that other strategies could not be used--just that they would cause greater inconvenience to the traveling public.

#### Drainage

The theory behind porous open-graded friction courses is that they allow for drainage through the mix and, if the transverse geometrics are correct, this drainage will leave the traveling surface by transverse movement (see Figure 1). One can note the effectiveness of this drainage by observing traffic movements during periods of heavy rainfall. Dense mixtures will tend to cause extensive splashing or whipping of surface water off the roadway surface and onto traveling vehicles, whereas surfaces that are open will reduce this tendency considerably. After periods of rainfall, one can observe the continuation of drainage for extended periods of time.

The importance of transverse geometrics cannot be overstated. The true effectiveness of an open-graded ACFC requires adequate movement of water off the roadway. When surface slopes are inadequate or subsequent densification of underlying pavement courses creates rutting, a collection basin can be formed that can create greater problems than the ones it was hoped the use of an open-graded ACFC would solve. In areas where temperatures reach freezing, the collection basin could become a hazard if the collected water freezes. It cannot be overemphasized that surface distortion and slope should be corrected by means other than the open-graded surface treatment. Consideration needs to be given to adequate cross slope and the minimal distances over which the water should be required to move. It would be better, for instance, to attempt to drain only half of an Interstate roadway by use of a crowned section than to attempt to drain the full width by cross-sloping.

Since realizing the complete benefits of an open-graded ACFC requires adequate drainage, it is imperative that consideration be given to optimizing all factors that influence drainage. Factors such as skid resistance and noise levels are also optimized by proper drainage.

#### Durability

Concern is often voiced over the inherent loss of mixture durability in open-graded ACFCs, since the openness of the mixtures is conducive to weathering, raveling, etc. When one considers the high asphalt contents used for these mixtures, it is apparent that the aggregate particles are being coated with films greater than those of routine dense mixtures. The greater film thicknesses help to retard the weathering of the mixture; however, planned preventive maintenance must be made a part of the total design strategy for these mixtures. A planned program for applying subsequent fog applications to add additional bitumen or rejuvenation materials should be considered before an open-graded ACFC is applied. By so doing, additional years of service life can be added and yearly performance greatly improved. If a planned maintenance program is not adhered to, a fog seal should be applied at the first indication of raveling. Experience has shown that, when open-graded mixtures ravel and no corrective action is taken, the result can be the development of rapid progressive failure by loss of the total surface. Once the failure has progressed to that point, patching is required and the loss of the desired surface texture is inevitable.

**Figure 1. ACFC drainage.**

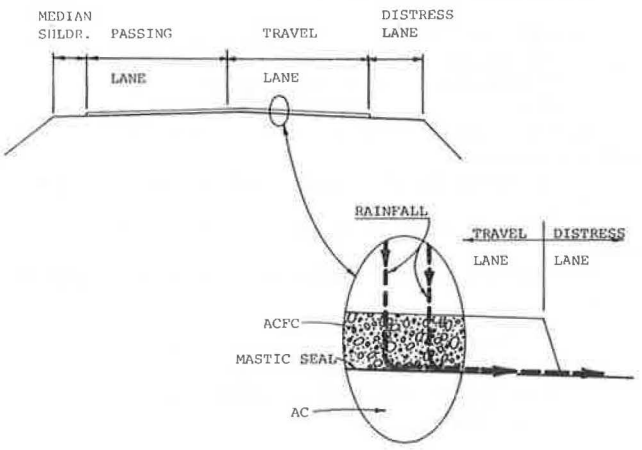

### Reflective Cracking

Recent national concerns have focused attention on the development of strategies for inhibiting cracking from reflecting through subsequent pavement courses. A study conducted in Arizona (6) indicated that test sections constructed with and without an open-graded ACFC perform quite differently. In effect, the open-graded ACFC, with its large, internal aggregate spacing, could easily "hide" the hairline crack at the surface and thus hide narrow cracks in an asphaltic concrete overlay (see Figure 2).

This ability to hide cracks must be viewed as an asset if one is primarily interested in roadway aesthetics. If one is interested in knowing that cracks do exist below the surface course, then it could be a disadvantage. At any rate, the use of open-graded ACFCs can be a means of inhibiting the appearance of reflective cracking. They also allow for subsequent fog-seal applications of rejuvenating agents to retard the growth of cracks.

## Placement Considerations

### Time of Year

Due to the open grading and the thickness of the lift, the air and surface temperatures during placement of open-graded ACFCs are critical. The mixture needs to be compacted immediately after placement, especially during periods of less favorable environmental conditions. In fact, the considerations for placement of the mixture parallel closely the requirements for the satisfactory placement of a chip seal. In Arizona, constraints imposed on allowable construction time depend on project elevation (see Figure 3). Seal coats are only allowed to be placed during set time periods. The placement season for open-graded ACFCs is only slightly longer than that for chip seals for the same elevation levels.

Experience in Arizona has shown that the allowable times for placement have worked quite satisfactorily. When deviations from the allowable timing have been permitted, by change order, we have on occasion had second thoughts regarding that decision because of subsequent construction problems. The net effect of proper placement and compaction is the ability of the surface to carry routine traffic very soon after placement, whereas with emulsion-chip seals a cure period is necessary.

Figure 2. Ability of ACFC to hide cracks in known cracking area.

Figure 3. Seasonal application of ACFC in Arizona.

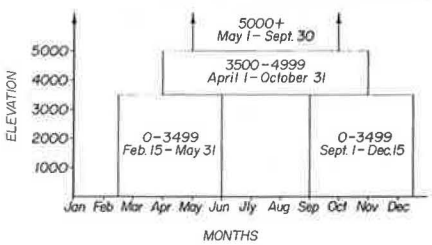


### Sealing of Roadway

One of the most important placement considerations is that of providing an adequate seal to the existing pavement surface (7). The ACFC must provide for lateral drainage and must not be a collection basin for vertical movement of water into the existing pavement structure.

Unfortunately, all too often this important aspect of placement is overlooked and the result is deterioration of the underlying structure and flushing or bleeding in the ACFC. The tack coat applied prior to placement of the ACFC must be uniform and adequate to seal. Currently, Arizona specifies 0.27 L/m² (0.06 gal/yd²) of asphalt cement for the tack coat. An emulsion tack can be applied as long as the residue effective for sealing is comparable to that required for an asphalt cement. Experience has shown a reluctance, however, to place an amount of emulsion tack coat that would be equivalent to the quantity of asphalt cement.

If the existing pavement cannot be adequately sealed, all of the other advantages sought from an ACFC may be overshadowed and it may be better to rely on a chip seal for the surface treatment.

### Movement of Binder

Another problem encountered in Arizona with the placement of the mixture is the movement of the binder to the bottom of the transport vehicle due to haul distance and heat. The excess asphalt ends up in concentrated areas during placement, which results in flushing or bleeding. In an attempt to overcome this problem, projects have been contracted in which 1 percent of the design bitumen content was withheld and, after placement of the mixture, the 1 percent effective asphalt was added to the mixture by a surface flush of an emulsion. There have been varying opinions on the true worth of this approach. In Arizona, we are currently back to placing the total asphalt into the mixture at the time of mixing. The adoption of placement seasons may have helped to negate the need for the other technique. At any rate, we can suggest it as a workable technique for those attempting to place ACFCs that are open graded in conditions of (a) high plant temperatures that result in low mixing viscosities, (b) high ambient temperatures, and (c) long hauling distances.

As our use of recycling strategies increases, we may be looking for ways to place ACFCs by a cold process. This involves slurry applications, which have the advantage of sealing a roadway surface during placement by "walking" the slurry along the pavement surface. The problem of getting adequate binder to the roadway surface for sealing purposes is eliminated.

## CONCLUSIONS

The following performance aspects of proper ACFC

design, construction, and maintenance are based on observations made over the past 25 years:

1. An open-graded ACFC will not drain properly unless there are proper transverse geometries. Reducing the distance the water must travel should be considered.
2. Although the film coatings on particles in an open-graded ACFC are thicker than in dense-graded designs, a planned maintenance program that requires a fog seal of rejuvenators and/or combined asphalt rejuvenators every two or three years is essential. Service-life performance is affected by the lack of such a program.
3. An open-graded ACFC has the ability to hide surface reflective cracking. It also provides space for subsequent fog seals of rejuvenating agents to retard cracking.
4. Since an open-graded ACFC is sensitive to bitumen quantity, temperature, and hauling distance, consideration should be given to control of the construction season.
5. Adequate sealing of the existing pavement surface before placement of an open-graded ACFC is essential.
6. Under high traffic volumes and speeds, an open-graded ACFC facilitates the handling of traffic during construction and reduces the effects of the splashing of surface water.

It is apparent that, as the need for safe surfaces for the vast highway network increases, more consideration will be given to the strategy of placing open-graded ACFCs. As traffic volumes increase, additional justification may be found for spending a greater initial amount of funds for wearing surfaces than is now considered feasible. At any rate, technology and experience have advanced to the point that the construction of premium surface courses cannot be justified, and there should be an increase in the applications of open-graded ACFCs in the years ahead.

As the era of asphalt-pavement recycling commences, its inherent advantages with regard to saving materials and energy continue to be discovered. The conception of saving energy by cold processing has carried over into the placement of ACFCs in that ACFCs can also be placed by cold-slurry processes. This ability to cold process an ACFC surface course makes it possible to consider an energy-saving strategy of cold processing for all pavement strategies on a rehabilitation project--the point being that, if one desires an ACFC and experience has been only with "hot" processing, it is possible to obtain a similar material by a cold-processing strategy.

ACKNOWLEDGMENT

The contents of this paper reflect our views, and we are responsible for the facts and the accuracy of the data presented. The contents do not necessarily reflect the official views or policies of the Arizona Department of Transportation.

REFERENCES

1. Maintenance of Open-Graded Asphalt Friction Courses. Committee on Maintenance, AASHTO, Washington, DC, Maintenance Aid Digest 11, July 1976.
2. R.W. Smith, J.M. Rice, and S.R. Spelman. Design of Open-Graded Asphalt Friction Courses. FHWA, Interim Rept. FHWA-RD-74-2, Jan. 1974.
3. Open-Graded Plant Mix Seals. FHWA, Notice HNG-23, May 28, 1973.
4. G.R. Morris and N.R. Scott. Arizona Experiences with Asphaltic Concrete Friction Courses. Proc., AASHTO Subcommittee on Maintenance, 60th Annual Meeting, Los Angeles, Nov. 12-15, 1973.
5. G.J. Allen, R.J. Peters, and H.W. Longfellow. Open-Graded Asphaltic Concrete Friction Courses. Presented at 63rd Annual Meeting, AASHTO, Birmingham, AL, Nov. 1976.
6. G. Way. Prevention of Reflective Cracking in Arizona Minnetonka-East (A Case Study). Arizona Department of Transportation, Phoenix, HPR 1-13 (224), Rept. 11, May 1976.
7. S.C. Britton, B.M. Gallaway, and R.L. Tomasin. Performance of Open-Graded Friction Courses. Texas Transportation Institute, Texas A&M Univ., College Station, Res. Rept. 234-1F, June 1979.

*Publication of this paper sponsored by Committee on Characteristics of Bituminous-Aggregate Combinations to Meet Surface Requirements.*

# Performance Comparison Between a Conventional Overlay and a Heater-Scarification Overlay

SAMUEL H. CARPENTER

**The heater-scarification technique has become one of the most commonly accepted forms of pavement surface recycling in use today. This has been due primarily to the record of successful performance exhibited by these projects over a relatively long period of time. The performance characteristics of a typical heater-scarification overlay project are analytically examined and compared with those of a conventional overlay. The comparison examines fatigue cracking caused by wheel loadings and thermal-fatigue cracking caused by daily temperature cycles. The results are presented for one combination of aged asphalt and recycling agent and one overlay type. The results show that for this combination the commonly held statement that a 19- to 25-mm (0.75- to 1.0-in) depth of heater scarification with 38 mm (1.5 in) of overlay will perform as well as 89 mm (3.5 in) of conventional overlay has some validity. The calculations illustrate the need for laboratory testing to select the best recycling agent for the particular asphalt being recycled and the need to tailor the characteristics of the recycled binder to produce the desired product.**

Heater scarification, one of the oldest forms of surface recycling, is used primarily to correct surface distress in bituminous pavements. Surface distress includes a number of types, such as rutting, raveling, weathering, and corrugations. Mixture problems such as asphalt content, gradation, or asphalt properties can also be altered during the

Figure 1. Typical heater-scarifier unit.

Figure 2. Variation of viscosity with depth for several pavement sections.

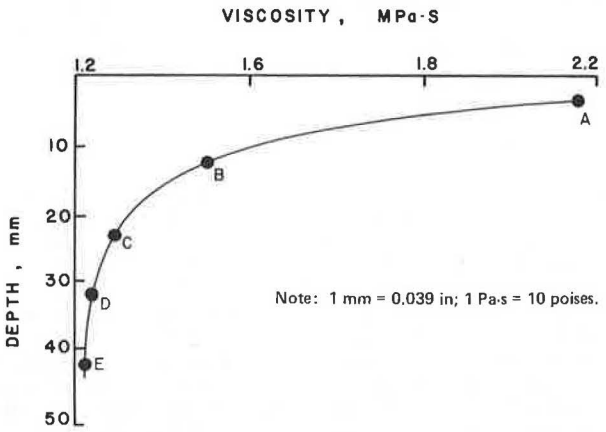


heater-scarification operation. It is this alteration of asphalt properties that provides a major performance improvement in the new pavement structure.

A typical heater-scarification unit is shown in Figure 1. There are a number of different units in operation today that accomplish basically the same result although the processes may differ slightly. The basic heater-scarification process follows a standard procedure:

1. The pavement surface is heated by indirect heat to a temperature in excess of 93°C (200°F) and to a depth of 25 mm (1.0 in) nominally.
2. Scarifier teeth pulled over the softened surface break up the pavement to a nominal depth of 25 mm.
3. A recycling agent may be added at this point to soften and rejuvenate the asphalt cement in the scarified mixture.
4. Mixture deficiencies may be corrected at this point by adding asphalt cement or aggregate and mixing it in with the scarified mixture.
5. The heater-scarified mixture may be compacted prior to application of the overlay, or a new asphalt concrete overlay is placed over the uncompacted heater-scarified layer and both are compacted simultaneously.

Heater scarification works with the "top inch" of the pavement, although multiple passes may be used to get greater depths of scarification. This top inch is important. The asphalt cement in the top inch is normally oxidized and hardened in any pavement of appreciable age. This is shown in Figure 2, which depicts the variation of viscosity with depth and age (1). The rejuvenation of this top inch of asphalt cement may return the pavement to an overall condition that resembles that of a new pavement, depending on the distress present.

The heater-scarification process removes the cracking present on the surface and buries it under 25 mm of rejuvenated asphalt concrete. An overlay on top of this further buries the cracked surface. Statements based primarily on observations of heater-scarified overlaid pavements have indicated that 25 mm of heater scarification with 38 mm (1.5 in) of overlay will give the same performance as 63-76 mm (2.5-3.0 in) of new hot-mix overlay over the original pavement surface. These statements have been based primarily on the observed rate of appearance of reflection cracks on the new surface.

Cracks in the old surface may be propagated by traffic or temperature cycles. Traffic loadings will produce fatigue cracking whereas temperature cycles will produce thermal-fatigue cracking. These inputs alone may develop cracks in a new pavement structure and, with existing cracks in the underlying surface, will propagate reflection cracks. The basic indication of the performance of an overlay may be indicated by how rapidly cracks work through the overlay. This can be determined from a fracture mechanics approach and a viscoelastic analysis and has been done previously (2).

## DETERIORATION IN THE OVERLAY

There are three methods by which deterioration in the form of cracking can be produced in an overlay over an old flexible pavement. These include

1. Development of normal fatigue cracking in the overlay,
2. Reflection cracking produced by vertical deformation at a crack as a result of wheel loadings, and
3. Thermal-fatigue cracking resulting from daily temperature cycles, which may produce a new crack in the overlay as well as propagate a reflection crack.

The crack-propagating mechanism that predominates for any one pavement will depend on the distress condition of the old pavement, the foundation support provided, the mixture variables, and the climate. The three mechanisms listed above are shown schematically in Figure 3.

If the surface is not badly cracked and mix deficiency is the only distress, reflection cracking will not be a problem in the overlay and fatigue cracking will be a possible distress while thermal-fatigue cracking may dominate. If the old pavement is very badly cracked, from whatever cause, it will provide a lower support value and fatigue cracking in the overlay will be prevalent. Thermal-fatigue cracking will also be active, but the thermal behavior of the old pavement will be minimized from the standpoint of reflection cracking. If the original pavement has transverse cracks spaced at regular intervals, reflection cracking and thermal-fatigue cracking will be important and the thermal characteristics of the old pavement will influence thermal-fatigue reflection cracking.

The mechanisms listed above are highly influenced by the support provided by the existing structural layers. Low support values will accelerate fatigue and reflection cracking that results from traffic, since these two forms of cracking are influenced by the same properties of the overlay, a resistance to

**Figure 3. Three modes of crack propagation in a heater-scarified overlaid pavement.**

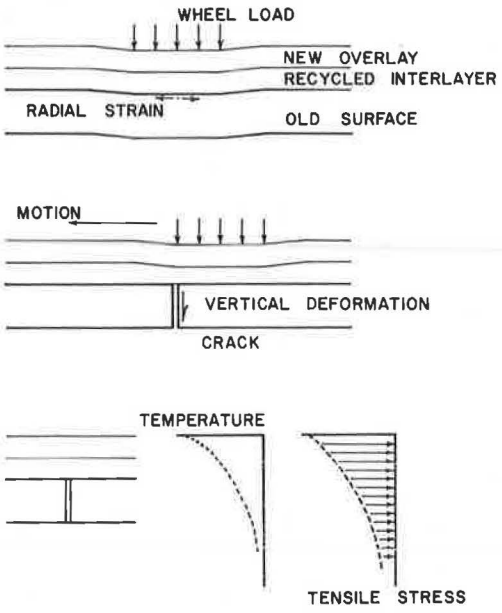


**Figure 4. Blend index chart for selecting proper amount of recycling agent to produce a selected consistency.**

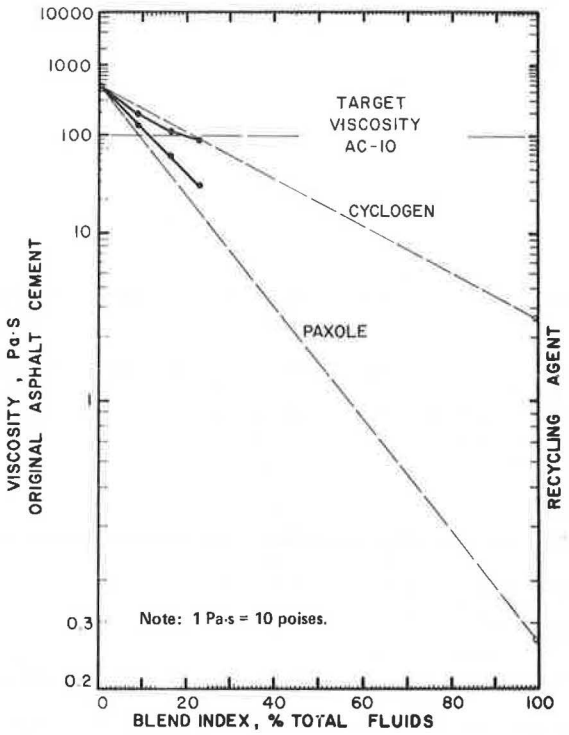


strain-induced cracking. Because both types of deterioration are influenced by the same properties and produced by the same input, fatigue cracking is examined to show the relative influence of the heater-scarified interlayer on performance. Fatigue distress is easier to characterize and clearly demonstrates the influence of the heater-scarification process. If exact life predictions were needed, the two distress types would have to be investigated separately. Exact predictions of cracking times are beyond the scope of this paper.

Thermal-fatigue cracking does not depend on support values from the old pavement. This form of deterioration depends solely on the viscoelastic and thermal contraction properties of the asphalt concrete layers. These properties may be most influenced by the heater-scarification recycling process, which uses a recycling agent.

In an initial study of thermal reflection cracking of overlays by Chang, Lytton, and Carpenter (2), the following conclusion was developed. To most effectively retard this cracking, the original pavement should be overlaid with a thin layer of low-modulus material and then with a higher-modulus material. Both materials should be as temperature insensitive as possible--i.e., there should be a low increase in stiffness with temperature drop.

This layer arrangement is easily attainable in the heater-scarification process. The stiffness characteristics of the heater-scarified interlayer may be controlled by the recycling agent used. The use of a stress-relieving interlayer such as this has been recognized for quite some time (3,4). The remainder of this paper presents the procedures used to analyze heater-scarified recycled materials, the input properties for these procedures, and the resulting differences in service life between the two rehabilitation methods.

## PAVEMENT PROPERTIES

The pavement being examined in this paper is from a class 1 surface mix in service as a shoulder on I-94 in Peoria, Illinois. Samples were brought to the laboratory and crushed, and the asphalt cement was extracted and recovered. The properties of the recovered asphalt cement are as follows: Penetration at 25°C (77°F) = 3.5 mm (0.13 in), viscosity at 60°C (141°F) = 480 Pa•s (4800 poises), and softening point (ring and ball) = 50.5°C (124°F). It should be recognized that these properties are the average over the entire thickness of 20.3 cm (8 in). For an actual heater-scarification operation, only the top 25 mm (1 in) should be evaluated. This would show an even higher viscosity, which would make it necessary to use a different amount of recycling agent to rejuvenate the aged binder.

The aged binder was rejuvenated to a viscosity of 100 Pa•s (1000 poises), the consistency of an AC-10 asphalt cement, by using Paxole 1009 recycling agent. The blending tests are shown in Figure 4. From this blend chart, a recycling-agent proportion of 12.5 percent by weight of aged binder (11.5 percent by weight of total fluids) was selected. The properties of this blend are given below for the blended material and the blended material following the thin-film oven test (TFOT) (ASTM D1754):

| Condition | Penetration at 25°C (mm) | Viscosity at 60°C (Pa•s) | Softening Point (ring and ball) (°C) |
|---|---|---|---|
| Before TFOT | 9.5 | 90 | 45 |
| After TFOT | 5.3 | 190 | 50 |

The TFOT values indicate properties that would exist in the recycled binder after mixing and compaction when the diffusion of the recycling agent into the aged binder is completed. The diffusion phenomenon was first reported by Carpenter and Wolosick (5) at the 1980 Annual Meeting of the Transportation Research Board.

A virgin AC-10 asphalt cement was selected from a construction project in central Illinois. This represents the virgin material that would be used in a

new overlay. The test properties for this asphalt cement are given below:

| Condition | Penetration at 25°C (mm) | Viscosity at 60°C (Pa•s) | Softening Point (ring and ball) (°C) |
|---|---|---|---|
| Before TFOT | 8.0 | 111 | 46.0 |
| After TFOT | 5.6 | 285 | 51.5 |

## Structural Characteristics

For comparative purposes in this paper, the original pavement was assumed to have 3.0 percent air voids, as was the overlay that used the AC-10. The air voids in the heater-scarified interlayer were reduced to slightly less than 3.0 percent by the addition of the recycling agent, which provided more total fluids to the mixture. The first structural property needed to characterize the performance of an asphalt concrete pavement is the stiffness modulus. Creep compliance and diametral resilient modulus are the two most common procedures used by researchers today to characterize the stiffness of asphalt concrete. The creep-compliance curve for the recycled mixture in cylindrical compression is shown in Figure 5.

These data can be obtained in any well-equipped research laboratory, and the tests should be performed whenever possible. When it is not possible, reasonably accurate comparisons can still be made by using any of the accepted nomographic procedures (6; 7; 8, p. 358). A computerized version of the Van der Poel nomograph was used to generate the stiffness relations used in this study (9). Basically, this involved calculating the entire relaxation-modulus curve for each material. Relaxation modulus is related to creep compliance by the following:

$$D(t) = [1/E(t)](\sin m\pi/m\pi) \quad (1)$$

where

D(t) = creep compliance at time t,
E(t) = relaxation (stiffness) modulus at time t, and
m = slope of the straight-line portion of the viscoelastic master curve that is being used.

The relaxation curves for the recycled material are shown in Figure 6. The laboratory data are superimposed, and the values of diametral resilient modulus are indicated. Figure 7 shows the computer-generated relaxation curves for the AC-10 overlay and for the original pavement, calculated in a similar manner. The calculations for the overlay and the recycled material were performed by using the asphalt cement properties after the TFOT aging because these values could be considered more typical of those that would exist in the finished pavement. It must also be realized that the surface layer, the AC-10 overlay, will age, whereas the heater-scarified interlayer will age little, if any. This difference in aging will stiffen the properties of the surface layer, making it more susceptible to cracking.

The master relaxation curves for each of the three materials are shown in Figure 8. The reference temperature is taken as 5°C (41°F). The

Figure 5. Creep-compliance curve for actual recycled material with resilient modulus data superimposed (138-kPa load range).

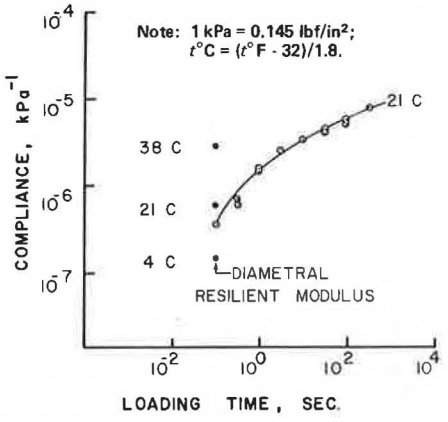


Figure 6. Computer-generated relaxation curves for recycled material examined with laboratory data superimposed.

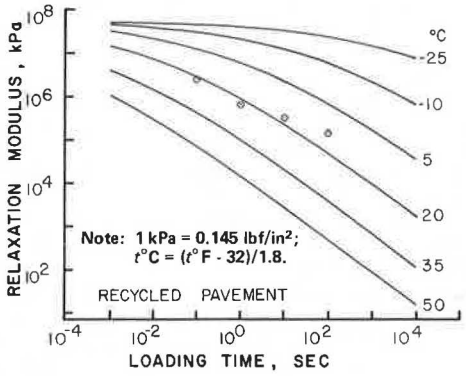


Figure 7. Computer-generated relaxation curves.

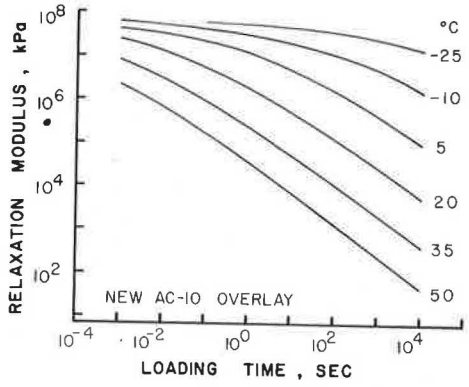


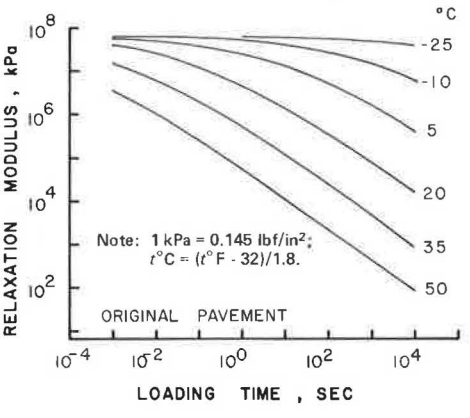

Figure 8. Master relaxation curves for materials examined.

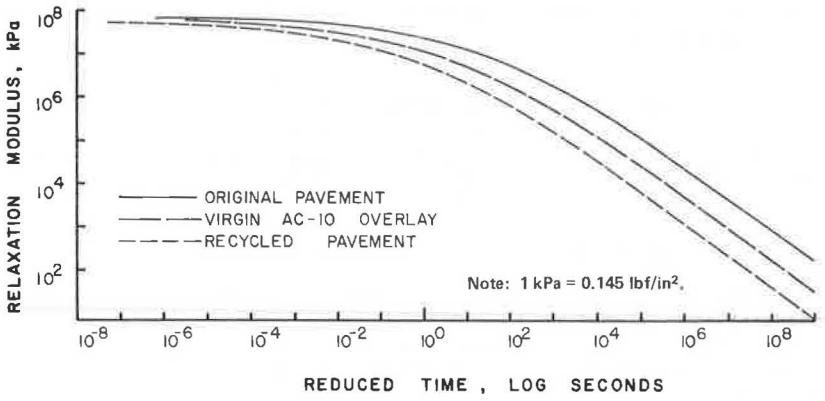


Figure 9. Fatigue curves predicted from asphalt cement and mix properties.

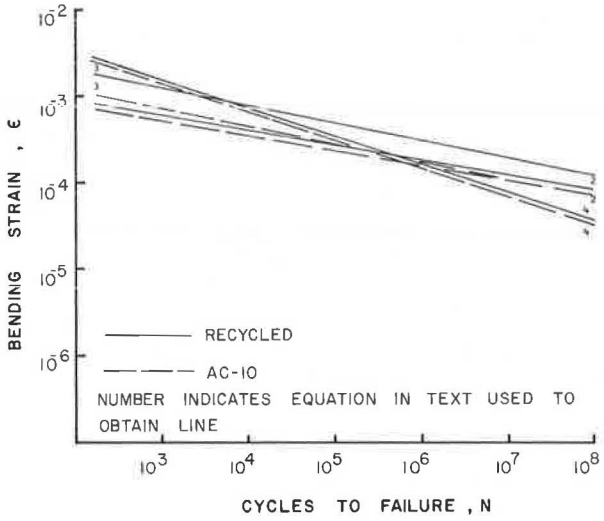


difference in the stiffness relations for these three materials is very dramatic. The original pavement is the stiffest; this is expected since it is composed of an aged asphalt cement. The difference between the AC-10 overlay and the recycled interlayer is greater than may have been expected. This emphasizes a difference in the aging characteristics of a recycled asphalt versus those of a virgin asphalt cement that has been noted by a number of researchers: A recycled asphalt cement will generally age less than a virgin asphalt cement in the same condition. Although the TFOT may not indicate long-term field aging precisely, the relative comparison it provides is valid and it does indicate what is in the pavement after mixing. It must be noted that the virgin AC-10 and the rejuvenated asphalt cement had similar properties according to the common classification tests before aging in the TFOT.

These computer-generated curves for relaxation (stiffness) modulus, the appropriate shift functions, and the asphalt cement properties are used in the next section of this paper to calculate thermal stresses, fatigue relations, and layer stiffnesses for performance comparisons of a conventional overlay and the heater-scarified overlay method.

## FATIGUE PROPERTIES

Nomographic procedures have been developed to estimate the fatigue curves for mixtures that use the binder and mix properties developed by the Shell research group in France (10). The equations they developed for constant stress and constant strain are, respectively,

$$\epsilon = (0.300 \times PI - 0.015 \times PI \times Vb + 0.08 \times Vb - 0.198) \times Sm^{-0.28} \times N^{-0.2} \quad (2)$$

and

$$\epsilon = (4.102 \times PI - 0.205 \times PI \times Vb + 1.094 \times Vb - 2.707) \times Sm^{-0.36} \times N^{-0.2} \quad (3)$$

where

$\epsilon$ = initial bending or radial strain,
PI = penetration index of the binder,
Vb = volumetric bitumen content of the mix,
Sm = stiffness modulus of the mix (Pa), and
N = number of cycles to failure.

Regression equations based on extensive analysis of fatigue-testing data reported in the literature were developed and reported in NCHRP Report 195 (11). The equation is as follows:

$$N = (1.213 \times 10^6)(PEN/10)^{0.22}(Va)^{-1.79}(Pb)^{-1.81}(Sm/10\,000)^{-0.71} \div (\epsilon \times 10^{-6}/100)^{-3.07} \quad (4)$$

where

PEN = penetration at 25°C,
Va = air voids in the total mixture,
Pb = asphalt content, and
Sm = mix stiffness modulus (lbf/in²).

These equations have been plotted in Figure 9 for the new overlay and the recycled material. The mixture properties are the same as those used to calculate the relaxation curves. The data shown in Figure 9 illustrate that the recycled interlayer material will have better fatigue properties than an overlay with the virgin AC-10 asphalt cement. The actual fatigue life of the pavement will depend on the thickness of the layers and the resultant strains produced by wheel loadings.

In analyzing an actual project, samples should be tested for the stiffness and fatigue data needed for a fatigue-life comparison of the different pavement structures being considered. The stiffness is needed as an input material property for the structural program to calculate the radial strain at the bottom of the asphalt layer. This strain is then used in the fatigue curve to calculate the number of load applications to failure.

The stiffness values used for the fatigue analysis were obtained from the computer-generated relaxation curves at a temperature of 20°C (72°F) and a loading time of 0.1 s for each asphalt layer being

Figure 10. Properties of pavement sections analyzed.

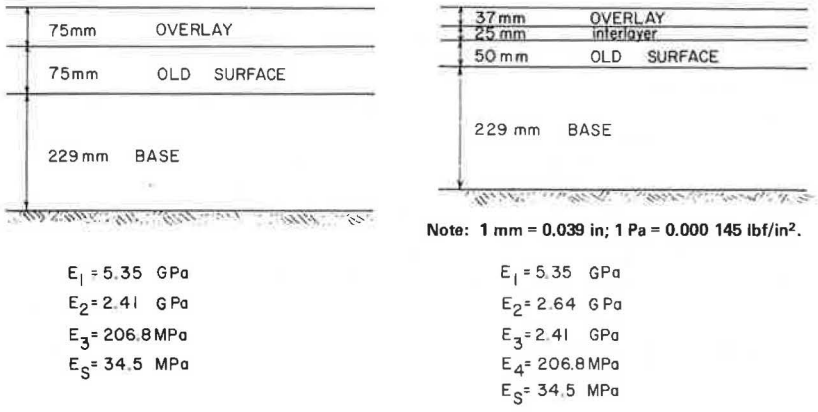


Note: 1 mm = 0.039 in; 1 Pa = 0.000 145 lbf/in².

Table 1. Input parameters for calculations of viscoelastic thermal stresses.

| Asphalt Cement | $D_1$ | m | $T_a$ | $\beta$ | $C_1$ | $C_2$ |
|---|---|---|---|---|---|---|
| Original Peoria | 7.463 | 0.68 | -204 | 43.23 | 38.20 | 496.11 |
| Rejuvenated Peoria (TFOT) | 6.553 | 0.71 | -170 | 33.74 | 29.72 | 425.25 |
| AC-10 (TFOT) | 7.260 | 0.79 | -200 | 38.88 | 34.45 | 489.34 |

Note: $\alpha = -1.35 \times 10^{-6}/°F$ for all materials, $D_1$ = compliance at intercept of straight-line portion of master curve and time log t = 0, m = slope of straight-line portion of master curve, $T_a$, $\beta$ = constants in the analytic solution to the Williams-Landell-Ferry equation, and $C_1$, $C_2$ = constants in the Williams-Landell-Ferry equation.

investigated. These stiffness values are shown in Figure 10. The stiffness value for the original layer has been reduced significantly to illustrate the loss in modulus due to extensive fatigue cracking, presumably the cause for the needed rehabilitation. The modulus of the granular layer also was selected to represent a saturated material. A linear elastic layer program was used to calculate radial strains at the base of the new material under an 80-kN (18-kip) single axle. The strains and estimated fatigue lives for the overlay (A) and 25-mm heater-scarified interlayer plus overlay (B) are given below (1 mm = 0.039 in):

| Layer | Thickness (mm) | Strain (mm/mm) | Cycles to Failure |
|---|---|---|---|
| A | 50 | $-1.83 \times 10^{-5}$ | $9.5 \times 10^{9}$ |
| | 76 | $-6.73 \times 10^{-5}$ | $1.4 \times 10^{7}$ |
| | 102 | $8.26 \times 10^{-5}$ | $5.1 \times 10^{6}$ |
| B | 63.5 | $9.08 \times 10^{-5}$ | $5.5 \times 10^{6}$ |
| | 89 | $+1.21 \times 10^{-4}$ | $1.3 \times 10^{6}$ |
| | 114 | $+1.22 \times 10^{-4}$ | $1.2 \times 10^{6}$ |

The prediction of fatigue lives from computer-generated pavement responses is highly dependent on the modulus values chosen for the original asphalt concrete and granular base. If the modulus value of the aged layer is used without a reduction for cracking [12 414 MPa (1 800 000 lbf/in²)], the predicted fatigue lives would be unrealistically high. The values calculated here may even be on the high side. Care must be exercised in selecting pavement parameters for an analysis of this nature. The numbers presented here indicate acceptable fatigue lives for both the overlay alone and the surface recycled pavement.

## THERMAL-STRESS REFLECTION CRACKING

### Thermal Stresses

Daily temperature cycles build up thermal tensile stresses in the asphalt concrete layers. These stresses will propagate a thermal-fatigue crack from the top downward in a pavement in which there are no cracks beneath the surface layer. This was recognized by Shahin (12) in his model, which attempted to quantify the appearance of thermal-fatigue cracking. When cracks exist beneath the surface layer, the temperature cycles will propagate a crack from the top and bottom toward the middle of the surface layer. The presence of the crack in the underlying layer provides such a stress concentration that crack initiation will most likely initiate at the bottom of the surface layer.

The first problem in predicting the rate of crack growth is in predicting the magnitude of the thermal stresses that are propagating the crack, a factor that has a considerable influence on the rate of crack growth. Thermal stress is dependent on the rate of temperature drop, the low temperature reached, and the viscoelastic time-temperature properties of the material. Previous attempts to predict these stresses have assumed "fictitious" loading times or have compared stresses at the assumed loading time of 20 000 s (12-14) to indicate which material is more susceptible to cracking.

A procedure developed for the solid-fuel rocket-propellant industry (15) and first applied to asphalt concrete pavements by Chang, Lytton, and Carpenter (2) has been shown to provide an accurate prediction of thermal stresses. This technique uses the viscoelastic curve, either relaxation or compliance, and actual climatic input for the temperature change. Previous examples have used laboratory-determined compliance data (2). Because these curves may not be readily obtained, the next best alternative is to use the nomographic procedures to develop the viscoelastic data. This procedure has been examined, and acceptable comparisons with laboratory data have been obtained.

The calculation procedures for the viscoelastic thermal stresses have been detailed elsewhere, and only the results are presented here. The input data extracted from the relaxation curves developed in the previous section are given in Table 1.

The temperature input data were developed from the heat-transfer program developed at the University of Illinois. The actual temperatures are for an average day in January at Abilene, Texas. These variations are not excessive and may be typical for a wide area of the Southwest. The surface temperature varied from 24° to 4°C (75°-41°F) from day to night. The temperature drop and time interval vary with depth into the pavement structure. This variation is shown in Figure 11 for the actual climatic data. These temperature and time values were used in the viscoelastic program.

The resulting thermal-stress distributions for

the three materials are shown in Figure 12, where it is assumed the materials were placed as a surface. The relative magnitude of the stress for each material is as expected from a cursory analysis of the viscoelastic curves. The recycled interlayer produces the largest reduction in thermal stresses. The benefit of the heater-scarification interlayer becomes more apparent when the thermal stresses in each material are arranged to correspond to their structural relations. This has been done in Figure 13. The stress level in the interlayer is a definite improvement compared with a normal 77-mm (3-in) overlay.

## Rate of Reflection Cracking

The rate of crack propagation can be effectively modeled by Paris' equation (16, p. 528). This relation has been verified by a number of researchers (17-19) as being applicable to asphaltic concrete:

$$Nf = \int_{Co}^{Cf} [1/A(\Delta K)^n]\, dc \quad (5)$$

where

Nf = number of cycles to failure,
Co = initial crack length,
Cf = final crack length following tensile-stress application,
A, n = viscoelastic and fracture properties of the mix,
$\Delta K$ = stress-intensity factor produced by thermal stress, and
dc = incremental crack growth.

From theory (17), the factor n can be calculated as 2 [1 + (1/m)] from the relaxation curve, where m is the slope of the linear portion of the curve.

Figure 11. Temperature variation used to calculate thermal stresses.

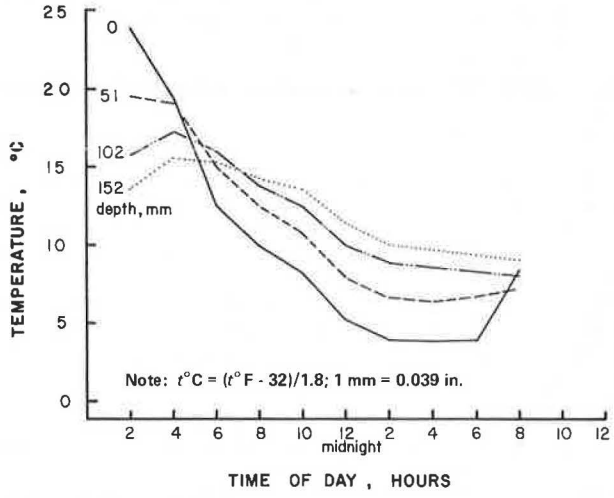


Figure 12. Variation in thermal stresses with depth for materials examined.

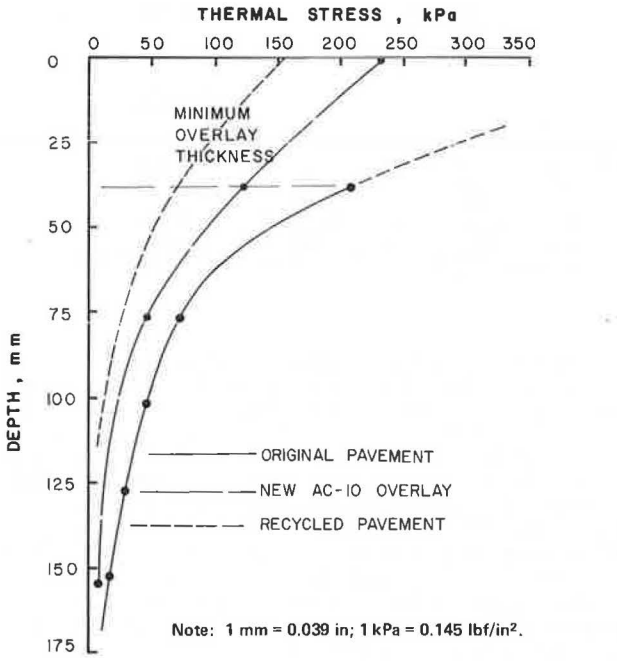


Figure 13. Variation in thermal stresses with depth for pavement sections analyzed.

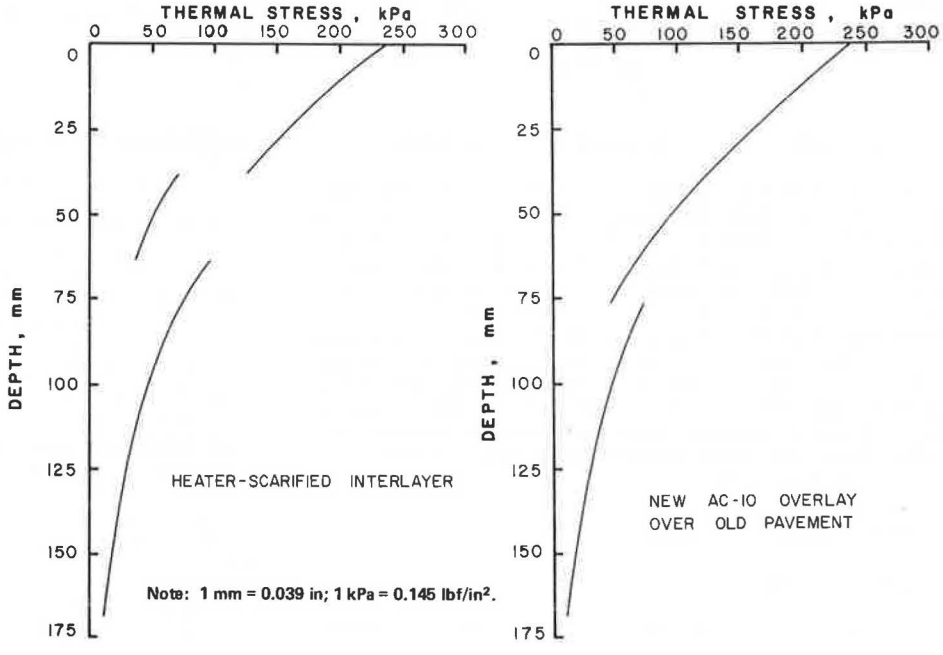

The fracture parameter A can only be estimated from the literature. Typical values will range from $10^{-14}$ to $10^{-12}$. There are not sufficient data available to relate the variation in A to asphalt properties. A value of $10^{-12}$ has been selected for calculations presented in this paper for all materials. The value of n will vary from 4.53 for the asphalt concrete overlay to 4.83 for the heater-scarified interlayer. These are representative of asphaltic materials.

The stress-intensity factor is needed to numerically integrate Equation 5 and obtain an estimate of the number of cycles to failure. In its simplest form, the stress will experience a singularity of the crack tip of magnitude $1/\sqrt{r}$, where r is the radius of the crack tip. The stress-intensity factor K is the magnitude of this increase. For similar geometric arrangements, r will be similar for all materials and the stress-intensity factors will be proportional to the tensile stress. If one uses this simplified approach with the tensile stresses indicating the stress-intensity factors, the number of cycles to failure will be proportional to the actual value obtained when the actual stress-intensity factors are used. The values obtained by integrating Equation 5 with tensile stresses are as follows: (a) For a new 76 mm (3-in) overlay, Nf = 400; (b) for a 25-mm (1-in) interlayer with a 38-mm (1.5-in) new overlay, Nf = 1200.

The results indicate that the heater-scarifier process could last nearly three times as long as a 76-mm overlay under the effects of thermal stresses. Assuming these stresses occur during a fourth of the year, the life of the overlay would be approximately 4 years whereas the heater-scarified pavement would last nearly 12 years. This life is considerably shorter than the period covered by the fatigue analysis. This indicates that the environmental influence in this example will be more severe than fatigue and that surface recycling will definitely show a benefit.

This performance level is highly dependent on the thermal stresses that develop. These stress levels will depend on the rejuvenating effect of the recycling agent on the aged binder. The factor of three may be an upper limit that results from a very good combination of the two asphalts examined in this study. A more in-depth study would examine the influence of several recycling agents to select the best combination to minimize thermal stresses but at the same time not adversely affect the fatigue characteristics of the pavement. Preliminary studies with another recycling agent, several reclaimed asphalts from pavements in Illinois, and virgin asphalt cements from new construction in Illinois are providing results similar to those presented here.

## CONCLUSIONS

The study discussed in this paper has shown that the materials produced in the heater-scarification recycling process have the potential to perform at least as well as a new overlay 76 to 102 mm (3-4 in) thick. Proper selection of recycling agent and virgin asphalt for the overlay can provide a far longer life for the heater-scarified overlaid pavement from a consideration of environmental damage. This fact combines well with the fact that surface recycling can be a very economical alternative.

The main point that should be obtained from this paper is that a technology does exist that allows relative performance to be accurately investigated. The performance comparisons can then be used to help justify surface recycling from considerations other than just cost. The performance comparisons commonly attributed to heater scarification have been based primarily on observations of in-service pavements. The results presented here are among the first analytic data to indicate why the observations show the heater-scarification process to be so successful. The soft interlayer lessens the accumulation of damage due to climatic influence without adversely affecting the fatigue life.

This paper presents numerical results for one actual material that was put through the recycling process and tested. The encouraging results indicate that further studies on the characteristics of a 100 percent recycled material with recycling agents added are needed if the full benefits of heater-scarification recycling are to be realized. This paper uses calculated or predicted values for fatigue and stiffness values. Further laboratory study is needed to characterize these 100 percent recycled materials to verify the validity of the predictive schemes for these materials and to quantify any problems that may develop through indiscriminate use of recycling agents with certain asphalts.

## ACKNOWLEDGMENT

This paper uses data developed as part of an Illinois Cooperative Highway Research Program project by the Department of Civil Engineering in the Engineering Experiment Station, University of Illinois at Urbana-Champaign, in cooperation with the Illinois Department of Transportation and the Federal Highway Administration.

The contents of this paper reflect my views, and I am responsible for the facts and the accuracy of the data presented. The contents do not necessarily reflect the official views or policies of the Illinois Department of Transportation or the Federal Highway Administration. This report does not constitute a standard, specification, or regulation.

## REFERENCES

1. R.F. Coons and P.H. Wright. An Investigation of the Hardening of Asphalt Recovered from Pavements of Various Ages. Proc., AAPT, Vol. 37, 1968, pp. 510-528.
2. H.S. Chang, R.L. Lytton, and S.H. Carpenter. Numerical Analysis of Thermal Crack Propagation in Pavement Overlays. Proc., 2nd International Conference on Numerical Methods in Geomechanics, Blacksburg, VA, 1976.
3. G.R. Morris and C.H. McDonald. Asphalt-Rubber Stress-Absorbing Membranes: Field Performance and State of the Art. TRB, Transportation Research Record 599, 1976, pp. 52-58.
4. N.F. Coetzee and C.L. Monismith. Analytical Study of Minimization of Reflection Cracking in Asphalt Concrete Overlays by Use of a Rubber-Asphalt Interlayer. TRB, Transportation Research Record 700, 1979, pp. 100-107.
5. S.H. Carpenter and J.R. Wolosick. Modifier Influence in the Characterization of Hot-Mix Recycled Material. TRB, Transportation Research Record 777, 1980, pp. 15-22.
6. W. Heukelom and A.J.G. Klomp. Road Design and Dynamic Loading. Proc., AAPT, Vol. 33, 1960, pp. 92-125.
7. N.W. McLeod. Asphalt Cements: Pen-Vis Number and Its Application to Moduli of Stiffness. ASTM Journal of Testing and Evaluation, Vol. 4, No. 4, 1976.
8. W. Heukelom. Observations on the Rheology and Fracture of Bitumens and Asphalt Mixes. Proc., AAPT, Vol. 35, 1966.
9. F.T. de Bats. The Computer Programs PONOS and POEL: A Computer Simulation of Van der Poel's

Nomograph. Koninklijke/Shell-Laboratorium, Amsterdam, External Rept. AMSR.0008.72, 1972.
10. F. Bonnaure, A. Gravois, and J. Udron. A New Method for Predicting the Fatigue Life of Bituminous Mixes. Presented at Annual Meeting of AAPT, Louisville, KY, 1980.
11. F.N. Finn, K. Nair, and J.M. Hilliard. Minimizing Premature Cracking in Asphaltic Concrete Pavement. NCHRP, Rept. 195, 1978.
12. M.Y. Shahin and B.F. McCullough. Prediction of Low-Temperature and Thermal-Fatigue Cracking in Flexible Pavements. Center for Highway Research, Univ. of Texas at Austin, Res. Rept. 123-14, 1972.
13. N.W. McLeod. Influence of Hardness of Asphalt Cement on Low-Temperature Pavement Cracking. Proc., Canadian Good Roads Assn., Ottawa, Ontario, 1970.
14. N.W. McLeod. Relationship Between Pavement Structural Integrity and Hardness of the Asphalt Cement. Proc., 3rd International Conference on Structural Design of Asphalt Pavements, London, Vol. 1, 1972, pp. 248-262.
15. Chemical Propulsion Information Agency. Joint Army-Navy-Air Force Solid Propellant Structural Integrity Handbook. Engineering College, Univ. of Utah, Salt Lake City, Rept. CE-72-160, Sept. 1972, pp. 107-136.
16. C.P. Paris and F.J. Erdogan. A Critical Analysis of Crack Propagation Laws. Journal of Basic Engineering, ASME, Series D, Vol. 85, 1963.
17. R.A. Schapery. Theory of Crack Initiation and Growth in Viscoelastic Media. International Journal of Fracture, Vol. 11, No. 1, Feb. 1975, pp. 141-159.
18. K. Majidzadeh, D.V. Ramsamooj, and T.A. Fletcher. Analysis of Fatigue of Sand-Asphalt Mixtures. Proc., AAPT, Vol. 38, 1969, pp. 495-518.
19. R.A. Schapery. A Theory of Crack Growth in Viscoelastic Media. Mechanics and Materials Research Center, Texas A&M Univ., College Station, Rept. MM 2764-73-1, 1973.

*Publication of this paper sponsored by Committee on Characteristics of Bituminous Paving Mixtures to Meet Structural Requirements.*

# Analysis and Repair of Water-Damaged Bituminous Pavement

G.W. MAUPIN, JR.

**An investigation of several bituminous concrete pavements on the Interstate system that experienced failures suspected to have been caused by stripping is reported. On two of the pavements, the degree of deterioration and potential serviceability was determined from the indirect tensile strength of cores and Dynaflect test results. Recommendations based on the investigation have resulted in repairs that are believed to be best suited to each situation. An emulsion mix design was developed for stripped bituminous concrete removed from a project with the expectation that it could be used as a surface mix on a highway with a low volume of traffic; however, because of risks involving performance, it was recommended for use as a base course. Resurfacing on a project that had experienced stripping failure is being monitored, and its performance is being evaluated.**

Stripping, which is the separation of the asphalt coating from the surface of the aggregate in flexible pavements, has resulted in considerable damage to several Virginia pavements in recent years. The deterioration that has resulted from the stripping has varied in severity from minor cracking to almost complete disintegration of the pavement. In 1978, stripping was suspected to be causing deterioration on several Interstate pavements, and an investigation was undertaken to determine the condition of several sections of distressed pavement and to recommend rehabilitative measures.

Although stripping problems in bituminous pavements have been encountered for many years, little attention has been given to selecting the most appropriate rehabilitative measures for particular situations. Usually, a resurfacing is applied as a temporary solution to the problem and no attempt is made to optimize the service life of the pavement. The initial step in deciding on the best type of repair for a given situation should be to determine the cause of failure, the degree of damage, and the strength of the overall pavement structure. The type of repair and rehabilitation selected should prevent further deterioration, where necessary, and strengthen the pavement structure so that it will provide satisfactory service. Other important factors that must be considered are limitations on the funds that are available and such construction-related restraints as the need to maintain the flow of traffic and the occurrence of minimum bridge clearances that limit the thickness of resurfacings. In Virginia, limitations on maintenance funds are becoming severe because of the reduction in tax revenue occasioned by reduced consumption of gasoline and inflation.

## TESTS USED

In the investigation reported here, a testing program was designed to determine the strength of the overall pavement structure and that of the asphaltic concrete courses under dry and wet conditions. Because pavements usually develop more distress under wet than under dry conditions, the wet strength was considered to be important.

Several sections of Interstate roads were investigated. The most extensive testing was conducted on sections of I-64 and I-85. In 1979, 34 and 30 cores were removed from I-64 and I-85, respectively. The cores were subjected to indirect tensile tests, as described later, to gain an indication of the overall strength and the loss in strength caused by moisture. In addition, a visual determination of stripping was made.

Viscosity and penetration measurements were made according to ASTM D2170 and ASTM D5, respectively,

**Figure 1. Chart used in determining thickness equivalency.**

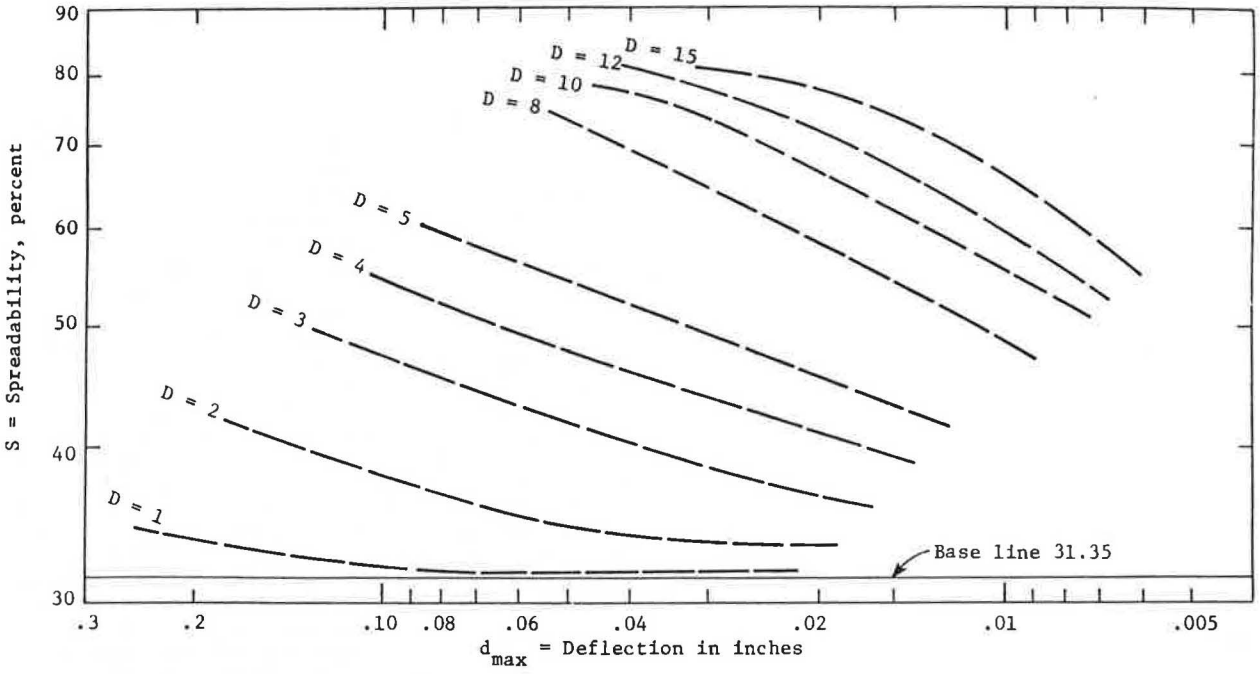


on asphalt cement recovered from cores by use of the Abson recovery procedure (ASTM D1856).

The strengths of the pavement structures were computed from the results of Dynaflect measurements. The results of these measurements were also used to predict the remaining service life of the pavement.

Pavement strengths were determined in terms of thickness equivalencies, which represent equivalent thicknesses of full-depth bituminous concrete. The maximum deflection, the shape of the deflection basin (spreadability), and the general evaluation chart shown in Figure 1 (1) were used to compute the thickness equivalencies. In this calculation, the maximum deflection is defined as the equivalent Benkelman beam deflection and the spreadability is defined as

$$S = [(d_{max} + d_1 + d_2 + d_3 + d_4)/5d_{max}] \times 100 \quad (1)$$

where $d_{max}$ is the deflection under the center of the applied load and $d_1$, $d_2$, $d_3$, and $d_4$ are the deflections at 1, 2, 3, and 4 ft from the center of the applied load.

## PAVEMENTS INVESTIGATED

The pavement sections investigated had exhibited various degrees of distress in the spring of 1978. Preliminary observations at that time revealed stripping damage; however, no extensive examinations of the pavements were made prior to the investigation reported here.

### I-64 in Goochland County

A section of I-64 approximately 10.5 miles long in Goochland County showed initial distress in the form of cracks. Later, potholes developed. A trench cut across the westbound traffic lane in the spring of 1978 revealed stripping throughout the full depth of the asphaltic concrete. The cracks were sealed prior to the application of a slurry-seal treatment in the summer of 1978; however, potholes continued to appear in the spring of 1979.

The pavement structure on this section consists of 6.0 in of stabilized soil cement, 8.0 in of no. 21-A crushed subbase material, 7.5 in of B-3 bituminous concrete base, 1.2 in of I-2 bituminous concrete, and 0.9 in of S-5 bituminous concrete surface. The design ranges for the 21-A dense-graded aggregate and the bituminous concrete mixture, respectively, were as follows (percentage by weight passing square mesh sieves) (2):

| Sieve Size | Percent Passing |
|---|---|
| 2 in | 100 |
| 1 in | 94-100 |
| 0.375 in | 63-72 |
| No. 10 | 32-41 |
| No. 40 | 16-24 |
| No. 200 | 8-12 |

| | Percent Passing by Mix Type | | |
|---|---|---|---|
| Sieve Size | S-5 | I-2 | B-3 |
| 1.5 in | | | 100 |
| 1 in | | 100 | |
| 0.75 in | | | 73-85 |
| 0.5 in | 100 | | |
| 0.375 in | | 63-77 | |
| No. 4 | 53-67 | 43-57 | 38-48 |
| NO. 8 | | | 28-35 |
| No. 30 | 19-27 | | |
| No. 50 | | 6-14 | |
| No. 200 | 4-8 | 2-6 | 2-6 |

The aggregate was from a quarry used only for the construction of the Interstate pavement. Although it had a high mica content, it passed all Virginia specifications for quality and soundness.

In June 1979, cores were taken and Dynaflect tests were performed approximately every 1 mile in the eastbound traffic lane (EBTL) and westbound traffic lane (WBTL) and every 2 miles in the passing lanes (PLs). Usually, three Dynaflect tests were performed within 150 ft of the area cored.

### Analysis of Cores

After they were separated into individual layers,

**Table 1. Indirect tensile strengths for cores from I-64.**

| Mix | Lane | Indirect Tensile Strength (lbf/in²) Dry | Vacuum Saturated | Dry Strength (%) |
|---|---|---|---|---|
| I-2 | WBTL | 90 | 57 | 63 |
| | EBTL | 67 | 32 | 48 |
| | PL | 134 | 120 | 90 |
| B-3 | WBTL | 91 | 50 | 55 |
| | EBTL | 85 | 39 | 46 |
| | PL | 180 | 100 | 56 |

**Table 2. Properties of recovered asphalt from I-64.**

| Mix | Penetration (mm) | Viscosity Dynamic at 140°F (poises) | Kinematic at 275°F (cSt) |
|---|---|---|---|
| B-3 | 40 | 8800-11 400 | 740-940 |
| I-2 | 21-23 | 49 000-66 000 | 1840-2120 |
| S-5 | 17-24 | 29 000-73 000 | 1580-2550 |

**Table 3. Thickness equivalency for I-64.**

| Lane | Thickness (in) Design | Needed for Current Traffic | Measured Avg | Measured Range |
|---|---|---|---|---|
| EBTL | 14.7 | 14 | 6.5 | 5.0-7.5 |
| WBTL | 14.7 | 14 | 9.0 | 8.0-10.5 |
| EBPL | 14.7 | 11 | 8.0 | 6.5-8.5 |
| WBPL | 14.7 | 11 | 9.0 | 8.0-11.0 |

half of the cores taken were dried and the other half were vacuum saturated with water. The cores were tested in indirect tension at a vertical deformation rate of 2 in/min and a temperature of 72°F. The mix in the surface course was not tested in indirect tension because of insufficient thickness. Penetration and viscosity tests were performed on asphalt cement recovered from several cores to obtain an indication of the brittleness of the pavement.

Table 1 gives the indirect tensile strengths of the I-2 and B-3 layers. It should be noted that the strength of the layers from the EBTL was less than that of the layers from the WBTL, especially for the I-2 mix. The materials used in both lanes were from the same source, and the traffic counts were approximately equal in both directions; therefore, the difference in strengths does not appear to be related to these items. The strengths for the passing lanes were considerably greater than those for the traffic lanes, probably because of the higher traffic volume carried by the latter.

The reductions in the strengths of the asphaltic concrete from the traffic lanes ranged from 37 to 54 percent when the material was vacuum saturated. These results indicate a significant reduction of pavement strength in late winter and early spring, when the pavement is wet. These results agree with the pavement performance, since failures occur more frequently in the wet seasons of late winter and early spring than at other times.

The properties of asphalt recovered from the cores were determined and are given in Table 2. All of the results except those for the B-3 cores indicated severe oxidation. The penetration for the asphalt from the S-5 and I-2 mixes averaged approximately 20 mm, and the B-3 material gave a value of 40 mm.

### Dynaflect Tests

The total pavement strength (thickness equivalency) was determined from the results of Dynaflect tests. Since the Dynaflect tests were performed in June 1979, the pavement should have been relatively dry. Table 3 gives the thickness equivalency values. The measured thickness equivalencies were from 5 to 7 in less than that needed for the current traffic volume, especially in the traffic lanes. These results can be interpreted to indicate that the pavement will not stand up under the current traffic volume for the design life and that there will be additional premature failures.

It was recommended that the structural strength be increased and the surface sealed to prevent the entrance of water because of the low strength of the overall pavement structure and of the asphaltic concrete when wet. Three of the worst sections were repaired by using a different method for each section: resurfacing with 1.4 in of hot mix, resurfacing with 1.4 in of hot mix and a fabric sealer, and resurfacing with 2.2 in of hot mix. The performance of these test sections will be evaluated to determine the most efficacious of the three methods. Recycling was not considered because of the poor performance of the original pavement.

## I-85 in Brunswick County

Cracking occurred in varying degrees of severity along a 20-mile section of I-85 in Brunswick County. Cores taken from one of the most deteriorated areas revealed extensive stripping through the full depth of the asphaltic layers. In 1978, this area was repaired with a slurry-seal treatment that seemed to alleviate the deterioration.

The pavement structure on this section of I-85 consists of 6 in of soil cement, 6 in of cement-treated stone, and 9-10 in of asphaltic concrete. The granitic aggregate used in the mixes was supplied from both a permanent and a temporary quarry.

Tests were performed on five 2-mile sections spaced throughout the 20-mile length because of traffic-control restraints. Cores were obtained in both the traffic and passing lanes, and Dynaflect tests were performed near the core locations.

### Analysis of Cores

Table 4 gives the dry and saturated indirect tensile strengths of the I-2 and B-3 layers. The strength of the layers in the saturated condition was only approximately 30-50 percent of the dry strength; therefore, the structural integrity of the pavement could be greatly reduced in the spring if water penetrated the pavement and drying conditions were poor.

The excellent performance of the slurry-sealed section probably can be attributed to the treatment preventing water from entering the pavement surface. The properties of the recovered asphalt, given in Table 5, indicate severe oxidation, especially for the I-2 and S-5 mixes. The asphalt is prone to cracking and failure because of brittleness.

### Results of Dynaflect Tests

The thickness equivalencies for the sections tested are given in Table 6. The measured thickness equivalencies of sections 1-3 were approximately equal to that necessary for the current traffic load; those

**Table 4. Indirect tensile strength for cores from I-85.**

| Mix | Section | Indirect Tensile Strength (lbf/in$^2$) Dry | Vacuum Saturated | Dry Strength (%) |
|---|---|---|---|---|
| I-2 | 1 | 86 | 34 | 40 |
| | 2 | 84 | 46 | 55 |
| | 3 | 85 | 34 | 40 |
| | 4 | - | - | - |
| | 5 | 93 | 27 | 29 |
| B-3 | 1 | 62 | 33 | 53 |
| | 2 | 89 | 55 | 62 |
| | 3 | 77 | 32 | 42 |
| | 4 | 92 | 36 | 39 |
| | 5 | 81 | 44 | 54 |

**Table 5. Properties of recovered asphalt from I-85.**

| Mix | Penetration (mm) | Viscosity Dynamic at 140°F (poises) | Kinematic at 275°F (cSt) |
|---|---|---|---|
| B-3 | 20-45 | 5300-38 000 | 820-1280 |
| I-2 | 19-21 | 40 000-50 000 | 1400-1570 |
| S-5 | 15-21 | 70 000-84 000 | 1670-2180 |

**Table 6. Thickness index for I-85.**

| Section | Thickness (in) Design | Needed for Current Traffic | Measured Avg | Range |
|---|---|---|---|---|
| 1 | 17.9 | 17.5 | 16 | 12-18 |
| 2 | 18.4 | 17.5 | 18 | 15-20 |
| 3 | 18.4 | 17.5 | 17 | 15-18 |
| 4 | 17.4 | 17.5 | 14 | 10-17 |
| 5 | 17.9 | 17.5 | 13 | 10-17 |

for sections 4 and 5 were slightly less.

Based on the Dynaflect results, which indicated that the present pavement strength is equal to or only slightly less than the design strength, it was not considered necessary to apply a hot-mix resurfacing. Since the strength of the asphaltic concrete was greatly reduced when saturated and the slurry seal that was applied to an adjacent section seemed to alleviate the deterioration, it was recommended that the pavement be sealed. A slurry seal was applied in July 1980 and should prevent or retard further deterioration.

## I-81 in Washington and Smyth Counties

Several sections of asphaltic concrete pavements on I-81 were found to have developed severe cracking and potholes. The makeup of the pavements on these sections varied as follows: 10-12 in of select material with a minimum California Bearing Ratio of 30, 6 in of crushed stone, 7.5 in of H-3(1) bituminous base (currently B-3 designation), 1.2 in of H-2 intermediate mix (currently I-2 designation), and 0.7 in of I-3 surface mix (currently S-5 designation). All of the sections investigated were covered with approximately 1.5 in of maintenance resurfacing (S-5).

The pavement distress had appeared in the form of cracks and potholes in the spring of 1978. An inspection revealed that damage was confined to the original surface and overlay and that it had resulted from severe stripping in the original surface. The maintenance resurfacings that had been applied to these sections were of two types: an S-5 nonpolishing mix and a sprinkle mix (3). Tests revealed that the sprinkle mix was very permeable and allowed water to reach the original surface mix, which contained a quartzite aggregate that is not now allowed for use in Interstate pavements because of its stripping history.

When the stripping problem was determined to have originated in the original surface, it was decided to remove approximately 1.5-2.0 in of the asphaltic concrete by cold milling and to apply a new surface. Recycling the removed material for the new surface was not considered because of past poor performance, but it was considered for use at other locations nearby.

Approximately 27 miles of the surface were removed, and there was a considerable amount of material to be reused or disposed of. It was anticipated that the removed surface could be used as a base material or in an emulsion surface mix on a low-traffic-volume highway. After an emulsion mix design was examined in the laboratory, it was decided not to use the material in this manner because of performance risks but to use it as an aggregate base material.

## Other Pavements

Another section of Interstate pavement was found to have a problem in a layer of asphaltic concrete containing an aggregate that, after construction, was banned from use in Interstate pavements because of its susceptibility to stripping. A 2.5-in maintenance resurfacing was applied to a limited area and is being observed to determine whether other areas can be treated similarly if the need arises. After one year, slight distress has been observed in several places; however, any conclusions at this time would be premature.

An additional section of Interstate pavement experienced considerable distress in late winter and early spring. The distress seemed to be confined to a maintenance resurfacing. An examination of cores removed from the pavement revealed an accumulation of water and lack of bond between the original surface and the maintenance resurfacing. A fabric sealer and resurfacing have been applied to some of the worst areas in an attempt to seal out the water and provide additional strength.

## SUMMARY

The importance of a thorough investigation before major pavement repairs are made is emphasized by the results of the investigation described in this paper. Although the pavement failures investigated had resulted from water damage, the individual cases required different rehabilitative measures. The popular repair technique of applying a hot-mix resurfacing would have been unwise in several of these cases because it would not have sealed out water or it would have been unnecessary from the standpoint of strengthening the pavement structure.

## ACKNOWLEDGMENT

I thank A.D. Newman, S.L. Hite, and W.A. Dennison for assisting in the necessary field testing and R.M. Cleek, Jr., and B.S. Byrd for providing traffic control. Appreciation is expressed to G.V. Leake and L.E. Wood, Jr., who conscientiously performed the field and laboratory tests, respectively. I also thank J.H. Dillard for his support and C.S.

Hughes III and K.H. McGhee for their professional advice on the conduct of the investigation and interpretation of the results. The investigation was financed with Highway Planning and Research funds administered by the Federal Highway Administration.

The opinions, findings, and conclusions expressed in this paper are mine and not necessarily those of the sponsoring agencies.

REFERENCES

1. N.K. Vaswani. Pavement Design and Performance Study: Phase B--Deflection Study. Virginia Highway Research Council, Charlottesville, Interim Rept. 3, Feb. 1971.
2. Road and Bridge Specifications. Virginia Department of Highways and Transportation, Charlottesville, Jan. 1, 1978.
3. J.H. Dillard and G.W. Maupin, Jr. Use of Sprinkle Treatment to Provide Skid-Resistant Pavments. Proc., AAPT, Vol. 40, 1971.

*Publication of this paper sponsored by Committee on Characteristics of Bituminous Paving Mixtures to Meet Structural Requirements.*

# Rational Approach to Design of Bituminous Stockpile Patching Mixtures

PRITHVI S. KANDHAL AND DALE B. MELLOTT

**Although a considerable amount of maintenance expenditure is spent on bituminous patching, the performance of conventional cold stockpile patching materials has been generally unsatisfactory. No concerted effort has been made to design these mixtures on a rational basis. The challenges of designing these mixtures are reviewed, and some new concepts vital for the survival of these mixtures in the adverse environment of potholes are presented. These concepts among others include the use of finer and predominantly one-sized gradation for the aggregate and the maximum dust content (minus 200 fraction) of two percent in the mixture. A formulation based on these concepts has been developed and used in the field during the past three years. The data obtained from the field and laboratory evaluation of the suggested formulation are reported. Laboratory test data indicate the effect of dust content on the workability of these mixtures. Attempts were made to quantify the workability of the mixtures by using a cement concrete penetrometer. However, the results were inconsistent and merely show a trend of higher penetrometer readings for mixtures with poor workability.**

After severe winters, potholes are certain to appear. Several estimates of the extent of the pothole problem have been attempted. According to a CBS Evening News broadcast of February 21, 1978, in 1977 there were an estimated 160 million potholes produced in nearly 4 million miles of roads and streets in the United States, which cost nearly $1 billion to repair. The most comprehensive damage estimates so far come from The Roads Information Program (TRIP), whose researchers estimated in a February 28, 1979, news release that 93 million potholes dotted roads around the country in 1979. According to TRIP, 5 million tons of asphalt mix, costing $256 million, was required just to fill the craters.

Pennsylvania's 72 418 km (45 000 miles) of state-administered highways constitutes the fourth largest such system in the United States. A value engineering study (1) conducted by the Pennsylvania Department of Transportation (PennDOT) for the Federal Highway Administration (FHWA) during the 1975-1976 fiscal year indicated that this vast network required a maintenance expenditure of $145 million, of which $25.8 million or 17.8 percent was required for bituminous patching. The cost for bituminous patching material alone was $5.7 million, or 22.1 percent of the total patching allotment. The remaining 77.9 percent covered the costs for equipment and labor. This study indicated that PennDOT should be providing a more permanent patch and reducing the number of repeat trips to the same area. To realize this goal, the need for using proper patching techniques cannot be overemphasized. O'Brien (2) has reported the annual costs per ton of patching material in place for five different patching techniques, taking into consideration the life of the patch. The annual cost per ton of the material was determined to be $307.68 when it was simply dumped in the pothole in one lift and hit with a shovel versus $61.41 when it was placed properly (proper placement includes shaping the area, removing loose debris, applying a tack coat, shoveling in the material, leveling with a lute, and compacting with a pug roller).

Many proprietary patching products have been promoted by various manufacturers. These mixtures are usually tailor-made with one stone type under strictly controlled conditions and supplied in 55-gal drums. The cost of such materials ranges from $100 to $500/ton, which makes their use prohibitive from the economic standpoint.

There is a need to develop a stockpile patching mixture that is economical, capable of withstanding some abuse in placement, and reasonably durable. It may be more cost effective to design mixtures for better durability. Information assembled from numerous sources, including a large number of highway and transportation departments (3), indicates the lack of a rational design procedure.

## CHALLENGES OF MIX DESIGN

It is difficult to design stockpile patching mixtures because the properties required in stockpiling and handling and after the material is placed in the pothole are contradictory. Some of these contradictory requirements are as follows:

1. Aggregate gradation--For good mixture workability, an open gradation is desired. After the mix is placed, however, a denser gradation is needed to improve durability.
2. Aggregate shape--To obtain good workability, angular aggregate shape should be avoided. However, once the mix is in place, a high degree of angularity is desirable for better stability.
3. Binder viscosity--Lower binder viscosity is

desired for storageability and workability, but after placement higher viscosity is desirable as soon as possible for better cohesion of the mixture.

4. Binder content--Greater residual bitumen content in the mixture is needed to obtain thicker films on the aggregate for stickiness and durability, but there is a possible binder drainage problem in the stockpile just after stockpiling while the mix is hot.

Use of highly absorptive aggregates can also pose problems. High moisture content in such aggregates often causes stripping and/or drainage problems in the stockpile. Selective absorption of the lighter fractions of the bituminous binder by such aggregates leaves a bituminous film that has undesirable characteristics and is significantly different from the original bituminous binder used.

It is not possible to use conventional methods of mix design generally used for hot asphaltic concrete, such as the Marshall and Hveem methods. Not only are the specimen preparation and testing difficult, but also the desired design criteria for the stockpile patching mixtures are unknown.

## NEW CONCEPTS

In the past, the use of larger-sized aggregate [12.5-19.0 mm (0.5-0.75 in)] in the stockpile mixture has been promoted to obtain higher stability. Such a mixture can be successful if the patching technique is ideal (for example, making edges vertical, cleaning, applying tack coat, and compacting adequately). However, ideal patching techniques are not always used and mixtures that contain larger aggregate start to ravel under traffic, which results in premature failure of the patch. Another concept is to disregard the stability and make the mixture finer and more pliable so that it will be more tolerant of abuse during placement and perform under traffic. This finer mix, if placed less than 76 mm (3 in) deep in one lift in a confined area, should be stable. For deeper and/or larger holes, the mixture has to be compacted in layers.

The cohesive and adhesive qualities of a mix depend mainly on the composition of the mortar (bituminous binder plus fines). If there are excessive fines or dust [material passing a 0.075-mm (no. 200) sieve] in the mixture, the mortar will be lean, less tacky, and friable. It is no coincidence that most of the expensive commercial patching products are made from clean stone. Several extraction tests run on such products have revealed that the fines (the minus 200 fraction) are usually less than 1 percent. In the absence of excessive fines, mixtures are very tacky; therefore, tack coating of the pothole will not be required. Many of PennDOT's conventional stockpile patching mixtures have not performed satisfactorily because of excessive fines. Such mixes are dull and friable and lack cohesive and adhesive qualities.

## PENNSYLVANIA'S IMPROVED FORMULATION

### Mixture Characteristics

In view of the challenges of mix design and new concepts, the characteristics discussed below appeared desirable for a satisfactory and economical stockpile patching mixture.

### Finer and Predominantly One-Sized Gradation

A gradation consisting of 100 percent passing the 9.5- or 4.75-mm (0.375-in or no. 4) sieve has the following advantages:

1. The mix is pliable and workable.
2. Due to increased surface area, more bituminous binder can be incorporated into the mix to improve the durability.
3. The mix remains pliable for a prolonged period of time and continues to densify easily under traffic and will continue to adapt to the changing geometry of the pothole. This characteristic enhances its chances of survival.

Normally, a finer dense gradation will not have good workability. However, if it is made of predominantly one-sized aggregate [100 percent passing the 9.5- or 4.75-mm sieve and mostly retained on the 1.18-mm (no. 16) sieve], the following advantages result: (a) the workability of the mixture is increased significantly, and (b) the mixture can cure effectively.

### Clean Aggregate

As discussed earlier, it is very important to keep the dust content (minus 200 fraction) in the mixture as low as possible to impart tackiness. This would significantly improve the adhesive and cohesive properties of the mixture.

### Angular Aggregate Shape

Angular aggregate shape is desirable for better stability. Since a finer and predominantly one-sized gradation is used, the effect of aggregate angularity on the workability of the mix is minimal. Angular crushed-stone aggregate is an ideal material.

### Use of Least Absorptive Aggregate

Highly absorbent aggregates should be avoided. The aggregate water absorption should be limited to approximately 1 percent.

### Adequate Binder Content

It has been determined that at least 4.5 percent residual bituminous binder is required in a stockpile patching mixture made from an aggregate whose water absorption is less than 1 percent. If the aggregate absorbs water in excess of 1 percent, the residual binder content should be increased a similar amount. For example, an aggregate that absorbs 1.5 percent water should have 5.0 percent mimimum residual bituminous binder. The factor limiting the maximum amount of the bituminous binder is drainage in the stockpile just after manufacture. The drainage can be minimized or eliminated by using lower mix temperatures and limiting the stockpile height to 1.2 m (4 ft) during the first 48 h.

### Proper Type and Amount of Antistripping Agent

The antistripping agent is a very important part of the formulation of the stockpile mixture. A mixture should retain its coating in the stockpile under adverse weather conditions, during handling, and in the pothole after placement. A stockpile patching mixture, which is more pervious than a densely graded hot mix, has to withstand by far the most severe weather and traffic effects. It has to survive in conditions that led to the creation of the pothole in the first place (such as poor base, inadequate drainage, and deteriorated adjacent pavement). Rain or melting snow provides water. The pneumatic tires of vehicles provide high pressures. This combination can emulsify the bituminous binder or displace it from the aggregate. If sufficient

stripping occurs as a result of this action, the traffic will dislodge the aggregate particles.

There are many commercially available antistripping agents in the market for use with the medium-curing (MC) cutback asphalts. Extensive testing in the PennDOT Bituminous Laboratory shows that there is no single additive that will work with all aggregate types. Therefore, it is essential that the type of antistripping agent and its amount be selected after testing with the aggregate that is actually being used in the mix. PennDOT requires its bituminous suppliers to conduct the wet coating test, static immersion test, and stripping test with the job aggregate.

## Specifications

The salient features of Pennsylvania's stockpile patching material specifications are discussed below.

### Description

The material shall consist of plant-mixed stockpile patching bituminous mixture composed of mineral aggregate coated with bituminous material. The material shall be capable of being stocked for at least six months without stripping and shall be workable at all times.

The material is intended for patching holes up to 76 mm (3 in) deep. For holes deeper than 76 mm, the material will be compacted in layers, each layer not exceeding 76 mm.

### Bituminous Materials

The listed bituminous materials shall meet the applicable requirements of PennDOT Bulletin 25 (Specification for Bituminous Materials):

| Class of Material | Type of Material |
|---|---|
| MC-250 | Cut-back petroleum asphalt |
| MC-800 | Cut-back petroleum asphalt |
| ME-250 | Emulsified cut-back asphalt |
| ME-800 | Emulsified cut-back asphalt |
| E-10 | Emulsified asphalt (high-float residue) |
| E-12 | Cationic emulsified asphalt |
| RT-4 | Coal tar |
| RT-6 | Coal tar |

Materials MC-250, ME-250, and RT-4 shall be used between November 1 and March 1; materials MC-800, ME-800, and RT-6 shall be used between March 1 and October 31; and materials E-10 and E-12 may be used throughout the year.

Materials MC-250, MC-800, ME-250, and ME-800 shall be treated with antistripping agents to meet the requirements of the wet coating test, the static immersion test, and the stripping test performed with the job aggregate. Materials E-10 and E-12 shall pass the dry and wet stone-coating test on the job aggregate.

The contractor shall furnish the sample of the job aggregate to the bituminous supplier for the coating and stripping tests specified in PennDOT Bulletin 25 and obtain a certificate that the bituminous material has been treated to suit the job aggregate. This certificate shall be produced when required by the engineer.

### Composition of Mixture

The contractor shall furnish the mixed material within the gradation limits specified below (1 mm = 0.039 in):

| Sieve Size (mm) | Percent Passing | |
|---|---|---|
| | Specified | Preferred |
| 9.5 | 100 | 100 |
| 4.75 | 40-100 | 85-100 |
| 2.36 | 15-40 | 10-40 |
| 1.18 | - | 0-10 |
| 0.075 | 0-2 | 0-2 |

The quantity of bituminous material in the mix shall be such that the minimum requirements on the percentage of residue specified below are met:

| Aggregate Type | Water Absorption (%) | Binder Residue (%) |
|---|---|---|
| Stone and gravel | <1.0 | 4.5 |
| Stone and gravel | 1.1 to 1.5 | 5.0 |
| Stone and gravel | 1.6 to 2.0 | 5.5 |
| Stone and gravel | 2.1 to 2.5 | 6.0 |

As far as possible, aggregate with less than 1.0 percent water absorption should be used. Exceptional cases where the minimum requirements of the preceding table are difficult to meet shall be referred to the Materials and Testing Division for approval.

### Preparation of Mixtures

All mineral aggregates and bituminous material shall be proportioned by weight or by volume. The mixture shall be such that it may be stocked, handled, placed, and finished without stripping of the bituminous material from the aggregate. To help prevent stripping, the mixed material shall be stocked no higher than 1.2 m (4 ft) for the first 48 h.

The mineral aggregate shall be clean and surface dry before mixing. The temperatures of the bituminous material, the aggregate, and the resulting mixture shall be maintained as follows [t°C = (t°F - 32)/1.8]:

| Material | Temperature Range (°C) | | |
|---|---|---|---|
| | Aggregate | Bituminous Material | Mixture |
| MC-250 | 4-66 | 57-82 | - |
| MC-800 | 4-66 | 74-96 | - |
| ME-250 | 4-66 | 79 max | - |
| ME-800 | 4-66 | 79 max | - |
| E-10 and E-12 | Appropriate for specified mix temperature | 60-79 | 88-121 |
| RT-4-C | 38-93 | 54-66 | 38-88 |
| RT-6-C | 38-93 | 54-79 | 38-88 |

When E-10 or E-12 emulsified asphalt is used, the temperature requirements on the aggregate and the mixture can be waived by the engineer if it is demonstrated that the mix can be prepared with unheated aggregate without any coating or stripping problems, during production and stockpiling. To help prevent drainage of bituminous binder in the stockpile, the mixing temperature shall be held as low as practicable within the ranges specified above.

The following two tests on the mixture, freshly prepared or taken from the stockpile, shall be performed by the contractor in the presence of a PennDOT representative before the samples are sent to the Materials and Testing Division for testing:

1. Water-resistance test--Fifty grams of mixture, whether freshly prepared or taken from the stockpile, shall be heated at 121°C (250°F) in a laboratory oven for 1 h, cooled at 93°C (200°F) in laboratory air, and then placed in 400 mL of boiling distilled water in a 600-mL glass beaker and stirred

Figure 1. Potholes filled with improved formulation (3 PX) and Sylvax (SX).

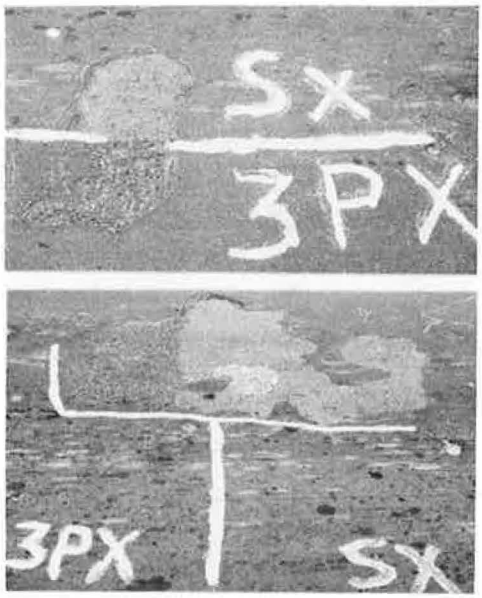


Figure 2. Trucks carrying different mixtures for comparative field evaluations.

Figure 3. Different mixes laid side by side in one patch.

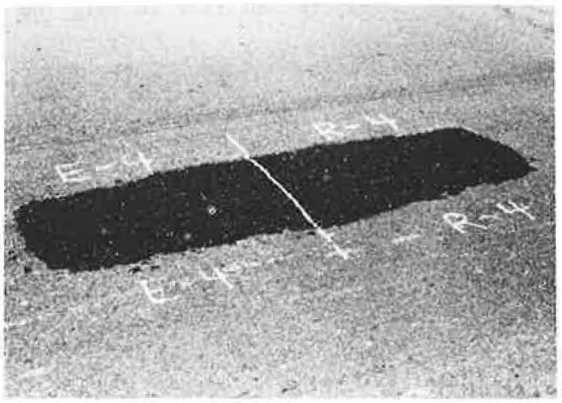

with a glass rod at the rate of 1 revolution/s for 3 min. The water shall be decanted, and the mix shall be spread on an absorbent paper for visual observation of the coating. The aggregate shall be at least 90 percent coated with a bituminous film.

2. Workability test--Approximately 2.3 kg (5 lb) of the mixture shall be cooled to -6.7°C (20°F) in the laboratory. After cooling, the mixtures shall be capable of being broken up readily with a spatula that has a blade length of approximately 203 mm (8 in). This test shall be performed when the mixture is produced or used between November 1 and March 1. If the mixture is not workable at -6.7°C, it shall be rejected and the composition of the mixture shall be properly modified (for example, by increasing the percentage of bitumen residue or by gradation changes).

## FIELD EVALUATIONS

The experimental (improved formulation) stockpile patching mixture discussed above was used in April 1977 at two locations: (a) US-22, Lebanon County, Stations 10-50; and (b) the road in front of the PennDOT Testing Laboratory, which carries city traffic. The improved formulation was used along with Sylvax UPM, supplied by Sylvax Chemical Corporation, Great Neck, New York. Sylvax UPM, a proprietary patching material, was determined to be significantly better than the standard cold mixes in field tests conducted by Public Technology, Inc. (4).

Both materials were placed in wet potholes without any preparation. Most of the evaluations conducted in March 1980 indicate that both materials are performing equally well. These patches are shown in Figure 1.

More field installations of these two stockpile patching mixtures were completed during the first two weeks of March 1978 on the various legislative routes and state and U.S. routes given below:

| County | Route | Location |
|---|---|---|
| Cumberland | LR-34, US-11 | North of Carlisle |
| Dauphin | LR-1, PA-147 | South of Halifax |
| | US-22,4; PA-225 | South of Halifax |
| | LR-769, I-83 | John Harris Bridge |
| Indiana | LR-54, US-422 | East of Indiana |
| | LR-63, US-119 | North of Indiana |
| Allegheny | LR-247, PA-51 | South of Pittsburgh |
| | US-22,70 | Liberty Bridge, Pittsburgh |

The weather generally met the criteria established for cold-weather patching with temperatures that ranged from -6° to 2°C (22°-35°F) with occasional snow flurries. The potholes filled ranged in size from about 0.05 to 3.72 $m^2$ (0.5-40 $ft^2$), and from 25.4 to 101.6 mm (1-4 in) deep. Many were wet, and some had ice in the bottom of the hole that was not removed. A total of 42 control patches and 251 Sylvax UPM patches were observed for performance. Most patches were observed regularly and photographed on each occasion to determine the extent of failures as they might occur. The observations were made after 1, 7, and 14 days, and 1, 2, and 6 months. Two of the locations have been observed after one year.

Again, as observed in the 1977 trials, most patches performed well, regardless of the technique or material used. No significant differences could be noted after the last observation. Failures have occurred in the areas surrounding many of the test patches, and additional patches have been placed. Figures 2 and 3 show the field installation of the patches in this comparative study.

## LABORATORY EVALUATION OF FIELD MIXTURES

Encouraged by the initial successful results of the improved formulation for the stockpile patching mixture, six engineering districts in Pennsylvania were selected for wide-scale field trials during the

**Table 1. Mix test data: good workability.**

| Item | District | Gradation (percent passing) | | | | Residue Asphalt (%) | Penetrometer Reading (N) | Marshall Test at -6.7°C | |
|---|---|---|---|---|---|---|---|---|---|
| | | 9.5 mm | 4.75 mm | 2.36 mm | 0.075 mm | | | Stability (N) | Flow (mm) |
| Sample | | | | | | | | | |
| 6444 | 4 | 100 | 72 | 27 | 2 | 5.0 | 489 | 3020 | 1.62 |
| 6451 | 9 | 100 | 58 | 26 | 1 | 4.0 | 445 | 5284 | 1.88 |
| 6783 | 8 | 100 | 62 | 28 | 2 | 3.5 | 623 | 4653 | 1.88 |
| 6872 | 8 | 100 | 79 | 23 | 2 | 5.2 | 578 | 1793 | 2.68 |
| 6887 | 10 | 100 | 69 | 27 | 1 | 5.6 | 445 | 4110 | 2.75 |
| 6888 | 8 | 100 | 70 | 26 | 2 | 4.3 | 534 | 5698 | 1.88 |
| 6906 | 9 | 100 | 50 | 27 | 2 | 4.7 | 267 | 1966 | 2.1 |
| 79-24 | 2 | 100 | 52 | 25 | 2 | 4.2 | 534 | 5623 | 2.25 |
| 13145 F | 8 | 100 | 65 | 26 | 2 | 4.4 | 356 | - | - |
| Mean | | 100 | 64 | 26 | 1.78 | 4.54 | 476 | 4017 | 2.12 |
| Standard deviation | | - | 9.6 | 1.4 | 0.44 | 0.65 | 111 | 1584 | 0.40 |
| 95 percent confidence limit | | | | | | | | | |
| Low | | 100 | 45 | 23 | 0.9 | 3.2 | 254 | 850 | 1.32 |
| High | | 100 | 83 | 29 | 2.7 | 5.8 | 698 | 7184 | 2.92 |

Note: 1 mm = 0.039 in; 1 N = 0.225 lbf.

**Table 2. Mix test data: fair workability.**

| Item | District | Gradation (percent passing) | | | | Residue Asphalt (%) | Penetrometer Reading (N) | Marshall Test at -6.7°C | |
|---|---|---|---|---|---|---|---|---|---|
| | | 9.5 mm | 4.75 mm | 2.36 mm | 0.075 mm | | | Stability (N) | Flow (mm) |
| Sample | | | | | | | | | |
| 6302 | 4 | 100 | 51 | 27 | 3 | 5.3 | 801 | 5578 | 2.38 |
| 6445 | 4 | 100 | 75 | 26 | 3 | 5.1 | 578 | 4341 | 1.62 |
| 6763 | 2 | 100 | 54 | 24 | 2 | 3.8 | 311 | 4070 | 1.62 |
| 6847 | 2 | 100 | 51 | 18 | 2 | 4.1 | 623 | 1922 | 3.25 |
| 6848 | 2 | 100 | 51 | 16 | 3 | 4.6 | 445 | 3879 | 3.15 |
| 6917 | 2 | 100 | 52 | 24 | 2 | 3.9 | 445 | 2304 | 1.35 |
| 6918 | 2 | 100 | 48 | 16 | 2 | 3.7 | 1068 | 1294 | 1.38 |
| 13145 C | 8 | 100 | 52 | 27 | 2 | 3.9 | 623 | 4301 | 1.50 |
| 123 | 9 | 100 | 74 | 24 | 3 | 4.2 | 756 | 4422 | 4.50 |
| Mean | | 100 | 56 | 22 | 2.44 | 4.29 | 627 | 3567 | 2.30 |
| Standard deviation | | - | 10.3 | 4.5 | 0.53 | 0.58 | 227 | 1401 | 1.10 |
| 95 percent confidence limit | | | | | | | | | |
| Low | | 100 | 35 | 13 | 1.4 | 3.1 | 173 | 765 | 0.10 |
| High | | 100 | 77 | 31 | 3.5 | 5.4 | 1081 | 6370 | 4.50 |

Note: 1 mm = 0.039 in; 1 N = 0.225 lbf.

1978-1979 winter. Whereas some producers met the specification requirements (cited earlier), others were either excessive in the 0.075-mm (minus 200) fraction or deficient in residual bitumen content. A laboratory evaluation of these accepted and rejected field mixtures was conducted in 1979. The following tests were conducted:

1. Extraction analysis--Aggregate gradation and residual binder content were determined.
2. Subjective workability test--The mix was cooled to -6.7°C (20°F) and its capability of being broken up readily with a spatula that had a blade length of approximately 203 mm (8 in) was observed. The workability was noted as good, fair, or poor.
3. Penetrometer test--An attempt was made to quantify the workability. The mix was placed in a Marshall mold and compacted at ambient temperatures by using two blows of a Marshall hammer to level the mix and to obtain consistency in packing. A concrete penetrometer (Soil Test CT-421) was used to measure the maximum force required to penetrate the surface. This penetrometer has a range from 0 to 3114 N (0-700 lb) and is graduated in 89-N (20-lbf) increments.
4. Marshall test--After the penetrometer test, the mix was compacted with 50 blows on both sides of the specimen. Since it was not possible to extract the specimen from the mold and test at ambient temperatures without damage, the specimen in the mold was cooled to -6.7°C (20°F), extracted, and tested for Marshall stability and flow at this low temperature.

The mix test data obtained by use of the above procedures are given in Tables 1-3, grouped by subjective workability rating. At the present time, the subjective workability test is the only reliable tool available to evaluate the mix. Figure 4 shows the effect of dust content (minus 200 fraction) and residual bitumen content on the mix workability at -6.7°C. Specification limits for a stone mixture (water absorption less than 1 percent) are shown by dotted lines on this figure and represent a minimum residual bitumen content of 4.5 percent (4.0 percent based on extraction) and a maximum of 2 percent minus 200 fraction (2.4 is rounded off to 2). The effect of the minus 200 fraction on the mix workability (or stiffness) is clearly evident. At dust content levels of 3 and 4 percent, even the increased bitumen content does not appear to help workability. This laboratory evaluation of the mixtures produced in various bituminous concrete plants lends support to the development of the new formulation.

Penetrometer test data (Tables 1-3) indicate a general trend toward higher readings for the mix-

**Table 3. Mix test data: poor workability.**

| Item | District | Gradation (percent passing) | | | | Residue Asphalt (%) | Penetrometer Reading (N) | Marshall Test at -6.7°C | |
|---|---|---|---|---|---|---|---|---|---|
| | | 9.5 mm | 4.75 mm | 2.36 mm | 0.075 mm | | | Stability (N) | Flow (mm) |
| Sample | | | | | | | | | |
| 6441 | 2 | 100 | 56 | 25 | 3 | 4.5 | 712 | 4 225 | 1.88 |
| 6446 | 4 | 100 | 73 | 27 | 4 | 5.4 | 890 | 4 724 | 2.00 |
| 6627 | 2 | 100 | 67 | 24 | 4 | 4.1 | 534 | 5 587 | 1.88 |
| 6768 | 2 | 100 | 54 | 25 | 3 | 3.9 | 1334 | 5 080 | 2.50 |
| 6927 | 9 | 100 | 70 | 22 | 3 | 4.0 | 934 | 8 727 | 2.12 |
| 6932 | 2 | 100 | 58 | 27 | 4 | 4.9 | 1601 | 9 043 | 2.00 |
| 6933 | 2 | 100 | 55 | 27 | 4 | 5.3 | 1112 | 9 768 | 1.75 |
| 6922 | 9 | 100 | 51 | 24 | 3 | 3.5 | 801 | 3 790 | 2.38 |
| Mean | | 100 | 60 | 25 | 3.50 | 4.45 | 988 | 6 370 | 2.05 |
| Standard deviation | | - | 8.3 | 1.8 | 0.53 | 0.69 | 347 | 2 406 | 0.25 |
| 95 percent confidence limit | | | | | | | | | |
| Low | | 100 | 43 | 21 | 2.4 | 3.1 | 294 | 1 557 | 1.55 |
| High | | 100 | 77 | 29 | 4.6 | 5.8 | 1681 | 11 183 | 2.55 |

Note: 1 mm = 0.039 in; 1 N = 0.225 lbf.

**Figure 4. Mix workability at -6.7°C (20°F).**

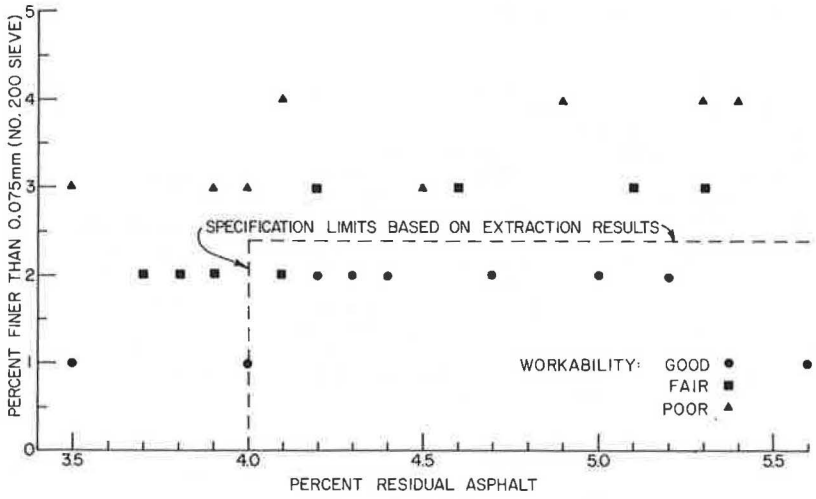


tures as workability decreases. But the data are inconsistent, and this test has failed to quantify the workability parameter. The configuration of aggregate particles at the spot tested seems to obscure the test data. A vane-shear type of device, to measure the maximum torque, is probably more appropriate.

Marshall test data (Tables 1-3) generally indicate higher Marshall stabilities for the mixtures with poor workability. Again, this test is not sensitive enough to evaluate the stockpile patching mixtures. The mixtures with good workability densify readily during the Marshall compaction and thus can also give higher stability values. The mixtures with poor workability can also give higher stability values on account of higher dust content and/or deficient bitumen content.

## FIELD PROBLEMS

The improved formulation was used by six Pennsylvania engineering districts in the 1978-1979 winter and by all 11 engineering districts in the 1979-1980 winter. Mix handling and performance have been generally satisfactory. In some instances, failures were reported, such as partial or complete loss of mix from the pothole and shoving of the mix in the pothole. The following mix characteristics and/or placement techniques are believed to be the probable causes of these failures:

1. Stripping of asphalt binder from the aggregate due to inadequate and/or improper type of anti-stripping agent in the binder;
2. Deficient binder content, which caused the mix to ravel, or excessive binder content, which caused the mix to shove (excessive binder will result at the bottom of the stockpile if the mix has drained);
3. Rounded or subrounded gravel particles (lack of aggregate angularity to provide good interlocking);
4. Excessive use of tack coat;
5. Potholes deeper than 76 mm (3 in) not compacted in layers; and
6. Excessive fines in the mix.

## ACKNOWLEDGMENT

We appreciate the assistance of Kim Truax and Richard Basso, Jr., in the field evaluation and Edward Macko in the laboratory evaluation of the stockpile patching mixtures. The assistance of Karen Ford in typing the manuscript is also appreciated.

This research project was sponsored by PennDOT. The opinions, findings, and conclusions expressed here are ours and are not necessarily those of PennDOT. This paper does not constitute a standard, specification, or regulation.

REFERENCES

1. W. Bortree and D. Mellott. Value Engineering Studies: Bituminous Patching. Pennsylvania Department of Transportation, Harrisburg, Oct. 1976.
2. L. O'Brien. Value Engineering in Pothole Patching. Rural and Urban Roads, Oct. 1976.
3. Bituminous Patching Mixtures. TRB, Synthesis of Highway Practice 64, Sept. 1979.
4. Field Test Evaluation Program: Sylvax UPM. Public Technology, Inc., Washington, DC, 1977.

*Publication of this paper sponsored by Committee on Characteristics of Bituminous Paving Mixtures to Meet Structural Requirements.*

*The Transportation Research Board does not endorse products or manufacturers. Trade and manufacturers' names appear in this paper because they are considered essential to its object.*

# Asphalt Mixtures: Comparative Analysis of Characterization for Design

RANDY B. MACHEMEHL AND THOMAS W. KENNEDY

**Direct relations among manifestations of pavement distress, materials evaluation, and techniques of asphalt mix design are desirable in the design of asphalt mixtures. Static and repeated-load testing, which estimate properties that have direct relations with distress, were used to evaluate asphalt mixtures designed and prepared by using the Texas blackbase design procedure. Three mixtures containing three different aggregate types and a range of asphalt contents were tested and evaluated at three test temperatures. Optimum asphalt contents were determined for various engineering material properties, including tensile strength, fatigue life, static modulus of elasticity, and permanent deformation. The differences between design asphalt contents and the values derived from experimental tests were often quite significant, depending on test temperature and material type. The asphalt contents obtained by the Texas procedure were found to be generally higher than the optimum values identified for distress-related material properties. Optimum asphalt contents for static tensile properties were generally less than those for repeated-load properties.**

The performance of asphalt pavements is frequently characterized by the presence or absence of fracture, distortion, or disintegration. These various distresses may manifest themselves through thermal or shrinkage cracking, fatigue cracking, permanent deformation or rutting, stripping, raveling, or other phenomena (1).

Direct relations among distress, materials evaluation, and mix-design techniques are obviously desirable. This investigation was designed to evaluate testing procedures that produce properties that can be directly related to distress through a comparison with a currently used mix-design procedure. The resulting data and analyses produced, in effect, an evaluation of a typical mix-design procedure that indicates how well this procedure could normally be expected to relate to pavement distress. The procedure was the blackbase mix-design procedure used by the state of Texas (2,3), which includes techniques for selecting the optimum asphalt content for both laboratory and field mixtures of blackbase that have maximum aggregate sizes of 45 mm (1.75 in).

## SELECTED TEST METHODS

The tests selected for this evaluation were the static and repeated-load indirect tensile tests, which are documented elsewhere (4-8) and are currently used by several agencies. Both forms of the indirect tensile test measure the tensile properties of pavement materials that directly relate to the common tensile failure and provide information on tensile strength, modulus of elasticity, and Poisson's ratio for both static and repeated loads, fatigue characteristics, and permanent deformation characteristics of pavement materials.

## EXPERIMENTAL PROGRAM

The basic experimental approach was to compare the engineering properties of blackbase mixtures at various asphalt contents with the properties of mixtures at the design asphalt content obtained by using the current Texas design procedure. The engineering properties were determined at 10°, 24°, and 38°C (50°, 75°, and 100°F). Three asphalt mixtures currently used in the construction of actual pavements by the Texas State Department of Highways and Public Transportation (TSDHPT) were tested by using the static and repeated-load indirect tensile tests and the unconfined compression test.

### Materials

The three basic aggregate combinations used in this investigation were obtained from Eagle Lake, Lubbock, and Lufkin, Texas. Each of these aggregates has been used in pavements and has performed satisfactorily; generally, however, when mixtures that contained these aggregates were tested in unconfined compression by TSDHPT, only the Lubbock mixture satisfied the specified strength requirements.

The Eagle Lake aggregate combination was a mixture of four different aggregates that might generally be described as a smooth, angular, nonporous, crushed river gravel. The asphalt cement mixed with the Eagle Lake aggregate was an AC-20 produced by the Exxon refinery in Baytown, Texas, the same as that used for an actual blackbase construction.

The Lubbock aggregate was a rough, subangular, porous crushed limestone (caliche). The asphalt cement used with this material was an AC-10 produced by the Cosden Oil refinery in Big Spring, Texas.

The Lufkin aggregate was a combination of two pit sands, mixed in equal proportions to obtain the desired gradation. The asphalt cement was an AC-20 produced by the Texaco refinery in Port Neches, Texas.

### Specimen Preparation

All specimens were mixed and compacted according to Texas test method Tex-126-E except that the mixing

was done by using an 11-L (3-gal) capacity Hobart mixer rather than by hand.

The specimens for the confined compression tests were about 200 mm (8 in) in height and 152 mm (6 in) in diameter. The specimens cut for the indirect tensile tests were generally 152 mm in diameter and 84 mm (3.3 in) in height. The specimens used in the repeated-load tests for the Eagle Lake gravel were also 152 mm in diameter but varied from 51 to 102 mm (2-4 in) in height. This variation in height was necessary because of the loading restrictions of the pneumatic repeated-load system.

### Testing Equipment

Three basic types of tests were conducted: the unconfined compression test and the static and repeated-load indirect tensile tests. The basic equipment used for these tests is described below.

The testing equipment for the unconfined compression tests included the Rainhart pressure pycnometer and the Texas gyratory-shear compaction device. The pressure pycnometer was used to subject the specimens to an 8300-kPa (1200-lbf/in²) hydrostatic water pressure at a water temperature of 65°C (150°F) for 15 min before actual testing (9). All unconfined compression tests were conducted by using the Texas gyratory-shear compactor, a testing device that is capable of testing 152-mm diameter specimens and applying compressive loads of approximately 89 kN (20 000 lbf) at an unloaded deformation rate of up to 254 mm/min (10 in/min).

The basic testing apparatus for the static indirect tensile tests was a Material Testing System (MTS) closed-loop electrohydraulic loading system. The vertical deformations were measured by a direct-current (dc) linear variable differential transducer (LVDT). Horizontal deformations were measured by two cantilevered arms wired with strain gages. The load-horizontal and load-vertical deformations were recorded on a pair of X-Y plotters: Hewlett-Packard models 7001A and 7000AR.

For the repeated-load tests, two loading systems were used: the MTS electrohydraulic loading system described above and a pneumatic system. The pneumatic system was driven by a source pressure of 620 kPa (90 lbf/in²), and the load was controlled by a regulator. The load was transferred to the specimen by means of a diaphragm-type air piston characterized by low frictional losses. The horizontal and vertical deformations were measured by dc LVDTs and recorded on the Hewlett-Packard X-Y plotters.

## TESTING PROCEDURE

### Unconfined Compression Tests

After compaction, the specimens were cured overnight at 60°C (140°F). The specimens were then pressure-wetted by being subjected to hydrostatic water pressure of 8300 kPa (1200 lbf/in²) at 65°C (150°) for 15 min (9).

Immediately after pressure wetting, the specimens were tested in unconfined compression. Duplicate specimens were tested at two different deformation rates: a fast rate of 245 mm/min (10 in/min) and a slow rate of 3.8 mm/min (0.15 in/min). The maximum load attained was recorded and used to calculate the unconfined compressive strength. These strength values were then compared with specifications (3) to determine whether the mixture was satisfactory.

### Indirect Tensile Tests

A preload of 90 N (20 lbf), which produced a tensile stress of approximately 4 kPa (0.6 lbf/in²), was applied to the specimens to prevent an impact loading and to minimize the effect of seating the loading strip. The specimens were then loaded at a constant deformation rate of 51 mm/min (2 in/min). In the repeated-load tests, the repeated load was applied at a frequency of 1 cycle/s (1 Hz) and a duration of 0.4 s, and there was a 0.6-s rest period. The relations for load-vertical and load-horizontal deformation were recorded by a pair of X-Y plotters. The tensile strength was calculated by using the ultimate load carried by the specimen.

## EXPERIMENTAL DESIGN

A factorial design was not used; rather, the various cells were selectively chosen so that optimum asphalt contents for the selected engineering properties could be found by using a minimum number of specimens. These tests were performed at 10°, 24°, and 38°C (50°, 75°, and 100°F) in controlled-environment chambers and at two stress levels that would produce reasonable fatigue lives for the repeated-load tests.

## ANALYSIS AND DISCUSSION OF TEST RESULTS

A laboratory design asphalt content, or an asphalt void ratio (AVR) design value, was determined for each material from the relations between asphalt content and total air voids (see Figure 1), which were calculated by using an in-mold AVR density and zero-air-void density. The asphalt contents determined by using this procedure were 4.5, 6.8, and 7.5 percent for the Eagle Lake gravel, Lubbock limestone, and Lufkin sand, respectively.

### Density

The AVR densities were generally greater than the densities obtained for specimens cut from the top and bottom of the compacted specimen. This can be explained by the fact that the AVR densities were determined while the specimens were confined in the mold and subjected to a compressive stress of 3450 kPa (500 lbf/in²) (3), whereas the densities for the top and bottom specimens were determined after the large compacted specimens had been removed from the mold, sawed, and measured in an unconfined state.

The optimum asphalt contents for maximum in-mold AVR density were 4.9, 7.6, and 7.5 percent for the Eagle Lake, Lubbock, and Lufkin mixtures, respectively. These asphalt contents are greater than or equal to the laboratory AVR design values. However, the optimum asphalt contents for maximum density for the top and bottom specimens were less than those for maximum in-mold AVR density, which indicates that the optimum for maximum density depended on both the technique and the portion of the specimen used to estimate density.

### Unconfined Compression Tests

Unconfined compression tests were performed on specimens at or near the AVR design asphalt content for both the fast and slow rates of deformation. None of the three mixtures satisfied the specification for unconfined compressive strength (3). The unconfined compressive strengths for the Eagle Lake gravel mixture were far below the minimum strength requirements for the poorest grade of blackbase at both the fast and slow speeds. The Lubbock limestone mixture exceeded the strength requirements at the slow speed but failed to meet the strength requirements at the fast speed. However, the unconfined compression previously conducted by TSDHPT indicated that the laboratory mixture satisfied the

Figure 1. Relation between asphalt content and total air voids.

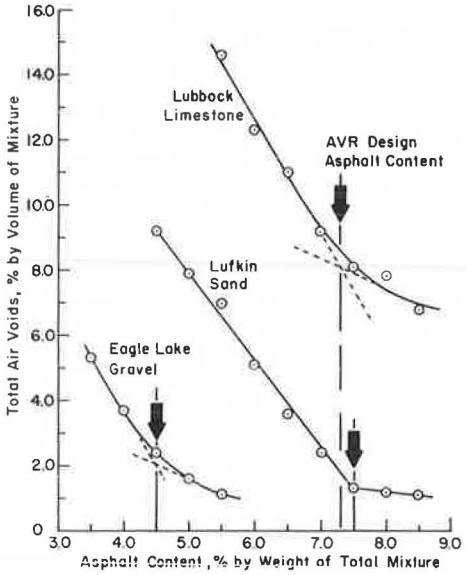


Figure 2. Effect of asphalt content and temperature on tensile strength.

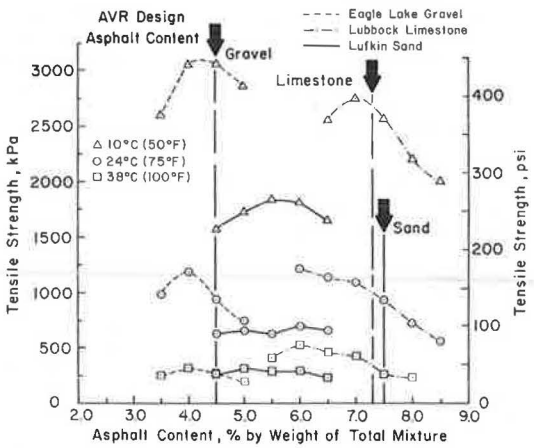


Figure 3. Effect of asphalt content and temperature on static modulus of elasticity.

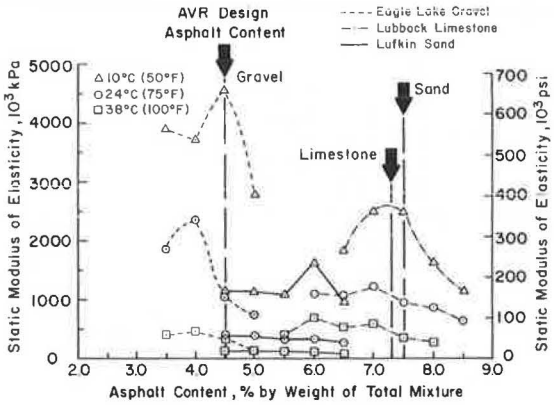


specified strength requirements for both speeds. It should be noted that the gradations of the laboratory and plant mixtures for the Lubbock limestone were significantly different. Since this investigation involved mixtures with the gradation of the plant mixture, differences in unconfined compressive strengths were expected.

Finally, the Lufkin sand mixture failed to satisfy the minimum strength requirements for the poorest grade of blackbase at the fast loading rate. The unconfined compressive strength at the fast loading rate was much less than the required strength. In addition, at the design asphalt content the slow-speed strengths failed to meet minimum strength requirements; however, the strengths were satisfactory for a small range of asphalt contents that were less than the AVR design optimum asphalt content, which indicates that a more satisfactory mixture might result at lower asphalt contents. It should be noted that the pressure pycnometer, which was used to saturate the specimens, severely damaged the specimens that contained Lufkin sand.

In conclusion, all mixtures failed to satisfy at least one of the standards for minimum unconfined compressive strength. Nevertheless, all mixtures have provided satisfactory pavement performance.

## Static Indirect Tensile Tests

Two engineering properties, tensile strength and static modulus of elasticity, were estimated by using the static indirect tensile test. The ultimate tensile strength and static modulus of elasticity for individual specimens were computed along with the values of Poisson's ratio.

For the range of temperatures studied, the optimum asphalt content for ultimate tensile strength increased slightly with a decreasing temperature for all three mixtures (see Figure 2), a result that agrees with previous findings (5-7,10).

The optimum asphalt contents for ultimate tensile strength for all mixtures and temperatures were from 0.2 to 2.5 percentage points less than the AVR design asphalt content, depending on the material and temperature. For the Eagle Lake and Lubbock mixtures, the optimum asphalt contents for tensile strength were from about 0.2 to 1.1 percentage points less than the AVR design values. For the Lufkin sand mixture alone, the optimums ranged from 1.5 to 2.5 percentage points less than the AVR design asphalt content.

The maximum tensile strengths for the Eagle Lake gravel mixture were from about 0 to 25 percent greater than the tensile strength at the laboratory AVR value; for the Lubbock limestone mixture, the maximum tensile strengths were from about 0 to 50 percent greater than the value at the AVR design value; for the Lufkin sand mixture, depending on the temperature, the estimated maximum tensile strengths were from 100 to 200 percent greater than the estimated values at the AVR design value of 7.5 percent. From the relations between asphalt content and ultimate tensile strength, it was found that at higher temperatures (lower strengths) the effects of asphalt content were small. At the higher temperatures the tensile strengths were essentially independent of asphalt content, whereas at lower temperatures (higher strengths) the asphalt content had a substantial effect on tensile strength.

Optimum asphalt contents for maximum static modulus of elasticity existed for all mixtures and temperatures (see Figure 3). At 24° and 38°C (75° and 100°F), however, the optimums for the Lufkin sand mixture were poorly defined. The optimum asphalt contents for the Eagle Lake gravel mixture ranged from 3.9 percent at 24°C to 4.4 percent at 10°C (50°F). For the Lubbock limestone mixture, the optimums ranged from 6.2 percent at 38°C to 7.2

Figure 4. Effect of stress difference on fatigue life at 24°C (75°F).

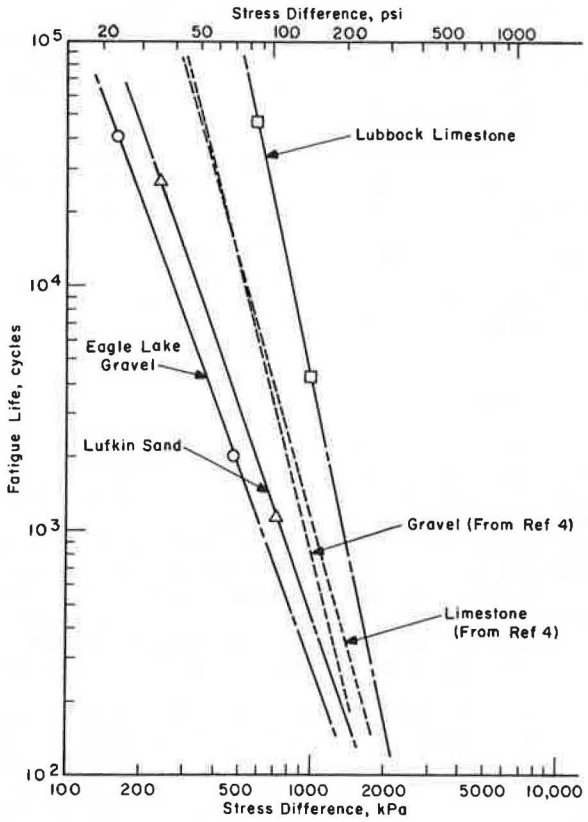


Figure 5. Effect of asphalt content and temperature on fatigue life.

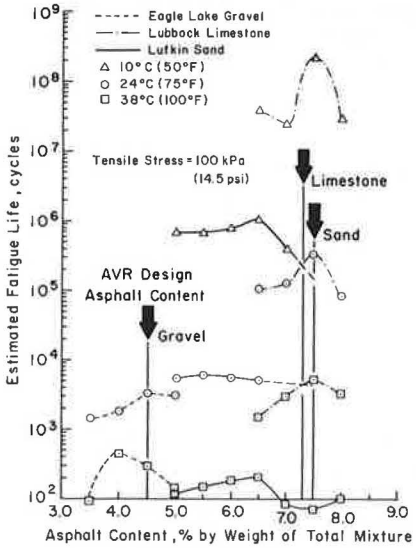


percent at 10°C. The optimum asphalt contents for the Lufkin sand mixture ranged from a poorly defined value of about 4.8 percent at 24°C to 6.0 percent at 10°C.

The optimum asphalt contents for maximum static modulus of elasticity for all mixtures and temperatures were less than the AVR design asphalt contents by as much as 0.1-2.7 percentage points, depending on the mixture and test temperature. The optimums for static modulus of elasticity for the Eagle Lake and Lubbock mixtures were 0.1-1.1 percentage points less than the laboratory AVR design value. For the Lufkin sand mixture alone, the optimums were 1.5-2.7 percentage points less than the AVR design value.

As a result of these differences, the maximum static modulus of elasticity for the Eagle Lake gravel mixture ranged from about 15 to 125 percent greater than the value at the AVR design asphalt content. For the Lubbock limestone mixture, the value of maximum static modulus of elasticity did not exceed the value at the AVR design value by more than 25 percent. Although the static modulus of elasticity was not obtained at the AVR value for the Lufkin sand mixture, it can be seen from Figure 3 that, depending on the temperature, the maximum values of static modulus of elasticity are probably significantly greater than the values at the AVR design value.

## Repeated-Load Indirect Tensile Tests

Repeated-load indirect tensile tests were conducted to evaluate the fatigue life, resilient modulus of elasticity, and resistance to permanent deformation of the materials being studied.

### Fatigue Life

The relation between stress difference and fatigue life for each material at 24°C (75°F) is shown in Figure 4. Stress difference was assumed to be equal to approximately four times the applied tensile stress (8). The two data points for each material indicated in Figure 4 represent the average values of maximum fatigue life at the respective stress actually applied to the specimen. Since the relation has been shown to be linear in previous studies (5,11-14), it was assumed to be linear for these materials.

From Figure 4, it can be seen that the Lubbock limestone mixture has the greatest resistance to fatigue, followed by the Lufkin sand and the Eagle Lake gravel mixtures. Also shown as having similar relations are a gravel and limestone of the same gradation, which were reported by Adedimila and Kennedy (5). Relations between fatigue life and asphalt content were developed for each material to study the effects of temperature and asphalt content. By using Figure 4, the applied stress, or stress difference, was normalized to eliminate the effect of differences in applied stress for each material. The estimated fatigue life for any set of conditions was determined at a stress difference of 400 kPa (58 lbf/in²) or a tensile stress of 100 kPa (14.5 lbf/in²) by assuming a linear relation between stress difference and fatigue life. This value was chosen to evaluate the effect of temperature and asphalt content because it minimized the need to extrapolate the relations between fatigue life and stress. The resulting relations are shown in Figure 5.

Correlation analyses were also made to determine the relations between actual fatigue life and both the initial tensile strain and the applied stress-strength ratio. These relations have been used by other investigators (5,7,11,12,15) to estimate the fatigue life of asphalt mixtures and would have decreased the amount of testing required to obtain fatigue-life estimates. The resulting correlations, however, were found to have very low coefficients of determination and therefore were of limited value.

An optimum asphalt content for maximum fatigue life that was consistent with previous findings (5,11,15-18) was found for all three mixtures and all test conditions studied. Depending on the temperature, the optimum asphalt content for maximum

fatigue life of the Eagle Lake gravel ranged from 4.0 to 4.6 percent, which is from 0.1 percentage point greater to 0.5 percentage point less than the AVR design asphalt content. For the Lubbock limestone mixture, the optimum asphalt content was 7.5 percent, regardless of temperature, which was approximately 0.2 percentage point greater than the AVR design value. However, for the Lufkin sand mixture, the optimum ranged from about 5.5 to 6.5 percent, which is 1.0-2.0 percentage points less than the AVR design value.

Thus, the optimum asphalt content for fatigue life tended to be less than the AVR design asphalt content for the Lufkin sand mixture. Because of these differences, the maximum fatigue life for the Eagle Lake gravel mixture was as much as 60 percent greater than the fatigue life at the AVR design value, depending on the temperature. For the Lubbock limestone mixture, the values of maximum fatigue life were 15-500 percent greater than the fatigue life at the AVR design value, the larger differences occurring at the lower temperatures. In addition, the percentage difference between maximum fatigue life and the value at the AVR value for the Lubbock limestone mixture increased with decreasing temperature. For the Lufkin sand mixture, fatigue lives were not available at the AVR value except at 38°C (100°F). For this condition, the maximum fatigue life was about 150 percent greater than the fatigue life at the AVR value. However, by estimating maximum fatigue life at 24°C (75°F) and 10°C (50°F), it can be seen that the maximum fatigue life could be anywhere from 150 to 1000 percent greater than the value at the AVR design asphalt content.

### Resilient Modulus of Elasticity

Although an optimum asphalt content for maximum resilient modulus of elasticity was evident for most of the mixtures studied, the actual value was not well defined, which indicated that this range of asphalt content did not have a substantial effect on resilient modulus. This agrees with the findings of other investigators (1,5,19).

The optimum asphalt contents for the Eagle Lake gravel mixture occurred only at 10° and 38°C (50° and 100°C) and were 4.2 and 4.4 percent, respectively. For the Lubbock limestone mixture the optimum asphalt contents ranged from 7.1 percent at 24°C (75°F) to about 7.3 percent at 10°C (50°F), and for the Lufkin sand the range was from 5.7 percent at 38°C (100°F) to 6.0 percent at 24°C (75°F).

The optimum asphalt contents for maximum resilient modulus of elasticity ranged from 0 to 1.8 percentage points less than the laboratory AVR design value. However, for the Eagle Lake and Lubbock mixtures combined, the range of optimum asphalt contents was 0-0.3 percentage point less than the AVR value. For the Lufkin sand mixture, the range was 1.5-1.8 percentage points less than the AVR value.

### Permanent Deformation

The analysis of permanent deformation was limited, since normalization of the applied stress was different for the various mixtures and test conditions. Since the relation between permanent deformation and applied stress is not well established, it was not possible to obtain information on permanent deformation for the same stress conditions. Therefore, the analysis primarily involved comparing the optimum asphalt contents for maximum resistance to permanent deformation with the AVR design asphalt content.

Although no definite trends were observed, it was found that temperature and stress level both influenced the optimum asphalt content. In addition, it appeared that asphalt content affected permanent deformation more at high temperatures than at low temperatures.

### Comparison of Optimum Asphalt Contents

Test results indicated that optimum asphalt contents existed for various engineering properties--i.e., indirect tensile strength, static modulus of elasticity, fatigue life, minimum permanent deformation,

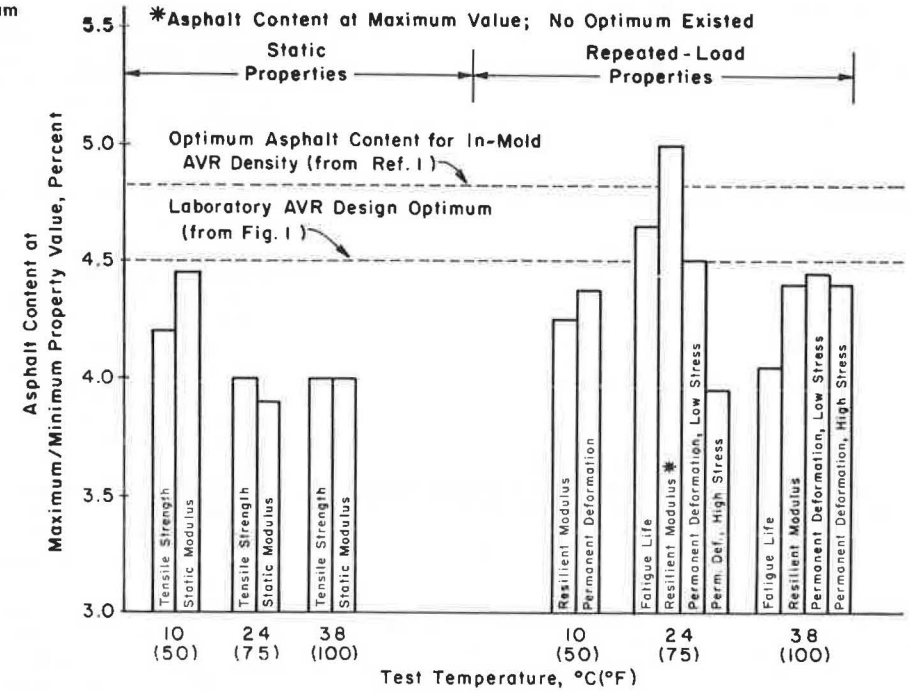


**Figure 6. Testing temperature versus optimum asphalt content for engineering properties of Eagle Lake gravel mixtures.**

and, to a certain extent, resilient modulus of elasticity. These optimums were different, however, and in addition were not the same as the AVR design asphalt content or the optimum for in-mold AVR density.

The relations between optimum asphalt content and test temperature for the properties are shown in Figures 6-8 for the Eagle Lake, Lubbock, and Lufkin mixtures, respectively. For comparison, the laboratory AVR design asphalt content and the optimum asphalt content for maximum in-mold AVR density are also shown.

Several general trends were observed in all three materials:

1. The selected AVR design value was approximately 0.3 percentage point less than the optimum for maximum in-mold AVR density except for the Lufkin sand mixture, for which the two optimums were equal.
2. Except for tests at 24°C (75°F) for the Eagle Lake gravel mixture and fatigue tests for the Lubbock limestone mixture, the optimum asphalt contents for all properties were less than the AVR design value.
3. The optimums for the static properties were less than those for the repeated-load properties. The optimum asphalt contents for static tensile properties of the Eagle Lake gravel and Lubbock limestone mixtures were 0.1-1.2 percentage points less than the AVR design asphalt content. The optimums for the Lufkin sand mixture were 1.5-2.7 percentage points less than the AVR design value.
4. The optimum asphalt contents for static modulus of elasticity were the smallest of the optimums identified.

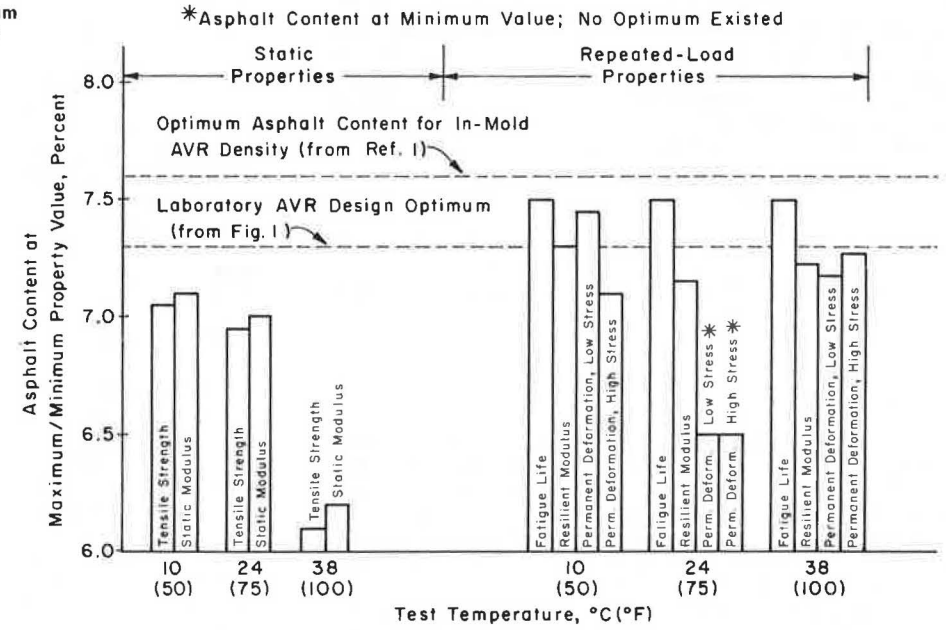


Figure 7. Testing temperature versus optimum asphalt content for engineering properties of Lubbock limestone mixtures.

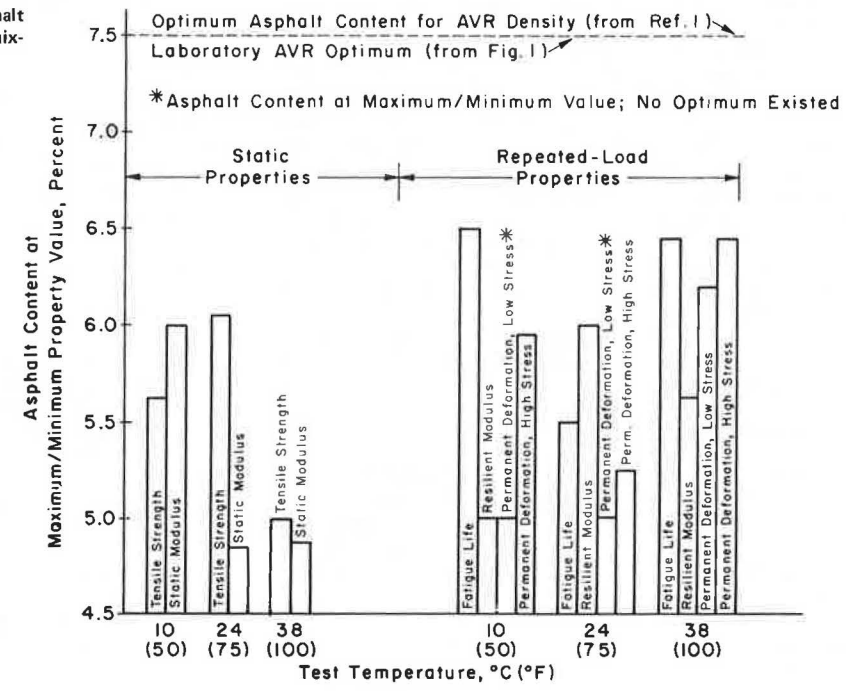


Figure 8. Testing temperature versus optimum asphalt content for engineering properties of Lufkin sand mixtures.

5. The optimum asphalt contents for tensile strength occurred at slightly richer asphalt contents at 24° and 38°C (75° and 100°F) than did the optimums for static modulus of elasticity.

6. The optimum asphalt contents for fatigue life were generally larger than the optimums for the other material properties studied, although this trend was not as strong in the Eagle Lake gravel mixture as in the other mixtures.

7. The optimum asphalt contents for resistance to permanent deformation and instantaneous resilient modulus of elasticity were generally greater than the optimums for static properties but less than the optimums for fatigue life.

From the preceding discussion and from Figures 6-8, it was concluded that the optimum asphalt content for static and repeated-load properties was generally less than the optimum asphalt content obtained by using the Texas design procedure. These test results indicate that, in terms of the engineering properties considered, optimum performance might occur at asphalt contents less than the design asphalt content. However, the adverse effect of moisture on the performance of an asphalt mixture that contains these lower asphalt contents was not considered in this investigation.

## CONCLUSIONS AND RECOMMENDATIONS

Within the limits of load, asphalt content, mixture, and temperature variables considered in this study, the following conclusions and recommendations are made.

### Conclusions

#### General

1. The design asphalt contents generally were higher than the optimum asphalt contents for the distress-related material properties of tensile strength, static modulus of elasticity, resilient modulus, fatigue life, and permanent deformation characteristics as measured by using the static and repeated-load indirect tensile test.

2. Optimum asphalt contents were determined for tensile strength, static modulus of elasticity, fatigue life, and permanent deformation. Well-defined optimums did not consistently occur for resilient modulus except at low temperatures.

3. Generally, the optimum asphalt contents for static tensile properties were less than the optimums for the repeated-load properties. The optimum for static modulus of elasticity was generally less than the optimum for tensile strength. The optimum for fatigue life was larger than the optimums for the other engineering properties. The optimums for permanent deformation and instantaneous resilient modulus of elasticity were generally less than the optimum for fatigue life and larger than the optimum for static tensile properties.

4. The static and repeated-load indirect tensile tests can be used to evaluate materials for mix-design purposes.

#### Static Characteristics

1. Asphalt content was very important with respect to tensile strength and static modulus of elasticity at low temperatures. The effect of asphalt content on tensile strength and static modulus of elasticity was not as important at higher temperatures.

2. The optimum asphalt contents for tensile strength and static modulus of elasticity increased as temperature decreased.

#### Repeated-Load Characteristics

1. Resilient modulus of elasticity also showed a reduced effect of asphalt content at higher temperatures, but the effect was smaller than that for tensile strength or static modulus of elasticity.

2. In general, the effect of asphalt content on resilient modulus of elasticity was small.

3. For the Lubbock limestone mixture, the optimum asphalt content for maximum fatigue life was essentially independent of temperature. For the Lufkin sand mixture, temperature did have an effect on the optimum for maximum fatigue life; the optimum at 24°C (75°F) was lower than the optimums at the other temperatures.

4. It was found that the rate of increase in permanent deformation was slightly greater wet of optimum asphalt content than dry or at optimum. All other properties were essentially the same wet and dry of optimum.

### Recommendations

1. It is recommended that static indirect tensile tests be performed on all blackbase mixtures as part of the current mix-design procedure used in Texas. If possible, repeated-load indirect tensile tests should also be conducted.

2. When possible, static and repeated-load indirect tensile tests should be performed on molded specimens of field mixtures. Ideally, specimens should be prepared at the plant to avoid reheating the mixture.

## ACKNOWLEDGMENT

The work presented in this paper is drawn from the eleventh in a series of reports dealing with the findings of a research project concerning tensile and elastic characteristics of highway pavement material. The work was sponsored by TSDHPT and the Federal Highway Administration (FHWA), and their support is gratefully acknowledged. Many individuals offered assistance, and their contributions are gratefully acknowledged. Special appreciation is due to David B. Peters, James N. Anagnos, and Pat Hardeman for their assistance in developing the testing program. Special thanks is also extended to Frank E. Herbert, Gerald Peck, and Robert E. Long of TSDHPT, who provided technical liaison and support for the project.

The contents of this paper reflect our views, and we are responsible for the facts and the accuracy of the data presented. The contents do not necessarily reflect the official views or policies of FHWA. This report does not constitute a standard, specification, or regulation.

## REFERENCES

1. D.B. Peters and T.W. Kennedy. An Evaluation of the Texas Blackbase Mix Design Procedure Using the Indirect Tensile Test. Center for Highway Research, Univ. of Texas at Austin, Res. Rept. 183-11, March 1979.
2. C. McDowell and A.W. Smith. Design, Control, and Interpretation of Tests for Bituminous Hot Mix Black Base Mixtures. Materials and Tests Division, Texas State Department of Highways and Public Transportation, Austin, Rept. TP8-71E, 1971.
3. Manual of Testing Procedures: Test Method 126-E. Texas State Department of Highways and Public Transportation, Austin, Jan. 1, 1974.
4. J.N. Anagnos and T.W. Kennedy. Practical Method of Conducting the Indirect Tensile

Test. Center for Highway Research, Univ. of Texas at Austin, Res. Rept. 98-10, 1971.
5. A.S. Adedimila and T.W. Kennedy. Fatigue and Resilient Characteristics of Asphalt Mixtures by Repeated-Load Indirect Tensile Test. Center for Highway Research, Univ. of Texas at Austin, Res. Rept. 183-5, 1975.
6. W.O. Hadley, T.W. Kennedy, and W.R. Hudson. A Method of Estimating Tensile Properties of Materials Tested in Indirect Tension. Center for Highway Research, Univ. of Texas at Austin, Res. Rept. 98-7, July 1970.
7. R.K. Moore and T.W. Kennedy. Tensile Behavior of Subbase Materials Under Repetitive Loading. Center for Highway Research, Univ. of Texas at Austin, Res. Rept. 98-12, Oct. 1971.
8. T.W. Kennedy and J.A. Anagnos. Procedures for Conducting the Static and Repeated-Load Indirect Tensile Tests. Center for Transportation Research, Univ. of Texas at Austin, Res. Rept. 183-14 (in preparation).
9. Manual of Testing Procedures: Test Method Tex-109-E. Texas State Department of Highways and Public Transportation, Austin, Jan. 1, 1978.
10. T.W. Kennedy and R.K. Moore. Tensile Behavior of Asphalt-Treated Materials Under Repetitive Loading. Proc., 3rd International Conference on Structural Design of Asphalt Pavements, London, England, Vol. 1, Jan. 1972.
11. J.A. Epps and C.L. Monismith. Influence of Mixture Variables on the Flexural Fatigue Properties of Asphalt Concrete. Proc., AAPT, Vol. 38, 1969, pp. 423-464.
12. P.S. Pell. Fatigue Characteristics of Bitumen and Bituminous Mixes. Proc., 1st International Conference on Structural Design of Asphalt Pavements, Univ. of Michigan, Ann Arbor, Aug. 1962.
13. J.A. Deacon. Fatigue of Asphalt Concrete. Transportation Engineering Division, Univ. of California, Berkeley, Ph.D. dissertation, 1965.
14. J. McElvaney. Fatigue of a Bituminous Mixture Under Compound Loading. Univ. of Nottingham, Nottingham, England, Ph.D. thesis, 1972.
15. C.L. Monismith, J.A. Epps, and D.A. Kasianchuk. Asphalt Mixture Behavior in Repeated Flexure. Institute of Transportation and Traffic Engineering, Univ. of California, Berkeley, Rept. TE 68-8, 1968.
16. R.A. Jimenez. Fatigue Testing of Asphaltic Concrete Slabs. ASTM, Philadelphia, Special Tech. Publ. 508, 1971, pp. 3-17.
17. R.A. Jimenez and B.M. Gallaway. Behavior of Asphaltic Concrete Diaphragms to Repetitive Loadings. Proc., 1st International Conference on Structural Design of Asphalt Pavements, Univ. of Michigan, Ann Arbor, Aug. 1962.
18. P.A. Pell. Fatigue of Asphalt Pavement Mixes. Proc., 2nd International Conference on Structural Design of Asphalt Pavements, Univ. of Michigan, Ann Arbor, Aug. 1967.
19. R.J. Schmidt. A Practical Method for Measuring the Resilient Modulus of Asphalt-Treated Mixes. HRB, Highway Research Record 404, 1972, pp. 22-32.

*Publication of this paper sponsored by Committee on Characteristics of Bituminous Paving Mixtures to Meet Structural Requirements.*

# Characteristics and Performance of Asphalt-Rubber Material Containing a Blend of Reclaim and Crumb Rubber

B.J. HUFF AND B.A. VALLERGA

**Asphalt cement, rubber extender oil, and a mixture of ground reclaim and crumb rubber, blended together at an elevated temperature in specific proportions and sequences, form a tough, durable, and adhesive membrane when hot-spray-applied to a surface and allowed to cool to ambient temperatures. This cast-in-place asphalt-rubber membrane has been found to be suitable for use in the construction of surface treatments for existing pavements (chip seals), stress-absorbing membrane interlayers (SAMIs) in the placing of asphalt concrete overlays, and waterproofing membranes for bridge decks and hydraulic linings (ponds, canals, and reservoirs). When hot-poured into pavement joints and cracks and allowed to cool, it also serves as an effective joint and crack filler. The concepts and proportions of the formulation and preparation of this material are presented together with information and data on its properties and applications. A discussion is presented of the results of two analytic studies on the applicability of asphalt-rubber membranes (a) in minimizing reflection cracking when used as a SAMI and (b) in producing a "multilayered aggregate structure" when used as a single-pass chip seal. A summary of the field performance observed to date on a number of installations of the asphalt-rubber material in its various applications is also included, together with observations on the efficacy of the material as a membrane and as a filler.**

Many attempts have been made to impart the desirable elastic and resilient properties of rubber to asphalt. The earliest of these involved the use of natural rubber and were relatively successful. However, because of the rapid buildup in viscosity of the blend as the percentage of rubber was increased, one could use only small percentages and still maintain a workable material. Obviously, this limited the benefit that could be added by the rubber.

In addition, the virgin polymers were susceptible to oxidation by the elements, and their beneficial properties dissipated rather rapidly with time. Their instability in relation to heat also created problems with their use. Overheating converted the rubber to an oil, which only served to soften the asphalt. This severely limited the production of the rubberized asphalt to jacketed kettles or as a latex in asphalt emulsions.

With the advent of synthetic rubber, the same exercises were repeated with essentially the same results. The synthetic rubber was somewhat cheaper than the natural rubber, but it also lacked some of the elasticity and tackiness of the natural rubber.

As the use of rubber increased, the growing pile of scrap tires was eyed as a cheap source of rubber for preparing rubberized asphalt. Early experiments showed that these tires could be ground and mixed with hot asphalt in large percentages to produce a material that had properties superior to those of the base asphalt. Since the rubber in these tires

was synthetically compounded and vulcanized to resist heat and weathering, the problems encountered with the virgin polymers were eliminated.

The synthetic vulcanized rubber, however, lacked the solubility of the virgin polymers. The only solubility observed was a drawing of the oils out of the asphalt by the rubber to produce swollen rubber particles with gellike surfaces. With time, this swelling would progress to the point that the swollen rubber particles would knit together within the asphalt matrix to form an asphalt-rubber sheet that was more resistant to the stresses that produce fracture in pavements than the asphalt itself.

This was a simple way to improve the asphalt, but it was not without its shortcomings. The drawing of the oils into the rubber particle adversely affected the cohesive and adhesive properties of the asphalt phase, thereby reducing its ability to bond to pavement surfaces or to bind together aggregate particles. The loss in bond strength, which occurred primarily in the early stages of service on the road when the rubber-asphalt matrix was being formed, could be counteracted to some degree by the use of a very soft asphalt rich in oils, but the resulting blend would remain somewhat soft and tender.

In addition, it was found that large quantities of rubber (in excess of 20 percent) were required to produce the desired effect--i.e., to form a matrix (1). The resulting mass had a viscosity much too high for most conventional asphalt applications. To counter this problem, kerosene was added and the material was applied as a cutback. This was quite successful but did create some problems with tenderness before curing and, for the most part, limited the use of the material to chip seals.

As this development was taking place, experiments were in progress to combine a reclaim scrap rubber, generally referred to as "devulcanized", with asphalt. This devulcanized scrap rubber is produced by a process of treating vulcanized scrap rubber with heat and oils, which, in effect, replasticizes it and makes it more soluble in asphalt. It offered advantages over the vulcanized scrap rubber in that it dispersed and dissolved in the asphalt to a greater degree and improved the binder properties (i.e., cohesion and adhesion) of the asphalt. Because of the greater dispersion, less rubber is required, which eliminates the need for solvents. Although it had some advantages, the devulcanized asphalt-rubber blends appeared to lack some of the toughness and resilience ultimately achieved with the vulcanized asphalt-rubber blends.

The "drying-up" effect previously noted with the vulcanized rubber was investigated, and it was found that asphalts that were low in aromatic oils had low-solubility effects on rubber and produced an asphalt-rubber that had poor adhesive properties (2). In going back to earlier work, it was realized that natural rubber contributed greater elasticity and adhesion to asphalt than did synthetic rubber. However, since the use of the virgin polymer still remained undesirable because of its instability and cost, vulcanized natural rubber available in certain scrap rubbers, especially those from truck tires, was tried and found to be highly suitable. When this high-natural-rubber scrap is added to hot asphalt, it is reconverted to the sticky, elastic material. Since the rubber is vulcanized, this conversion proceeds more slowly and thus allows for a greater heat stability than if the virgin polymer were used.

In addition to the rubberlike properties contributed by the scrap rubber, there are valuable components in this compound that are often overlooked but might well contribute to the improvement of the asphalt. Examples of these are the following:

1. Carbon black--Scrap rubber contains more than 20 percent carbon black, an element that has been shown to add reinforcing properties to asphalt (3,4).
2. Antioxidants--For the tire to survive weathering, it is necessary that antioxidants be added to the rubber compound. It is believed that these chemicals contribute an additional measure of durability to the asphalt-rubber.
3. Amines--Although they are added to the rubber compounds for other reasons, particularly during the devulcanizing process, amines are closely related to the antistrip compounds and current laboratory studies indicate that they do aid in resistance to stripping.
4. Aromatic oils--Aromatic oils are the same oils that are used in recycling to rejuvenate the old asphalt and in emulsion form to restore oxidized asphalt pavements. By their presence, these oils will prolong the life of the asphalt-rubber material.

By using the foregoing knowledge of the behavior of combinations of various types of ground rubber and asphalt based on both laboratory and field experiments and observations, a formulation of asphalt, extender oil, and scrap rubber was developed that produced an asphalt-rubber material found to be particularly useful in forming a tough, durable, and adhesive membrane when hot-sprayed or hot-poured and allowed to cool. As a hot-spray application, it is suitable for use in the construction of surface treatments for existing pavements (chip seals), stress-absorbing-membrane interlayers (SAMIs) in the placing of asphalt concrete overlays, and waterproofing membranes for bridge decks and for hydraulic linings in ponds, canals, and reservoirs. As a hot-pour application, it serves as an effective joint and crack filler.

## COMPOSITION OF ASPHALT-RUBBER MATERIAL

The asphalt-rubber material used in the work described in this paper is the product ARM-R-SHIELD produced by Arizona Refining Company. The product is designed to combine the desired properties of the various types of rubbers and react this rubber blend with an asphalt that has been modified with extender oil to improve its quality and its compatibility with the rubber. The ARM-R-SHIELD material is described in detail in U.S. Patent 4,068,023 (5).

The asphalt proposed for use is tested first to determine its compatibility with rubber, which is an indicator of its relative aromatic content. If the asphalt appears to be deficient in aromatic oil, a small amount (2-6 percent) of a highly aromatic rubber extender oil (lube extract) is blended with the asphalt. The modified asphalt is then mixed at 350°-400°F with 20 ± 2 percent of a blend of rubber that contains 40 percent powdered devulcanized rubber and 60 percent powdered vulcanized rubber high in natural rubber (30 percent minimum). By this process, the flexibility and solubility of the devulcanized rubber, the elasticity, toughness, and adhesion of the natural rubber, and the resilience of the insoluble synthetic rubber are incorporated into the asphalt-rubber blend.

Figure 1 shows schematically the composition and formulation of the asphalt-rubber material. The combining of the ingredients and the mixing at elevated temperature are straightforward and can be done readily by a batching process in any tank in which adequate provision is made for (a) mixing by recirculation, stirring, air agitation, or other appropriate means; and (b) heating by appropriate heat-exchanging and temperature-control devices. A conventional distributor truck can serve this purpose if care has been taken to maintain it in good

**Figure 1. Composition of asphalt-rubber-membrane system.**

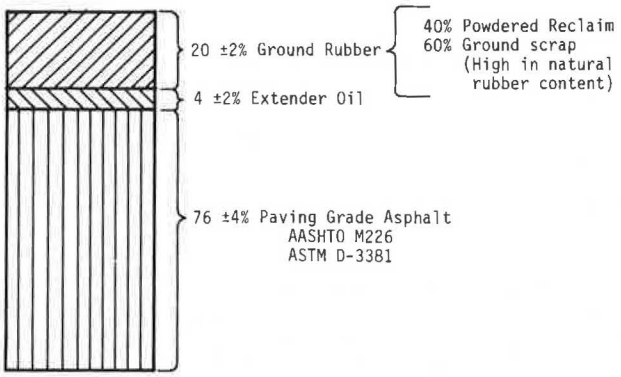


**Table 1. Consistency-temperature characteristics of asphalt-rubber material compared with base asphalt.**

| Property | Test Method | AR-4000 Asphalt | Asphalt-Rubber Material[a] |
|---|---|---|---|
| Penetration | ASTM D-4 | | |
| 39.2° F | | 9 | 17 |
| 77.0° F | | 76 | 101 |
| Softening point (ring and ball) (° F) | ASTM D-36 | 120 | 132 |
| Dynamic viscosity at 140° F (poises) | ASTM D-2171 | 1800 | 7580 |
| Kinematic viscosity (cSt) | Brookfield | | |
| 165° F | | – | 165 000 |
| 170° F | | 45 600 | – |
| 190° F | | 6 200 | – |
| 212° F | | 1 984 | – |
| 230° F | | 860 | – |
| 250° F | | 450 | – |
| 265° F | | – | 3 400 |
| 277° F | | 194 | – |
| 310° F | | 82 | – |
| 330° F | | 58 | – |
| 350° F | | 42 | 912 |
| 400° F | | – | 720 |

[a]Contains 78.4 percent AR-4000 asphalt, 1.6 percent extender oil, and 20 percent rubber blend.

operating condition and the heating system can be adequately controlled.

## CHEMICAL AND PHYSICAL PROPERTIES

Determining the chemical properties of a blend of asphalt, extender oil, and ground rubber particles is extremely difficult. Most of the conventional tests are not readily adaptable to the material. Research is currently under way at several government and private laboratories, and it is expected that progress will be reported in the literature in due course.

From the standpoint of chemical properties, composition can be analyzed and the solubility characteristics of the separate ingredients can be measured (6, ASTM D-297, and ASTM D-2007). However, once the ingredients are combined and formed into a product, the interactions among the asphalt, extender oil, and rubber particles are complex and dependent on both time and temperature. Moreover, a method of determining the chemical state of the blend is not available. For example, the fraction of rubber dissolved into the asphalt at any time would seem to be a significant factor, but reliable laboratory procedures and techniques for making this determination are not yet available.

From the standpoint of physical properties, the situation is more favorable although by no means satisfactory. The main physical properties of interest and applicability are consistency, durability, and adhesion. With appropriate modifications to account for the small particles of rubber dispersed in the asphalt, the various viscosity-measuring devices can be used as well as various tests for bonding and resistance to weathering.

### Consistency

Table 1 gives data on consistency versus temperature for an AR-4000 asphalt and the same AR-4000 blended with extender oil and ground rubber in accordance with the formulation presented above. The tabulated results are typical of the change in viscosity characteristics of an asphalt when the extender oil and rubber blend are incorporated into the asphalt at an elevated temperature in the manner and sequence specified (5). Figure 2 shows a plot of these data on a special asphalt consistency versus temperature chart that provides for plotting together test data from the various test methods commonly used for determining the flow characteristics of asphalt.

The consistency versus temperature data show that the influence of the rubber on the base asphalt is to decrease its susceptibility to temperature. In the high temperature range particularly, the improvement in viscosity is substantial: There is approximately a 15-fold increase in viscosity at 140°F and above. Improvement of cold-weather properties is also indicated by the significant increase in penetration value at 39.2°F.

### Durability

The resistance to weathering of the asphalt-rubber material was measured by exposing various blends to direct sunlight in the Phoenix, Arizona, climate for a two-year period. Specimens 0.25 in thick and 4 in in diameter were cased in metal pans and placed on the roof of the laboratory. Kinematic viscosity was measured at 140°F before and after exposure. Table 2 gives the results obtained.

The data indicate that the ratio of viscosity after exposure to original viscosity was lower when extender oil was included in the blend. This improvement is considered significant and attests to the benefit of incorporating the oil extender in the asphalt-rubber material.

More sophisticated durability testing, including comparisons with other materials of known durability characteristics, is currently under way. These results will be published when they are available.

### Adhesion

Preliminary evaluation of the adhesion characteristics of the asphalt-rubber material was performed in a cold-bond test. In this case, a comparison was made with the base asphalt used in making the asphalt-rubber material.

The cold-bond test was run in a specially modified ductility tester designed to pull a specimen with 1x1-in cross section and 2-in length between two brass blocks. The specimens were cast (hot-poured) in a mold so that the two ends adhered to the brass blocks. After a specimen is conditioned in a refrigerated alcohol bath for 10 min, it is quickly transferred to the modified ductility tester and elongated 0.5 in (i.e., 25 percent) at a standard rate. The specimen is removed from the ductility apparatus and again brought to temperature in the alcohol bath and stretched 0.5 in to half again its original length. This step is repeated until the specimen has been elongated a full 2 in, or twice its original length.

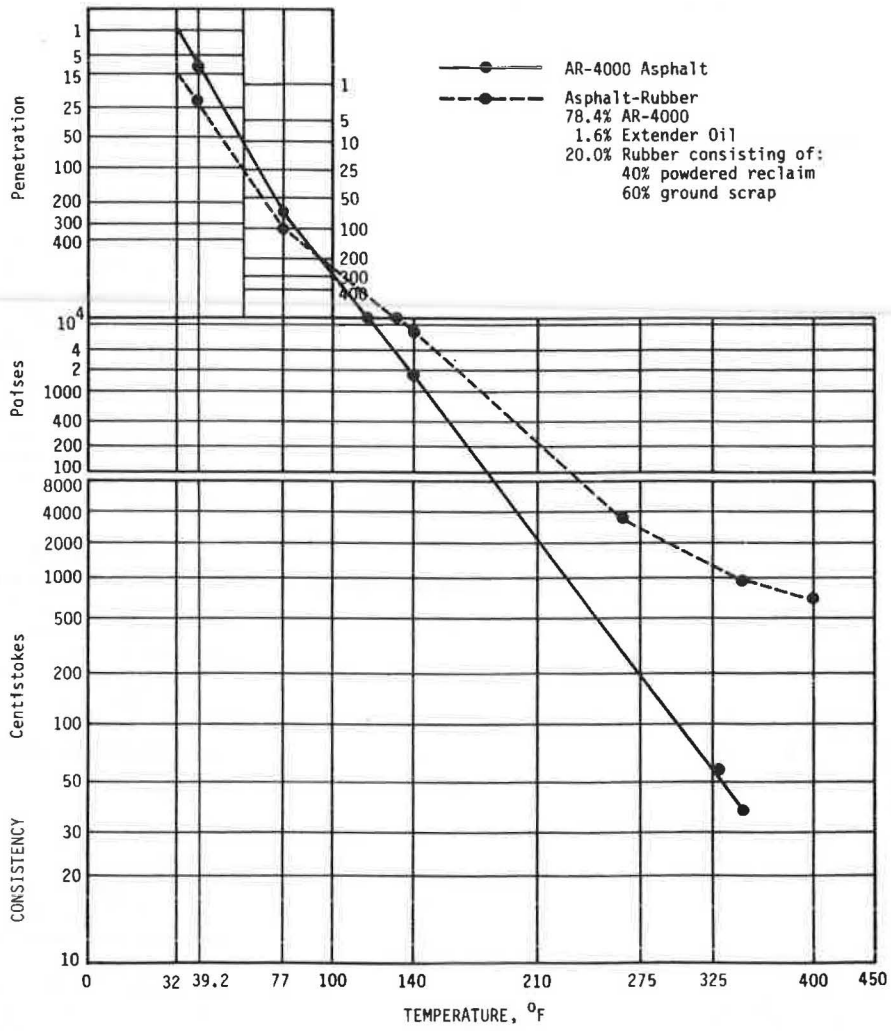


**Figure 2. Effect of addition of reclaim and crumb-rubber blend on consistency-temperature relation of AR-4000 asphalt.**

**Table 2. Results of durability study of asphalt-rubber blends.**

| Test No. | Composition of Blend (%) | | | Exposure Time (months) | Viscosity at 140° F (poises) | | Viscosity Ratio |
|---|---|---|---|---|---|---|---|
| | Asphalt | Extender Oil[a] | Ground Rubber[b] | | Before | After | |
| 1 | 80[c] | -- | 20 | 15 | 5704 | 18 034 | 3.16 |
| 2 | 78.4[c] | 1.6 | 20 | 15 | 5204 | 12 341 | 2.37 |
| 3 | 72.6[d] | 7.4 | 20 | 15 | 5978 | 15 759 | 2.64 |

[a]Shell Dutrex 739.
[b]U.S. Rubber Reclaiming Company G-274, consisting of 40 percent powdered reclaim (i.e., devulcanized) rubber and 60 percent crumb (i.e., ground scrap) rubber high in natural rubber content.
[c]AR-4000.
[d]AR-8000.

Table 3 gives the results of this test for adhesion characteristics. Observations were made of adhesion, cohesion, and reduction in cross-sectional area. After 100 percent elongation, the specimens were cut free from one of the blocks and returned to the low-temperature bath, and measurements were made of recovery in elongation at time intervals of 1 and 10 min. Test series were run on separate specimens at 40° and 60°F.

From a study of these data, it can be seen that the asphalt-rubber maintains its ductility at the lower temperature and has the ability to recover elastically about half of the elongation imparted to the specimen whereas the asphalt has essentially no ductility at the lower temperature and no elastic recovery. The asphalt-rubber also exhibited less reduction in cross-sectional area during testing than the base asphalt under the same conditions of temperature and elongation.

## CHARACTERIZATION OF ASPHALT-RUBBER

Since the asphalt-rubber material is being widely used as an SAMI in pavement resurfacing operations and therefore becomes an integral part of the structural section of a pavement system, it became necessary to determine the stiffness characteristics of the asphalt-rubber membrane in terms of a stiffness modulus. This was done in a creep mode of loading.

The procedure used in this "tensile creep test" was to cast test specimens in a mold that consisted of the end pieces of the ASTM D-113 ductility test

**Table 3. Results of tests for adhesive and cohesive characteristics of asphalt-rubber material.**

| Material | Test Temperature (°F) | Characteristic | Test Observations at Elongation of 25% | 50% | 75% | 100% | Recovery Time 1 min | 10 min |
|---|---|---|---|---|---|---|---|---|
| AR-4000 asphalt | 40 | Adhesion | Pass | – | – | – | | |
| | | Cohesion | Fail | (brittle fracture) | | – | | |
| | | Reduction in cross-sectional area (%) | 0 | – | – | – | | |
| | | Recovery (%) | | | | | 0 | 0 |
| | 60 | Adhesion | Pass | Pass | Pass | Pass | | |
| | | Cohesion | Pass | Pass | Pass | Pass | | |
| | | Reduction in cross-sectional area (%) | 9 | 22 | 30 | 35 | | |
| | | Recovery (%) | | | | | 0 | 0 |
| Asphalt-rubber[a] | 40 | Adhesion | Pass | Pass | Pass | Pass | | |
| | | Cohesion | Pass | Pass | Pass | Pass | | |
| | | Reduction in cross-sectional area (%) | 14 | 14 | 24 | 33 | | |
| | | Recovery (%) | | | | | 30 | 55 |
| | 60 | Adhesion | Pass | Pass | Pass | Pass | | |
| | | Cohesion | Pass | Pass | Pass | Pass | | |
| | | Reduction in cross-sectional area (%) | 5 | 14 | 19 | 24 | | |
| | | Recovery (%) | | | | | 45 | 55 |

[a]Contains 78.4 percent AR-4000 asphalt, 1.6 percent extender oil, and 20 percent rubber blend.

mold and 5.8-in long, straight side pieces in place of the conventional wedge-shaped ones. The side pieces were coated with a release agent of glycerine and kaolin to facilitate removal. The restricted portion of the test specimen cast in this mold had parallel straight sides 6.2 in long and a uniform cross section of 0.3 $in^2$. Gage marks were placed 4 in apart on the center section of the restricted length.

The specimens were then subjected to creep loading in tension under various constant loads at temperatures of 40°, 70°, and 100°F by placing them in a constant-temperature ductility bath modified so that one end of each specimen was fixed while the other end was supported by a floating "raft" made of wood and polystyrene foam. A hanging weight was used to apply the load to the specimen through a thread that passed over essentially frictionless pulleys and was attached to the raft. During the test, the 4-in distance between the gage marks on the specimen was followed with dividers, and readings were taken at 1-min intervals. Each specimen was temperature-conditioned by placing it in the constant-temperature bath for at least 90 min before the start of the test. Figure 3 shows the test setup and a measurement being taken with calipers between the gage marks.

A separate specimen was creep-tested in tension at each temperature, and various loads were applied sequentially, in increasing order, to a single specimen. For each loading, stress and elongation were calculated on the basis of the length and cross-sectioned area at the time of application of that particular load (see Table 4).

An analysis of the test results given in Table 4 was made in connection with an analytic study of the effects of the asphalt-rubber material, when used as an SAMI, in the distribution of stress and strain in an asphalt concrete overlay (7). Assuming that 70°F is a representative temperature for the asphalt-rubber membrane layer, the stiffness for the asphalt-rubber material at times of loading of 0.02-0.05 s, considered representative of moving traffic, was estimated to range from 7500 to 3600 $lbf/in^2$. In their analytic study, Coetzee and Monismith (9) chose to use a stiffness modulus of 5000 $lbf/in^2$.

## APPLICATION CONSIDERATIONS

Immediately after mixing, the asphalt-rubber material described above is generally ready for application by either hot spray or hot pouring within a temperature range of 375°-425°F. If a delay occurs when the material is ready to be applied, the heat is turned off until the job resumes.

The material may also be allowed to stand overnight and be applied the following day, provided the heat is turned off and restarted at a time interval prior to application sufficient to ensure that the application temperature is again within the range of 375°-425°F. Mixing by recirculation or stirring, or combinations thereof, must be maintained during reheating to obtain uniformity of temperature and to avoid localized overheating, which will damage the asphalt-rubber material.

## USES OF ASPHALT-RUBBER MATERIAL

The principal uses of the asphalt-rubber material described above are in connection with membrane systems designed for pavement maintenance and rehabilitation. The four asphalt-rubber membrane systems most widely used are the following:

1. Surface treatment--A hot-spray, cast-in-place asphalt-rubber membrane into which clean, dry rock chips are embedded (i.e., chip seal);
2. SAMI--A hot-spray, cast-in-place asphalt-rubber membrane placed on an existing asphalt or portland cement concrete (PCC) pavement before resurfacing to reduce the transfer of stresses to the resurfacing layer from the underlying pavement structure and hence minimize reflection cracking (clean, dry chips or sand particles are spread on the membrane while it is hot to provide a working surface for placing the overlay);
3. Waterproofing membrane--A hot-spray, cast-in-place asphalt-rubber membrane used on such structures as bridge decks and hydraulic linings to prevent passage of water to the underlying regions; and
4. Joint and crack filling--A hot pour of asphalt-rubber into joints and cracks to serve as a

Figure 3. Test setup for tensile creep test of asphalt-rubber material: (top) overall view of equipment with pulley system and (bottom) calipers used to measure total strain over gage length.

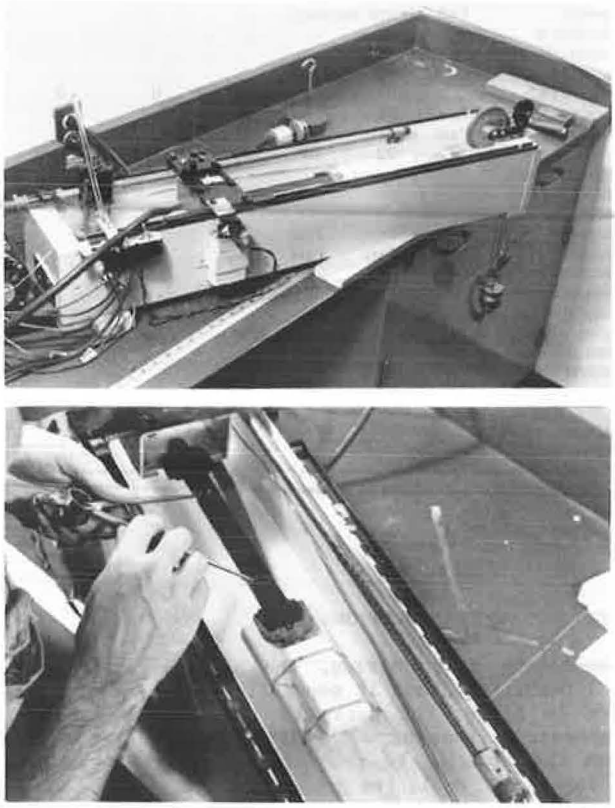

Table 4. Results of tensile creep test on asphalt-rubber material.

| Temperature (°F) | Cross-Sectional Area ($cm^2$) Initial | Final | Load (g) | Elongation at 1000 s (%) | Stress ($g/cm^2$) |
|---|---|---|---|---|---|
| 40 | 2.0 | 1.89 | 300 | 6.03 | 150 |
| | 1.89 | 1.79 | 400 | 5.21 | 212 |
| | 1.79 | 1.64 | 600 | 9.46 | 335 |
| | 1.64 | 1.36 | 1000 | 20.2 | 611 |
| 70 | 2.0 | 1.73 | 20 | 15.4 | 10 |
| | 1.73 | 1.20 | 40 | 38.4 | 23 |
| | 1.20 | 1.03 | 60 | 16.2[a] | 50 |
| 100 | 2.0 | 1.68 | 2 | 18.9[a] | 1.0 |
| | 1.68 | 1.00 | 4 | 69.0[a] | 2.4 |

Notes: 1 $cm^2$ = 0.155 $in^2$; 1 g = 0.0022 lb; and 1 $g/cm^2$ = 0.0064 $lbf/in^2$.
Asphalt-rubber material contains 78.4 percent AR = 2000 asphalt, 1.6 percent extender oil, and 20 percent rubber blend.
Metric units were used because U.S. customary units were too large to give meaningful measurements.
[a]Percentage elongation at 240 s.

seal against the intrusion of water and debris.

Other uses may evolve in time in any case where the unique properties of the asphalt-rubber material may prove to be beneficial. One such case is the use of asphalt-rubber as a binder with open-graded asphalt concrete to impart better adhesion and cohesion characteristics over a wider range of climatic conditions.

## PERFORMANCE CHARACTERISTICS

Since the first experimental installations in the 1975 construction season, the asphalt-rubber material has been incorporated into many and varied projects throughout the United States under the auspices of various user agencies. A chronological listing of these projects has been maintained together with data sheets that record construction details for use in subsequent evaluations of condition and performance. Periodically, condition surveys have also been made and the results have been recorded on forms specifically designed for the purpose. These are filed with the original construction data sheets.

Based on evaluations of the data obtained so far from field construction records and from surveys of present condition, the following general observations are made:

1. The handling characteristics of the asphalt-rubber material from blending to application are uncomplicated. Mixing of the ingredients and application of the finished blend can be successfully accomplished in any tank that has adequate means for mixing and temperature control. For example, a conventional pressure-distributor truck is suitable for the purpose if it is in good operating condition and equipped with appropriate heating equipment and good temperature-control devices.
2. The resulting asphalt-oil-rubber blend is smooth in texture and uniform in consistency. It is free of clusters of undispersed rubber particles or of nonuniformly blended ingredients.
3. Hot-spray applications are readily performed with conventional spray equipment, within the temperature range of 375°-425°F. Hot-pour applications are similarly easy to make by using any of the standard pouring devices within the same range of application temperatures.
4. When the asphalt-rubber is hot-sprayed or hot-poured, it is sufficiently adhesive so that the application of a tack coat is generally not required, provided the surface is broomed clean of loose debris.
5. The general performance of surface treatments made with the asphalt-rubber material has been exceptionally good. Some very early problems with soft binder and loss of aggregate have been corrected by making several small modifications in product formulation and avoiding completely the use of wet or dirty aggregate chips. It is essential that, as a minimum requirement, the aggregate be clean and dry. Although the use of hot, precoated aggregates is ideal, it has not been found to be necessary with this material. Of particular interest in connection with asphalt-rubber-membrane surface treatments is the observation that this type of construction is not limited by the "one layer of chips" concept associated with conventional asphalt-seal test construction. Field trials have shown that one can successfully construct a "multilayered chip seal" with a single heavy application of the asphalt-rubber material (as much as 1 gal/$yd^2$ or more) if sufficient aggregate is applied to embed in the membrane and still produce a textured aggregate surface (8).
6. The general performance of SAMIs made with this asphalt-rubber material has been most promising. Results from various field installations have been reported in the literature (9).
7. The general performance of bridge-deck waterproofing membranes made with this material appears to be promising although the installations have not yet been fully tested. Time will tell whether or not the asphalt-rubber membrane will provide sufficient waterproofing to protect the underlying concrete decks from the intrusion of water. It should be noted that the bridge-deck membranes must be covered with a protective sheet, such as asphalt-

impregnated fiber mats, to provide a working surface for placing the overlay.

8. The general performance of joints and cracks filled with hot-poured asphalt-rubber material has been exceptionally good, especially where the joints and cracks are air-blown clean and free of debris. However, a well-designed control experiment with other types of fillers is needed in order to compare the performance of the asphalt-rubber with that of materials that have service records in this kind of use.

As a consequence of the above evaluations of field experience with the asphalt-rubber material, a series of guide specifications has been initiated to delineate the materials and procedures to be followed for achieving the desired results. The first of these is a material specification (10) to cover the preparation of the asphalt-rubber material itself from selected ingredients that must be blended together under carefully controlled conditions in the manner, proportions, and sequence given to ensure uniformity in properties and behavior. This specification is basic to all systems that use the asphalt-rubber material, whether hot-sprayed or hot-poured.

Besides the material specification, two construction specifications have been developed to cover the placement of an asphalt-rubber-membrane surface treatment (11) and an asphalt-rubber SAMI (12). Both of these specifications are considered to reflect the best practice from experience accumulated to date.

## ANALYTIC STUDIES

In conjunction with the evaluation program, two special analytic studies were undertaken to develop a better understanding of the behavior of the asphalt-rubber-membrane systems. The first of these was a study of how to design an asphalt-rubber surface treatment based on a multilayer chip concept. The second was a study of how an asphalt-rubber SAMI functions to minimize reflection cracking in asphalt concrete overlays.

### Design of Asphalt-Rubber Surface Treatment

The study related to the design of an asphalt-rubber surface treatment with a multilayered aggregate structure consisted of conducting a field audit of an experimental project on Van Buren Road in Phoenix in which the quantities of asphalt-rubber material and aggregate chips were varied from section to section and all sections produced a highly satisfactory surface treatment in all respects over more than five years of field service. In the audit, the range of asphalt-rubber was found to vary from 0.4 to 1.95 gal/yd² and the range of aggregate chips retained ranged from 22 to 68 lb/yd². The thickness of the surface treatment was also measured for each section. Details of this study are described in Specification M-101 of Arizona Refining Company (11), which also presents a nomograph for use in designing chip-seal surface treatments with a multilayered aggregate structure.

### Effects of Asphalt-Rubber Interlayer on Reflection Cracking

The analytic study of the effect of applying a thin (0.25- to 0.375-in) asphalt-rubber membrane of low stiffness and high deformability at the interface between the underlying and overlay pavements on minimizing reflection cracking in asphalt concrete overlays consisted of finite-element analyses of pavement overlay systems with and without the asphalt-rubber interlayer. This study was undertaken at the University of California, Berkeley, and a report was issued in June 1978 (7).

Conventional methods of overlay design, whether empirical or theoretically based, generally give thickness requirements that are adequate to provide the needed structural strength to accommodate anticipated traffic volumes and loadings for a projected design life. However, these overlays, although structurally functional, are susceptible to the development of cracks caused by the "reflection" of cracking patterns that exist in the underlying pavement. The mechanism for the development of these reflection cracks is not fully understood but is believed to be directly related to the transfer of high stresses to the underside of the overlay at discontinuities in the underlying pavement.

A two-dimensional finite-element model of the pavement system, with and without the SAMI present, was used in this study to analyze the pavement structure for response to traffic loads. The mesh used in the analysis had elements as small as 0.06x0.015 in at the crack tip because of the very high stress and strain gradients encountered at this location.

The results obtained from the finite-element analysis are presented as contours of effective stress distribution that show the concentration of high stresses at the crack tip. For the specific case of a 2-in asphalt concrete overlay on an 8-in PCC pavement, a 0.25-in-thick asphalt-rubber SAMI with a stiffness modulus of 5000 lbf/in² reduces the maximum stress at the crack tip from about 600 to about 100 lbf/in², a sixfold decrease. The corresponding contours of shear-strain distribution for the same case show that the shear strain is reduced approximately fourfold, from about $30 \times 10^{-3}$ to $7 \times 10^{-3}$ in/in.

Various studies were made on the effects of varying such parameters as the stiffness moduli of the asphalt-rubber (1000-20 000 lbf/in²), subgrade (5000-10 000 lbf/in²), asphalt concrete (100 000-1 500 000 lbf/in²), and PCC (1 000 000-4 000 000 lbf/in²) as well as cross-sectional dimensions of the pavement overlay system and the crack width. Figure 4 is most interesting because it clearly demonstrates that, although the effect of overlay thickness is to reduce crack-tip stress when the asphalt-rubber SAMI is not present, it has little effect when the asphalt-rubber SAMI is present. For this case, the asphalt-rubber appears by extrapolation to be equivalent to a 9-in asphalt concrete overlay. However, further study is needed to determine whether such an equivalency relation exists.

As part of this analytic study, a limited analysis was also conducted to estimate stresses in the pavement overlay system, with and without the asphalt-rubber SAMI, resulting from temperature change. For a temperature drop of 40°F, with and without the asphalt-rubber SAMI layer, a 30-fold drop in horizontal shear at the crack tip, from about 3000 to 100 lbf/in², is obtained. For this analysis, the temperature change was attenuated with depth and the stiffness modulus of the asphalt concrete was held constant. Since the modulus is a time-dependent parameter, it is likely that the stress difference in the two cases may not be as large as that stated. Nevertheless, there is indication of a substantial reduction in thermally induced stresses as a result of the use of the asphalt-rubber SAMI.

## CONCLUSIONS

The general concept of combining a blend of 40 percent powdered reclaim rubber--i.e., devulcanized

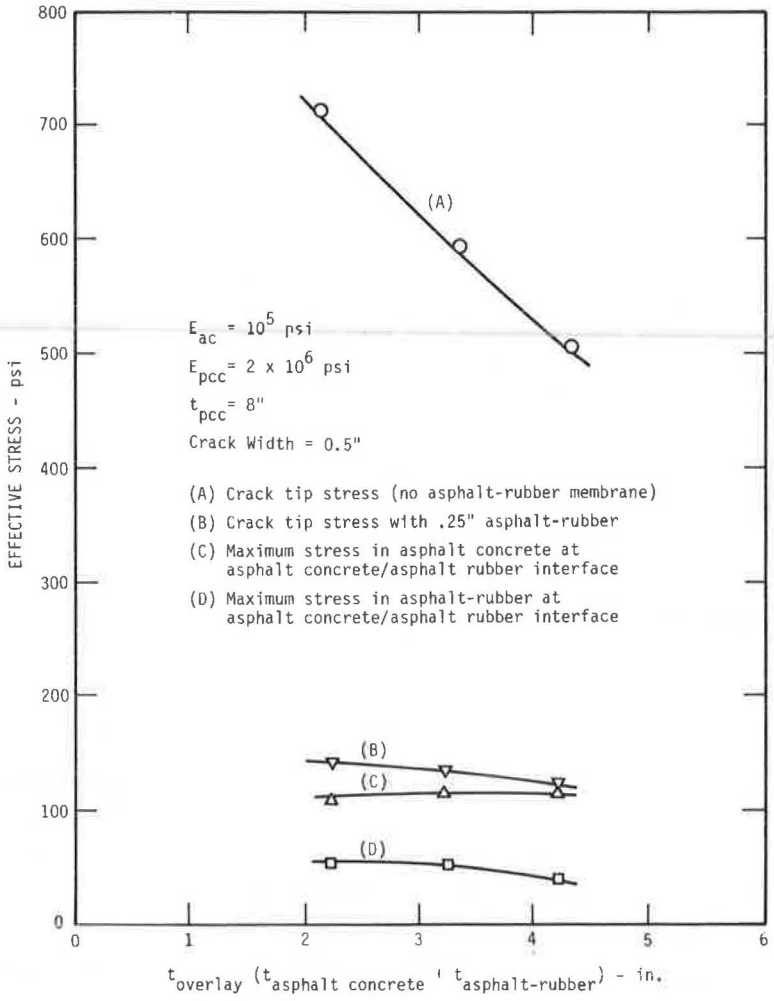


**Figure 4. Effect of thickness of overlay on effective stress at crack tip with and without asphalt-rubber SAMI and on maximum stress in asphalt concrete and SAMI.**

scrap--and 60 percent powdered vulcanized scrap rubber high in natural rubber content with a paving-grade asphalt supplemented with rubber extender oil to produce an asphalt-rubber material with the desirable properties of both the asphalt and the rubber is valid. Laboratory experiments, analytic studies, and field experience to date support the following conclusions:

1. The asphalt-rubber material is easily prepared from its three basic ingredients with the equipment and know-how currently available in the field of asphalt construction.
2. The resulting asphalt-rubber product is smooth in texture and uniform in consistency and can be readily spray-applied or poured within a temperature range of 375°-425°F by using conventional asphalt spreading or pouring equipment.
3. When hot-sprayed on a surface and allowed to cool, the material forms a tough, durable, and adhesive asphalt-rubber membrane of low stiffness and high deformability that makes it useful for the construction of (a) surface treatments with a multilayered aggregate structure, (b) SAMIs, and (c) waterproofing membranes for bridge decks and hydraulic linings.
4. When hot-poured into clean and debris-free pavement joints and cracks and allowed to cool, the material forms an effective filler that resists the intrusion of water and debris but still has the low stiffness and high deformability to accommodate displacements associated with loading and thermal stresses.

Although there has been much development work with this asphalt-rubber material since its inception in 1975, further studies are needed at both the laboratory and field stages to develop better methods of determining its properties, characterizing its behavior, and documenting its performance in each of its many applications.

REFERENCES

1. C.H. McDonald. A New Patching Material for Pavement Failures. HRB, Highway Research Record 146, 1966, pp. 1-16.
2. B.D. LaGrone and B.J. Huff. Utilization of Waste Rubber to Improve Highway Performance and Durability. Presented at 52nd Annual Meeting, HRB, 1973.
3. F.S. Rostler, R.M. White, and E.M. Dannenberg. Carbon Black as a Reinforcing Agent for Asphalt. Proc., AAPT, Vol. 46, 1977.
4. B.A. Vallerga and P.F. Gridley. Carbon Black Reinforcement of Asphalts in Paving Mixtures. ASTM, Philadelphia, Special Tech. Publ. 724, 1979, pp. 110-128.
5. D.L. Nielsen and J.R. Bagley. Rubberized Asphalt Paving Composition and Use Thereof. U.S. Patent 4,068,023, Jan. 10, 1978.
6. F.S. Rostler and R.M. White. Composition and

Changes in Composition of Highway Asphalts, 85-100 Penetration Grade. Proc., AAPT, Vol. 31, 1962.
7. N.F. Coetzee and C.L. Monismith. An Analytical Study of the Applicability of a Rubber-Asphalt Membrane to Minimize Reflection Cracking in Asphalt Concrete Overlay Pavements. Department of Civil Engineering, Univ. of California, Berkeley, Geotechnical Engineering Rept., June 1978.
8. B.A. Vallerga and J.R. Bagley. Design of Asphalt-Rubber Single Surface Treatments with Multilayered Aggregate Structure. ASTM, Philadelphia, Special Tech. Publ. 724, 1979, pp. 22-38.
9. B.A. Vallerga, and others. Applicability of Asphalt-Rubber Membranes in Reducing Reflection Cracking. Proc., AAPT, Vol. 49, 1980, pp. 330-353.
10. Specification for ARM-R-SHIELD. Arizona Refining Co., Phoenix, Spec. M-101, 1976.
11. Construction Specification for ARM-R-SHIELD Surface Treatment. Arizona Refining Co., Phoenix, Spec. C-201, 1976.
12. Construction Specification for ARM-R-SHIELD Stress Absorbing Membrane Interlayer. Arizona Refining Co., Phoenix, Spec. C-202, 1976.

*Publication of this paper sponsored by Committee on Characteristics of Nonbituminous Components of Bituminous Paving Mixtures.*

# Modification of Paving Asphalts by Digestion with Scrap Rubber

JOHN W.H. OLIVER

**The service performance of sprayed surface treatments laid where traffic-induced stress is severe or where the existing pavement is cracked can be significantly improved if comminuted scrap rubber is digested in the asphaltic cement before spraying. Work performed to identify the factors that are of importance in optimizing asphalt performance is reported. Measurement of the deformation response of the rubber digestions to sinusoidal loading indicated that the modified binder had improved response under the loading produced by traffic at high pavement temperatures and that produced by thermal contraction at low pavement temperatures. A simple and rapid test procedure was developed to measure the response under loading conditions similar to these. The procedure is to subject a prism of the binder at 60°C to a shear strain of 1.0-in creep and then determine the elastic recovery when the stress is removed. The most important factor affecting elastic recovery was found to be the morphology of the rubber particles as determined by the comminution process used in their manufacture. A simple bulk-density test was used to characterize this morphology. Digestions of natural (truck-tire) rubber are generally superior to those that incorporate synthetic (car-tire) rubber but are more affected by changes in the time or temperature of digestion. Where a cryogenic comminution process had been used, only digestions of natural-rubber particles produced a significant improvement in asphalt properties. Elastic recovery of strain is linearly related to rubber concentration.**

Rubber modifiers have been used in bituminous materials for many years. They have usually been specially prepared natural and synthetic rubbers, and their concentration has been limited to less than 5 percent by mass of the asphaltic cement because greater concentrations have caused problems in handling (pumping and spraying) and because of their high cost. At these concentrations, the improvement in binder performance obtained in pavement service has been marginal unless a satisfactory polymer network has been formed in the asphalt.

A major improvement in this situation occurred as a result of the work of McDonald (1) and Morris and McDonald (2), who introduced the use of digestions of scrap rubber in asphalt that contained up to 25 percent by mass of comminuted tire-tread rubber. A sprayed layer of this material has been widely used in the United States to prevent cracks in the substrate from being reflected through overlays. It is normally applied as either a chip-seal surface treatment with approximately 20 percent rubber added to the asphalt, commonly known as a stress-absorbing membrane, or as an interlayer of rubber-asphalt binder and aggregate (stress-absorbing membrane interlayer) overlaid by a thin course of asphaltic concrete.

In Australia, the main use of the scrap rubber-asphalt digestions has been in sprayed surface treatments where the advantages are considered to be

1. The sealing of cracked pavements to prevent, or delay the onset of, reflection cracking, and
2. The retention of chips in hot weather under severe traffic stress conditions (such conditions occur when seals are used to provide surface texture on high-speed roads where a conventional asphalt seal is unable to provide satisfactory stone retention at bends or in acceleration and deceleration areas).

## DEFORMATION TESTING OF RUBBER-MODIFIED ASPHALTS

### Sinusoidal Loading

A useful means of evaluating the deformation behavior of asphalts and rubber-modified asphalts is by their response to sinusoidal loading in simple shear. This provides basic information on the behavior of the materials, but specialized equipment is required and testing is slow. The sinusoidal loading procedure was therefore used only to determine the appropriate test conditions (temperature, rate of strain, etc.) for the rubber-asphalt digestions, and a simpler apparatus, operated near the required conditions, was then used for routine testing.

In the sinusoidal loading procedure, a force applied to the material produces a sinusoidal displacement that lags behind the force (see Figure 1). The magnitude of the phase-angle difference between the force and the displacement ($\phi$) is an indication of the partitioning of the response between viscous and elastic behavior. The phase angle is zero for purely elastic behavior and 90° for purely viscous behavior. The ratio of the maximum value of the force to the maximum value of the displacement is proportional to the complex

Figure 1. Deformation response of viscoelastic material to repeated sinusoidal loading.

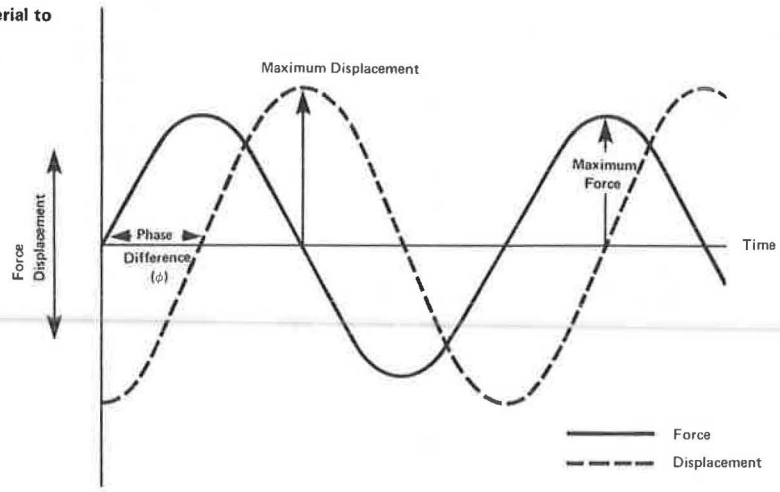


Figure 2. Modification of viscoelastic response of asphalt at 5° and 60°C by digestion with scrap rubber.

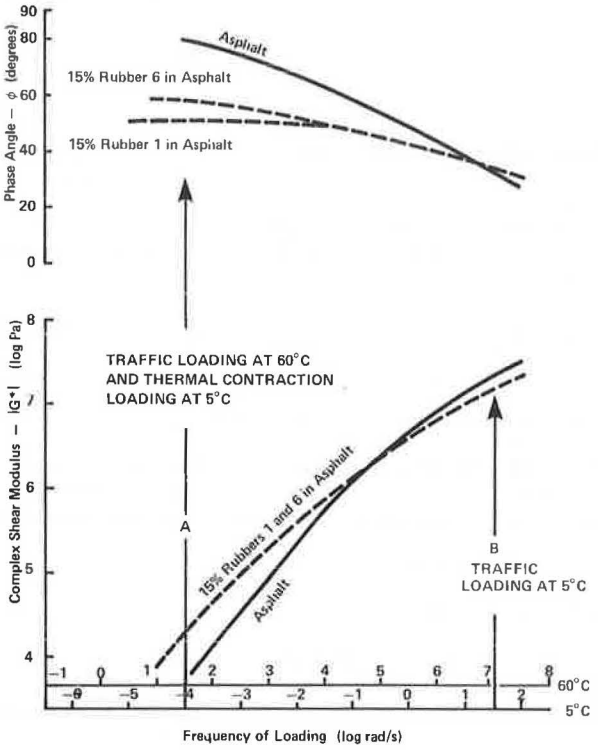


shear modulus of the material (|G*|).

The responses of an asphalt alone and after it has been modified by digestion with two different scrap rubbers [15 percent by mass of scrap rubber digested for 1 h at 200°C (sample 6) and 220°C (sample 1)] are shown in Figure 2. The response at 60°C can be determined by reference to the upper of the two frequency scales on the horizontal axis and at 5°C by reference to the lower scale. Details of the rubber samples are given in Table 1.

Sample 6 has depressed the increase of the phase angle at low loading frequencies to a constant value just below 60°. Sample 1 is even more effective, reducing the angle to about 50°. At these very slow rates of strain or high temperatures, the response of the unmodified asphalt is that of a viscous liquid, whereas the modified binders show behavior typical of a low-modulus elastic solid.

Table 1. Samples used in bulk-density test.

| Sample | Rubber Composition | Preparation Method |
|---|---|---|
| 1 | Synthetic | Industrial tire grinding |
| 2 | Synthetic | Laboratory drilling of tire tread A |
| 3 | Synthetic | Laboratory rasping of tire tread B |
| 4 | Synthetic | Laboratory rasping of tire tread C |
| 5 | 60 percent synthetic | Laboratory drilling of tire tread D |
| 6 | Synthetic | Tire retreader's buffings |
| 7 | Synthetic | Laboratory drilling of tire tread C |
| 8 | Synthetic | Industrial cryogenic |
| 9 | Synthetic | Laboratory cryogenic |
| 10 | Natural | Laboratory rasping of tire tread E |
| 11 | Natural | Laboratory drilling of tire tread E |
| 12 | Natural | Industrial tire buffings |
| 13 | Natural | Undisclosed industrial process |
| 14 | Natural | Laboratory cryogenic |
| 15 | Natural | Undisclosed industrial process |

## Relation to Pavement Loading

Two kinds of loading are of particular importance in relation to the performance of thin bituminous surfacings. The first, due to vehicles passing over the surfacing, is assumed to be periodic and has a loading time of between, say, 20 and 50 ms, depending on vehicle speed. The second, due to thermal contraction by diurnal temperature change, has a duration of the order of $10^4$ s. The magnitude of the strains produced in the binder by such loading is not known precisely, but the high-stress locations in the surfacing are where the binder films are thin (3). In such locations, the strain in the binder will be high.

Vehicle loading can cause distress in a surfacing at either end of the range of pavement surface temperatures. At high pavement temperatures, the binder can be too fluid and not resist the plucking and shearing action of vehicle tires; at low pavement temperatures, the binder can be so hard (particularly after a long period of service) that vehicle loading causes brittle fracture of the binder films. Thermal-contraction loading is critical at low pavement temperatures when the binder (again, particularly after long-term exposure) is at its hardest. Since both modes of loading induce overall, gross tensile strains in the surfacing, they will augment each other to produce the cracking that eventually occurs at low surface temperatures.

These important rate-of-loading conditions at the appropriate pavement temperatures for Australian conditions are given in Table 2 and are indicated by arrows A and B in Figure 2.

## Selection of Test Procedure and Test Conditions for Rubber-Modified Asphalts

Consideration of Figure 2 indicates that the important modification of deformation response by the addition of scrap rubber, so far as performance in the pavement surfacing is concerned, is for traffic loading at high road temperatures and thermal contraction at low road temperatures (arrow A). For traffic loading at 5°C (arrow B), there is no significant change in the phase angle or modulus level.

To compare the effectiveness of different scrap-rubber digestions in asphalt, it is desirable to have a simple and rapid method of evaluating the deformation response of the product. To assess the relative benefit in pavement service, such testing should be done at about 60°C, at a rate of loading equivalent to traffic loading and to relatively high strains.

A simple method of measuring creep and elastic recovery in shear was developed by using a modification of the Shell sliding-plate rheometer. This instrument enables a higher strain (1.0) to be realized than is possible with sinusoidal loading and permits rapid testing at the test temperature selected (60°C).

The above discussion indicates the desirability of using test methods that indicate the basic deformation and flow behavior of the rubber-asphalt digestions under the critical pavement service conditions. These materials have properties intermediate between those of asphalt and those of rubber, and empirical procedures used to evaluate asphalts may not be suitable. The deformation behavior of rubber-modified asphalts and methods of testing are discussed in greater detail by Dickinson (4).

## EXPERIMENTAL PROGRAM

### Digestion Procedure

The primary method of evaluation of different rubber-asphalt systems was the laboratory digestion, under controlled conditions, of mixtures of the comminuted scrap rubber and asphalt followed by deformation testing of the product. The laboratory digestion procedure required that the rubber sample be dried in a vacuum oven prior to addition to the hot asphalt in a reaction flask maintained at the desired temperature. The mixture was continuously stirred, and samples were withdrawn and cast, when hot, into sliding-plate rheometer test molds.

Laboratory digestion simulates the heat treatment applied prior to spraying of the product in road construction operations. In Australia, this normally takes the form of circulation of the materials in an asphalt sprayer at about 200°C for between 30 min and 1 h (5).

### Deformation Testing of Digestions

An extensively modified sliding-plate rheometer was used to measure the deformation properties (creep in shear) of the binder specimens. A diagram of the apparatus is shown in Figure 3. Although the instrument is simple to use, it is necessarily delicate and is more suited to research needs than to routine quality-control work.

To test a sample, a mass of 20 g was applied to a 10-mm-thick specimen until a strain of 1.0 was obtained. The load was then automatically removed by a motor-driven mechanism, and the sample was permitted to recover under a "no-load" condition. Movement of the free plate was recorded by using a displacement transducer.

The parameters calculated for analysis were time under stress (i.e., time to reach a strain of 1.0) and percentage elastic recovery (defined as the percentage of this strain recovered when the load is removed and after a recovery period that is 10 times the straining period). Time under stress can be regarded as a simple measure of resistance to deformation at the test temperature (60°C), whereas elastic recovery is an indication of the elastic component of this deformation.

Normally, a particular asphalt-rubber combination was digested for 2 h in the reaction vessel at a controlled temperature. Samples were removed for testing after digestion for 0.5, 1, and 2 h. Three

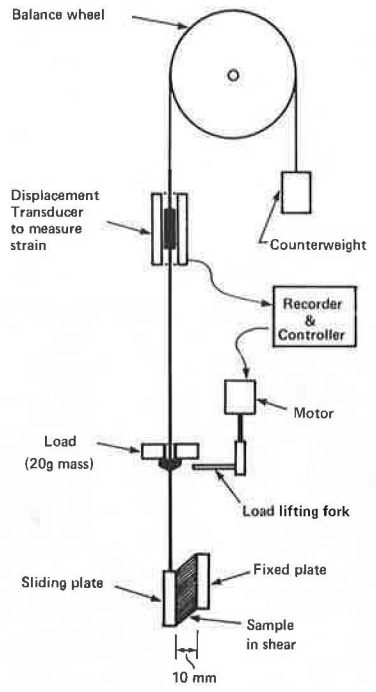


**Figure 3. Diagram of apparatus used to measure elastic recovery of strain.**

**Table 2. Rate of loading conditions for bituminous surfacings.**

| Loading Mode | Surfacing Temperature | Loading Duration (s) | Approximate Frequency of Sinusoidal Loading (log rad/s) | Distress Mode |
|---|---|---|---|---|
| Moving traffic | High 60°C[a] | 0.02-0.05 | +1.5 | Shearing and plucking of aggregate |
| | Low 5°C[b] | 0.02-0.05 | +1.5 | Brittle fracture of binder films |
| Thermal contraction | Low 5°C[a] | $10^4$ | -4.0 | Cracking of surfacing |

[a]Arrow A, Figure 2. [b]Arrow B, Figure 2.

specimens were prepared from material removed after each digestion time. A test result is the mean value obtained for these three specimens. Repeat testing on an asphalt-rubber combination, which was relatively insensitive to changes in time and temperature of digestion, indicated that the confidence limits (95 percent probability) of a test result were ±1.4 s for time under stress and ±3.1 percent for elastic recovery.

## Materials Evaluated

Two asphalts representative of Australian production were used. Both were 85/100 penetration grade. The material used for the bulk of the testing was the vacuum distillation residue from Kuwait crude petroleum, air-blown to grade. The second asphalt, which was more aromatic in character, was a blend of the vacuum distillation residue from a Kuwait crude petroleum and the propane-precipitated asphalt from this residue.

The bulk of the rubber granulate used for asphalt work in Australia is the material produced during the preparation of used tires for retreading. A series of rotating saw blades contact the tread area of the tire, and the buffings are drawn off by a vacuum system. Normally, the buffings supplied for asphalt work are a mixture of natural (truck-tire) and synthetic (car-tire) rubbers, the car-tire rubber predominating.

Products from two other comminution processes supply the remainder of the asphalt market. One of these is the cryogenic method, which involves hammer milling of the rubber after it has been cooled with liquid nitrogen. At a sufficiently low temperature, the rubber behaves as a brittle solid. Another process, for which full details have not been disclosed, involves softening and swelling of the tire by solvent immersion followed by size reduction and solvent recovery.

Industrially produced scrap-rubber particles can be of variable and indeterminate composition. As part of the study, comminuted rubber prepared from cured sheets of vehicle-tire feedstock of known composition were examined. The laboratory comminution processes used included rasping, drilling, hand cutting, and cryogenic embrittlement followed by crushing.

# RESULTS

## Rubber Particle Morphology

The gross morphology (structure) of the rubber particles, as determined by the way they are produced, was found to be the most important factor affecting the elastic properties of the rubber-asphalt digestions. The difference in the morphology of particles produced by three different processes is clearly illustrated in the scanning electron photomicrographs produced in Figures 4-6. The particles shown all passed a 600-µm sieve and were retained on a 300-µm sieve when sieved dry. A summary of the appearance of the particles and their composition and production method together with the elastic recovery value of an asphalt digestion of each sample is given in Table 3.

Examination in the scanning electron microscope of rubber particles produced by a number of processes indicated that there are two main types of morphology: one where the surface is covered in porous, "spongelike" nodules and one where the surface is smooth. These two extremes are shown by the photographs in Figures 4 and 6, respectively. Particles with intermediate morphology generally have either a smooth surface with some porous nodules attached or a mixture of smooth and nodular-surfaced particles.

There appeared to be a relation between the number of porous nodules present in a sample and the elastic recovery of strain of a digestion of the sample in asphalt. Accordingly, a simple means of characterizing particle morphology was devised, and the relation between this property and elastic recovery of strain was examined. The property measured was the bulk density in water of particles

Figure 4. Electron micrograph of laboratory-ground synthetic tire-tread rubber.

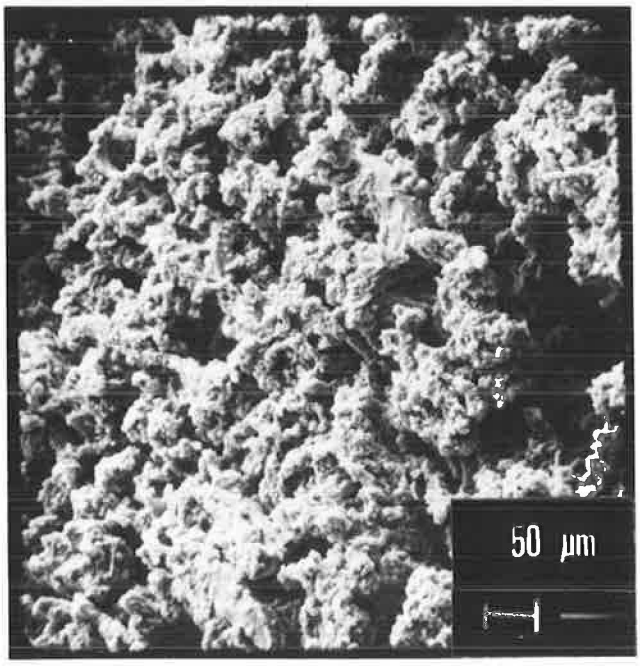


Figure 5. Electron micrograph of laboratory-drilled synthetic tire rubber.

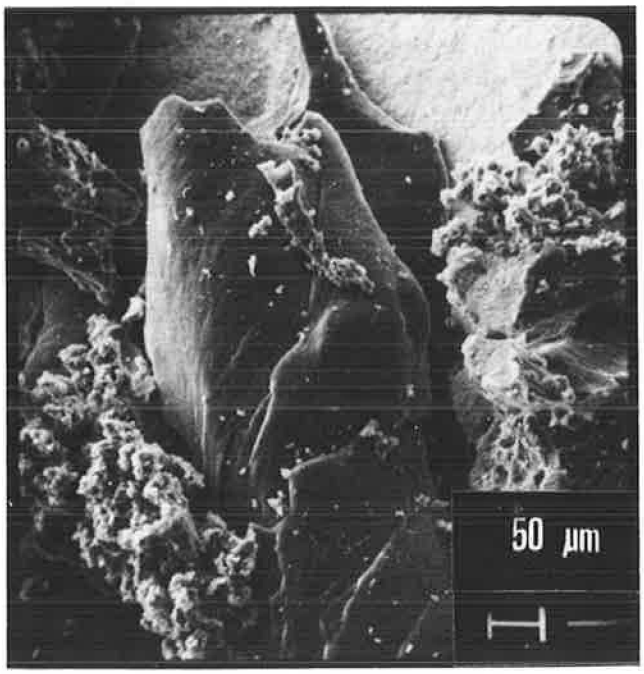

**Table 3. Properties and appearance of samples shown in Figures 4-6.**

| Figure | Material and Production Process | Gross Morphology | Elastic Recovery[a] (%) |
|---|---|---|---|
| 4 | Laboratory-produced car-tire grindings | Particle surface completely covered with porous nodules | 35 |
| 5 | 100 percent styrene-butadiene, cured tire feedstock, laboratory drilled | Generally smooth, rounded particles with a few porous nodules attached | 17 |
| 6 | 100 percent styrene-butadiene, cured tire feedstock, embrittled in liquid nitrogen and crushed | Smooth-faced, angular, cracked particles | 3 |

[a]Fifteen percent by mass rubber in air-blown asphalt digested at 200°C for 0.5 h.

**Figure 6. Electron micrograph of cryogenically crushed synthetic tire rubber.**

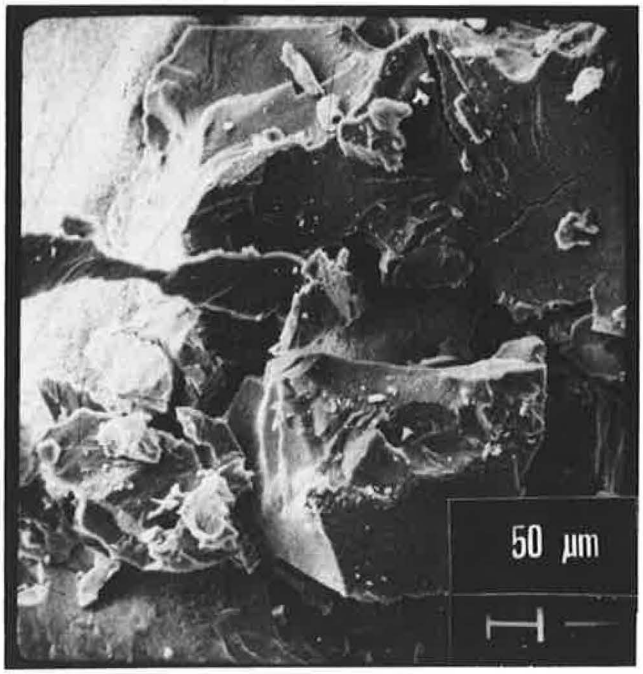


**Figure 7. Relations between elastic recovery and bulk density for natural and synthetic rubbers.**

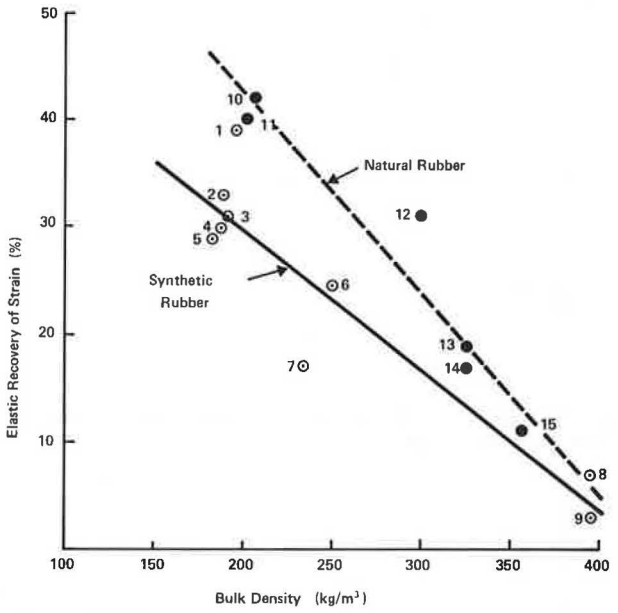


separated between the 300- and 600-µm sieves (6).

To determine the bulk density, 7.5 g of sieved rubber particles was first boiled in 100 mL of water to remove trapped air, and then a weak detergent solution was added to ensure reproducible wetting of the particles. The volume of the rubber was measured after the sample had been allowed to settle in the water for 15 min. Replicate testing indicated that the confidence limit at the 95 percent probability level of the mean of two tests was ±8.2 kg/m³.

The relation between percentage elastic recovery (0.5-h digestion at 200°C of 15 percent by mass rubber in the air-blown asphalt) and bulk density is shown in Figure 7 for a number of rubbers. The desirable condition, for pavement service, is for the rubber-asphalt digestion to show a high value of elastic recovery. The rubber samples are identified by specimen number, and brief details of their composition and method of preparation are given in Table 1. Separate regression lines are drawn for natural and synthetic rubbers. The Pearson correlation coefficient is 0.96 for natural rubbers and 0.93 for synthetic rubbers.

The results show that there is a strong correlation between particle morphology (as measured by the bulk-density test) and the elastic recovery of strain of the rubber-asphalt samples. The digestion conditions used are the ones most commonly used for spraying of rubberized binders in Australia.

## Digestion Conditions

The effect of time and temperature of digestion on the elastic recovery of synthetic and natural rubber-asphalt digestions, made from industrially produced rubber buffings, is shown in Figures 8 and 9. For both rubber types, elastic recovery increases with both time and temperature of digestion up to 220°C. At 240°C, there is no further increase for the 2-h synthetic rubber digestion and a marked reduction in elastic recovery for the 1- and 2-h natural rubber digestions. Figure 10 shows the time-under-stress results for natural rubber. These results suggest that, with this rubber, thermal degradation can occur at temperatures as low as 180°C but that the elastic properties of the mixture are not immediately affected. The synthetic rubbers tested generally had a time-under-stress value of between 5 and 10 s regardless of digestion conditions.

The significance of these results, with regard to asphalt spraying operations, is that both natural and synthetic rubbers behave satisfactorily under normal digestion conditions in the sprayer. However, if overheating occurs, the properties of natural-rubber digestions are more rapidly degraded than are those of synthetic-rubber digestions. Since time and temperature of digestion are interdependent, the same difficulty can arise from extended digestion times at normal spraying temperatures.

## Rubber Composition

Results presented in the previous sections indicate

Figure 8. Effect of time and temperature of digestion on elastic recovery for synthetic-rubber tire buffings.

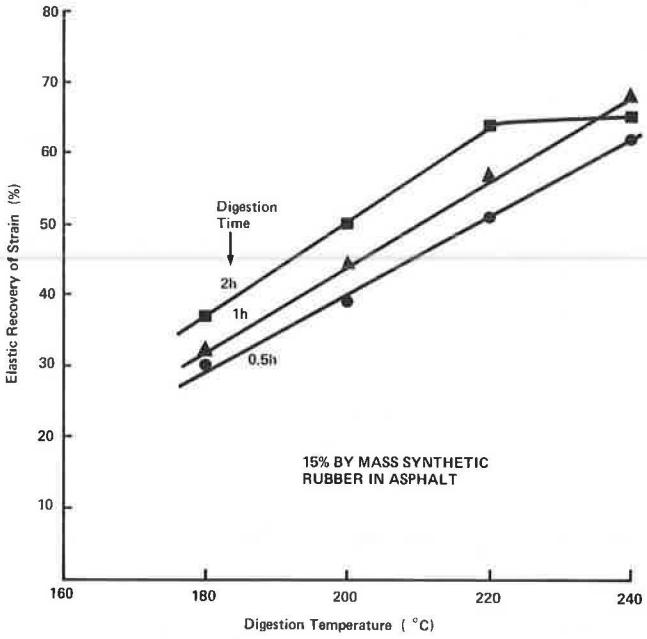


Figure 9. Effect of time and temperature of digestion on elastic recovery for natural-rubber tire buffings.

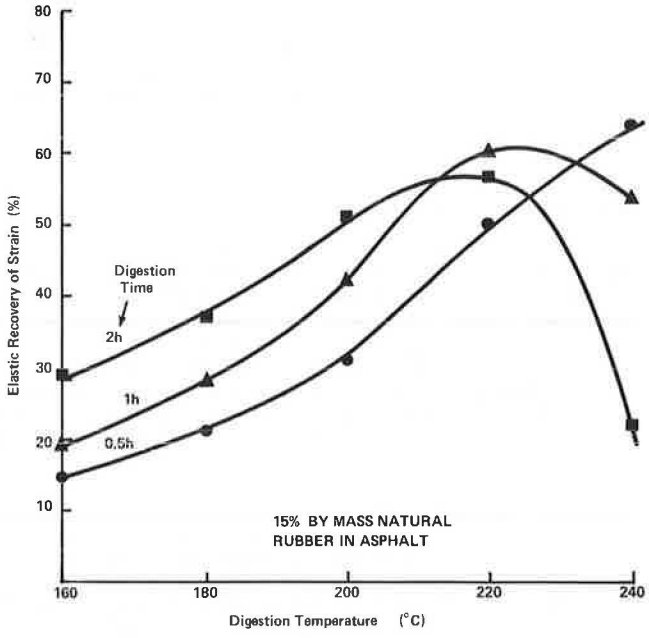


that rubber composition is an important variable that interacts with both particle texture and digestion conditions. As an example, digestions of cryogenically prepared natural rubber improved significantly (in terms of elastic recovery) as digestion time increased, whereas digestions of cryogenically prepared synthetic rubber did not.

## Rubber Concentration

The effect of rubber concentration on elastic recovery of strain is shown in Figure 11 for typical spraying conditions (tire retreader's buffings

Figure 10. Effect of time and temperature of digestion on consistency of digestions of natural-rubber tire buffings.

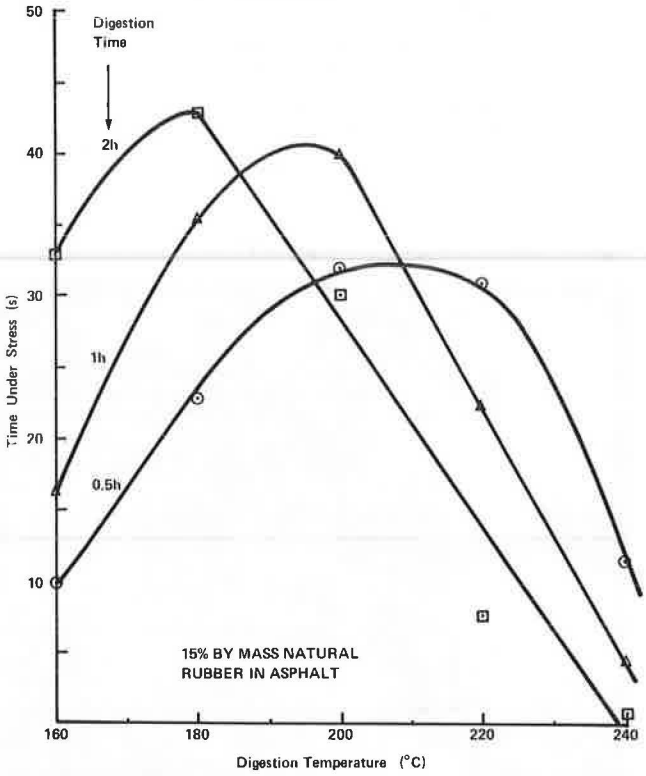


digested in air-blown asphalt at 200°C).

Linear relations, with correlation coefficients of 0.99, apply for the three digestion periods studied. Linear relations were also found to apply for a high-elastic-recovery material that could, however, only be tested over a narrow concentration range because the highest-concentration samples were impossible to pour.

## Rubber Particle Size

For tire retreader's buffings (mainly synthetic), there was a small, regular increase in elastic recovery as particle size decreased. This may be due to the smaller-sized fractions containing a higher proportion of porous (low-bulk-density) particles than the larger-sized fractions. In the case of cryogenically prepared synthetic rubber, there was very little modification of the parent asphalt properties even when a sample of the rubber was reduced in size so that it all passed a 150-µm sieve and 25 percent passed a 75-µm sieve.

## Bitumen Composition

There was no significant difference between the air-blown and the propane-precipitated Kuwait asphalt in respect to elastic recovery of strain. This was true for both natural and synthetic rubber specimens and for rubber particles with a porous (low-bulk-density) or a smooth (high-bulk-density) appearance.

## Curing of Rubber-Asphalt Binders After Application

To determine whether structural changes can occur in rubber-asphalt binders after they have been sprayed, the behavior of specimens during extended laboratory storage was observed. A storage temperature of 55°C was selected as typical of the maximum surface

Figure 11. Rubber concentration versus elastic recovery.

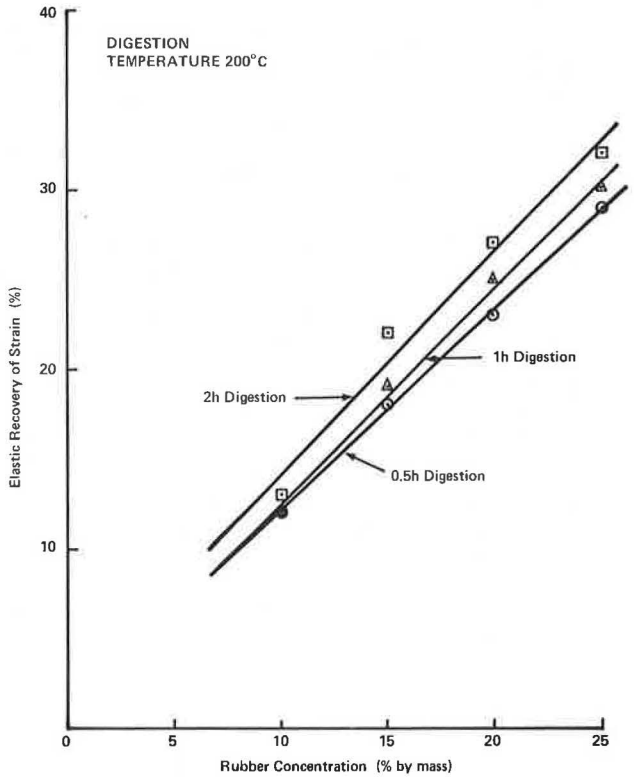


temperature likely to be encountered and to ensure that any changes that occurred did so at a detectable rate.

Two rubber samples were used: industrial retreader's buffings and new-car-tire buffings. These were typical of rubber samples that gave a low and a high elastic recovery. Each sample was used to prepare specimens digested at (a) conditions that gave optimum elastic recovery and (b) conditions that gave below-optimum elastic recovery. For both sets of samples and conditions, there was little or no change in elastic recovery with time of storage.

## DISCUSSION OF RESULTS

The main factors that affect the behavior of rubber-asphalt digestions have been identified and studied. However, the list is by no means exhaustive and there may be others, such as rubber particle shape and the "nonrubber" additives in tire rubber, which could be important.

The morphology of the rubber particles has been shown to play an important role in determining the properties of rubber-asphalt digestions. The form of the particles seems to be determined by the disintegration method used. Tearing apart the bulk rubber at near-ambient temperatures so that stretching of the rubber takes place before fracture produces a much more "active" material than brittle fracture at low temperatures. Experimentation with different manufacturing procedures is planned in order to obtain low-bulk-density products.

Production by the cryogenic process appears unsatisfactory, particularly for predominantly synthetic rubber materials. Either further treatment of the product is required, or this method of comminution should be restricted to natural rubber scrap.

The bulk of scrap rubber used in asphalt is predominantly synthetic, and digestion conditions are not particularly critical. If a low-bulk-density product were to be introduced, smaller concentrations might be as effective as high concentrations of currently used scrap rubbers. Digestion conditions could, however, become more important, and this would certainly be true if the product contained a high percentage of natural rubber. There is a need for a simple quality-control test to evaluate the deformation properties of rubber-asphalt digestions. In the interim, the bulk-density test and analysis of the composition of the rubber can be used as a guide to quality.

A separate test will be needed to indicate whether improved digestions can be sprayed by using conventional equipment and procedures. If spraying of these materials proves to be difficult, such a test could be used to evaluate the effectiveness of measures designed to improve sprayability. Since the process of forcing a viscoelastic fluid through an orifice under pressure to produce a regular flow pattern is not well understood, the best approach may be to simulate the field spraying condition in the laboratory. An apparatus has been constructed that allows rubber-asphalt digestions to be sprayed from a regular slotted jet nozzle at the pressure and temperature used in road sprayers. This apparatus will be commissioned shortly.

In Australia, as the demand for scrap rubber has increased, so has the price. It is possible that specially formulated synthetic polymers may soon become competitive. Dispersions in asphalt of one group of these materials, known as block copolymers, have the advantage of having very little effect on the asphalt at spraying temperatures but developing marked rubberlike properties through the formation of a network structure at service temperatures. New types of block copolymers are coming onto the market, and these should be evaluated to determine the minimum effective concentration in asphalt.

There is little information on the long-term durability of rubber-asphalt digestions, although they have given satisfactory service in Australia for more than five years now. Laboratory durability tests developed for asphalts (7) may not be appropriate for this type of material, but there could be a need to determine whether these modified asphalts maintain their elastic behavior under the long-term exposure of pavement service.

Road trials are planned in Australia to investigate the effect of concentration and type of rubber on long-term service performance of sprayed seals, both in high-traffic-stress situations and as overlays for cracked pavements.

## CONCLUSIONS

Modification of asphaltic cements by use of scrap rubber improves deformation response under traffic loading at high pavement temperatures and loading due to thermal contraction at low pavement temperatures. A simple and rapid laboratory test procedure was developed to assess the degree of improvement obtained from various rubbers and digestion procedures. This procedure is as near as practicable to the loading and straining conditions described above.

The major findings for digestions of scrap tire rubber in asphalt were as follows:

1. Rubber particle morphology, as determined by the process used to manufacture the particles, is the most important of the factors that affect the elastic properties of rubber-asphalt digestions. This morphology can be characterized by a simple bulk-density test.
2. Natural-rubber digestions tend to be superior

to those containing synthetic rubber, but digestion conditions (time and temperature) are less critical for synthetic rubber.

3. The elastic recovery of strain of the digestions is linearly related to the rubber concentration.

4. For car-tire retreader's buffings, the elastic recovery of the digestions tends to increase as the size of the rubber particles used decreases.

5. Little or no change in the elastic recovery of certain specimens was observed when they were stored at 55°C (which imitated curing over an extended period in road service).

ACKNOWLEDGMENT

This paper is presented with the permission of the executive director of the Australian Road Research Board. Views expressed in the paper are solely my own.

REFERENCES

1. C.H. McDonald. A New Patching Material for Pavement Failures. HRB, Highway Research Record 146, 1966, pp. 1-16.
2. G.R. Morris and C.H. McDonald. Asphalt-Rubber Stress-Absorbing Membranes: Field Performance and State of the Art. TRB, Transportation Research Record 595, 1976, pp. 52-48.
3. E.J. Dickinson and H.P. Witt. The Deformation Behaviour of Thin Films of Asphalt Confined Between Rigid Surfaces and Subjected to Rates of Loading Simulating Traffic Over a Pavement. Division of Petroleum Chemistry, American Chemical Society, Symposium on Science of Asphalt in Construction, preprint, Vol. 16, No. 1, 1971, pp. D156-D164.
4. E.J. Dickinson. Assessment of the Deformation and Flow Properties of Polymer-Modified Paving Bitumens. Australian Road Research, Vol. 11, No. 3, 1981, pp. 11-18.
5. J.D. Bethune. Use of Rubber in Bituminous Surfacing. Proc., 9th Conference of Australian Road Research Board, Vol. 9, No. 3, Session 24, 1978, pp. 9-32.
6. J.W.H. Oliver. A Bulk Density Test to Characterize the Morphology of Rubber Particles. Australian Road Research Board, Vermont, Victoria, Internal Rept. AIR 286-3, 1981.
7. E.J. Dickinson. The Hardening of Middle East Petroleum Asphalts in Pavement Surfacings. Proc., AAPT, Vol. 49, 1980, pp. 30-63.

*Publication of this paper sponsored by Committee on Characteristics of Nonbituminous Components of Bituminous Paving Mixtures.*

# Effect of Aggregate Top Size on Asphalt Emulsion Mixture Properties

MICHAEL S. MAMLOUK AND LEONARD E. WOOD

**Since base-course aggregate gradations have top sizes larger than 25.4 mm (1 in) in most cases, the adequacy of using the standard Marshall procedure in evaluating asphalt-stabilized base courses has been questioned. The findings of a comprehensive laboratory investigation that focused on the evaluation of the effect of aggregate top size on the Marshall test results of cold-mixed asphalt emulsion mixtures are reported. Marshall specimens were prepared by using a high-float asphalt emulsion, HFMS-2s, and aggregate top sizes of 19 and 38 mm (0.75 and 1.5 in). Other factors included in the study were asphalt emulsion content, aggregate type, and aggregate gradation. Marshall tests were performed at 22°C (72°F) to evaluate the mixture properties. Test results for such factors as stability, flow, stiffness, and index were obtained. Other mixture properties, such as specific gravity, air voids, retained moisture, and total liquid, were also evaluated. According to the test results, increasing the aggregate top size in the asphalt emulsion mixture from 19 to 38 mm increased the bulk specific gravity and decreased the air voids. The retained moisture and total liquid in the mixture after curing were not largely affected by the aggregate top size. The modified Marshall test results were altered to some extent by the change in aggregate top size. It is recommended that the effect of aggregate top size be taken into consideration when the standard Marshall procedure is used in designing asphalt emulsion mixtures with large aggregate top sizes.**

In recent years, a great deal of interest has been shown in, and much effort has been devoted to, the development of various types of stabilized materials for use in pavement construction. The use of asphalt emulsions as stabilizing agents has increased tremendously in the past two decades, precipitated by apparent economic and environmental benefits (1). Asphalt emulsions can be mixed at ambient temperatures, which saves both the cost and amount of fuel needed for hot mixes. Asphalt emulsion mixtures also eliminate the dust and combustion pollutants that result from the drying and mixing of the aggregate. In spite of their widespread use, the behavior of these mixtures has not been sufficiently well understood to enable the development and acceptance of a rational design procedure and set of criteria (2).

According to the standard preparation procedure of Marshall specimens [102 mm (4 in) in diameter by 64 mm (25 in) high], the aggregate top size should not exceed 25.4 mm (1 in). Since base-course aggregate gradations frequently have top sizes greater than 25.4 mm, the adequacy of the standard Marshall procedure in the design of asphalt-stabilized base courses has been questioned. This study reports the findings of a comprehensive laboratory investigation that focused on the evaluation of the effect of aggregate top size on the Marshall test results of cold-mixed asphalt emulsion mixtures. Two aggregate top sizes were used: 19 and 38 mm (0.75 and 1.5 in). One asphalt emulsion type, three asphalt emulsion contents, two aggregate types, and two aggregate gradations were included in the study. A modified Marshall test was used in the evaluation process. Marshall test results such as stability, flow, stiffness, and index were obtained at a test temperature of 22°C (72°F). Other mixture properties, such as specific gravity, air voids, and retained moisture, were also evaluated.

Figure 1. Aggregate gradations.

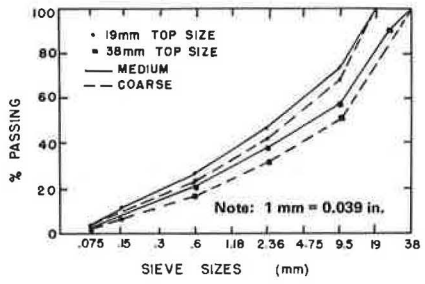


Table 1. Experimental design.

| Gradation | Asphalt Residue (%) | 19-mm Top Size: Sand and Gravel | 19-mm Top Size: Limestone | 38-mm Top Size: Sand and Gravel | 38-mm Top Size: Limestone |
|---|---|---|---|---|---|
| Medium | 2.5 | O | O | O | O |
| | 3.25 | X | X | X | X |
| | 4.0 | O | O | O | O |
| Coarse | 2.5 | O | O | O | O |
| | 3.25 | X | X | X | X |
| | 4.0 | O | O | O | O |

Note: O = two replicates and X = three replicates.

Figure 2. Autographic Marshall equipment.

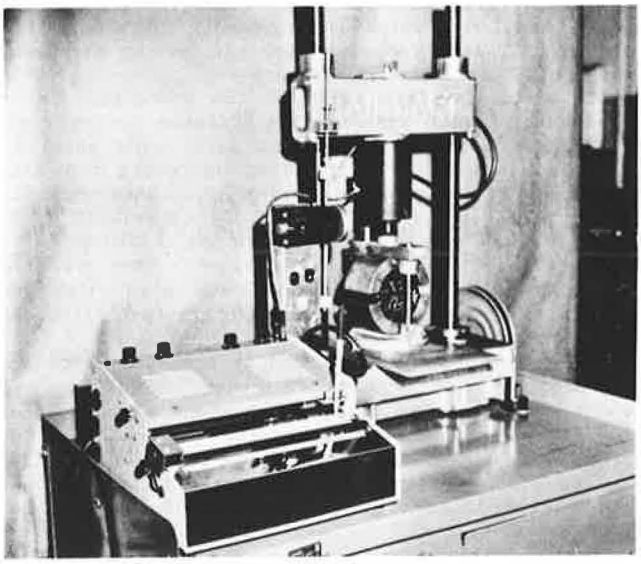

## MATERIALS

### Aggregate Types, Gradations, and Top Sizes

Two aggregate types were used in the study. The first type was totally a mixture of sand and gravel that consisted approximately of 50 percent calcareous and 50 percent siliceous pieces. About 60 percent of gravel particles retained on the 4.75-mm (no. 4) sieve had crushed faces. The second type was totally crushed limestone. Two aggregate gradations were used--a medium and a coarse gradation with a maximum size of 38 mm. The medium gradation followed the midspecification of the Indiana State Highway Commission (ISHC) no. 53-B gradation band. The coarse gradation was selected at the "quarter point", midway between the midpoint and the lower limit of the specification band. The two gradations were also scalped at the 19-mm sieve to provide similar aggregate gradations with a 19-mm top size. The scalped percentage was balanced over the remaining sizes, which changed the gradation curves as shown in Figure 1. Other properties of the aggregates are given below:

Figure 3. Marshall stability, flow, stiffness, and index.

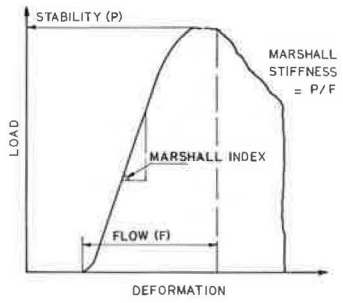


| Property | Sand and Gravel | Limestone |
|---|---|---|
| Apparent specific gravity | 2.710 | 2.741 |
| Bulk specific gravity | 2.644 | 2.696 |
| Absorption (%) | 1.560 | 1.280 |

### Asphalt Emulsion

A high-float asphalt emulsion of one type and grade was used: HFMS-2s (ASTM D977). The physical properties of the emulsion were as follows (25°C = 45°F):

| Property | Value |
|---|---|
| Saybolt Furol viscosity (s) | 50+ |
| Residue by distillation (%) | 70.0 |
| Penetration of residue after distillation (25°C, 5 s, 100 g) | 200+ |
| Specific gravity of residue after distillation (25°C) | 0.999 |

## SPECIMEN PREPARATION

Specimens 102 mm (4 in) in diameter and 64 mm (2.5 in) high were prepared according to the mix procedure suggested in previous studies (3,4). One initial added moisture content of 3 percent of the aggregate dry weight was used. Three asphalt emulsion contents were evaluated to provide residue contents of 2.5, 3.25, and 4 percent of the aggregate dry weight. Specimens were compacted at a room temperature of 22°C by using 50 blows of a standard Marshall hammer on each side of the specimens. Either two or three replicate specimens were prepared for each factor combination (see Table 1). All specimens were cured for three days at room temperature.

### Testing Procedure

After specimens were cured, the bulk specific gravity was determined according to ASTM D2726. Specimens were tested at a room temperature of 22°C by using the Marshall equipment shown in Figure 2. The machine was connected to a chart recorder to provide a continuous recording of load versus deformation throughout the test (see Figure 3). The modified Marshall stability and Marshall flow were determined according to standard American Society for Testing and Materials (ASTM) procedure except for test temperature. Two other parameters were also obtained--Marshall stiffness and Marshall index (3,4). Marshall stiffness is defined as the ratio between Marshall stability and flow, and Marshall

index is the slope of the linear portion of the load versus deformation trace. Other properties of the mixture, such as density, voids content, and moisture content at time of testing, were evaluated. After the test was completed, specimens were broken apart and dried and the oven-dry bulk specific gravities were obtained.

Statistical analysis was performed on the data to determine the effect of aggregate top size on the asphalt emulsion mixture properties as well as Marshall test results. Other factors, such as aggregate type, aggregate gradation, and asphalt emulsion content, were also evaluated. A level of significance of 5 percent was used throughout the analysis.

## ANALYSIS OF STUDY RESULTS

### Specific Gravity and Air Voids

The specific gravity of the asphalt emulsion mixture is a useful parameter for the mixture evaluation. In this study, specific gravity was used to measure the effect of changes in the mixture ingredients. High specific gravities of the mixture are recommended in order to reduce further compaction by traffic, which results in rutting of the pavement. High specific gravities also reduce moisture absorption, which affects the potential of stripping. On the other hand, a certain amount of air voids in the mixture is needed to enhance the rate of curing of the mixture and to improve drainage.

Two types of specific gravities were evaluated: the air-cured bulk specific gravity at time of testing and the oven-dry bulk specific gravity. According to the test results, the aggregate top size had a marked effect on the air-cured bulk specific gravity of the specimens. Large top-size aggregates provided higher values of air-cured specific gravity than small top-size aggregates, as Figure 4 shows. The average air-cured specific gravities of all specimens in the study were 2.258 for the 19-mm top-size aggregates and 2.304 for the 38-mm top-size aggregates. This effect was more apparent for the limestone mixtures than for the sand and gravel mixtures. In addition, the air-cured specific gravities of mixtures with 19- and 38-mm top sizes were highly correlated. The correlation coefficient between the two variables was 0.953 for all mixtures included in the study.

Figure 4. Air-cured bulk specific gravity of mixtures with 19- and 38-mm aggregate top sizes.

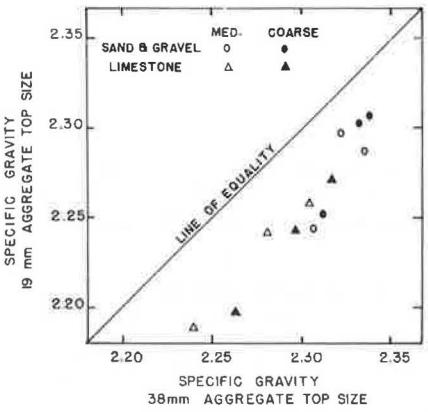


Figure 5. Air voids of mixtures with 19- and 38-mm aggregate top sizes.

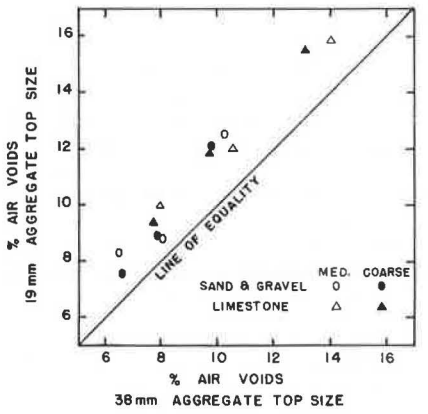


On the other hand, asphalt emulsion content showed a significant effect on the air-cured bulk specific gravity of the specimens. Increasing the asphalt emulsion content in the mixture fills the voids among aggregate particles and also allows for more compaction to occur due to lubrication. Therefore, higher percentages of asphalt emulsion content increase the bulk specific gravity of the mixture. At 2.5, 3.25, and 4 percent asphalt residue contents, average values of 2.251, 2.290, and 2.302 of air-cured specific gravities were obtained, respectively. In addition, the sand and gravel mixtures provided a larger average specific gravity than the limestone mixtures.

The oven-dry bulk specific gravity of specimens followed the same general pattern as the air-cured specific gravity. Mixtures with large aggregate top sizes had high values of oven-dry bulk specific gravity. This effect was apparent in all mixtures, especially the limestone mixtures.

The amount of air voids in the compacted specimens after curing was markedly affected by aggregate top size. Small percentages of air voids were obtained for mixtures with 38-mm aggregate top size compared with mixtures with 19-mm aggregate top size (see Figure 5). A correlation coefficient of 0.987 was obtained between air voids for mixtures with small and large aggregate top sizes. Moreover, the air voids showed trends highly correlated with, and almost the reverse of, those for the air-cured specific gravity.

The air voids were affected by aggregate type and asphalt emulsion content. Larger values of air voids were obtained for the limestone mixtures than for the sand and gravel mixtures. In addition, increasing the asphalt emulsion residue content from 2.5 to 3.25 and 4 percent decreased the average air voids from 12.887 to 9.730 and 8.001 percent, respectively.

### Retained Moisture and Total Liquid

The moisture included in the asphalt emulsion mixture comes from the water added during the initial mixture preparation as well as the moisture included in the asphalt emulsion itself. The moisture portion is very important in the preparation of the cold-mixed asphalt emulsion mixture because it increases the workability of the mix and provides a uniform coating of asphalt residue on the aggregates. However, a large amount of moisture has an adverse effect on the mixture and reduces the strength. During the curing process the water evaporates, leaving the asphalt residue adhering to the aggregate. The rate of strength development of the asphalt emulsion mixture is directly related to the rate at which the mixture loses moisture.

The effect of aggregate top size did not show a significant influence on the amount of moisture retained in the compacted specimens after curing.

Both mixtures with small and large aggregate top sizes gave approximately the same moisture content values for the corresponding cases, as shown in Figure 6. The average retained moisture was 1.109 percent of the aggregate dry weight for mixtures with 19-mm aggregate top size, whereas the corresponding value for mixtures with 38-mm aggregate top size was 1.032 percent.

Aggregate type and gradation did not change the amount of retained moisture in the mixture to a large extent. On the other hand, mixtures with high asphalt emulsion contents had low air-void contents, which resulted in the reduction of moisture loss from the specimens during curing. In addition, increasing the asphalt emulsion content increased the initial water content in the mixture because of the water included in the asphalt emulsion itself. Average values of retained moisture were 0.70, 1.16, and 1.35 percent for mixtures with 2.5, 3.25, and 4 percent asphalt residue contents, respectively.

The total liquid in the compacted specimens after curing is one of the characteristics used frequently in the evaluation of asphalt emulsion mixes. The liquid content in the mixture is the sum of the asphalt emulsion residue content and the amount of retained moisture. In this study, the total liquid content was not largely affected by the changes in the aggregate top size. The average total liquid content was 4.36 percent of the aggregate dry weight for all mixtures with the small-sized aggregate and 4.28 percent for mixtures with the large-sized aggregate. The influence of change of aggregate top size is illustrated in the following table:

| Aggregate | Total Liquid (%) | |
|---|---|---|
| Top Size (mm) | Sand and Gravel | Limestone |
| 19 | 4.318 | 4.399 |
| 38 | 4.217 | 4.347 |

The total liquid content, like the retained moisture content, was also affected by other factors.

## Marshall Stability and Flow

The Marshall test is commonly used to characterize hot-mixed asphalt mixtures (the test has not been standardized for cold-mixed asphalt emulsion mixtures). In this investigation, Marshall stability and flow values of the mixture were obtained at room temperature. The effect of aggregate top size on the modified Marshall test results was evaluated.

In most cases (see Figure 7), mixtures with a 19-mm top-size aggregate resulted in higher modified Marshall stability values than mixtures with 38-mm top-size aggregate. However, the difference between these values for the two mixtures was not large. An average stability value of 6.09 kN (1370 lbf) was obtained for specimens with small top-size aggregate, whereas the average value for specimens with large top-size aggregate was 5.76 kN (1296 lbf).

Other factors in the study showed some effects on the modified Marshall stability. The crushed limestone mixes achieved a significantly higher stability than the sand and gravel mixes in spite of their lower specific gravities. Both aggregate types, however, showed the same trends in stability values for the different asphalt emulsion contents. The interaction effect of the different factors is shown in Figure 8. A peak stability was obtained at the middle asphalt emulsion content level. As the figure shows, the asphalt emulsion content variable is influential for all mixes except those with 38-mm limestone aggregate.

The modified Marshall flow did not show a consistent trend for the two aggregate top sizes (see Figure 9). Although mixes with the large top-size aggregate had slightly higher flow values than those with the small top-size aggregate, the difference was not great. Due to the variability of the data, aggregate type, aggregate gradation, and asphalt emulsion content did not show a marked effect on the flow values. The largest flow values were obtained for mixes with 38-mm aggregate top size, coarse gradation, and 2.5 percent asphalt emulsion residue.

Figure 7. Modified Marshall stability of mixtures with 19- and 38-mm aggregate top sizes.

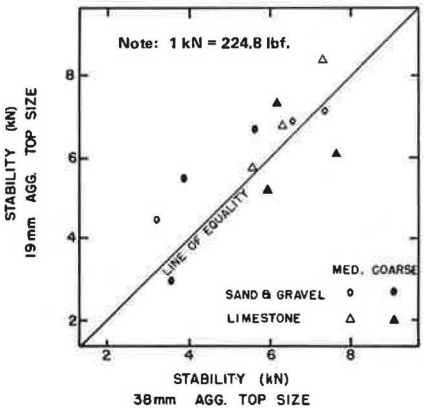


Figure 6. Retained moisture of mixtures with 19- and 38-mm aggregate top sizes.

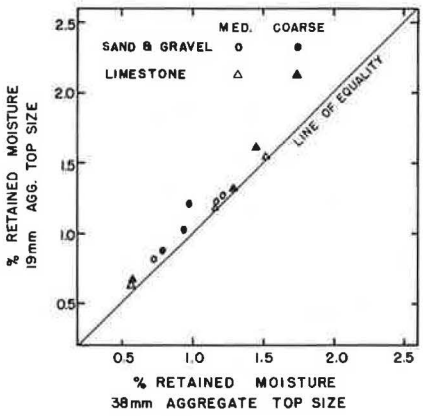


Figure 8. Effect of aggregate top size, type, and gradation and asphalt emulsion content on Marshall stability.

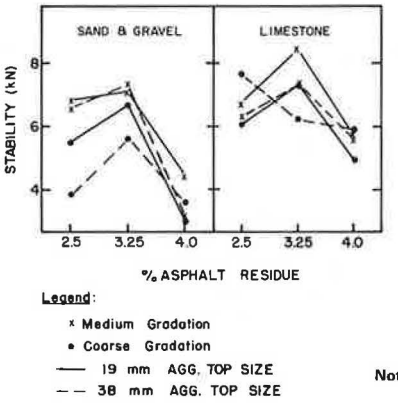

Figure 9. Modified Marshall flow of mixtures with 19- and 38-mm aggregate top sizes.

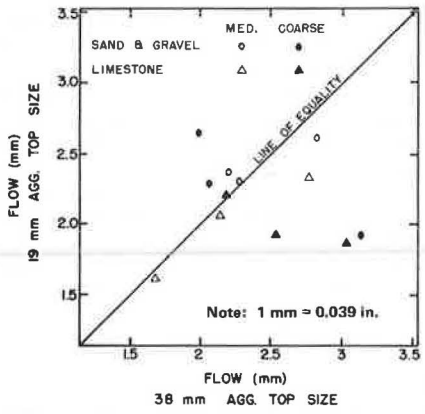


Figure 10. Marshall stiffness of mixtures with 19- and 38-mm aggregate top sizes.

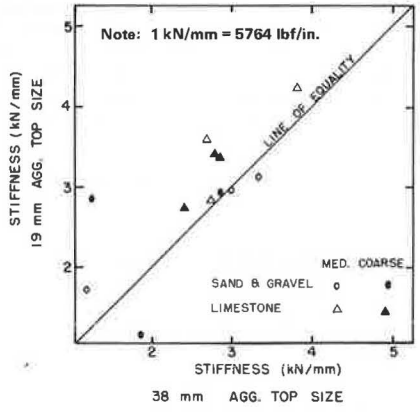


## Marshall Stiffness and Index

Mixtures with the small top-size aggregate resulted in larger Marshall stiffness values than mixtures with large top-size aggregate in most cases, as shown in Figure 10. Average Marshall stiffness values of 2.98 and 2.63 kN/mm (17 000 and 15 000 lbf/in) were obtained for mixtures with small and large top-size aggregates, respectively. In addition to aggregate top size, larger Marshall stiffness values were obtained for limestone mixes than for sand and gravel mixes. In addition, asphalt emulsion content showed some effect on the Marshall stiffness. Large values of stiffness were obtained for 2.5 and 3.25 percent asphalt emulsion residues in comparison with 4 percent residues. Moreover, medium-graded mixtures resulted in larger stiffness values than coarse-graded mixtures in almost all cases.

The Marshall index showed the same trend as the stiffness values, although the pattern was slightly different. There was no consistent trend in aggregate top size for the different factor combinations. However, large index values were obtained for limestone mixtures compared with the corresponding values for sand and gravel mixtures. In addition, increasing the asphalt emulsion residue content from 2.5 to 3.25 and 4 percent resulted in a decrease in the index values in most cases. The average Marshall index values of specimens with 19- and 38-mm aggregate top sizes for the two types of aggregates are given below:

| Aggregate Top Size (mm) | Marshall Index | |
|---|---|---|
| | Sand and Gravel | Limestone |
| 19 | 4.530 | 7.121 |
| 38 | 4.349 | 9.048 |

## SUMMARY AND CONCLUSIONS

A comprehensive laboratory investigation was performed to evaluate the performance of cold-mixed asphalt emulsion mixtures used in black bases. The study concentrated on the influence of aggregate top size on the mixture characteristics. The effect of aggregate type, aggregate gradation, and asphalt emulsion content was also investigated. A modification of the Marshall test was used in the study. Marshall stability, flow, stiffness, and index were obtained at room temperature (approximately 22°C). Other mixture parameters were also evaluated, such as specific gravity, air voids, retained moisture, and total liquid after curing.

Based on the results of the study, some conclusions were derived. Increasing the aggregate top size in the asphalt emulsion mixture from 19 to 38 mm increased both the air-cured and oven-dried bulk specific gravities and decreased the amount of air voids. The retained moisture and total liquid in the mixture after curing were not largely affected by the aggregate top size. At the same time, modified Marshall stability, flow, stiffness, and index were altered to some extent by the change in aggregate top size. Therefore, the effect of aggregate top size should be taken into consideration when the standard Marshall procedure is used in designing asphalt emulsion mixtures with large aggregate top sizes.

The results of this study serve several purposes. They provide highway engineers with a better understanding of the influence of different factors on the design parameters and properties of asphalt-emulsion-treated mixtures by use of Marshall equipment. Furthermore, the results provide additional design parameters that could be used in conjunction with the conventional parameters for the Marshall method of mix design to better control the mixture properties.

## ACKNOWLEDGMENT

The work reported in this paper is based on a study performed by Bradley V. Saxton as a part of his master's degree requirements at Purdue University (5). Financial support from the Joint Highway Research Project at Purdue University, ISHC, and the Federal Highway Administration is duly acknowledged. Appreciation is also extended to those who helped in preparing the graphs and typing the manuscript. The contents of this paper reflect our views, and we are responsible for the facts and the accuracy of the data presented.

## REFERENCES

1. Bitumuls Mix Manual. Chevron Asphalt Co., San Francisco, 1977.
2. G.K. Fong. Mix Design Methods for Base and Surface Courses Using Emulsified Asphalt: A State-of-the-Art Report. FHWA, Rept. FHWA-RD-78-113, 1978.
3. A.A. Gadallah, L.E. Wood, and E.J. Yoder. A Suggested Method for the Preparation and Testing of Asphalt Emulsion Treated Mixtures Using Marshall Equipment. Proc., AAPT, Vol. 46, 1977.
4. M.S. Mamlouk and L.E. Wood. A Laboratory Evaluation of Asphalt Emulsion Mixtures Using the Marshall and Indirect Tensile Tests. TRB, Transpor-

tation Research Record 754, 1980, pp. 17-22.
5. B.V. Saxton. A Laboratory Evaluation of the Influence of Crushed Stone, Aggregate Top-Size, and Binder Type on AETM Properties. Joint Highway Research Project, Purdue Univ., West Lafayette, IN, JHRP-77-9, 1977.

*Publication of this paper sponsored by Committee on Characteristics of Bituminous Paving Mixtures to Meet Structural Requirements.*

# Overview of Pay-Adjustment Factors for Asphalt Concrete Mixtures

RICHARD M. MOORE, JOE P. MAHONEY, R.G. HICKS, AND JAMES E. WILSON

**In the fall of 1979, the Oregon State Highway Division and Oregon State University, with participation from the University of Washington, initiated a research project to study the impact of variations in material properties on asphalt pavement life. The study is aimed at developing a rational approach to assessing the effects of variations from specification limits so that a firm basis can be established for the development of pay factors. To collect information on the status of quality-control procedures and the use of pay-adjustment factors, a questionnaire was distributed to all state agencies, the District of Columbia, and the Federal Highway Administration. Each agency was asked to respond to questions on their current method for acceptance or rejection of asphalt concrete paving materials and related pay-adjustment factors. The results of the questionnaire are summarized. Analysis of the results indicates the following: (a) Most state agencies will accept one or more property characteristics of asphalt concrete that are outside specification tolerances, (b) most state agencies apply a pay-adjustment factor to accepted materials that are outside specification tolerances, (c) only 26 percent of the state agencies consider their pay factors to be proportional to reduced pavement serviceability, (d) approximately half of the agencies consider pay-factor plans to be effective in encouraging compliance with specifications, and (e) there is a wide disparity in the pay-adjustment factors used by the different agencies.**

In the fall of 1979, the Oregon State Highway Division and Oregon State University initiated a research project to study the impact of variations in material properties on asphalt pavement life. The University of Washington is cooperating in the study with Oregon State University. The questionnaire was prompted by an increase in the occurrence of pavement problems during recent years and in the proportion of pavements constructed with a significant amount of material outside of specification limits (1). The effect of construction noncompliance on pavement serviceability has been questioned by highway agencies and has resulted in frequent controversy with contractors on the assessment of pay adjustments. The general result is reduced pay to the contractor for material that is determined to be outside the specification tolerances. The current study is aimed at developing a rational approach to assessing the effects of variations from specification limits so that a firm basis can be established for the development of pay factors.

The American Association of State Highway Officials (AASHO) Road Test (1958-1960) emphasized to the highway industry the significance of the relation of the variability of material test properties to highway specifications (2). As a result, many agencies have been developing and experimenting with various combinations of statistically based specifications to provide a more accurate evaluation of the end products and to allow acceptance of noncompliance work in conjunction with a reduced payment for that work. In 1976, 33 states were using or had tried some form of statistically oriented end-result specification (3).

In an effort to collect current information on the status of quality-control procedures and the use of pay-adjustment factors, a questionnaire was developed and distributed to all state agencies, the District of Columbia, and the Federal Highway Administration (FHWA) in November 1979. Questionnaires were returned by all except four states (a 92 percent response rate). Each agency was asked to respond to seven questions concerning their current method for acceptance or rejection of asphalt concrete paving materials. The items of emphasis on the questionnaire included

1. Acceptance of noncompliance construction and materials with or without pay adjustments,
2. Identification of properties tested for acceptance and the method of test used,
3. Pay-adjustment factors used in relation to each tested property,
4. Rationale used in establishing pay-adjustment factors,
5. Relation of pay-adjustment factors to pavement serviceability or other criteria,
6. Effectiveness of pay-adjustment factors in encouraging compliance with specifications, and
7. Summary opinions regarding the use of pay adjustments.

Although the required information could be placed on the questionnaire, the states were encouraged to include copies of supplemental information that would assist in the overall evaluation. Most states did provide supplemental materials.

Although emphasis in this paper is placed on the results of current state practice, a rational approach is presented and discussed that shows significant promise in developing pay factors. The rational development of pay factors is based on selected material properties that can be developed in the laboratory. Preliminary test results and corresponding pay factors are shown for one recent paving project constructed in the state of Oregon.

## QUESTIONNAIRE RESULTS

Seven primary questions were contained in the questionnaire. The responses received for each of these questions are discussed below.

### Acceptance of Below-Specification Work and Materials

Question 1 was, Do you accept asphalt concrete pavement construction and materials that do not satisfy specification requirements? The responses to this question are summarized below:

| Response | Agencies No. | Percent |
|---|---|---|
| Will not accept | 4 | 9 |
| Accept without pay adjustment | 4 | 9 |
| Accept with pay adjustment | 30 | 64 |
| Combination acceptance | 9 | 18 |
| Total | 47 | |

Of the 47 agencies that responded, only 4 indicated that they do not accept construction work or materials that are below specification. All of the remaining agencies (91 percent) accept some aspects of the work or materials when they are below specifications. "Combination acceptance" indicates acceptance of some deficient materials with pay adjustment and some without.

The key concept illustrated is that 82 percent of the agencies use some form of pay-adjustment factors when accepting one or more of the evaluated criteria. However, only four states indicated a possible acceptance of below-specification work or materials on every evaluated property considered in the questionnaire. All other agencies identified certain criteria that would not be accepted if below specification limits. A detailed discussion of these criteria is included in the analysis of questions 2 and 3 of the questionnaire. The 18 percent labeled "combination acceptance" indicates agencies that accept below-specification work and materials by using a combination of pay adjustment and no pay adjustment, depending on the criteria being considered.

## Properties Evaluated to Determine Pavement Acceptability

Question 2 was, What properties do you evaluate to establish the acceptability of an asphaltic pavement? The questionnaire listed eight properties commonly evaluated during or after completion of construction. These properties were thickness, smoothness, compaction, asphalt content, asphalt properties, aggregate quality, mix moisture content, and mix gradation. Each agency was asked to identify which properties are evaluated and controlled by their specifications and to indicate the method of testing used. The table below summarizes data received concerning which properties are evaluated:

| Property | Agencies That Test Property No. | Percent |
|---|---|---|
| Thickness | 31 | 66 |
| Smoothness | 37 | 79 |
| Compaction | 43 | 91 |
| Asphalt content | 43 | 91 |
| Asphalt properties | 44 | 94 |
| Aggregate quality | 39 | 83 |
| Mix moisture content | 21 | 45 |
| Mix gradation | 45 | 96 |

The data for the method of testing are discussed in conjunction with question 3, which deals with the use of pay factors. All property criteria except mix moisture content are evaluated by at least two-thirds of the agencies.

## Pay-Adjustment Factors for Properties Evaluated

Question 3 was, What are your pay-adjustment factors for each of the properties identified in question 2? The data summaries that relate to pay-adjustment factors and methods of testing are given in the tables that follow. Each table deals with a different property, and each is discussed individually.

A review of the questionnaire results indicates that the basis for applying pay factors can be broken down into the following five categories:

1. Statistical--The concepts of random sampling are used in collecting test data. The statistical methods used to evaluate the measurements can include the use of simple averaging, a range of measurements, the normal distribution, and the Student's t-distribution.
2. Guide in specification--The agency makes use of a pay-adjustment-factors guide, usually in tabular form, which is part of the specification in which statistical methods are not used.
3. Schedule (not in specification)--The agency has established guidelines for use in applying pay factors, but they are not a part of the specifications. For example, one state has a "price adjustment committee", which determines pay adjustments for each case individually. The state has a guide to pay factors, which may be used at the committee's discretion.
4. None--Since materials below specification are not accepted, no pay factors are involved.
5. Negotiated--The agency accepts below-specification work and materials based on negotiations with the contractor. These negotiations include pay adjustment.

It is important to note that many of the agencies that make use of pay-adjustment factors retain a process of decision making by the agency's project engineer. The pay factors are applied only if the below-specification work or material is accepted.

### Thickness

The questionnaire information on thickness evaluation is summarized below:

| Item | Agencies That Use Method No. | Percent |
|---|---|---|
| Test method | | |
| Cores | 23 | 74 |
| Other depth measurements | 8 | 26 |
| Basis of pay factors | | |
| Statistical | 5 | 16 |
| Guide in specification | 7 | 23 |
| Schedule | 2 | 6 |
| None | 14 | 45 |
| Negotiated | 3 | 10 |

Thirty-one agencies evaluate the thickness of the finished pavement, and 74 percent of this total use cores in measurement of the final thickness. The remaining agencies use other methods, such as measuring the uncompacted thickness at the paver and applying a predetermined coefficient based on density to determine final thickness. Although it is not indicated, all state agencies probably evaluate this property either by direct or indirect evaluation procedures.

Almost half of the agencies do not accept a pavement thickness below specification tolerances. Most of these agencies specify that an overlay is required to bring the thickness up to specification, the contractor assuming all costs. The remaining agencies accept final thicknesses that are below specification in conjunction with some form of pay adjustment.

### Smoothness

The table below summarizes the questionnaire data regarding smoothness:

| Item | Agencies That Use Method No. | Percent |
|---|---|---|
| Test method | | |
| Straightedge | 26 | 70 |
| Profilograph | 4 | 11 |
| Roadmeter | 3 | 8 |
| Not identified | 4 | 11 |
| Basis of pay factors | | |
| Statistical | 6 | 16 |
| Guide in specifications | 6 | 16 |
| Schedule | 4 | 11 |
| None | 18 | 49 |
| Negotiated | 3 | 8 |

Thirty-seven of the agencies evaluate the smoothness of the finished pavement surface. Of these, 70 percent use a straightedge as the basis of their measurements, 11 percent did not identify a method of testing, and the remaining 19 percent use either the profilograph or roadmeters such as the Portland Cement Association (PCA) Roadmeter.

As in the case of the thickness evaluations, approximately half of the agencies accept pavements that do not meet the smoothness specification tolerances. Most of these apply a pay-adjustment factor to account for the increased maintenance requirements. The other half of the agencies do not accept pavement surfaces outside the tolerance limits, but most of them allow a contractor to bring the surface up to specification with placement of an overlay at the contractor's expense.

## Compaction

The results of the questionnaire data on compaction are given below:

| Item | Agencies That Use Method No. | Percent |
|---|---|---|
| Test method | | |
| Nuclear gage | 26 | 60 |
| Cores | 3 | 7 |
| Procedure specification | 4 | 9 |
| Other AASHTO | 8 | 19 |
| Not identified | 2 | 5 |
| Basis of pay factors | | |
| Statistical | 11 | 26 |
| Guide in specification | 11 | 26 |
| Schedule | 3 | 7 |
| None | 16 | 37 |
| Negotiated | 2 | 5 |

Of the 43 agencies that evaluate compaction, 60 percent use nuclear gage methods and 7 percent use pavement cores. The 9 percent that use their own procedural specification gave detailed procedures of the test requirements without reference to any of the standard test methods.

Almost two-thirds of the agencies accept pavement sections that have not been compacted to specification requirements. Note that both statistically and nonstatistically based pay-adjustment factors are used equally. Although 37 percent of the agencies indicated they would not accept pavement that was improperly compacted, the available information was insufficient to identify the procedures used to remedy the deficiency.

## Asphalt Content

The testing methods used and the basis for the pay-adjustment factors that are applied when below-specification material is accepted are summarized below:

| Item | Agencies That Use Method No. | Percent |
|---|---|---|
| Test method | | |
| Extraction | 32 | 74 |
| Tank sticking | 3 | 8 |
| Procedure specification | 7 | 16 |
| Not identified | 1 | 2 |
| Basis of pay factors | | |
| Statistical | 17 | 40 |
| Guide in specification | 6 | 14 |
| Schedule | 3 | 6 |
| None | 15 | 35 |
| Negotiated | 2 | 5 |

Forty-three of the agencies evaluate asphalt content, and 74 percent of these use extraction methods. The remaining agencies use other methods, such as tank sticking.

Approximately one-third of the agencies do not accept material outside the tolerance limits of the specifications. Most of those agencies check the asphalt content on a regular basis during construction so that adjustments can be readily made without great losses of time or materials. Therefore, pay adjustments are often not needed. The majority of the agencies accept materials that have asphalt contents outside specification tolerances. The most commonly used basis for pay-adjustment factors among these agencies is statistical in nature.

## Asphalt Properties

Forty-four agencies, or 94 percent of those that responded to the questionnaire, provide for the evaluation of the asphalt properties in their specifications. A summary of the test methods and pay-adjustment factors used by these agencies is given below:

| Item | Agencies That Use Method No. | Percent |
|---|---|---|
| Test method | | |
| Producer test | 10 | 23 |
| Agency test | 31 | 70 |
| Not identified | 3 | 7 |
| Basis of pay factors | | |
| Statistical | 8 | 18 |
| Guide in specification | 13 | 30 |
| Schedule | 3 | 7 |
| None | 16 | 36 |
| Negotiated | 4 | 9 |

The majority (70 percent) use a combination of various American Association of State Highway and Transportation Officials (AASHTO) test methods to evaluate the individual characteristics of the asphalt.

Slightly more than one-third of the agencies do not accept asphalt that has properties outside the specification tolerances. These agencies evaluate the properties before the asphalt is used in mixes; thus, unacceptable asphalt can be rejected with little loss in time or money. The remaining two-thirds of the agencies accept asphalt that has properties that do not meet specification tolerances. The majority of these have a pay-factor guide in their specifications, but only 18 percent base their pay factors on statistical concepts.

## Aggregate Quality

Thirty-nine of the agencies that responded provide for evaluation of aggregate quality in their specifications. Several agencies indicated that they do

not evaluate the aggregate quality as part of the contractor's specifications because the aggregate source is supplied by the state. The test methods and the basis of the pay factors currently used are summarized below:

| Item | Agencies That Use Method No. | Percent |
|---|---|---|
| Test method | | |
| Approved source | 9 | 23 |
| AASHTO | 28 | 72 |
| Not identified | 2 | 5 |
| Basis of pay factors | | |
| Statistical | 3 | 8 |
| Guide in specification | 2 | 5 |
| Schedule | 4 | 10 |
| None | 27 | 69 |
| Negotiated | 3 | 8 |

Of those agencies that evaluate aggregate quality, 72 percent make use of AASHTO test procedures.

More than two-thirds of the agencies do not accept aggregate below specification quality. Since most testing is completed prior to delivery of material to the construction site, there is seldom a need to accept inferior aggregate. For the few situations in which below-specification aggregate is accepted, there is no dominant method of developing pay-adjustment factors.

### Mix Moisture Content

Less than half (21) of the agencies evaluate the mix moisture content as part of their specifications. The test methods and the basis for pay factors used by these agencies are summarized below:

| Item | Agencies That Use Method No. | Percent |
|---|---|---|
| Test method | | |
| Modified AASHTO | 7 | 33 |
| Standard moisture test | 11 | 52 |
| Not identified | 3 | 15 |
| Basis of pay factors | | |
| Statistical | 1 | 5 |
| Guide in specification | 1 | 5 |
| Schedule | 1 | 5 |
| None | 15 | 71 |
| Negotiated | 3 | 14 |

Very little information relating to test methods was given in the responses on mix moisture content. Most of the agencies simply indicated the use of standard moisture tests.

Of the agencies that use mix moisture content as a specification criterion, 71 percent do not accept material outside the tolerance limits of the specifications. This is a property that can be controlled during the construction process, often with little loss in time or materials, so that no pay adjustments are necessary. For the few situations in which below-specification materials are accepted, there is no dominant method of developing pay-adjustment factors.

### Mix Gradation

All but 2 of the 47 agencies that responded evaluate mix gradation as part of their acceptance criteria. A summary of the questionnaire results concerning the test methods and basis for pay factors used in evaluating mix gradation is given below:

| Item | Agencies That Use Method No. | Percent |
|---|---|---|
| Test method | | |
| AASHTO | 35 | 78 |
| Own test | 7 | 15 |
| Not identified | 3 | 7 |
| Basis of pay factors | | |
| Statistical | 18 | 40 |
| Guide in specification | 8 | 18 |
| Schedule | 2 | 4 |
| None | 14 | 31 |
| Negotiated | 3 | 7 |

Most of the agencies use an extraction test followed by a sieve analysis.

Slightly more than two-thirds of the agencies accept mixes that have gradations that do not satisfy specification tolerances. Of these, the majority base their pay-adjustment factors on statistical concepts. The 31 percent that do not accept below-specification mixes indicated that they control the gradation during material preparation. This allows rejection and modification of mixes on a continuing basis, which results in small losses of time or material. Therefore, no pay factors are necessary.

### Method of Establishing Pay-Adjustment Factors

Question 4 was, How were your pay-adjustment factors established? This question was used in an effort to identify the background for justification and development of pay-adjustment factors. The four categories listed were laboratory results, field studies, experience, and other. Each agency indicated which categories they relied on in accepting below-specification work or materials and determining the pay adjustments. The table below summarizes the background characteristics used by the various agencies in their specification development:

| Method | Agencies That Use Method No. | Percent |
|---|---|---|
| Laboratory results | 8 | 17 |
| Field studies | 11 | 23 |
| Experience | 28 | 60 |
| Other | 11 | 23 |
| Pay factors not used | 10 | 21 |

Sixty percent of the agencies indicated that experience is predominant in the development of pay factors. The remaining background categories are about equally used by the agencies. Since several agencies have relied on more than one background category, the total percentage is greater than 100 percent of the 47 agencies responding.

It should also be noted that a fifth category is added to the results in the preceding table to account for those agencies that do not use pay factors. The 21 percent given includes the four agencies that do not accept anything below specification and the six agencies that occasionally accept one or more properties below specification on a negotiated basis.

### Relation Between Pay Adjustment and Pavement Serviceability

Question 5 was, Is your pay adjustment proportional to the value of the reduction in pavement serviceability resulting from specification noncompliance? This question (as well as questions 6 and 7) required the person who responded to the questionnaire to express an opinion on behalf of his or her agency. It is important to note that, since opin-

ions vary within agencies, the response from an agency may be a function of who answered the questionnaire. Therefore, the corresponding data and figures should not be considered absolute agency policy.

The following table summarizes the responses regarding the relation of pay factors and pavement serviceability:

| | Agencies | |
|---|---|---|
| Response | No. | Percent |
| Yes | 12 | 26 |
| No | 23 | 48 |
| No response | 12 | 26 |

Twenty-six percent of the agencies indicated that they believed their pay adjustments to be proportional to reduced pavement serviceability. However, several of those agencies also indicated that they used engineering judgment and experience to develop that rationale and that they could not verify it in terms of engineering principles. Forty-eight percent of the agencies claim little relation between their pay factors and pavement serviceability, and the remaining 26 percent did not respond to this question.

The responses to the second part of this question, in which other rationales for establishing pay-adjustment factors were identified, are summarized below:

| | Agencies That Use Rationale | |
|---|---|---|
| Rationale | No. | Percent |
| Cost of replacement | 4 | 17 |
| Discourage noncompliance | 7 | 30 |
| Estimate effect on pavement life | 3 | 13 |
| Recommendation of FHWA | 5 | 22 |
| Cost of production | 1 | 4 |
| Cost of quality control | 1 | 4 |
| Pay factors not used | 2 | 10 |

The 23 agencies that responded "no" on the first question gave six different rationales for determining pay factors. Thirty percent use pay factors in their specifications to discourage noncompliance. Another 22 percent are following recommendations made in standard specifications of FHWA.

### Effectiveness of Pay Factors in Encouraging Compliance with Specifications

Question 6 was, Do you feel your pay-adjustment factors are effective in encouraging compliance with specifications? The responses to this question are summarized below:

| | Agencies | |
|---|---|---|
| Response | No. | Percent |
| Yes | 25 | 53 |
| No | 8 | 17 |
| Don't know | 5 | 11 |
| No response | 9 | 19 |

Slightly more than half of the agencies indicated that they felt their pay-adjustment factors to be effective in encouraging compliance with specifications, whereas 17 percent do not feel they are effective.

### Agency Opinion on Pay Adjustments and Other Acceptance Methods

Question 7 was, Summarize your opinion regarding the need for pay adjustments or the success of your method for acceptance of paving materials. The opinions given in answer to this question cover the full spectrum, from "don't believe in pay factors" to "end-result specifications are the way to go". The wide range of positive and negative comments and the lack of agreement among agencies illustrate the controversial nature of this topic and the need to develop a rationale that is consistent with engineering principles acceptable to a majority of the agencies and equitable to all parties. Some of the advantages of the pay-adjustment method identified by the responding agencies are that it (a) induces contractors to improve quality control, (b) creates a uniform procedure for accepting work that does not comply with specifications, (c) reduces problems associated with contract administration, (d) reduces litigation, and (e) requires fewer state personnel.

Among the disadvantages of the method are that (a) it needs to be based on sound engineering approaches, (b) contractors resist, (c) contractors may increase bids, (d) it may result in poor-quality work if pay factors are not severe, (e) it cannot measure reduced serviceability, and (f) it can cause administration problems.

## EXAMPLES OF CURRENTLY USED PAY FACTORS

In responding to question 3 of the questionnaire, each agency was requested to identify pay-adjustment factors for the eight properties listed (thickness, smoothness, compaction, asphalt content, asphalt quality, mix moisture content, and mix gradation). A majority of the states included either a tabulation of their current pay factors or partial sections from their specifications. Some of the agencies did not submit detailed information. With this in mind, examples and comparisons of pay factors for the two material properties of compaction and asphalt content are presented. These two factors are selected because of their relative importance in the production of quality asphalt concrete and to reduce the number of properties discussed to provide an overview of the kind of data received and summarized. Detailed presentations of pay-factor information will be available in a subsequent project report.

There are several general considerations that affect the application of pay-adjustment factors regardless of the property being evaluated. These considerations include lot size, the identification of contract pay items affected by pay adjustments, and the effects of multiplicative relations of pay adjustments. As important as these considerations are, a detailed treatment is not provided in this paper.

### Compaction

Twenty-three state agencies submitted information on their use of pay-adjustment factors for noncompliance with compaction requirements. There is a wide disparity between the agencies: Ten different approaches are used to determine level of compaction. In addition, the agencies that use the same approach have widely varying values for a pay factor applied to a common level of compaction. Table 1 gives the 10 approaches used and the number of agencies that use each approach.

There is little value in comparing the various approaches and their effect on the contract unit price unless the actual, required data necessary for each are obtained on a common sample. Unfortunately, this is beyond the scope of the existing research. However, the tendency for wide divergence within approaches can be demonstrated. It is this divergence that may cause confusion and dissatisfac-

**Table 1. Approaches used by state agencies to determine pay adjustment for noncompliance with compaction requirements.**

| Approach | No. of Agencies |
|---|---|
| Percentage reduction in contract price computed by formula based on statistics | 3 |
| Pay factors for percentage of target density | 7 |
| Pay factors for percentage of control strip density | 4 |
| Pay factors for percentage of voidless density | 1 |
| Pay factors for daily mean air-void content | 1 |
| Pay factors based on deviation of air-void content | 1 |
| Price adjustment for percentage of deficiency | 1 |
| Pay factors based on computed quality level | 2 |
| Pay factors based on computed quality index | 1 |
| Pay factors for percentage within limits | 2 |

**Table 2. Approaches used by state agencies to determine pay adjustment for noncompliance with asphalt content requirements.**

| Approach | No. of Agencies |
|---|---|
| Percentage of reduction in contract price computed by formula based on statistics | 3 |
| Pay reduction for percentage out of tolerance | 3 |
| Pay factors for average deviation from job mix | 13 |
| Pay factors for deviation of sample average as percentage | 1 |
| Pay reduction for deviation of sample average as percentage | 1 |
| Pay factors based on deviation of mean above or below mix tolerances | 1 |
| Price adjustment computed by specified procedure based on percentage of asphalt above or below mix design tolerance | 1 |
| Pay factors for degree of nonconformance of moving average | 1 |

tion among paving contractors who undertake work in several states.

The use of pay-adjustment factors determined by comparing the in-place density with the target or laboratory density appears to be the most common approach (seven agencies). The in-place density is typically determined with a nuclear gage, and the target or laboratory density is determined from samples prepared by use of the Marshall or Hveem mixture design procedures. The percentage of the target density achieved is then compared with predetermined values in the agency's specifications. This concept is demonstrated below for the state of Mississippi:

| Target Density Achieved (%) | Pay Factor (%) |
|---|---|
| 94.9-100 | 100 |
| 94.2-94.8 | 90 |
| 93.5-94.1 | 70 |
| 92.8-93.4 | 50 |
| <92.8 | 0 |

The table below compares three target densities for the seven state agencies that can be compared:

| Target Density (%) | Pay Factor (%) | No. of Agencies |
|---|---|---|
| 100 | 100 | 7 |
| 95 | 100 | 5 |
| | 93 | 1 |
| | 90 | 1 |
| 90 | 90 | 1 |
| | 75 | 1 |
| | 69 | 1 |
| | 50 | 2 |
| | 40 | 1 |
| | 0 | 1 |

For 100 percent of target density, all seven agencies provide for full pay (100 percent pay factor), as would be expected. For 95 percent of target density, the amount of pay received by a hypothetical contractor could range from 90 to 100 percent. This variability increases significantly for 90 percent of target density. The percentage pay received by a contractor could range from 0 to 90 percent depending on the state in which the contractor was performing the work.

The information resulting from the analysis of the questionnaire further reveals that, for most of the seven agencies cited, achievement of at least 95 percent of target density qualifies for full payment for the material in a given lot. If the target density is in the 90 percent range, a number of agencies either apply severe (low) pay factors or require the project engineer to make further evaluations as to whether the lot should be accepted at reduced pay or be totally rejected. Most agencies also give contractors an option of accepting the pay adjustment or removing and replacing the material at their own expense in an effort to achieve work that is in compliance.

## Asphalt Content

Information on pay-adjustment factors for asphalt content was submitted by 25 agencies. This material characteristic also showed a wide disparity in pay factors among the state agencies. Table 2 gives the eight different approaches used and the number of agencies using each approach. Again, there is little value in comparing the various approaches due to the lack of supportive data. However, as in the case of the compaction criteria, the tendency for significant divergence within approaches can be demonstrated.

The use of pay-adjustment factors determined by computing the average deviation of the asphalt content from the job mix criteria appears to be the most common approach (13 agencies). The target value established for asphalt content is then used for comparison with the actual asphalt content of the lot samples. This concept is demonstrated below for the state of Nebraska:

| Avg Deviation | Pay Factor (%) |
|---|---|
| 0.0-0.31 | 100 |
| 0.32-0.37 | 95 |
| 0.38-0.41 | 90 |
| 0.42-0.45 | 80 |
| 0.46-0.49 | 70 |

Note that an equal pay adjustment is applied when the deviation is either above or below the job mix target value.

The table below compares three levels of average deviation from the job mix target for the 13 state agencies obtained by using this evaluation method:

| Avg Deviation | Pay Factor (%) | No. of Agencies |
|---|---|---|
| 0.20 | 105 | 1 |
| | 100 | 11 |
| | 90 | 1 |
| 0.40 | 100 | 5 |
| | 95 | 3 |
| | 90 | 2 |
| | 80 | 1 |
| 0.55 | 100 | 1 |
| | 95 | 1 |
| | 80 | 3 |
| | 70 | 2 |

For an average deviation of 0.20 (e.g., asphalt

binder content range of 5.8-6.2 percent for a 6 percent target content), 11 agencies provide for full pay (100 percent pay factor), one agency provides a pay factor of 105 percent (which involves a bonus for high uniformity), and one agency provides a pay factor of 90 percent. For an average deviation Of 0.40, the amount of pay received by a contractor could range from 0 to 100 percent, although the majority of the state agencies would provide payments of at least 95 percent. At an average deviation of 0.55, the payment provisions vary from 0 to 100 percent, but the majority of the agencies severely penalize the contractor. One agency gave no pay factor for deviations of 0.40, and five agencies gave no pay factor for deviations as high as 0.55. These agencies could either reject the material at zero pay or accept the noncompliance material at a negotiated pay factor.

## RATIONAL PAY-FACTOR DEVELOPMENT

In an attempt to develop more rational pay factors, work is currently under way to evaluate the effects of known mix variations on pavement life. When these effects are known, pay factors can be assigned. The effects of density, gradation (particularly minus 0.074 mm), asphalt content, and aggregate quality are currently being evaluated at Oregon State University.

The procedure being used to develop pay factors is to evaluate the performance of asphalt mixes in fatigue and permanent deformation. The diametral test (4) is used to evaluate these properties. Fatigue ($\varepsilon_E$ - N) for permanent deformation ($\varepsilon_p$ - N) curves are developed for each mix combination. The fatigue curve shown in Figure 1 indicates the effect of density on fatigue life.

Once developed, pay factors can be determined for any strain level as given in Table 3. The table gives pavement life (repetitions) associated with various mix densities and the pay factors developed with respect to some standard (in this case, 96 percent of maximum density). As indicated, the pay factors developed range from about 5 to 45 percent for poorly compacted specimens (∿90 percent of maximum) to 45-65 percent for specimens compacted to 92 percent of maximum. It should also be noted that specimens compacted to 100 percent would yield fatigue levels about 3.5-4 times greater than the standard condition; however, these mixes may have a greater tendency to bleed or rut. This effect is still being studied.

The important point is that improved mix evaluation methods can lead directly to pay factors if noncompliance in a mix exists. These pay factors should more accurately reflect how a mix will perform in the field than the methods now being used. A detailed presentation of the development of pay factors using this approach will be available in subsequent project reports.

## SUMMARY AND CONCLUSIONS

The pay-factor questionnaire prepared and distributed by the Oregon State Highway Division has proved to be extremely useful in evaluating the current status of quality-control procedures and the use of pay-adjustment factors in the construction of asphalt concrete pavement projects. The 92 percent response rate by the state agencies is a key factor

**Figure 1. Effect of mix density on fatigue life.**

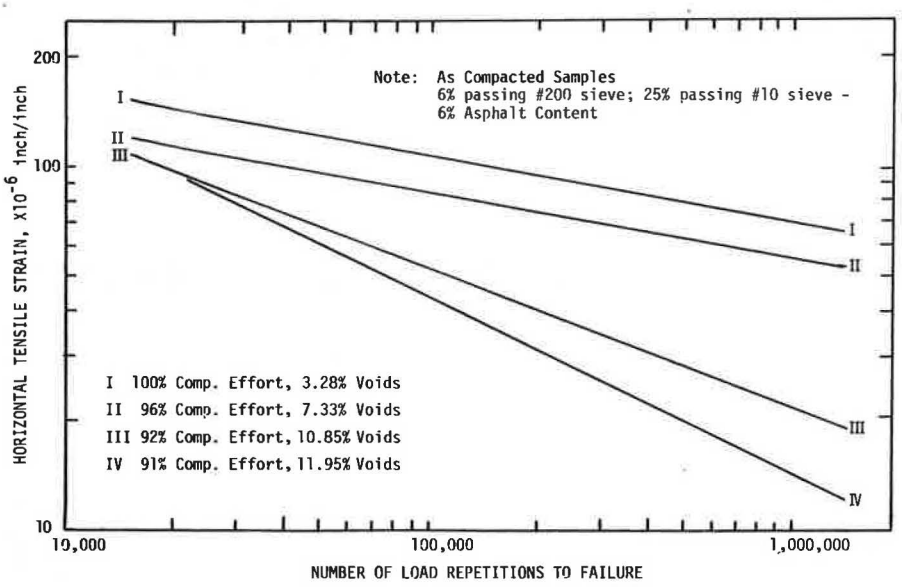


**Table 3. Estimated reduction in pavement life and associated pay factors based on fatigue criteria and varying mix densities.**

| | | Strain Level | | | |
|---|---|---|---|---|---|
| | | Heavy-Duty | | Primary | |
| Compaction (%) | Mix Bulk Specific Gravity | 50 με (000 000s) | Pay Factor (%) | 100 με (000 000s) | Pay Factor (%) |
| 96 | 2.31 | 1.62 | 1.00 | 0.0406 | 1.00 |
| 100 | 2.41 | 6.44 | 3.98 | 0.148 | 3.65 |
| 92 | 2.22 | 1.04 | 0.64 | 0.0182 | 0.45 |
| 91 | 2.19 | 0.0788 | 0.05 | 0.013 | 0.32 |

in the value of this report and is also an indication of the intense interest in this aspect of the construction process.

The data from the questionnaires were summarized, and the analysis of the results indicates the following:

1. Most state agencies (91 percent) will accept one or more properties in the construction and materials of asphalt concrete pavement that are outside of specification tolerances.
2. The specific properties that are accepted outside of specification tolerances by a large majority of agencies, generally with a pay adjustment, are compaction asphalt content, asphalt properties, and mix gradation. Pavement thickness and smoothness are additional properties accepted outside of specification tolerances by approximately half of the agencies.
3. Most of the agencies that accept construction and materials outside of specification tolerances apply a pay adjustment in reducing the compensation to the contractor. It is significant that the current philosophy is to penalize the contractor for properties that are below specification. A few agencies are considering the provision of a bonus for properties that are found to be above specification and provide increased pavement serviceability or life. Illinois appears to be the only state agency that currently provides a bonus for high quality and uniform work.
4. The background most relied on for establishing pay factors is experience.
5. Only 26 percent of the agencies consider their pay factors to be proportional to reduced pavement serviceability. Other widely used rationales for pay factors are to discourage noncompliance by application of the penalty and to comply with the recommendations of FHWA.
6. Approximately half of the agencies consider the use of pay-factor plans to be effective in encouraging compliance with specifications. The remaining agencies either will not use specified pay factors or do not believe the plans currently available are sufficient.
7. There is a wide disparity in the pay-adjustment factors currently used by the different state agencies. Several approaches are used to determine pay factors for each material property evaluated. In addition, agencies that use the same approach have widely varying values for the pay factor applied to a common level of material quality.

ACKNOWLEDGMENT

The study described in this paper was supported by FHWA. FHWA has not reviewed the findings presented. The contents of this paper reflect our views, and we are responsible for the facts and accuracy of the data presented. The contents do not necessarily reflect the official views or policies of either the Oregon Department of Transportation or FHWA.

REFERENCES

1. J.E. Wilson and R.G. Hicks. Evaluation of Construction and Short-Term Performance Problems for Asphalt Pavements in Oregon. Proc., AAPT, Feb. 1979.
2. The AASHO Road Test: Report 5--Pavement Research. HRB, Special Rept. 61E, 1962.
3. Statistically Oriented End-Result Specifications. NCHRP, Synthesis of Highway Practice 38, 1976.
4. R.S. Schmidt. A Practical Method for Measuring the Resilient Modulus of Asphalt-Treated Mixes. HRB, Highway Research Record 404, 1972, pp. 22-31.

*Publication of this paper sponsored by Committee on Quality Assurance and Acceptance Procedures.*

# Texturing of Cement Concrete Pavements by Chip Sprinkling the Fresh Concrete

F. FUCHS

**One of the research projects on slipperiness being conducted by the Centre de Recherches Routières in Belgium concerns the chip sprinkling of cement concrete pavements. Of all the surface treatments for fresh concrete, this technique is the only one that permits the use of polishable aggregates in the bulk of the concrete without prejudicing skid resistance. This is an obvious economic advantage in regions that do not have sufficient reserves of materials with a high resistance to polishing. The large-scale application of the procedure has required the construction of a chip-sprinkling machine, which is now operational for works carried out with both fixed and slip forms. Between 1974 and 1980, a number of large works have been completed in Belgium and France. Guidelines for optimal execution have been published that deal with the laying of the concrete and the chip sprinkling. Existing experimental roads have demonstrated the effectiveness and durability of the technique. The degree of skid resistance is related to the quality of the chipping stones used. The surface rolling noise is less annoying than the noise produced by transverse grooved concrete and is comparable to the rolling noise of other types of skid-resisting pavements that have a random surface texture.**

For several years, a major effort has been under way in various countries to improve the skid-resisting properties of pavements. Up to now, research has shown that high skid resistance on wet road surfaces is linked to the following factors (1): (a) a coarse macrotexture, obtained by applying a suitable surface treatment, and (b) a harsh microtexture, obtained by excluding polishable aggregate from the surface of the pavement.

The most widespread surface treatment used today for cement concrete pavements is the deep transverse grooving of the fresh concrete. This treatment has evolved tremendously during the past 15 years or so, both in Europe (2,3) and, more recently, in the United States (4). The application of this technique gives excellent results with regard to skid resistance and ensures effective transverse draining of the road. Nevertheless, the simple and inexpensive technique is sometimes criticized for the in-

Figure 1. Appearance of concrete after chip sprinkling at rate of 7 kg/m$^2$ with 14- to 20-mm-gauge stones.

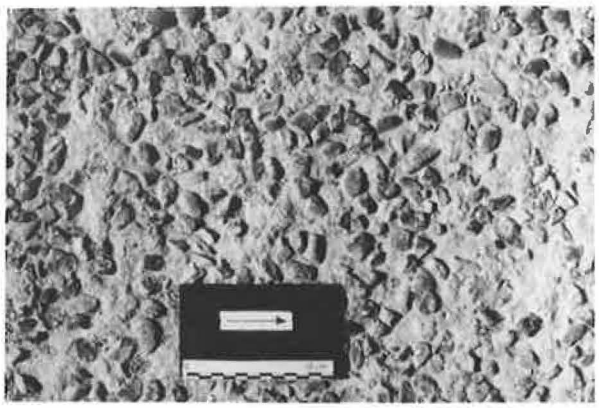

Figure 2. Rear view of chipping machine on rails.

crease in rolling noise it produces. Variable spacing of the grooves lessens, but cannot eliminate, this disadvantage.

This has been one of the main reasons, apart from economic considerations (discussed below), behind the search for new types of nonskid pavement, a search that has led to two techniques: (a) chip sprinkling the fresh concrete or (b) stripping the aggregate in its surface (5). These techniques have now been perfected to the point that they are completely operational for use with both fixed forms and slip forms and are permitted by Belgian official specifications as alternatives for deep transverse grooving (6).

Stripping of the aggregate consists of removing the superficial mortar of the concrete so that the aggregate is exposed. The treatment can be carried out by simultaneously sprinkling water and brushing the surface of the fresh concrete with a rotating brush. The sprinkled water is subsequently removed with the laitance from the surface of the concrete. Another technique, used in Denmark since 1976 (7) and more recently in Belgium, consists of spraying a retarder onto the surface of the fresh concrete. The following day, after the concrete has hardened, the surface is brushed vigorously with a metal-bristled brush so that the surface mortar is removed.

The chief advantage of the chip-sprinkling technique, according to the studies carried out by the Centre de Recherches Routières (8), is that, in contrast to grooving and stripping of the aggregate, it permits the use of polishable aggregate in the bulk of the concrete without affecting skid resistance. Indeed, in this case the contact area between the pavement and vehicles tires is essentially made up of chippings that have a high resistance to polishing. The intention of this paper is to expound the latest developments in this technique, particularly its large-scale application, made possible by the mechanization of the slip-form technique.

## BASIC PRINCIPLE AND ADVANTAGES OF CHIP SPRINKLING

The chip sprinkling of cement concrete pavements consists in evenly strewing polish-resistant stones of a determined size--e.g., 14-20 mm--onto the surface of the already compacted and profiled fresh concrete and setting them in such a way that they slightly protrude from the surface, creating a coarse macrotexture (see Figure 1).

The main economic advantage of the procedure is that it permits the use of local aggregates in the bulk of the concrete, even those aggregates that do not stand up well to polishing, such as limestone. This is of particular interest to those countries or regions whose local geology does not allow the cheap supply of hard materials that have a high resistance to polishing.

In countries such as Belgium, where the available aggregates are polish-resistant or polishable, according to the location of the building site, contractors and directing officials are free to choose the cheapest materials without changing techniques or construction equipment: Chip sprinkling is always possible. Moreover, the chipping materials can be chosen to suit the site, the volume of traffic, and the maximum permitted speed. It is thus possible to obtain a high level of skid resistance at dangerous spots, or on heavily trafficked roads, by selecting chipping stones that have a very high resistance to polishing. Even in that case, the extra cost of chip sprinkling remains low because of the limited quantities of chippings required (6-8 kg/m$^2$) and is amply compensated for by the savings on the concrete aggregate.

## MAIN PHASES IN DEVELOPMENT OF THE PROCEDURE

The application of the procedure has taken place in two main phases. The first phase, from 1949 to 1969, consisted in setting up rather limited experiments that used manual techniques on heavily trafficked roads (9). The results obtained from these roads showed that (a) the chipped areas showed a significant improvement in the sideway force coefficient (SFC) in comparison with untreated areas and (b) these chipped areas stood up well to long-term use (20-25 years).

As early as 1973, the Centre de Recherches Routières, in collaboration with a machine constructor, began studies on the mechanization of the procedure. These studies led to the construction of a chip-sprinkling machine that is capable of simultaneously ensuring that the exact amount of chipping stones is spread evenly over the surface and that the stones are driven the correct depth into the fresh concrete by means of a vibrating tamping beam (10). The machine has been operational since 1974 for fixed-form operation (8,11), and since 1979 for slip-form work (12). Thus far, this machine has been used to lay more than 400 000 m$^2$ of pavement, in both Belgium and France.

The fixed-form machine is an independent unit that has the following functions (see Figure 2):

1. Supplying chippings from a storage hopper that is filled by means of bins and a loading system built into the machine,

2. Dosing and uniform spreading of the chippings on the surface of the concrete,
3. Driving the chippings into the fresh concrete with a vibratory tamping beam, and
4. After chipping, spraying the fresh concrete with a curing agent.

Thus far, about 150 000 m² of pavement has been laid by using this machine, both for experimental and normal construction, in widths ranging from 3 to 7.5 m. This makes it possible to draw conclusions regarding both the improvement of the technique (13) and its adaptation to slip-form operations.

At the outset, it was possible to imagine two different systems: (a) an independent chipping machine mounted on tracks and (b) a chip-sprinkling machine incorporated in a slip-form paver. Eventually, the second type was selected because (a) it provided easier vertical alignment of the tamping beam (moreover, tamping at the working level of the slip-form paver makes it possible to correct the surface of the concrete, particularly after dowels are inserted by vibration) and (b) it eliminates the necessity of replacing the form work during tamping (this operation is carried out between the sliding forms of the slip-form paver).

Broadly speaking, the machine is made up of the same components as the fixed-form machine (see Figure 3) (8):

1. A storage hopper for the chippings that has a capacity of approximately 800 kg per meter of width;
2. A spreader drum whose speed of rotation can be regulated and that has an adjustable opening for the passage of the chippings so that the chipping rate can be precisely adjusted; and
3. A vibrating tamping beam whose lower face is slightly inclined in relation to the direction of advance so that the chippings will be pushed progressively down into the concrete (the level of the beam can be adjusted while the machine is in operation by means of hydraulic jacks, and the vibrating frequency can be altered in relation to the plasticity of the concrete).

The storage hopper is loaded with chippings by means of a hydraulic grab, mounted either on the lorry that is carrying the chippings or, for large widths, on the slip-form paver itself. Incorporating the chipping equipment into the slip-form paver makes it possible to mount the vibratory dowel-inserting device in front of this equipment. The curing agent is sprayed by a separate machine that follows immediately behind the slip-form paver. This permits finishing touches to be made by hand, if necessary, after the surface has been laid. The chip-sprinkling equipment is operated from an autonomous control station located at the rear of the machine so that the operator has a good view of the work.

Three works had been completed at the time this paper was written. Two experimental works were carried out in Belgium: one at Bernissart toward the end of 1979 and another at Aisemont toward the end of 1980. The first work involved laying a continuous reinforced concrete pavement about 2700 m long and 2x3.5 m wide. The second pavement was 2400 m long and consisted of 6-m slabs separated by doweled contraction joints. The chipping equipment was mounted at the rear of a Guntert and Zimmerman slip-form paver (see Figures 3 and 4).

At Aisemont, the dowels were inserted into the fresh concrete by vibration simultaneously with the chip sprinkling. The concrete was made by using local limestone aggregate, which is usually rejected because of its poor (0.37-0.40) polished stone value (PSV) (14). In one section at Aisemont, the concrete also contained local crushed sand. Chipping was carried out by using 14- and 20-mm and 10- and 14-mm aggregate with a PSV of 0.55, spread at an approximate rate of 6 kg/m².

On the whole, the results obtained can be regarded as excellent with respect to the actual execution--the even spreading of the chippings and the uniform penetration of the stones into the fresh concrete. The works aroused much interest, particularly in France, where the chipping technique used in conjunction with slip forms is a key point in the construction of motorway pavements in cement concrete because there is not a sufficient supply of aggregate with a high PSV. Although the application of surface dressings to new concrete roads gives good results with respect to skid resistance, it has not entirely solved the problem because of generally

Figure 3. Cross section of slip-form paver incorporating chipping equipment.

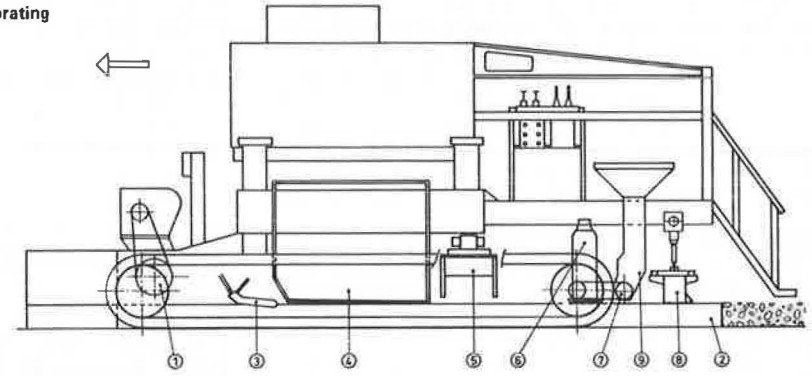


Slip-form paver:
1. Screw distributor
2. Slip-form
3. Internal vibrator
4. Extrusion box
5. Device for dowel insertion
6. Smoothing beam

Chipping equipment:
7. Spreader drum
8. Tamping beam
9. Storage hopper

Figure 4. Slip-form paver at work at Bernissart site over 3.5-m width.

Figure 5. Sélestat bypass under construction in 8-m-wide sections.


poorer durability (5-7 years) and the relatively high cost of the technique (15).

The first large-width application was carried out near Strasbourg in France during the summer of 1980, on a motorway section 17 km long and 2x8 m wide (autoroute A35, the Sélestat bypass) (see Figure 5). This time the equipment was incorporated into a "CMI autograde" slip-form paver. The concrete, laid on a lean concrete base, uses rounded aggregate from the Rhine that is gathered from a ballast pit near Sélestat. The surface was chip sprinkled with hard crushed stone of 16- and 20-mm gauge. The spreading rate was approximately 6 kg/m². The Californian method of concrete laying was used: short slabs of 4.5-6 m separated by undoweled contraction joints sawed in the hardened concrete. The average rate of advance of the machine was about 2 m/min.

As a sequel to these works, another chip-sprinkled concrete project is planned for the spring of 1981 on the Calais-Arras motorway. A concrete pavement 2x8 m wide and consisting of 32- to 38-cm-thick slabs will be laid over a length of 30 km.

## RECOMMENDATIONS FOR ACHIEVING SATISFACTORY RESULTS

Based on the experience gained on existing experimental roads, the following recommendations can be drawn up for the construction of chipped cement concrete pavements.

### Composition of Concrete

When a surface is to be chip sprinkled, the concrete used does not have to have any special composition as long as it has a uniform consistency and retains sufficient plasticity after compaction to allow insertion of the chippings. In Belgium, continuously graded 0/32 concrete is normally used. It has a high cement content (400 kg/m³) and contains no air-entraining agents. Slump measurements that use Abram's cone vary from 1 to 2 cm for works carried out with fixed forms and from 2 to 4 cm for slip forms. The concretes used in France are probably closer to those encountered in the United States and have a cement content of 330 kg/m³ and an air content of 3-6 percent (16). Slump values vary from 1 to 5 cm according to the type of machine used. In this respect, it should be pointed out that the quality of the mortar, and particularly its cement content, can have a long-term effect on the durability of the chip-sprinkled surface, since the surface mortar anchors the chippings into the pavement.

### Execution of Chip Sprinkling

The chipping stones should be 14- to 20-mm or 10- to 14-mm gauge. They should be angular, cube shaped, hard, and clean. Official requirements (6) set a minimum PSV of 0.50 for general use and 0.60 for dangerous spots or for use on heavily trafficked roads.

The stones are sprayed just before they are used so that they are wet, which helps them to stick well to the concrete. The rate of chipping is adjusted so that the surface is covered as much as possible without pockets of chippings being formed. For the gauges mentioned above, this usually lies between 6 and 8 kg/m².

The stones are driven into the fresh concrete so that they are properly anchored to the pavement, remain visible on the surface, and provide a coarse surface texture. Nevertheless, the covering of a certain proportion of the chippings with a thin film of mortar can be tolerated, since this film wears off later under traffic. Before the section is opened to traffic, the surface should be swept mechanically in order to remove any loose chippings.

Recommendations have been published for operations carried out with fixed forms (13). These recommendations will be supplemented in due course by the new experience gained and adaptations made for the slip-form method.

## PERFORMANCE OF CHIP-SPRINKLED CONCRETE

In addition to the technological aspects, several variants were tried out on experimental works in chipped cement concrete that were constructed between 1969 and 1975. These variants had mainly to do with the composition of the concrete and the characteristics of the chipping stones.

Systematic measurements of the surface characteristics of these pavements show the following:

1. The average texture depth (H), determined by the sand-patch test (17), usually lies between 2 and 2.5 mm at the completion of the works. This depth rapidly stabilizes after a few months of traffic wear and will not be subsequently affected except by the wear of the chipping stones and the mortar due to traffic; this wear turns out to be insignificant if hard chippings are used.
2. Skid resistance--as typified, for example, by the SFC--is very satisfactory and depends mainly on the qualities of the chipping stones used. By way of an example, Table 1 summarizes the results of measurements made on the Hasselt bypass (constructed in 1975) five years after it was opened (the traffic density is 5000 vehicles of all categories per day). From these measurements, it can be concluded that (a) the SFC changes in direct relation to the PSV of the chipping stones and (b) the use of bulk aggregate that has poor resistance to polishing does not affect the SFC.
3. No loss of chippings caused by traffic was ob-

**Table 1. Results of measurements made on experimental road at Hasselt in November 1980.**

| PSV | | | | | |
|---|---|---|---|---|---|
| Stones in Concrete Aggregate | Chipping Stones | H (mm) | SFC[a] At 20 km/h | SFC[a] At 80 km/h | Δ SFC[a] at 20-80 km/h |
| 0.55 | 0.71 | 1.71 | 0.81 | 0.59 | 0.22 |
| 0.55 | 0.58 | 1.83 | 0.72 | 0.55 | 0.17 |
| 0.55 | 0.50 | 2.20 | 0.72 | 0.55 | 0.17 |
| 0.39 | 0.58 | 1.75 | 0.75 | 0.55 | 0.20 |

[a]Measured with a TRRL-type odoliograph fitted with a Permanent International Association of Road Congresses smooth tire; water temperature on the pavement reduced to 20°C.

served, nor did frost or the action of deicing salts have any adverse effects.

4. Possible effects of the chipping technique on surface evenness have not been substantiated. On the whole, chip-sprinkled pavements offer satisfactory comfort to the road user. Moreover, the tamping beam acts as a profile corrector, particularly when dowels are inserted by vibration.

5. As far as the noise problem is concerned, a research project currently in progress has succeeded in providing evidence that there is a relation between the geometric characteristics of a surface and the rolling noise due to it, both inside and outside the vehicle (18). The results show that for chip-sprinkled cement concrete--which, like chip-sprinkled bituminous concrete, cement concrete with exposed aggregate, and surface dressings, has a random texture--the noise spectrum does not behave in the same way as it does for transverse grooved cement concrete, where a single wavelength related to groove spacing dominates and occasionally causes an annoying whistle. Furthermore, it appears that noise levels are adversely affected by surface irregularities whose wavelengths exceed 10 mm, which indicates that less noisy chip-sprinkled surfaces could be obtained, in built-up areas, for example, by making use of appropriate gauges of chippings. Further research is planned in this area.

## CONCLUSIONS

Chip sprinkling of fresh concrete is, to the best of my knowledge, the only surface treatment that makes it possible to construct cheap and durable skid-resistant cement concrete pavements in areas where there are large formations of polishable materials. Savings are possible both on the aggregate used in the bulk of the concrete and on transportation costs. The projects completed to date have demonstrated that chip-sprinkled surfaces perform well, particularly with respect to skid resistance and durability. The existence on the market of an operational machine for works carried out with both fixed and slip forms has contributed to the large-scale development of this procedure since 1980.

## ACKNOWLEDGMENT

I wish to express my sincere thanks to the Institut pour l'Encouragement de la Recherche Scientifique dans l'Industrie et l'Agriculture for its financial support. The Centre de Recherches Routières also extends its thanks to the Ministry of Public Works, to its French colleagues, and to private enterprise for their cooperation during the construction of the experimental roads. Finally, I wish to thank all those persons who have taken an active part in constructing and perfecting the chip-sprinkling machine and all those who have contributed, through their care and devotion, to the success of the experiments and the measurements made on the roads.

## REFERENCES

1. Committee on Slipperiness: Report. 14th World Road Congress, Prague, 1971, Permanent International Assn. of Road Congresses, Paris, 1971.
2. J.-P. Leyder and J. Reichert. Techniques for Achieving Non-Skid Pavement Surfaces, Especially by Deep Transverse Grooving of Fresh Cement Concrete. TRB, Transportation Research Record 523, 1974, pp. 141-150.
3. J.-P. Leyder. Dix Ans d'Expérience de Striage Transversal Profond du Béton à l'État Frais. 2nd Symposium Européen des Routes en Béton, Berne, Switzerland, 1973, C-8, pp. 311-323.
4. E.E. Rugenstein. Summary and Evaluation of Concrete Pavement Texturing Practices. Proc., International Conference on Concrete Pavement Design, Purdue Univ., West Lafayette, IN, 1977, pp. 557-563.
5. J.-P. Leyder. New Types of Anti-Skid Surfacings. 16th World Road Congress, Vienna, Austria, 1979, Permanent International Assn. of Road Congresses, Paris, Tech. Committee Rept. on Surface Characteristics, 1979, pp. 63-83.
6. Cahier des Charges Type n° 150. Fonds des Routes, Administration des Routes, Ministère des Travaux Publics, Brussels, Belgium, 1978.
7. S. Leksø. Concrete Test Road on M20 (Ølby-Ringsted). Statens Vejlaboratorium, Roskilde, Denmark, 1978.
8. F. Fuchs. Actual Experience Regarding the Chipping of Cement Concrete. TRB, Transportation Research Record 624, 1976, pp. 90-94.
9. G. Van Heystraeten. Connaissances Acquises en Matière de Béton de Ciment Clouté. La Technique Routière, Vol. 19, No. 1, Brussels, Belgium, 1974, pp. 25-50.
10. Belgian Patent 810.023: Road Chip-Sprinkling Machine. Centre de Recherches Routières, Brussels, Belgium, 1974.
11. G. Van Heystraeten. La Rugosité des Revêtements: le Béton de Ciment Clouté. La Technique Routière, Vol. 20, No. 4, Brussels, Belgium, 1974, pp. 1-20.
12. G. Van Heystraeten. Une Nouvelle Technique de Réalisation de Revêtements Antidérapants en Béton de Ciment par le Cloutage du Béton Frais. International Colloquium on Concrete Roads, Cembureau, Besançon, France, 1978, pp. 195-203.
13. Code de Bonne Pratique pour l'Exécution d'un Revêtement en Béton de Ciment Clouté Entre Coffrages Fixes. Centre de Recherches Routières, Brussels, Belgium, Recommendations CRR-R 41/78, 1978.
14. Methods for Sampling and Testing of Mineral Aggregates, Sand, and Fillers. British Standards Institution, London, BS812:1975, 1975.
15. J.P. Roussel and P. Brun. Efficacité des Enduits Superficiels. Bulletin de Liaison des Laboratoires des Ponts et Chaussées, Paris, Sept. 1978, pp. 253-262.
16. Directive pour la Réalisation des Chaussées en Béton de Ciment. Direction des Routes et de la Circulation Routière, Ministère des Transports, Paris, 1978.
17. Mode Opératoire: Essai à la Tache de Sable--Méthode de Mesure. Centre de Recherches Routières, Brussels, Belgium, CRR-MF 32/69, 1969.
18. G. Descornet. Experimental Study of the Rolling Noise of a Test Car on Various Existing Road Surfaces in Belgium. International Tire Noise Conference, Stockholm, 1979.

*Publication of this paper sponsored by Committee on Rigid Pavement Construction.*

# Magnitude of Horizontal Movement in Jointed Concrete Pavements

I. MINKARAH, J.P. COOK, AND J.F. McDONOUGH

**A section of US-23 near Chillicothe, Ohio, has been used as a test pavement for the past seven years. Variables included in the test section are slab length, type of subbase, saw-cut configuration, type and coating of dowel bars, and skewed joints. Both hand and electronic measurements of horizontal movement have been made. The hand measurements, made monthly, gave the long-term movements. The electronic measurements were continuous readings taken for one-week periods for each set of joints. Enough data have been collected to set up a computer program on a statistical basis to interpret the results. The results show that the short-term movements are greater than the long-term movements. The short-term movements are as great as 0.25 in (6.44 mm) regardless of whether the slab length is 40 or 21 ft (12.2 or 6.4 m). The long-term movements are much smaller and are almost directly proportional to slab length. It is recommended that the preformed seal be designed for the long-term movements but be able to accommodate the larger short-term movements as an upper limit. The bond between the seal and the joint face should be able to take some tension as a further guarantee of holding the seal in place in case of large joint openings.**

Jointed concrete pavements have been in use in this country for more than 100 years. Over that time span, many theories have been proposed to account for pavement movement. In recent years, a body of research has been accumulating that demonstrates that actual measurements of pavement movement in different regions of the country provide the best method for predicting movements. This paper presents data taken from 7 years of measurements on a test pavement in the midcentral region of the country (1).

The joints in portland cement concrete (PCC) pavements are usually formed by sawing a transverse contraction slot to a depth of at least 0.16T, where T is the slab thickness. This provides a weakened plane for cracking, and the drying shrinkage of the concrete causes the slab to crack through the remainder of the depth. The joint is usually bridged by a system of dowel bars that provides load transfer from one section of the slab to the next.

There are a large number of variables that may afffect the behavior of a pavement. Although it is possible to study the effect of some of these variables theoretically, the net result is that the actual in-service behavior of the pavement is quite different from its predicted behavior.

To study experimentally the effect of these variables on the behavior of pavements, a test pavement was constructed in Chillicothe, Ohio, as part of US-23. Combinations of the variables that were considered of prime importance, such as type of subbase, variation of joint spacing, type and coating of dowel bars, configuration of the saw cut, and the use of skewed joints, were incorporated into the pavement. The pavement has been monitored since 1972, and a great number of data on its behavior have been collected (2-4). This paper, however, is limited to a discussion of the magnitude of the horizontal movement of the contraction joint.

## TEST PAVEMENT

The test pavement is a 3225-ft (983-m) section of the southbound roadway on US-23 in Chillicothe. It is a tangent section located between two bridges, built on fill that ranges from 20 to 35 ft (6.1-10.7 m) in depth. The profile of the highway provides an easy grade of -0.28 percent into a 600-ft (183-m) vertical curve, which is followed by a +2.0 percent grade.

The pavement is mainly reinforced PCC [24 ft (7.3 m) wide and 9 in (229 mm) thick] laid over a granular subbase [grade A, 7.5 in (190 mm) thick]. A 183-ft (55.8-m) section was left plain, with no dowels, and with right-forward-skew joints at 17-ft (5.2-m) spacing. The subbase over a 776-ft (236-m) section was changed to a 4-in (102-mm) layer stabilized with asphalt.

The spacing of the joints was set at 17, 21, and 40 ft (5.2, 6.4, and 12.2 m). Both plain steel and plastic-coated dowels were used. The configuration of the transverse joints was also varied. There are some 0.25-in (6-mm) standard joints, 0.25-in joints with 0.125-in (3-mm) bevel on each side, and some 0.5-in (12-mm) saw-cut joints. Table 1 gives the location and type of the different variables introduced in the test pavement.

## FIELD MEASUREMENTS

The following types of measurements were taken on the pavement:

1. During the early life of the pavement, monthly hand-gage measurements of horizontal movement were made over the entire length of the project. These measurements were reduced later to four sets a year.
2. In 1979, selected large cracks in the pavement were instrumented for hand horizontal measurements. Readings across the cracks were taken by the hand gage at the same time as measurements were made on the rest of the joints.
3. Electronic measurements of horizontal movement were made on groups of joints. The measurements were taken continuously over a period of approximately one week during each of the seasons of the year.
4. Electronic measurements of vertical movement were made on one joint in each group during each season of the year.
5. Hand measurements of spalling and cracking were taken during each season of the year.
6. Periodically, Dynaflect readings were taken across all joints and selected cracks.
7. Electronic measurements of the temperature of the middle of the slab were made simultaneously with the electronic horizontal measurements.

## INSTRUMENTATION

### Hand-Gage Measurements

The hand gage consists of a base bar with two 45° pointed probes, one fixed and one movable. An Ames dial gage graduated to 0.001 in (0.025 mm) is mounted on top of the base bar between the two probes.

Brass plugs were set into the pavement on either side of each joint. These brass plugs are approximately 6 in (152 mm) apart and are set so that the top surface of the plug is just below the pavement surface. The tops of these plugs are center drilled with a 0.0625-in (1.6-mm) hole and countersunk to

**Table 1. Variables included in test pavement.**

| Joint Group | Joints Nos. | Total | Type | Spacing (ft) | Subbase Type | Dowel Type |
|---|---|---|---|---|---|---|
| 1 | 1-7 | 7 | 0.125-in bevel sawcut | 40 | Granular | Standard |
| 2[a] | 8-16 | 9 | Standard 0.25-in sawcut | 40 | Granular | Standard |
| 3 | 17-24 | 8 | Standard 0.25-in sawcut | 21 | Stabilized | Standard |
| 4 | 25-34 | 10 | Standard 0.25-in sawcut | 40 | Stabilized | Standard |
| 5[b] | 35-44 | 10 | Standard 0.25-in sawcut | 17 | Stabilized | None |
| 6 | 45-53 | 9 | Standard 0.25-in sawcut | 21 | Granular | Plastic coated |
| 7 | 54-63 | 10 | Standard 0.25-in sawcut | 40 | Granular | Plastic coated |
| 8 | 64-73 | 10 | 0.5-in sawcut | 40 | Granular | Standard |
| 9 | 74-84 | 11 | Standard 0.25-in sawcut | 40 | Granular | Standard |
| 10 | 85-94 | 10 | Standard 0.25-in sawcut | 21 | Granular | Standard |
| | 95-96 | 2 | Standard 0.25-in sawcut | 40 | Granular | Coated[c] |
| | 97-100 | 4 | Standard 0.25-in sawcut | 40 | Granular | Standard |
| | 101 | 1 | Expansion | 40 | Granular | |

Note: 1 in = 25.6 mm; 1 ft = 0.3 m.

[a]Chlorinated rubber base cure.
[b]Right forward skew and plain pavement.
[c]Experimental coating being evaluated by state of Ohio.

45° to receive the points of the probe.

The hand gage has a separate calibration bar of Invar, and countersunk holes receive the points of the probe.

## Electronic Measurements of Horizontal Movement

Horizontal movement was measured with 1-MΩ Bournes linear motion transducers (model 3049L), which were mounted on the side of the slab, at middepth and not on the riding surface. Each joint was fitted with a drilled and tapped aluminum plate on one side of the joint and a short section of 1.5x1.5-in (38x38-mm) aluminum angle on the other side of the joint.

The transducers were connected to double-channel Rustrak recorders (model 291) so that one recorder could serve two transducers. The recorder was powered by a 12-V battery. A resistor was connected to the recorder in series with the transducer to limit the current from the 12-V batteries to 50 μA, which is the full range of each channel.

One recorder had one channel calibrated for a motion transducer and the other channel calibrated for a temperature sensor. The temperature sensor is a model 1441 from Yellow Springs Instrument Company and is calibrated from -10° to +150°F (-23° to 66°C). This temperature sensor is mounted in a hole drilled at the middepth of the slab.

All strip-chart recorders have a chart speed of 0.25 in/h (6.4 mm/h) so that one week of continuous readings on a given set of joints is obtained in a 42-in (107-cm) length of chart paper.

The joints were arranged in the groups given in Table 1. Within each 10-joint group, the joints were wired in pairs so that one recorder could serve two joints. A short section of steel signpost was driven into the berm midway between two joints to serve as an anchoring post. At each joint, the shoulder material was excavated down to the bottom of the slab. Each joint was filled with a cutout box made of sheet metal, complete with cover. The recorder, two controls, and a 12-V battery to power the recorder served as a unit for each pair of joints. The entire unit was enclosed in a watertight welded aluminum box, which was bolted to the anchoring post and then locked. The transducers were connected to the recorders by wires threaded through a flexible rubber hose that stretched from the hole at the edge of the pavement to the aluminum box. The rubber hose protected the wires from traffic that might accidentally pass over the shoulder at that point.

Each time a set of readings was taken, either manual or electronic, both the air temperature and the pavement surface temperature were recorded. The thermometer used was a Pandux surface temperature thermometer (model 309F), graduated from -50° to +250°F (-46° to 121°C).

## CALIBRATION

Very few, if any, transducers are truly linear over the entire range of the instrument. Consequently, each horizontal measuring transducer was calibrated for a particular channel of a particular recorder and was so marked. The transducers were not shuffled indiscriminately from one recorder to another.

Two serious problems were encountered during the horizontal measurements: (a) water and (b) fade in the transducer response.

Instruments often had to be moved from one joint group to another during a hard rain. Even though the test section was built on fill and was generally well-drained, there were times during a hard rain when water running down the top of the joint would fill the cutout hole faster than the underdrains could carry the water off. Consequently, there were some times when the transducer was forced to operate while actually immersed in water. For this reason, a separate calibration was carried out in the laboratory in which the transducer was immersed in water. No significant change from the dry calibration was found.

Fade in the transducer response was another problem. After a period of three months under adverse weather conditions, the data were found to be quite unreliable. Consequently, after 10 weeks in the field, the units were returned to the laboratory, fitted with all new transducers, recalibrated, and returned to the field. All calibrations, of course, were carried out by using the same battery source and controls used in the field.

Ten batteries were used on the project. There were, at all times, five batteries in the field powering the units and another five back in the laboratory for recharging.

## RESULTS

The electronic measurements of horizontal movement gave a continuous reading of the movement of the joint, plus or minus from a given zero setting. For purposes of data analysis, discrete points were needed. Consequently, the magnitude of the movements at 6:00 a.m., noon, 6:00 p.m., and midnight were chosen for use all through the analysis.

The hand-gage horizontal measurements also provided, over the years, a large number of readings.

The values used to plot the frequency curves were obtained from the difference between the readings of two consecutive months taken at the same joint.

The frequency curves of both types of measurements are shown in Figures 1-4. Figures 1 and 2 show the electronic measurements of the movement of a pavement with 21- and 40-ft (6.4- and 12.2-m) slabs. Figures 3 and 4 show these movements as measured by hand. Positive values indicate expansion of the slab or closing of the joint.

It is easily seen by comparing Figures 1 and 2 with Figures 3 and 4 that the magnitude of the movement is virtually the same. A statistical F-test was conducted to compare the movement for the 40-ft (12.2-m) spacing of joints with that for the 21-ft (6.4-m) spacing. The results show no significant difference in movement due to joint spacing. The main reason for this behavior is that, over time, a midslab crack developed in most 40-ft spans. A detailed joint-by-joint study of the movements shows that, within any particular group, most of the movement is taking place at one joint and the joints before and after it are moving very little.

The distribution curves for the measurements show

**Figure 1. Frequency curve for horizontal movement in 21-ft spans: electronic measurement.**

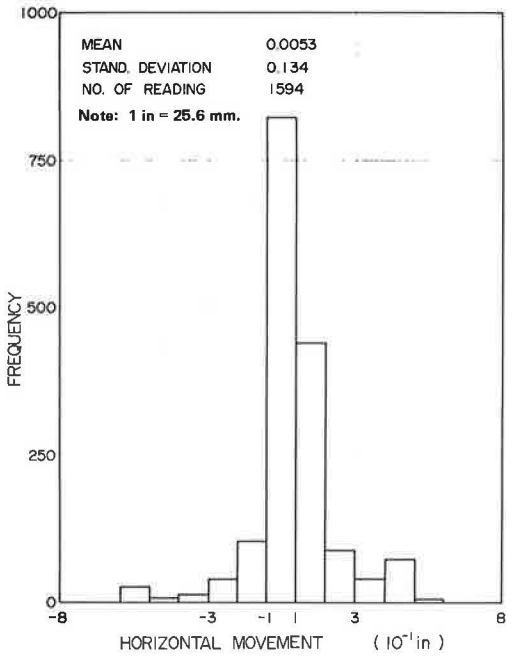


**Figure 2. Frequency curve for horizontal movement in 40-ft spans: electronic measurement.**

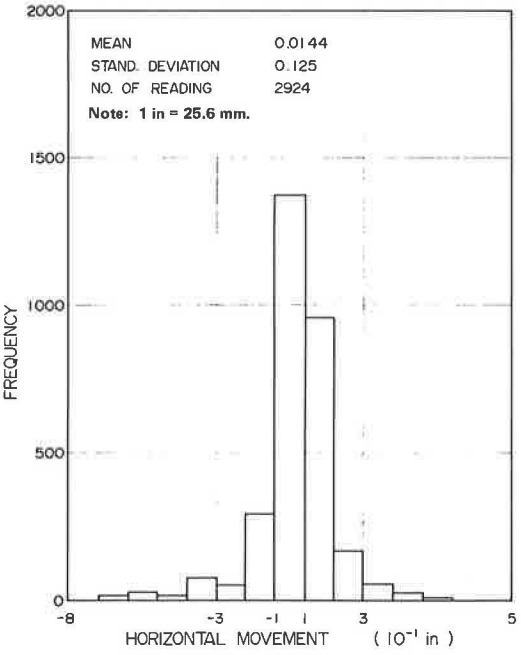


**Figure 3. Frequency curve for horizontal movement in 21-ft spans: hand measurement.**

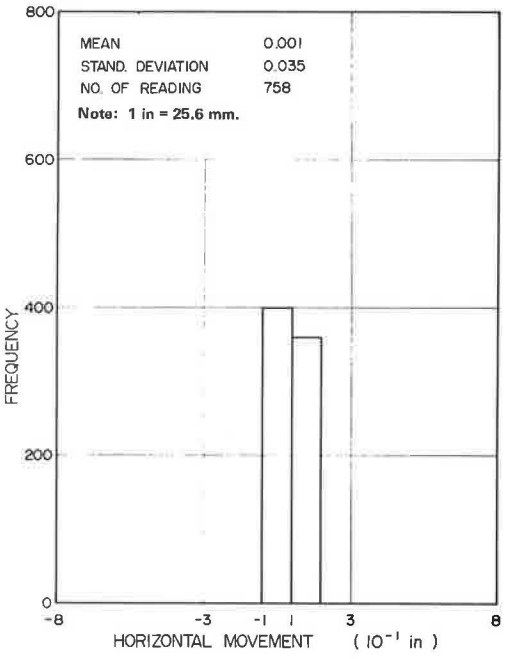


**Figure 4. Frequency curve for horizontal movement in 40-ft spans: hand measurement.**

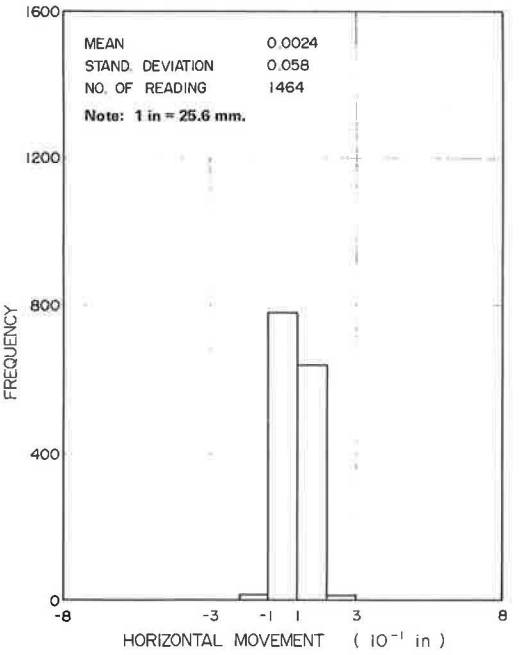

that the movement of 97 percent of the joints lies between ±0.1 in (±2.5 mm) when movement is measured by hand whereas only 78 percent of the movement is within this band when movement is measured electronically. It is important to note, however, that the movement of most of the joints within this band is close to zero.

Joints that show little or no movement at a particular time are not necessarily frozen into a fixed position. Any particular joint may show little or no movement at one time and then later show a large movement. This point is currently being double-checked by spot measurements of both the joints that show large movements and the two or three joints that precede and follow them.

For analysis of the data, normal distribution curves have been superimposed on the frequency distributions. Figures 5 and 6 show the normal distribution curves for the 21- and 40-ft (6.4- and 12.2-m) slabs. Figure 7 shows the normal distribution curves for a combination of all the movements.

The magnitude of the movement at a joint is of extreme importance in the design of the jointing material, whether this material is premolded or field molded. To determine the magnitude of the movement, 90 and 95 percent confidence limits ($C_1$ and $C_2$) were calculated by using the normal distribution curves corresponding to the frequency distributions of hand and electronic measurements. Figures 8-13 show the normal curves and the values of $C_1$ and $C_2$ for all cases under study. The values are also given in Table 2. The nomenclature used in the statistical analysis is based on the work of Miller and Freund (5). The calculations are

**Figure 5. Superposition of normal curve for 21-ft spans: electronic measurement.**

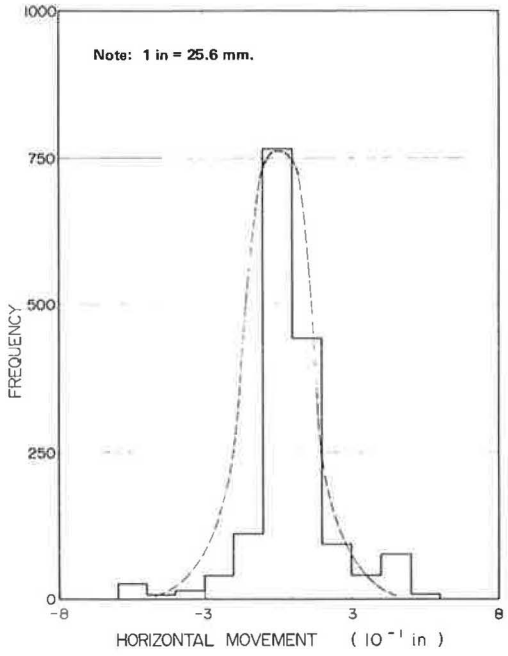


**Figure 6. Superposition of normal curve for 40-ft spans: electronic measurement.**

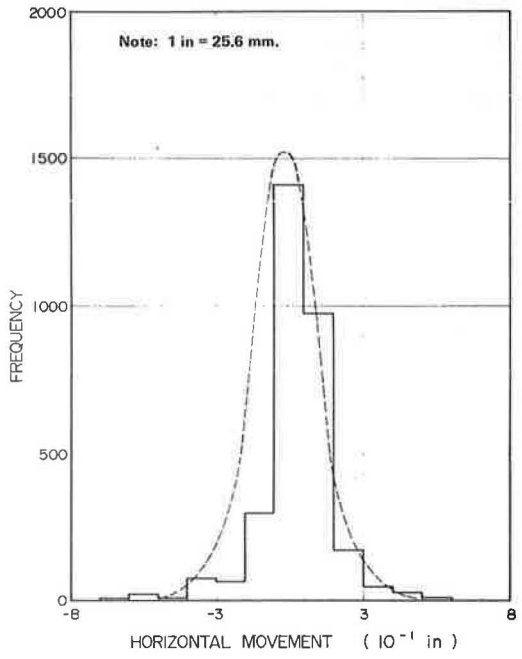


**Figure 7. Superposition of normal curve for all spans: electronic measurement.**

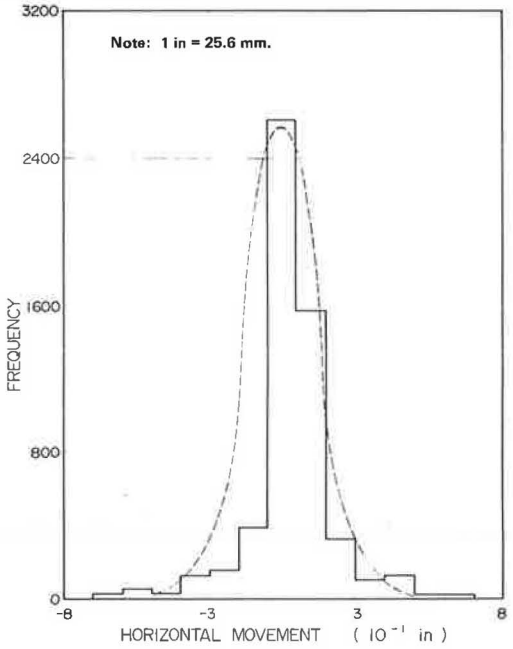


**Figure 8. Normal distribution curve for 21-ft spans: electronic measurement.**

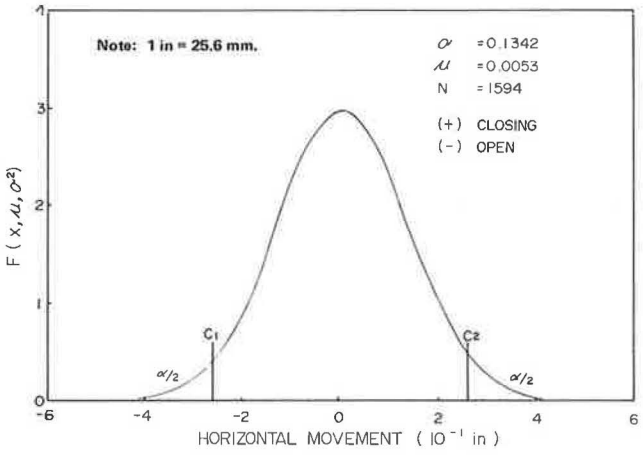

based on the following formulas:

$$C_1 = \mu - (Z_{\alpha/2})\sigma \quad (1)$$

$$C_2 = \mu + (Z_{\alpha/2})\sigma \quad (2)$$

where

$\mu$ = mean of the normal distribution,
$\sigma$ = standard deviation,
$Z_{0.025} = \pm 1.96$, and
$Z_{0.05} = \pm 1.645$.

It is apparent that the value of $C_1$ and $C_2$ for electronic measurements can be taken as $\pm 0.25$ in (6.4 mm) and is the same for 40- and 21-ft (12.2- and 6.4-m) slabs. The electronic measurements give the short-term movements, since they were taken by continuous recording. The hand measurements show the aggregate movement obtained over a long period

**Figure 9. Normal distribution curve for 40-ft spans: electronic measurement.**

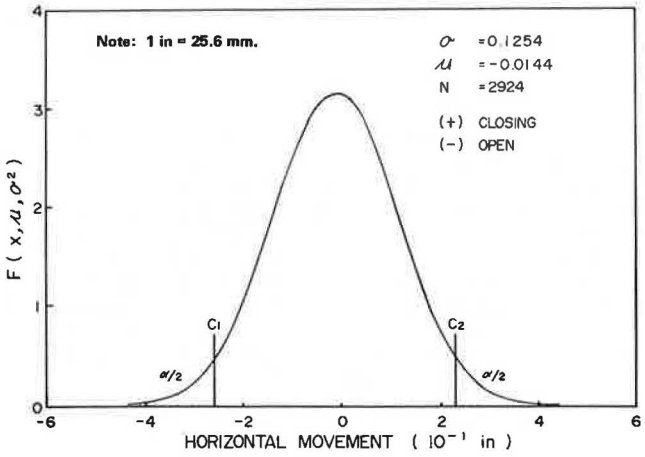


**Figure 10. Normal distribution curve for all spans: electronic measurement.**

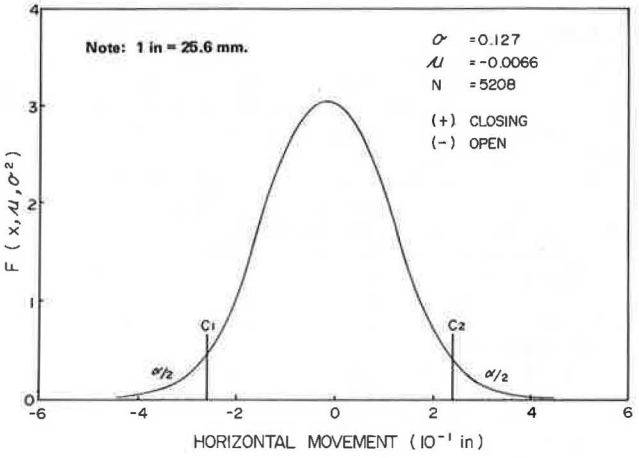


**Figure 11. Normal distribution curve for 21-ft spans: hand measurement.**

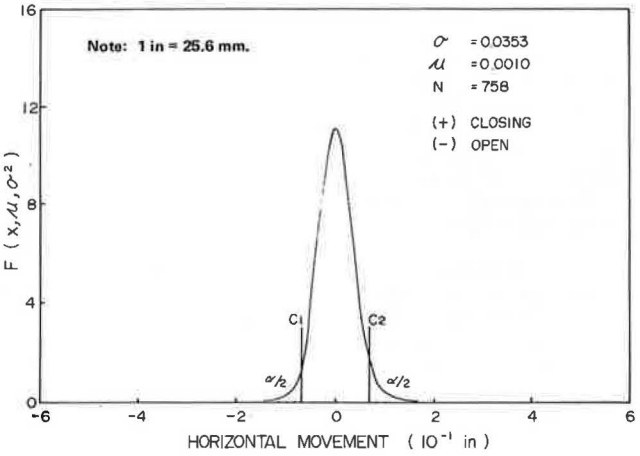


**Figure 12. Normal distribution curve for 40-ft spans: hand measurement.**

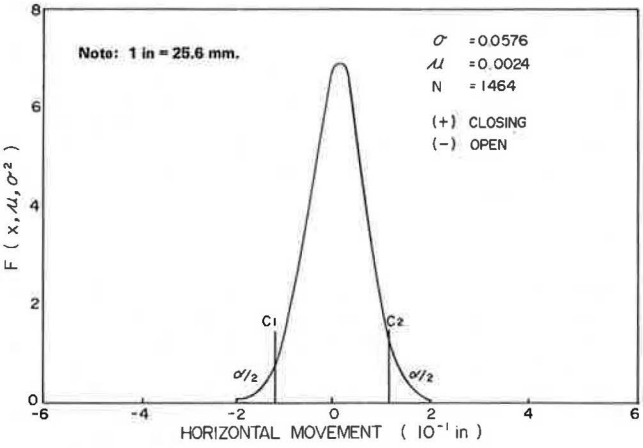


**Figure 13. Normal distribution curve for all spans: hand measurement.**

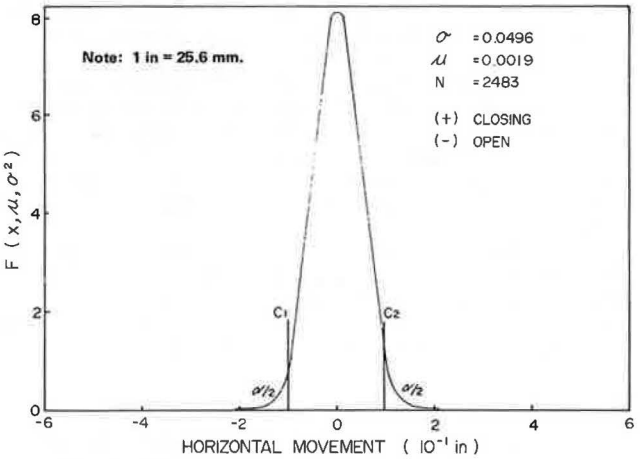


**Table 2. Probable magnitude of joint movements.**

| Measurement Type | Joint Spacing (ft) | Movement (in) 95 Percent Confidence Limits $C_1$ | 95 Percent Confidence Limits $C_2$ | 90 Percent Confidence Limits $C_1$ | 90 Percent Confidence Limits $C_2$ |
|---|---|---|---|---|---|
| Electronic | 40 | -0.26 | 0.23 | -0.22 | 0.19 |
| | 21 | -0.26 | 0.27 | -0.22 | 0.23 |
| | | -0.26 | 0.24 | -0.22 | 0.20 |
| Hand | 40 | -0.12 | 0.11 | -0.10 | 0.10 |
| | 21 | -0.07 | 0.07 | -0.06 | 0.06 |
| | | -0.10 | 0.10 | -0.08 | 0.08 |

Note: 1 in = 25.6 mm; 1 ft = 0.3 m.

of time, since they were based on a monthly difference in the movement. Over this longer time span, the slabs had time to adjust themselves to the temperature and moisture change and more of the slabs took up their share of the movements. It is interesting to note that the long-term movement of a 40-ft slab is almost double that of a 21-ft slab, whereas the short-term movements are almost equal.

The midslab temperature was also measured at one joint in every group. This measurement was taken simultaneously with the horizontal movement. The temperatures include not only hot summers but also some of the worst winters Ohio has seen in many years.

## INTERPRETATION OF RESULTS

In the experimental pavement, the jointing material used was a standard 0.7-in (17.5-mm) premolded seal inserted into a 0.25-in (6.4-mm) saw-cut groove. The pavement was cast and the joints were sawed under almost ideal weather conditions. Enough shrinkage had occurred to crack all joints through before sealing. Neither the vertical edges of the pavement nor the longitudinal pavement shoulder joint was sealed.

### Short-Term Movements

Many of the joints, on a short-term basis, have shown movements as great as 0.25 in (6.4 mm). However, it is not always the same joint that repeatedly shows these large movements. A statistical analysis of the data shows a probability of only 2.5 percent that a particular joint will move this much.

In general, the joints after seven years are still in excellent shape. Close inspection shows no joints completely closed and no joints in which the jointing material has slipped completely to the bottom of the saw-cut groove. However, there are joints in which the seal has lost contact with the joint face over a portion of its length and has slipped, which results in a "scalloped" effect.

The preformed seal will slip if contact with the concrete face of the joint is lost and vibration due to traffic causes it to migrate downward. Tire pressure on compacted snow may cause the same effect. This will happen if the preformed seal opens completely and the adhesive between the seal and the concrete fails.

Therefore, the short-term movement of ±0.25 in (6.4 mm) could be considered as the ultimate movement of a joint. The jointing material should be capable of resisting an occasional extension and compression of 0.25 in without failure.

### Long-Term Movements

It is apparent from Table 2 that long-term movements are appreciably smaller than short-term movements: i.e., $C_1$, $C_2$ = ±0.12 in (3.0 mm) for a 40-ft (12.2-m) slab, and $C_1$, $C_2$ = ±0.07 in (1.8 mm) for a 21-ft (6.4-m) slab. These values should be considered as the actual movements of contraction joints in the midcentral region of the United States (1). If the jointing material is designed to sustain a short-term maximum movement of 0.25 in (6.4 mm), the factor of safety ranges from 2.08 for a 40-ft slab to 3.57 for a 21-ft slab. Similar values can be obtained for different slab lengths and different environmental regions of the United States. The values given above correspond very closely with the values obtained in a 1956 Michigan study (6) for pavements with similar contraction joints and a similar spacing between expansion joints. The tabulated measured values take into account the combined effects of temperature, moisture, and shrinkage.

Although the short-term movements are appreciably larger than the long-term movements, experience has shown that it takes a large number of these cycles to cause a preformed seal to fail. The Ohio study shows that, although these large movements have occurred, the probability of these movements occurring repeatedly at any given joint is less than 3 percent.

### Present Practice

In most areas of the country, the following well-known formula is used to calculate movement:

$$\text{Movement} = \alpha_c (\Delta T) L \quad (3)$$

However, actual measurements do not verify the formula and its use is not recommended. Note that the formula contains three variables, none of which can be estimated with sufficient accuracy. The coefficient of expansion ($\alpha$) varies with different concretes. The temperature range is indeterminate because it has not been shown whether movement varies with air temperature, slab surface temperature, or midslab temperature. Even the slab length is indeterminate because measurements show that, in the short term, two or three slab units may act together. In addition, the formula does not take into account the change in slab length due to moisture.

## CONCLUSIONS AND RECOMMENDATIONS

From the discussion in this paper, it becomes obvious that the present practice of using the temperature-change formula in the calculation of the horizontal movement at a joint in order to design a sealant is not adequate. Neither the length nor the change in temperature nor the coefficient of thermal expansion can be determined with any degree of accuracy. The best approach is to physically measure the movement and get a statistical value of the probable movement.

There are two different types of movements to be considered: short term and long term. The short-term movement, which is large and does not seem to be dependent on the spacing of the joints, is equal to ±0.25 in (6.4 mm) for 21- and 40-ft (6.4- and 12.2-m) spacing. The long-term movement is dependent on joint spacing and is much smaller than the short-term movement. It is recommended that the long-term movement be used in the design of the seal in spite of the fact that it is smaller. The short-term movement can be considered as an upper limit or ultimate value that has to be allowed for rather than being used for design.

Values of long-term movements can be determined for different regions in the United States and other countries by using a statistical analysis of hand measurements similar to the method reported in this article. There is no need for expensive electronic measurements when the same result can be obtained by taking hand measurements at closer intervals--say, every 6 h. Such a measurement could be undertaken on a pavement with 60- or 80-ft (19.2- or 25.6-m) spacing of joints to conform the insensitivity of short-term movements to joint spacing.

In view of the above, the following recommendations are made:

1. A movement of 0.07 in (1.8 mm) should be used as a basis for the design of seals with 20-ft (6.1-m) spacing of joints or less in the midcentral region of the country (1).
2. A movement of 0.12 or 0.125 in (3 or 3.2 mm) should be used for the design of seals with 40-ft (12.2-m) spacing of joints in the midcentral region (1).

3. A similar study should be undertaken in other regions to determine the value of the movement to be used as a basis for the design of seals. These values could be tabulated and used in lieu of Equation 3.
4. A check should be made on short-term movements to confirm that they are in the order of ±0.25 in (6.4 mm) for longer spans.
5. A seal should be designed to accommodate the long-term movement and to resist the short-term movements as an upper limit.
6. The bond between the seal and the face of the joint should be able to take some tension as a further guarantee of holding the seal in place in case of a large opening of the joint.

ACKNOWLEDGMENT

This paper was prepared in cooperation with the Ohio Department of Transportation and the Federal Highway Administration, U.S. Department of Transportation. The contents reflect our views, and we are responsible for the facts and the accuracy of the data presented. The contents do not necessarily reflect the official views or policies of the Ohio Department of Transportation or the Federal Highway Administration. This paper does not constitute a standard, specification, or regulation.

REFERENCES

1. P.J. Nussbaum and E.C. Lokken. Portland Cement Concrete Pavements: Performance Related to Design-Construction-Maintenance. FHWA, Rept., FHWA-TS-78-202, Aug. 1977, revised Nov. 1978.
2. J.P. Cook and I. Minkarah. Development of an Improved Contraction Joint for Portland Cement Concrete Pavements. Ohio Department of Transportation, Columbus, Aug. 1973.
3. I. Minkarah and J.P. Cook. A Study of the Field Performance of an Experimental Portland Cement Concrete Pavement. Ohio Department of Transportation, Columbus, May 1975.
4. I. Minkarah and J.P. Cook. A Study of the Effect of the Environment on an Experimental Portland Cement Concrete Pavement. Ohio Department of Transportation, Columbus, Aug. 1976.
5. I. Miller and J.E. Freund. Probability and Statistics for Engineers. Prentice-Hall, Englewood Cliffs, NJ, 1977.
6. H.C. Coons. Report on Experimental Project in Michigan. HRB, Res. Rept. 17-B, 1956, pp. 35-88.

*Publication of this paper sponsored by Committee on Sealants and Fillers for Joints and Cracks.*

# Design for Minimizing Detrimental Vibrations from Construction Blasts

YONG S. CHAE

**Effects of ground vibrations on structures and people in the vicinity of construction blasts have become a major environmental concern and problem to engineers and contractors as well as to the general public. Understanding of the propagation characteristics of stress waves produced by blasting and structural response to ground vibration is essential in planning and design for safe blasting operations to minimize or eliminate legitimate damage claims and complaints. Both the theoretical and empirical propagation laws for ground motions resulting from blasting are analyzed; by this means, the intensity of ground vibration can be predicted on the basis of weight of explosives, distance from point of detonation, dynamic properties of transmitting medium, and other variables. Existing damage criteria by which the damage to a structure can be related to the intensity of ground vibration are reviewed to show that, although dynamic analysis (such as the response-spectrum technique) may provide the most rational approach, peak particle velocity appears to be the best and most practical criterion for use in design of safe blasting operations. However, the currently recommended design criterion of 50-mm/s (2-in/s) peak particle velocity, applicable uniformly to all types of structures, is found to be inadequate. Revised design criteria based on the type, age, and stress history of the structure are proposed. Structures are classified into four categories, and the safe design value is recommended for each. Human response to vibration is found to be very critical and sometimes a controlling factor in the design. A case study is presented to illustrate a design based on the revised design criteria.**

With the expansion of construction activities and a growing public awareness of and demand for improved environmental quality in recent years, the problem of detrimental vibrations resulting from construction activities has become increasingly important to engineers and contractors. The problem is normally associated with surface activities such as quarry operations and construction projects in residential areas. Specifically, the problem of the effect of vibrations on structures and people becomes most acute when explosives are used in rock excavation for foundations and transportation facilities (tunnels and highways), quarry operations for construction materials, and the mining of natural resources. On the other hand, as Figure 1 (1) shows, operation of construction equipment causes less vibration unless the distance from the source to the affected point is extremely close.

Because the general public is directly involved in the problems of blasting vibration, many investigations have been conducted, both in this country and abroad, on the effects of air and ground vibrations on residential and other structures. Although many of these studies focused on quarry operations, construction blasting raises many of the same problems. There are, however, problems unique to construction blasting that have not received special attention.

To minimize or eliminate legitimate damage claims and complaints, the engineer needs a reliable basis on which to plan and conduct blasting operations. To ensure an environment free from nuisance and annoyance, the engineer must, therefore, be able to determine the maximum weight of explosives that can be detonated without causing damage to adjacent structures and, at times, without having detrimental effects on the human beings in those structures.

The design for minimizing detrimental vibrations

Figure 1. Ground vibration from construction activities.

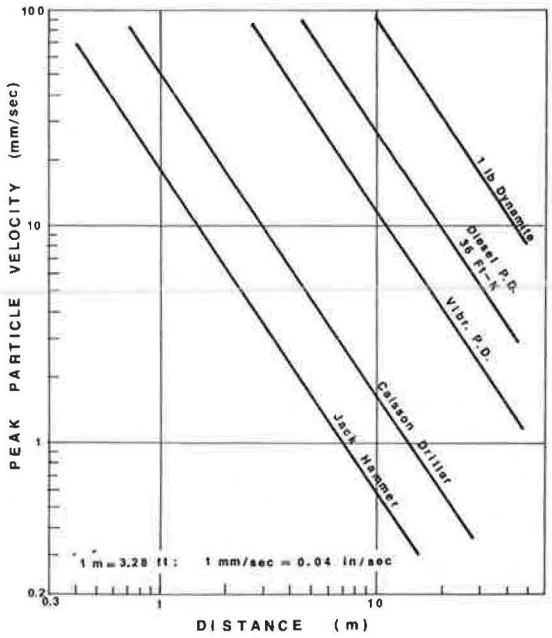


Figure 2. Geometrical attenuation of ground vibration.

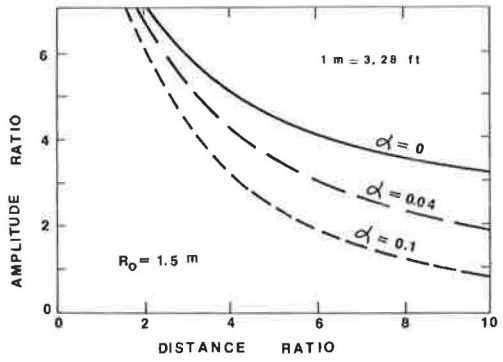


from construction blasts requires the establishment and understanding of (a) the propagation law for ground motions resulting from blasting, whereby the intensity of ground vibration can be predicted on the basis of weight of explosive, distance from point of detonation, dynamic properties of the transmitting medium, and other variables; and (b) reliable damage criteria for different types of structures, whereby the damage produced in a structure can be related to the intensity of ground vibration.

## PROPAGATION LAW FOR GROUND VIBRATIONS

Some of the waves generated by a surface blast move through the rock, and others travel along the surface of the ground. The body waves are propagated in the form of compressive and shear waves, and Rayleigh and other minor waves propagate as the surface waves. Each of these elastic waves travels with a unique velocity that depends on the physical characteristics of the material. Compressive and shear waves propagate with the following velocities, respectively:

$$v_c = [(\lambda + 2G)/\rho]^{1/2} \quad (1)$$

$$v_s = (G/\rho)^{1/2} \quad (2)$$

where $\lambda$ and G are Lame's constants and $\rho$ is the mass density. The velocity of Rayleigh waves is roughly equal to shear-wave velocity.

The rate at which elastic waves decay as they travel also depends on the physical properties of the material. Attenuation of surface-wave energy can be expressed by Bornitz's equation (see Figure 2):

$$A/A_o = \sqrt{R_o/R}\exp[-\alpha(R - R_o)] \quad (3)$$

where A, $A_o$ are amplitudes of ground vibrations at distances R and $R_o$ from the source and $\alpha$ is the coefficient of wave energy absorption. The coefficient $\alpha$ is dependent on the soil types and indicates the degree of deviation from the properties of an ideally elastic medium. The velocities of these waves are greatest in rock and least in unconsolidated soil, and the rate of energy decay is greater in soil than in rock due to considerable frictional losses.

The attenuation equation, Equation 3, is given in terms of displacement amplitude ratio and does not contain the terms for charge weight and other related factors. For theoretical analysis, therefore, it is convenient and useful to use a dimensional analysis that involves the following dependent variables (2):

- $\delta$ = maximum ground displacement,
- v = maximum velocity of displaced particle at a given point,
- a = maximum acceleration of displaced particle at a given point, and
- f = frequency of motion of displaced particle.

The most convenient independent variables to use are

- W = energy released by explosion,
- R = distance from the point of detonation to the point of observation,
- $\rho$ = mass density of the material,
- c = seismic velocity within the material, and
- t = time elapsed.

By applying the Buckingham Pi theorem, the dependent variables can be shown to be related to dimensional groups of independent variables, as follows:

$$\delta/R = g_1[(tc/R), (W/\rho c^2 R^3)] \quad (4)$$

$$v/c = g_2[(tc/R), (W/\rho c^2 R^3)] \quad (5)$$

$$aR/c^2 = g_3[(tc/R), (W/\rho c^2 R^3)] \quad (6)$$

where $g_1$ through $g_3$ are unknown functions of the dimensionless groups of independent variables. An examination of all of the above equations indicates that, for explosions of different yields in a given transmitting medium ($\rho c$ = constant), the range scales as the cube root of the energy released.

It may be generalized, therefore, that for a given transmitting medium ($\rho c$ = constant) the propagation law for ground motion can be written as

$$Y = d(R/W^b)^a \quad (7)$$

where Y is the peak amplitude of ground motion (either displacement, velocity, or acceleration) and a, b, and d are constants associated with the dynamic properties of the transmitting medium and other variables. It is noted from this equation

**Figure 3. Peak particle velocity versus scaled distance.**

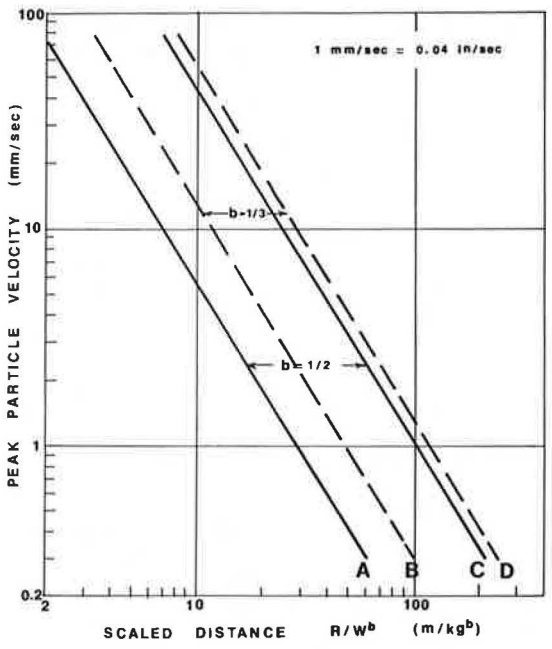


**Figure 4. Damage criteria for structures.**

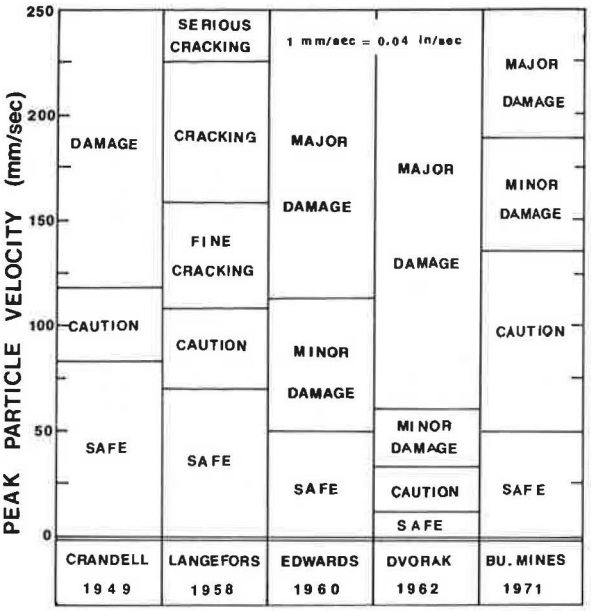


that the peak amplitude of vibration is directly proportional to the quantity $R/W^b$, called scaled distance. This relation is linear when plotted on a log-log scale, as shown in Figure 3, where Y is expressed as a peak particle velocity. Lines A and C show the lower and upper bounds of all velocity data obtained by the U.S. Bureau of Mines (3) by using square-root scaling (b = 1/2). These two lines are the envelopes to hundreds of test points, and the upper-bound line represents the most severe vibration. Lines B and D represent the lower- and upper-bound lines obtained by using cube-root scaling (b = 1/3), based on data compiled by Hendron (4). The relative merits of square-root and cube-root scaling are subject to debate, but the relation given by square-root scaling is generally more conservative.

Although the relation given in Figure 3 may be used as a guideline for preliminary calculation of the intensity of ground vibration at a given site (in terms of peak particle velocity), test blasts should be conducted at the project site to establish the propagation law because, as Figure 3 shows, there is a wide spread between the upper and lower bounds of the relation. If test blasts are not conducted, the amplitude may be assumed by using the upper-bound line. It should be noted that, if one uses this line, for a peak particle velocity of 50 mm/s (2 in/s) the scaled distance is 9 $m/kg^{1/2}$ (20 $ft/lb^{1/2}$) and for the velocity of 13 mm/s (0.5 in/s) the scaled distance is 22 $m/kg^{1/2}$ (50 $ft/lb^{1/2}$).

## DAMAGE CRITERIA FOR STRUCTURES

Fundamentally, the property of wave motion that governs the effects of vibrations on people and structures is the energy that the waves deliver to structures. This may, as previously described, be expressed by the peak amplitude of motion produced (displacement at a certain frequency), by the peak acceleration generating the force that moves a structure, or by the energy itself expressed as the particle velocity of the motion it produces. All of these quantities are subject to direct measurement, and various combinations of them have been used as numbers against which to define damage conditions.

One of the first damage criteria developed was the energy ratio (ER) of Crandell (5), defined as the square of the ratio of peak acceleration to frequency:

$$ER = (a/f)^2 \quad (8)$$

If the ground motion is assumed to be sinusoidal in character, then

$$ER = 4\pi^2 \cdot v^2 \quad (9)$$

ER is, therefore, directly proportional to the square of the peak particle velocity. It can also be shown that the particle velocity is a measure of radial strain in the mass, as follows:

$$\epsilon_r = v_r/c \quad (10)$$

where

$\epsilon_r$ = peak radial strain,
$v_r$ = peak radial particle velocity, and
c = seismic wave velocity.

Based on these theoretical concepts and field observations, many researchers have arrived at the conclusion that the best criterion to use in defining damage-causing vibrations is energy expressed in terms of peak particle velocity (5-10). In 1971, the U.S. Bureau of Mines published a comprehensive report that presented the results of a 10-year program to study the problem of air blast and ground vibrations generated by blasting (3). This study contained a review of all available data in this country and abroad, including the original study the U.S. Bureau of Mines made during the period from 1935 to 1942 and the studies of Crandell (5), Langefors (8), Edwards and Northwood (9), Dvorak (10), and Wiss and Nicholis (11). The conclusion of this report, drawn from the consensus of these researchers, is that peak particle velocity is the best criterion for evaluating the damage potential due to vibration. Figure 4 summarizes the findings of the researchers referred to above. It is apparent from this figure that a peak particle velocity of 50 mm/s (2 in/s) is a conservative safe

**Table 1. Recommended design criteria.**

| Class | Description | Peak Particle Velocity (mm/s) |
|---|---|---|
| 1 | Structures of substantial construction | 100 |
| 2 | Relatively new residential structures in sound condition | 50 |
| 3 | Relatively old residential structures in poor condition | 25 |
| 4 | Old residential structures in very poor condition | 13 |

Notes: 1 mm = 0.039 in.
If structure is subjected to repeated blasting or blasting is done without instrumentation, lower class by one.

**Figure 5. Maximum charge weight versus distance.**

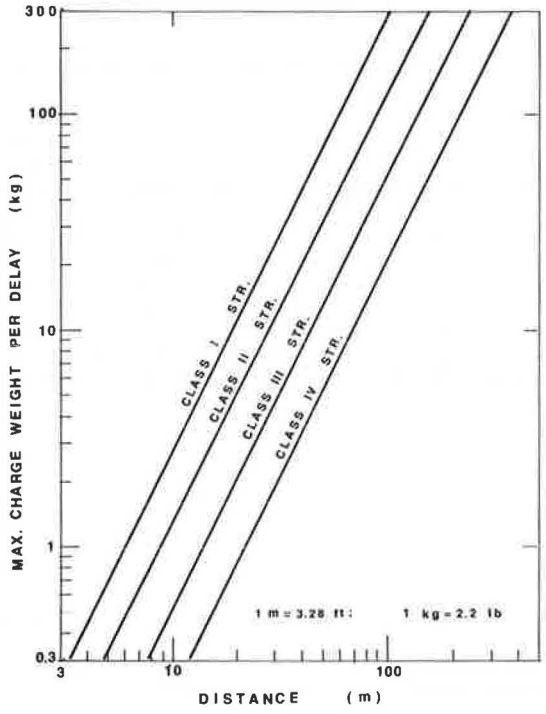


limit--i.e., causing no damage to structures. The U.S. Bureau of Mines has recommended this value as the safe blasting limit.

The most recent development in establishing design criteria is the use of the response-spectrum technique (4,12), which has been used extensively in the analysis of structural response to earthquake-induced ground motion. The response-spectrum technique takes into account the dynamic characteristics of the structure being analyzed and is applicable to the entire frequency range rather than the limited frequency range represented by the velocity bound. This technique is more rational because (a) it accounts for dynamic excitation of the structure, which may be magnified several times over the input ground motion, and (b) a response spectrum reflects all of the variables related to structural response to ground motion.

## RECOMMENDED BLAST DESIGN CRITERIA

In the use of peak particle velocity as the design criterion, the value of 50 mm/s established by the U.S. Bureau of Mines has been widely followed. During the past several years, however, there have been indications that this limit may not be adequate. Vibration levels much lower than 35 mm/s (1.4 in/s) have caused many complaints (13), and there have been incidences in which damage to structures occurred when the velocity was as low as 6 mm/s (0.25 in/s). On the other hand, in many other instances, a maximum value of 178 mm/s (7 in/s) has been proved quite safe. A close examination of the U.S. Bureau of Mines report (3) indicates that more than half of the structures studied suffered no damage from blasts that produced particle velocities greater than 100 mm/s (4 in/s) whereas minor damage to some structures occurred when the velocity was as low as 23 mm/s (0.9 in/s).

The 50-mm/s damage criterion for structures may, therefore, be too conservative for some structures and not safe enough for others. This is because, as previously discussed, the criterion is based solely on ground motion and does not take into account the dynamic characteristics of the structure itself. In other words, the response of a structure to ground vibration will also depend on the type of structure involved, the type of construction, the stress history (age), and the vibration-time history (peak value as well as duration).

The best way to determine the dynamic response of a structure to ground motion is, therefore, a complete dynamic analysis of the structure by numerical integration, phase diagram, Fourier analysis, or response spectra, where ground motion is used as input. Although there may be occasions that require a dynamic analysis of structural response to blasting vibrations, such a method is expensive and time-consuming and requires an actual time history; in most cases, such an analysis is not warranted.

It is recommended, therefore, that peak particle velocity be used as the design criterion but that the type, age, and condition of the structure be taken into account. To this end, structures are classified into four categories. Table 1 gives the recommended design criterion for each. Admittedly, the description for each category is rather broad and is subject to the evaluation and judgment, as well as the conservatism, of the engineer. Currently, the descriptions are being refined based on case studies. Another aspect being studied is the effect of frequency on the safe velocity value for each of the four different categories of structures.

It is essential that test blasts be conducted at the project site to establish the propagation law. In the absence of such tests, however, one may use the upper-bound line of Figure 3 for preliminary analysis. The recommended design values for scaled distance based on the upper-bound line are given below:

| Class | Recommended Scale Distance (m/kg) |
|---|---|
| 1 | 6 |
| 2 | 9 |
| 3 | 14 |
| 4 | 22 |

Figure 5 shows a nomogram that has been constructed based on these recommended design values for use in estimating the safe charge per delay or minimum safe distance for the four classes of structures. Note that, for a distance of 30 m (100 ft) between the blast point and a class 4 structure, 1.8 kg (4 lb) of explosive per delay could be safely used. The safe amount of explosive per delay is increased to about 45 kg (100 lb) for a class 1 structure located at the same distance. This is about 25 times as much explosive per delay.

## EFFECTS OF BLAST VIBRATIONS ON PEOPLE

The human perception of vibration to alternating or

Figure 6. Human response to vibration.

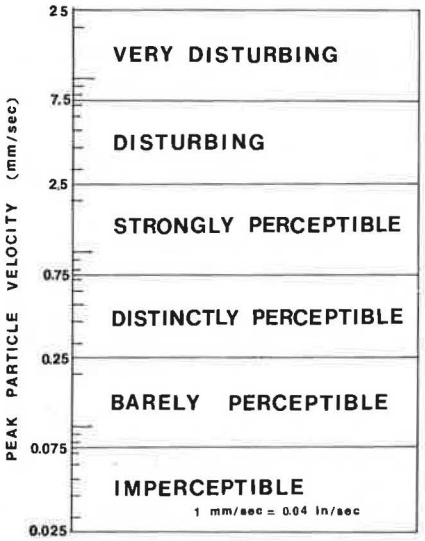


Figure 7. Propagation law for ground motion at site.

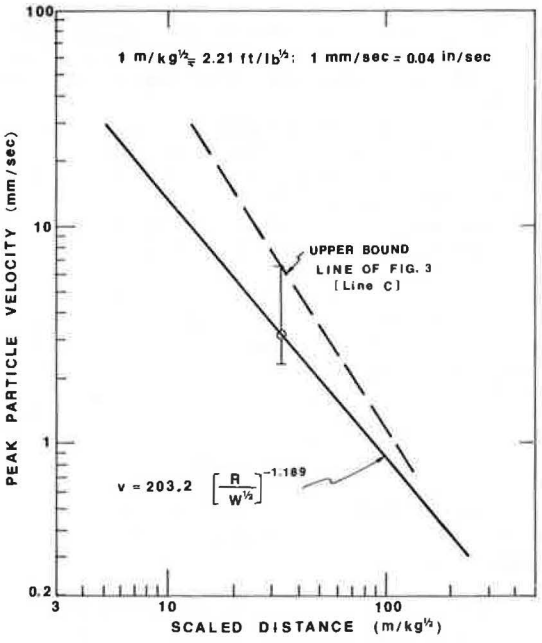


shaking force is a very complex problem because it depends on many factors, such as displacement, frequency, velocity, and acceleration. In addition, it is highly variable among individuals. In addition, a tolerance to vibration may be built up over a period of repeated exposure. Continual exposure to vibration accelerations in excess of 1.0 g can cause severe discomfort. Vibration frequency appears to play an important part in these cases: Tolerance is lowest in the low-frequency range--say, 5-20 cycles/s--and increases with increasing frequency.

Several investigations have been conducted to evaluate human perception to steady-state vibrations. A study by Reiher and Meister (14) has been the most frequently cited. However, vibration associated with blasting is transient in nature, and the human response to such vibration must be characterized not only by acceleration and velocity or by displacement and frequency, which is sufficient for the steady state, but also by the decay rate (damping attenuation) of the vibration. An experimental work by Wiss and Parmelee (15) is the most recent one to study the human response to transient vibration. The effect of damping was found to reduce the vibration perception of human beings.

Based on the results cited above and considerations of uniformity in the presentation of human-response regions, it is proposed that the human-response ratings shown in Figure 6 be used for design criteria. It is readily seen in this figure that velocities of 13-100 mm/s (0.5-4 in/s), which have been defined as the safe limits for structures, will be quite objectionable to human beings. Therefore, depending on the character of the area in which blasting is to be conducted, safe velocities might be as small as 8 mm/s (0.3 in/s), if one takes the upper boundary of "disturbing" as the safe limit for preventing possible complaints from residents.

## CASE STUDY

An old navy facility in Brooklyn, New York, is being rehabilitated to build a new water-pollution control plant. This required removal of massive concrete piers and foundations to prepare for the new plant. The only economical way of removing these structures was by blasting. Unfortunately, there were a number of old residences (class 4 structures) near the blasting site, and the utmost care had to be exercised in blasting so as not to cause any damage to the residences.

During the period from December 18, 1978, through February 22, 1979, three series of test and monitoring blasts were conducted at the site. This provided a total of 163 test data points. It should be noted that, of this total, 19 points yielded "no vibration", which can mean vibration levels of anywhere from 0- to 0.25-mm/s (0- to 0.01-in/s) peak particle velocities. The 0.25-mm/s velocity appears to be the lowest vibration level that the equipment used could detect. Since 19 out of 163 data points represents a significant portion of the data obtained, these points were included in the data analysis.

Figure 7 shows the results of the regression analysis on data for particle velocity versus scaled distance for all three test series (163 data points). The upper-bound line of Figure 3 is also shown. To avoid confusion, each data point is not given, but the midpoint of the data is represented by a symbol and the length of the line represents the range of the data. The vertical line through the midpoint represents one standard deviation. Based on the regression analysis, the wave-propagation law for ground motion at the project site may be established as

$$v = 203.2\,(R/\sqrt{w})^{-1.189} \qquad (11)$$

Note that the standard deviation is rather small and there is a good correlation between peak particle velocity and scaled distance.

Because of the very poor structural condition of the residential houses in the case study, the safe peak particle velocity had to be set at an extremely low value equal to the vibration level caused by heavy trucks passing by [1.0 mm/s (0.04 in/s)]. However, based on human susceptibility to vibration, the limit was recommended to be 2.5 mm/s (0.1 in/s). Based on the propagation law for ground motion established for the project site and given in Equation 11, the maximum safe explosive charges for limiting the vibration levels below the specified values can be calculated as

Figure 8. Design maximum safe charge weight versus distance.

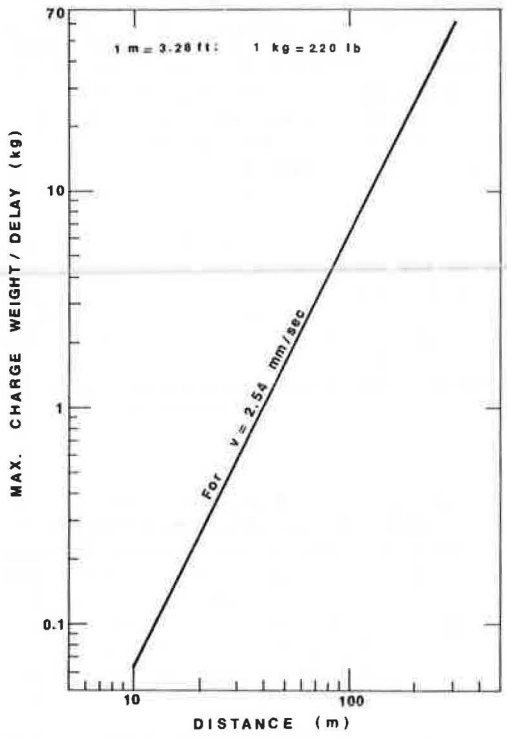


$$W = (R/94.63)^2 \quad (12)$$

Figure 8 shows a graph for estimating safe charge and distance limits for the above criterion. By using this method, the contractor was able to proceed with construction without unnecessary delay and without causing any damage to the structures.

## CONCLUSIONS

1. In most situations, dynamic analysis (including response spectra and Fourier analysis) of structural response to blasting vibrations is not warranted. Thus, peak particle velocity becomes the best criterion for safe design.
2. Peak particle velocities ranging from 13 to 100 mm/s (0.5-4 in/s) are recommended as design criteria for four different categories of structures based on type, age, and structural soundness.
3. Levels of human tolerance to ground vibrations are considerably lower than safe vibration limits for structures. The human response level can therefore be used to ensure safe blasting operations.
4. A case study is presented to illustrate a design based on the peak-particle-velocity concept and structural categorization.

## REFERENCES

1. J.R. Wiss. Vibrations During Construction Operations. Journal of Construction Division, Proc., ASCE, Vol. 100, No. CO3, Sept. 1974, pp. 239-246.
2. N.R. Ambraseys and A.J. Hendron. Dynamic Behavior of Rock Masses. In Rock Mechanics in Engineering Practice (K.G. Stagg, ed.), Wiley, New York, 1968.
3. H.R. Nichols and others. Blasting Vibrations and Their Effects on Structures. U.S. Bureau of Mines, Bull. 656, 1971.
4. A.J. Hendron. Engineering of Rock Blasting on Civil Projects. In Structural and Geotechnical Mechanics, Prentice-Hall, Englewood Cliffs, NJ, 1977, pp. 242-277.
5. F.J. Crandell. Ground Vibrations Due to Blasting and Its Effects upon Structures. Journal of Boston Society of Civil Engineers, April 1949, pp. 222-245.
6. Y.S. Chae. Ground Motions: Part II--Multi-Protection Design of Structures. Defense Civil Preparedness Agency, U.S. Department of Defense, TR-20, 1973, pp. 75-224.
7. Y.S. Chae. Design of Excavation Blasts to Prevent Damage. Civil Engineering, April 1978, pp. 77-79.
8. U. Langefors and others. Ground Vibrations in Blasting. Water Power, Sept. 1958, pp. 335-338; Oct. 1958, pp. 390-395; Nov. 1958, pp. 421-425.
9. A.T. Edwards and T.D. Northwood. Experimental Studies of the Effects of Blasting on Structures. The Engineer, Vol. 210, Sept. 1960, pp. 538-546.
10. A. Dvorak. Seismic Effects of Blasting on Brick Houses. Prace Geofyrikeniha Ustance Ceskoslovenski Akademie, Ved. 169, Geofysikalni Sbornik, 1962, pp. 189-202.
11. J.F. Wiss and H.R. Nicholis. A Study of Damage to a Residential Structure from Blast Vibrations. ASCE, New York, 1974, pp. 1-73.
12. C.H. Dowding. Ground-Structure Response to Blasting Vibrations. Proc., 14th Annual Meeting, Society of Engineering Science, Lehigh Univ., Bethlehem, PA, Nov. 1977, pp. 1085-1097.
13. D.V. Power. A Survey of Complaints of Seismic-Related Damage to Surface Structures Following the Salmon Underground Nuclear Detonation. Bull., Seismological Society of America, Berkeley, CA, Vol. 56, Dec. 1966.
14. H. Reiher and F.J. Meister. The Effect of Vibration on People. Headquarters, Air Material Command, Wright Field, OH, Rept. F-TS-616-RE, translation, 1946.
15. J.F. Wiss and R.A. Parmelee. Human Perception of Transient Vibrations. Journal of Structural Division, Proc., ASCE, Vol. 100, No. ST4, 1974, pp. 773-787.

*Publication of this paper sponsored by Committee on Earthwork Construction.*

# Behavior and Repair of Deteriorated Reinforced Concrete Beams

I. MINKARAH AND B.C. RINGO

**The results of a study on reinforced concrete beams subjected to deterioration effects such as those caused by the action of deicing salts are presented. Included are descriptions of the basic problems in the field, including the corrosion mechanism, and the experimental results. Beam tests are described that show the behavior of beams with specific conditions of interrupted cover and/or bond. Specific signs of distress useful in field inspection are emphasized. Also described is a series of tests of those same beams after repair. Specific attention is given to how much of the beam's original strength can be expected to be recovered after rehabilitation.**

The purpose of the experimental and analytic study described in this paper is to provide quantitative information concerning the effect of loss of cover and flexural bond on the strength of reinforced concrete beams and to experimentally determine the response of the beam after repair. The overall study leads to effective repair for beams subject to these deficiencies as well as to an understanding of the behavior of these members.

To initiate this study, a total of 40 reduced-scale 5-in x 10-in x 9.5-ft (12.7-cm x 25.4-cm x 2.9-m) reinforced concrete beams were constructed with predetermined and varying amounts of cover removal and bond loss in the region of varying flexural stress (1-3). The beams were loaded until failure occurred. As load was applied, the progressive values of strain in the reinforcing steel bars, as well as load and deflection increments, were recorded. The presentation includes fabrication details, testing details, and conclusions on the beam's behavior when bond or cover does not exist and on the flexural capacity restored to the beam by the repair process (4,5).

The loss of significant amounts of cover and flexural bond in reinforced concrete beams has become a widespread problem. The problem is most commonly found in bridges and parking garages that are subjected to deicing salt. The salt releases chloride ions that enter the concrete and corrode the reinforcing steel. The corrosion products increase in volume, which results in cracking of the concrete cover and progressive loss of flexural bond. Insufficient research has been conducted to date to determine whether loss of cover and flexural bond significantly reduces the strength of reinforced concrete beams and to quantify that loss. Little or no information exists to document quantitatively the behavior of the beam after repair. This project addresses these subjects.

## CORROSION PROCESS

This work deals with the reinforced concrete beam subjected to the detrimental effects of actions equal to or similar to those of deicing salt applications. In view of this, it is appropriate to briefly present a description of the corrosion process.

Chemically, concrete can be characterized as a saturated solution of calcium hydroxide and is very alkaline in nature. Good-quality, uncontaminated concrete has a pH of approximately 12.5. The reinforcing steel bar, chemically iron, is unstable in an oxygen environment. Initially, the bar's corrosion rate is high and forms a passive oxide film around the steel bar, which in turn acts as a barrier to moisture and oxygen. At this point, the corrosion rate decreases markedly and the reinforced concrete beam is stable. This passive oxide film is very stable in the high-pH environment; thus, the steel reinforces the concrete, and the alkaline nature of the concrete stabilizes the oxide film on the steel, preventing further corrosion.

The resultant effect of the application of deicing salts is to destroy this protective oxide film. Both calcium chloride and sodium chloride are largely chloride (64 and 61 percent, respectively). Both materials ionize rapidly in water, which leaves the chloride ion free to migrate into the concrete. The chloride ion ($Cl^-$) is chemically aggressive and will lower the pH of the concrete. The lower pH allows the passive oxide film to dissolve and exposes the reinforcing bar to additional moisture and oxygen.

The basic corrosion mechanism, then, is as follows: Salt is introduced into the reinforced concrete. The salt dissolves and the chloride ion penetrates the concrete through cracks, voids, and surface pores, lowering the pH of the concrete. The existing oxide film dissolves, separates from the steel bar, and exposes it to moisture and oxygen. The process continues with corrosion of the steel and separation of the oxides. The process builds up pressures on the order of 4000 psi (27.6 MPa) as a result of the expansion of the corrosion product. The surfaces above and below the reinforcing bar are separated and thus delaminated by the internal stresses. This is a continuing process unless specifically arrested by rehabilitation (6). The delamination breaks at the surface of the concrete and forms a spall that is in turn removed by freeze-thaw cycles and the general service performance of the beam. The amount of deterioration and its duration will depend on numerous factors, such as the ratio of cover to bar diameter, the general arrangement of bars within the section, and the porosity of the concrete (7;8, p. 79).

In summary, then, it is the attack of the chloride ion ($Cl^-$) and the changing pH of the concrete that lead to the deterioration of the reinforced concrete. The time element of this deterioration is highly variable. It is severely affected by weather conditions, including the number of freeze-thaw cycles, the nature and quality of the concrete mix itself, the amount of protection (cover) afforded the steel bars, and the amount of deicing salts applied to the concrete surface, in addition to other variables. Severe deterioration has been observed in parking garages in as short a time as two years. This paper deals with the structural behavior and strength of these deteriorated reinforced concrete beams.

## TEST BEAMS

A total of 40 beams were constructed. Each beam had a basic cross section 5 in (12.7 cm) wide and 10 in (25.4 cm) deep, and the reinforcement consisted of two no. 4 bars placed at an effective depth of 8.25 in (21 cm). Stirrups made of 0.187-in (4.8-mm) diameter smooth wire were placed at 4 in (10.2 cm) center to center in the approximate outer thirds of

the beam to avoid a premature shear failure. Five control beams were cast without any interruption of cover and/or bond. The cross section is shown in Figure 1 and the steel placement in Figure 2.

To achieve an effective loss of cover and loss of cover and bond in the laboratory beams, concrete was blocked out in the casting process in order to simulate deterioration. This was done for 35 beams. For a loss of the 1.5-in (3.8-cm) cover, concrete was blocked out from the bottom of the reinforcing bar to the bottom of the beam. For a loss of both cover and flexural bond, concrete was blocked out from the top of the reinforcing bar to the bottom of the beam in such a way that a piece of paper could be inserted in between the bar and the cast concrete. This pattern is shown in Figure 1. The concrete was vibrated briefly to ensure complete filling of the form work. Both cover and bond were removed for distances of 1-6 ft (0.3-1.8 m), in 1-ft increments, symmetrically about the beam's centerline. A total of 12 beams with both cover and bond removed from 1 to 3 ft (0.3-0.9 m) were repaired, after they were initially tested to failure. The repair was done in two ways. One group was repaired by using a 6000-psi (41.4-MPa) mortar mix without preapplication of a bonding agent, and one similar group was repaired by using the same mortar mix after application of a bonding agent. All 12 beams were then again tested to failure.

The beams were 10 ft (3 m) long and spanned 9.5 ft (2.9 m). The load was applied as one concentrated load on a 5-in (12.7-cm) square bearing pad located at a point just outside the zone of simulated deterioration. The bonding agent used was a Type II epoxy (5) and is described later in this paper.

## MATERIALS

The materials were representative of those conventionally used in reinforced concrete construction such as parking garages and bridges. The reinforcing bars were no. 4 standard deformed bars with an average tensile yield point of 63.5 ksi (438 MPa) and a range of 62.0-65.0 ksi (427-448 MPa). Stirrups were fabricated of 0.187-in (4.8-mm) round smooth wire. The concrete used throughout the project was supplied by a local ready-mix plant. The 28-day compressive strength averaged 6350 psi (43.8 MPa) and ranged from 6100 to 6600 psi (42-45.5 MPa). The modulus of rupture averaged 700 psi (4.8 MPa). Failure models of the cylinders were consistent and typical of the anticipated conical splitting usually observed in well-made cylinders. Curing was done at a temperature range of 76°-78°F (24.4°-25.6°C), room temperature in the laboratory, and under taped plastic sheets for all beams and cylinders. The five control beams, those without any interruption of cover or bond, were tested over the two-year term of this project. The failure loading was an average of 11 ± 0.5 kips (48.9 ± 2.2 kN), and the testing error was estimated at less than ±0.2 kip (0.9 kN). The slump of the concrete, which used a bank-run gravel 0.375-in (9.5-mm) maximum-size coarse aggregate and portland cement, averaged 2.5 in (6.4 cm). It is the judgment of the investigators that the material properties and beam properties produced were sufficiently consistent as to have no practical or significant effect on the results and conclusions of the test program.

Figure 1. Beam details.

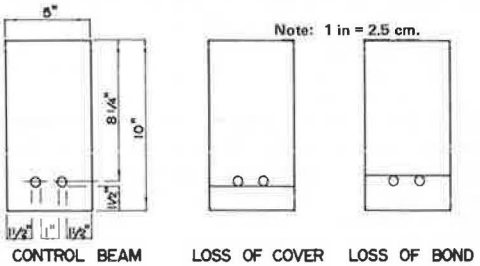


## BONDING AGENT

In the beam-repair process, only one bonding agent was used: a clear, amber-colored amino-amine epoxy system that contained no mineral filler (5). It suited the procedures of the test project in the laboratory because of its convenient physical properties. With a pot life of slightly more than 1 h, it could be applied in temperatures of 60°F (15.6°C) and above, was tack free in less than 2 h, and was hard dry after one overnight curing period. It was a relatively thick syrup but was readily applied by brush. It should be noted that it was not the purpose of this project to test the various bonding agents available (4) but rather to ascertain their integral effect on the repair process of the beam.

## TEST PROCEDURE

The beam tests were performed by using a self-containing testing-installation structural frame and the MTS hydraulic testing machine manufactured by MTS Systems Corporation of Minneapolis, Minnesota.

This allowed a consistent application of the load in 500-lb (227-kg) increments, at a rate of 20 lb/s (9 kg/s) at 3-min intervals. Deflection measurements and strain gage readings were recorded immediately before and after each 500-lb load increment was applied. Deflections were measured at midspan by using a Soiltest 0.001-in (0.025-mm) dial gage.

Twenty-six of the beams were tested with the location of the concentrated load at a point 3 ft (0.9 m) from the left-hand reaction. Others were tested with the load 1.5 ft (0.46 m) from that support due to the increased length of simulated deterioration. These locations are also shown in Figure 2. This created in the test beams a con-

Figure 2. Dimensions of test beam.

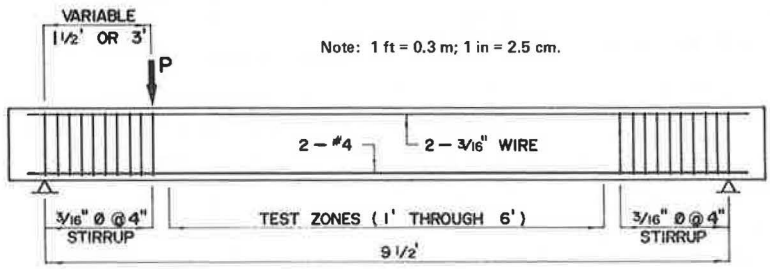

Figure 3. Structural mechanics.

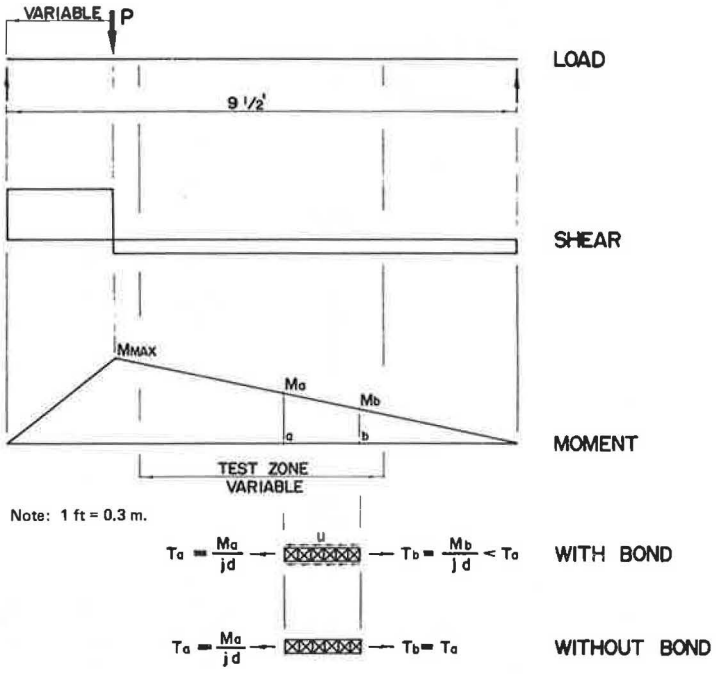


Figure 4. Strain-gage locations.

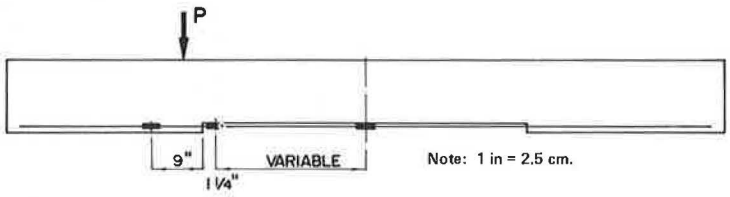


stantly changing moment gradient, which is necessary to induce variable tensile stresses in the reinforcing bar and the corresponding magnitudes of flexural bond. This is shown in Figure 3, where the fundamental behavior of the composite reinforced concrete beam is indicated.

Each beam that was eventually repaired went through two series of loadings. Before each beam was repaired, it was loaded to 3 kips (13.3 kN) in order to initiate cracking. The 3-kip load produced the kind of working stress to which a parking-garage beam would likely be exposed. The first set of beams tested was loaded with several cycles of this working-stress load, but cycles other than the first failed to increase the size of any cracks. For this reason, only one cycle of loading was used thereafter. After each beam had been loaded in this way, it was tested to failure. Catastrophic failure was avoided in all except three situations. Beams intended for repair were then removed, repaired, and retested to ascertain the maximum load-carrying capacity of the restored beam. Each beam was loaded until the concrete failed (usually in the compression zone). The beam was considered to have failed when it would accept no more load.

## INSTRUMENTATION

To determine the effect of the different beam types (the nature and amount of simulated deterioration) on the reinforcing steel, strain gages were attached to one reinforcing bar on each beam in several locations. The locations of the gages were selected on the basis of data obtained from the report by Bryars (1). A minimum of two gages per altered beam was used in locations that were thought to be the most critical (see Figure 4).

The strain gage used was the Baldwin-Lima-Hamilton type AB-19 bakelite gage. This is not normally a desirable gage for strain measurements of reinforcing bars because of the involved application process, but an abundance of these gages was readily available. The application process was tested and proved to be satisfactory. After applying the gages to the reinforcing rods, the gages were waterproofed and padded to reduce the risk of damage during the concrete placement. The V/E-20A digital strain gage indicator, equipped with the V/E-25 scan controller, the V/E-21A switch, balance, and calibration module, and the V/E-22B printer, was used to read, scan, and print the numerous strain measurements. These instruments are manufactured by Vishay Instruments of Malvern, Pennsylvania.

## RESULTS AND DISCUSSION

The testing procedures used over the two-year span are considered quite successful (1-3). Results were reproducible, and numerical values over the two years were quite consistent and well within the magnitudes of error inherent in any testing procedure. Of equal importance was the success of the techniques used to simulate the deteriorated beam. Again, test results were consistent and acceptable. All test results are summarized in Table 1, which contains both experimental results and relevant calculations based thereon.

There are two main areas of importance that must be presented in these results. The first, of course, is the set of numerical test results ob-

**Table 1. Experimental results.**

| Loss of Cover (ft) | Loss of Bond (ft) | Repaired | | Test Results | | | | Coefficient of Strength[a] | |
|---|---|---|---|---|---|---|---|---|---|
| | | Without Bonding Agent | With Bonding Agent | Maximum Load (kip) | Maximum Moment (kip-ft) | $f'_c$ (ksi) | $f_y$ (ksi) | Loss | Recovery |
| 0 | 0 | - | - | 10.5 | 21.55 | 7.0 | 64 | - | - |
| 0 | 0 | - | - | 11.5 | 23.60 | 6.2 | 65 | - | - |
| 0 | 0 | - | - | 11.0 | 22.58 | 6.2 | 65 | - | - |
| 0 | 0 | - | - | 18.0 | 22.74 | 6.8 | 63 | - | - |
| 0 | 0 | - | - | 17.5 | 22.10 | 6.8 | 63 | - | - |
| 1 | 0 | - | - | 10.9 | 22.34 | 7.0 | 64 | 0.991 | - |
| 1 | 0 | Yes | - | 9.5 | 19.50 | 7.0 | 64 | - | 0.864 |
| 1 | 0 | - | Yes | 11.0 | 22.58 | 7.0 | 64 | - | 1.000 |
| 1 | 1 | - | - | 11.0 | 22.58 | 6.2 | 65 | 1.000 | - |
| 1 | 1 | - | - | 10.8 | 22.17 | 7.0 | 64 | 0.982 | - |
| 1 | 1 | Yes | - | 9.5 | 19.50 | 7.0 | 64 | - | 0.864 |
| 1 | 1 | - | Yes | 11.0 | 22.58 | 7.0 | 64 | - | 1.000 |
| 1 | 1 | - | - | 11.0 | 22.58 | 6.2 | 65 | 1.000 | - |
| 2 | 0 | - | - | 10.4 | 21.35 | 7.0 | 64 | 0.945 | - |
| 2 | 0 | Yes | - | 9.5 | 19.50 | 7.0 | 64 | - | 0.864 |
| 2 | 0 | - | Yes | 11.0 | 22.58 | 7.0 | 64 | - | 1.000 |
| 2 | 2 | - | - | 11.0 | 22.58 | 6.2 | 65 | 1.000 | - |
| 2 | 2 | - | - | 11.0 | 22.58 | 6.2 | 65 | 1.000 | - |
| 2 | 2 | - | - | 10.0 | 20.52 | 7.0 | 64 | 0.909 | - |
| 2 | 2 | Yes | - | 10.0 | 20.52 | 7.0 | 64 | - | 0.909 |
| 2 | 2 | - | Yes | 11.0 | 22.58 | 7.0 | 64 | - | 1.000 |
| 3 | 0 | - | - | 9.5 | 19.50 | 7.0 | 64 | 0.864 | - |
| 3 | 0 | Yes | - | 9.5 | 19.50 | 7.0 | 64 | - | 0.864 |
| 3 | 0 | - | Yes | 11.0 | 22.58 | 7.0 | 64 | - | 1.000 |
| 3 | 3 | - | - | 11.0 | 22.58 | 6.2 | 65 | 1.000 | - |
| 3 | 3 | - | - | 9.9 | 20.30 | 7.0 | 64 | 0.900 | - |
| 3 | 3 | Yes | - | 9.5 | 19.50 | 7.0 | 64 | - | 0.864 |
| 3 | 3 | - | Yes | 10.5 | 21.55 | 7.0 | 64 | - | 0.955 |
| 4 | 0 | - | - | 18.0 | 22.73 | 6.8 | 63 | 1.000 | - |
| 4 | 0 | - | - | 17.5 | 22.10 | 6.8 | 63 | 0.986 | - |
| 5 | 0 | - | - | 19.0 | 24.00 | 6.8 | 63 | 1.000 | - |
| 5 | 0 | - | - | 19.0 | 24.00 | 6.8 | 63 | 1.000 | - |
| 6 | 0 | - | - | 18.0 | 22.74 | 6.8 | 63 | 1.000 | - |
| 6 | 0 | - | - | 19.5 | 24.63 | 6.8 | 63 | 1.000 | - |
| 4 | 4 | - | - | 17.0 | 21.47 | 6.8 | 63 | 0.958 | - |
| 4 | 4 | - | - | 16.0 | 20.21 | 6.8 | 63 | 0.901 | - |
| 5 | 5 | - | - | 15.5 | 19.58 | 6.8 | 63 | 0.873 | - |
| 5 | 5 | - | - | 14.5 | 18.32 | 6.8 | 63 | 0.817 | - |
| 6 | 6 | - | - | 14.0 | 17.68 | 6.8 | 63 | 0.789 | - |
| 6 | 6 | - | - | 15.5 | 19.58 | 6.8 | 63 | 0.873 | - |

Note: 1 kip = 4.45 kN; 1 kip-ft = 1.356 kN·m; 1 ksi = 6.89 MPa.

[a]Altered Pu/original Pu.

tained. One of the main objectives of this project has been achieved in that quantitative results have been obtained that describe the percentage of strength lost or gained by simulated deterioration and subsequent repair. The second area of importance is that of the behavior of the beams as indicated by the crack patterns on the beam. The crack pattern produced by a particular beam has proved to be predictable, reliable, and directly related to the amount and type of deterioration as well as to the nature of the repair used. Figures 5-7 show the typical crack patterns.

To describe the relative strength of these 40 beams, we have selected the ratio of the experimental load value, for various situations, to the load capacity of the control beams. This ratio is referred to as the coefficient of strength (CS). A CS value of unity indicates perfect agreement between the tested beam and the control beam--in other words, no loss of strength or full recovery of strength as the case may be.

Table 1 gives the loss of strength for deteriorated beams as well as the recovery after subsequent repair. It is significant to note that the greatest loss of strength occurred for the beam with no cover and no bond over a distance of 6 ft (1.8 m). This was not unanticipated. The CS value was 0.789. In other words, even when the cover and bond were prevented for as much as 63 percent of the span, only 21 percent of the member's strength was lost! It is also of significance to note that 99 percent

**Figure 5. Basic crack patterns.**

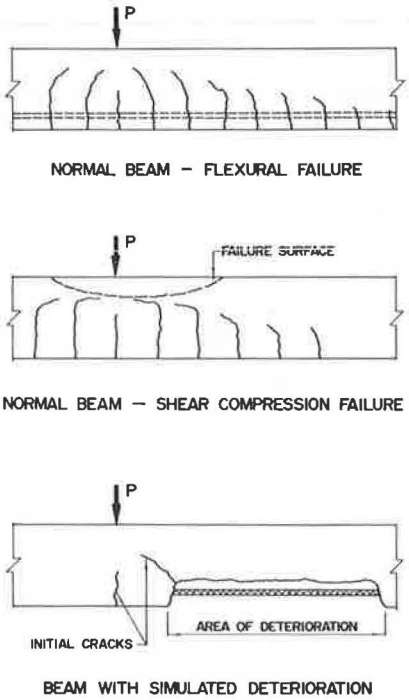

Figure 6. Crack patterns of deteriorated beams.

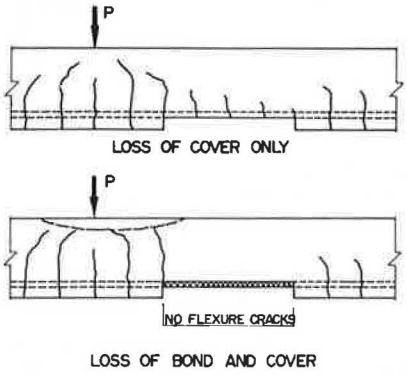


Figure 7. Crack patterns of repaired beams.

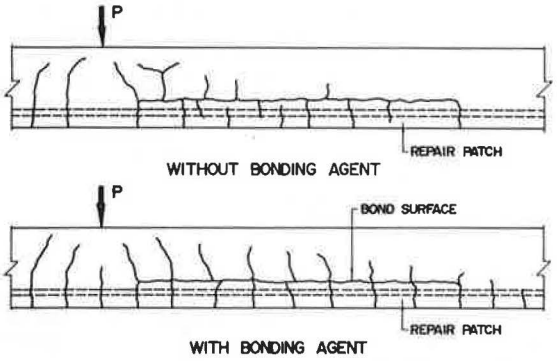


(CS = 0.991) of the strength was recovered when beams subjected to losses up to 3 ft (0.9 m) (31.5 percent of the span) were repaired. In the short term, then, the beam loses little strength and can be completely repaired.

At the point where flexural bond loss begins, all of the tensile stress is instantaneously directed into the reinforcing steel, which results in stress concentration. Stress concentration is demonstrated by the locations of initial yielding of steel and initial cracking of concrete at the reentrant corner (see Figure 5). When bond between the concrete and steel is lost, there is nothing to reduce the tensile stress in the steel. Theoretically, the stress in the reinforcing steel is constant in the region of bond loss; however, strains in the test beams indicate that stress in the region of bond loss is not constant. This apparently results from the mechanical bond that remains between the concrete and the unbonded steel. The magnitude of tensile stress is increased in the region of bond loss, and it cannot be redistributed through bond stress. This results in premature yielding of the reinforcing steel in the region of bond loss.

Figures 5-7 describe the behavior of the beams under action of loading. The crack patterns are indicative of the distress being felt by the particular beam.

The behavior of beams with loss of cover and/or bond was radically different from that of the control beams. Figure 6 shows the crack pattern of a beam with loss of cover only. It behaves essentially as a control beam and has the same crack pattern as the control beam. Even though further deterioration would certainly occur in the field under service conditions, it is apparent that there is sufficient bond on the bar, when only cover is "removed", for the beam to behave normally for short-term loading. Values of CS were consistently above 0.864. However, for the beam without cover and without bond, there is a radical change in behavior and a greater decrease in strength.

For such beams without bond, the CS value varied from a high of 1.000 to a low of 0.789 for bond loss up to 6 ft (1.8 m) (63 percent of the span). Along with this loss of strength, a radical crack pattern was apparent. The first crack appeared at about 50 percent of service loading, which corresponded to a concentrated loading of 1.5 kips (6.7 kN) for the beams loaded 1.5 ft (0.46 m) from the left support. This crack was quite wide at its origin, was singular, and extended to within 2 in (5 cm) of the top of the beam. The crack width was dramatic in every test. At higher load levels, additional flexural cracks formed under the load, as shown in Figures 5 and 6. As the load approached maximum for the beam, an additional horizontal crack opened at the top of the original crack and at right angles to it. This crack propagated toward the load and toward the center of the beam. This "tree-shaped" crack always occurred at the onset of failure.

Because of the lack of composite action between the concrete and the steel in beams with no bond, there were no flexural cracks in the region of simulated deterioration. The mechanics of this behavior are shown in Figure 3. The absence of cracking also indicated that the concrete was generally in compression. Although it is not the purpose of this paper to perform an in-depth analysis of the structural mechanics of the deteriorated beam, it is of interest to note that there is a combination of effects present here. They could be described as a combination of tied-arch behavior with bending. Certainly, the actual behavior is also influenced by the nature of the loading. In this case, there was no loading over the region of no bond. If such loading existed, the crack pattern would certainly reflect this change of internal stresses.

In some of the beams where there was loss of cover and bond, horizontal cracks formed at the level of the reinforcing steel at the far end of the test zone. This type of crack usually indicates a loss of bond between the concrete and steel as the steel begins to pull out of the concrete. The localized bond failure was due to a stress concentration at the point where the steel bars reentered the concrete. This stress concentration is a result of the lack of composite action between the concrete and steel in the test zone. As Figure 3 indicates, in a normal beam flexural bond stress acts to reduce the tensile stress in the steel by transferring stress to the concrete (9). When bond between the concrete and steel is lost, no bond stress exists to reduce the tensile stress in the steel. Theoretically, the tensile force in the exposed reinforcing steel is constant. This neglects a possible frictional effect. Although the strains measured in the exposed bars were not constant, they were higher than those measured in the control beams and beams with loss of cover only. Thus, at the near end of the test zone, the exposed portion of the steel was more highly stressed than the portion that was bonded to the concrete; a stress concentration existed at this point. Figure 5 shows typical crack patterns observed in beams with loss of bond.

In all the beams with loss of cover and bond, the strain gage near the reentrant corner was the first to reach yield. This was undoubtedly due to a large stress concentration at this point. Just inside the reentrant corner, where flexural bond is provided between the concrete and steel, a portion of the tensile stress in the steel is transferred to the

concrete. At the point where flexural bond loss begins, all of the tensile stress is instantaneously directed into the reinforcing steel so that there is a severe stress concentration at this point. Figures 5 and 6 indicate the resultant crack pattern.

One of the most dramatic aspects of the behavior of the beams with loss of cover and bond was the ultimate failure. The failure was a very sudden shear-compression failure of the concrete under load along the surface defined by the horizontal crack described earlier (Figures 5 and 6). The deflections of the beams with loss of bond were linear and nearly identical to those of the control beam up to the failure load. At failure, the beams with loss of bond showed only a slight increase in deflection. The slow, ductile failure exhibited by the control beams was not shown by those with loss of bond. One beam showed a particularly dramatic failure. As the last increment of load was applied, the beam literally exploded as the concrete in the compression zone flew off the beam. This sudden release of energy split the beam longitudinally for almost the entire length of the test zone.

## CONCLUSIONS

The following summary conclusions may be made as a result of the project described in this paper:

1. Regardless of the length involved, the loss of no more than the cover to the reinforcing steel has little short-term effect on the behavior and strength of the beam. As long as substantial bond remained between the concrete and that part of the bar surrounded by concrete, the beams tested showed no practical reduction in strength. It should be noted that, in actual service conditions, it is unlikely that the loss of cover would occur without some loss of bond also. It is also important to note that this type of deterioration is a continuing process unless specifically arrested and repaired; therefore, there is a time effect on exposed steel and concrete that has not yet been included in this project.
2. The loss of both cover and flexural bond significantly alters the behavior of the reinforced beam and substantially lowers its strength. This reduction in strength increases as the length of bond loss increases. The decrease in strength, as well as the change in behavior, is due to the loss of composite action inherent in conventional reinforced concrete beams. The type of failure and the crack pattern preceding that failure change; such failures are sudden and of the shear-compression type. The behavior over the region of the beam that had no cover and no flexural bond is similar to that of a tied arch with secondary effects.
3. When beams that have lost cover are repaired, the rehabilitation is complete. In these laboratory tests, without the use of the bonding agent, more than 86 percent of the original strength was recovered. When the bonding agent was used, the strength recovery was 100 percent in all beams tested. These conclusions hold for simulated deterioration 1, 2, and 3 ft (0.3, 0.6, and 0.9 m) in length. Repairs have not yet been tested for deterioration greater than 3 ft, which is 31.6 percent of the span.
4. When beams previously subjected to a loss of both cover and flexural bond are repaired, the strength recovery and behavior under load depend on the use of a bonding agent. The strength recovery of beams without a bonding agent averaged 88 percent of the original beam, and the minimum value was 86 percent. The cracking pattern under increasing load showed a lack of adhesion between the patch and the original concrete. When a bonding agent was used, the recovery was nearly complete: The average was 99 percent of the original beam, and the minimum test result was 96 percent. The cracking pattern in this case was similar to that in the normal beams (Figures 5 and 7).

## RECOMMENDATIONS

The investigation described in this paper is ongoing. In brief, the following features and variables must be incorporated into the overall project:

1. Partial loss of flexural bond with respect to the diameter of the reinforcing bar must be included in the testing phases.
2. The loading system should be altered so as to more closely represent uniform loading and/or truck loading, as is more typical of service conditions.
3. Reinforcing steel must be altered to represent loss of shape and/or area, as would occur by means of actual corrosion over an extended period of time.
4. Alternative methods of repair, with and without a bonding agent, should be considered and tested. In such a procedure, beams must be repaired without physically inverting the beam, as was done for convenience in the laboratory procedures of this project.
5. If possible, the conclusions derived and the results measured should be verified by some amount of field testing on real structures.

## ACKNOWLEDGMENT

Particular acknowledgment for their significant efforts is due to the following graduate students of the University of Cincinnati: Eric Bryars, James Miller, Greg Sliger, Jerry Wong, and Mike Toensmeyer. Without the contributions of these individuals, this work could not have been accomplished.

We must express our gratitude for the assistance rendered by T.M. Baseheart, Associate Professor of Civil Engineering; Ross Martin of Reading Central Mixed Concrete, Inc.; and the following members of the senior class of the University of Cincinnati: Mike Frank, Patti French, Dave Holstrom, Mark Lookabaugh, Jon Reed, Brian Pickering, Mike Sturdevant, and Jerry Holman.

We are also grateful for the financial support provided by the University of Cincinnati and Reading Central Mixed Concrete, Inc.

## REFERENCES

1. E. Bryars. The Effect of Loss of Cover and Bond in Regions of High Flexural Stress on the Strength of Reinforced Concrete Beams. Univ. of Cincinnati, master's thesis, June 1979.
2. J. Miller. The Effect of Restoring Loss of Cover and Bond in Regions of High Flexural Stress on the Strength of Reinforced Concrete Beams. Univ. of Cincinnati, master's project, June 1980.
3. G. Sliger. The Effect of Large-Scale Loss of Cover and Bond on the Strength and Behavior of Reinforced Concrete Beams. Univ. of Cincinnati, master's project, June 1980.
4. J. Warner. Epoxies: "Miracle" Materials Don't Always Give Miracle Results. Civil Engineering, Feb. 1978, pp. 48-55.
5. Epoxies for Concrete Repair and Restorations. Concrete Construction, Vol. 24, No. 3, March 1979, pp. 169-174.
6. The Repairability of Concrete. Concrete Construction, Jan. 1980, pp. 41-44.
7. Concrete Manual, 8th ed. Bureau of Reclamation,

U.S. Department of the Interior, 1975, pp. 1-32, pp. 131-144, pp. 393-437.
8. H. Woods. Durability of Concrete Construction. ACI, Detroit, Monograph 4, 1968.
9. C.-K. Wang and C.G. Salmon. Reinforced Concrete Design, 3rd ed. Harper and Row, New York, 1979, pp. 24-178.

*Publication of this paper sponsored by Committee on Adhesives, Bonding Agents, and their Uses.*

*Notice: The Transportation Research Board does not endorse products or manufacturers. Trade and manufacturers' names appear in this paper because they are considered essential to its object.*

*Abridgment*

# Repair of Torsionally Inadequate Concrete Beams by Use of Adhesively Bonded Plates

MICHAEL R. TOENSMEYER AND JOHN P. COOK

**The results of a study conducted to determine the feasibility of repairing torsionally inadequate reinforced concrete beams by using externally bonded steel plates are presented. The test program consisted of three sets of beams. Set A consisted of beams that had failed under torsional loading. Set B consisted of the same beams that failed as set A but were repaired by using epoxy adhesive to bond plates to the sides of the beams in the exterior thirds of the beam span. For set C, the plates were bonded to the sides of the beams before any testing. In the repaired beams, the external plates not only restored the integrity of the failed members but also increased the load-carrying capacity by 20 percent. For equal loads, the repaired beams had deflections approximately 6 percent less than those of the original beams. Set C, the control set, had 20 percent more carrying capacity than the concrete beams and also had deflections 20 percent lower. However, the plate configuration used did not force the members to fail in a flexural mode. The repair method was shown to be feasible, but more research is recommended to determine the best plate configuration and plate size.**

The use of externally bonded steel plates to strengthen reinforced concrete beams is not new. Fleming and King (1) in South Africa have used bonded plates in the tension zone of concrete beams. Irwin (2) in the United Kingdom has done similar work. In the United States, at least one bridge in California has been strengthened by Byrd, Tallamy, MacDonald, and Lewis. However, all of these applications have been directed toward increasing the flexural capacity of the members.

Until this time, no work has been done on increasing the torsional capacity of reinforced concrete members. One principal type of structure that exhibits torsionally inadequate spandrel beams is the parking garage. Typically, the facade of a garage with several bays will be surrounded by spandrel beams, and very heavy loads, such as automobiles, will be parked at some distance from the spandrel beam. This loading produces a torsional moment, which in turn produces torsional stresses in the spandrel beam. Depending on the location in the member, these torsional stresses can add to the shear stresses.

Most prior testing of torsionally loaded members has been for the analysis and design of new members, but very little information is available on the repair of torsionally inadequate members.

## OBJECTIVE OF THE PROGRAM

The objective of this study was to propose a method of repair for torsionally inadequate reinforced concrete spandrel beams. The proposed solution was to adhesively bond steel plates to the vertical faces of the beams in the high-shear and high-torsion regions by using an epoxy adhesive. The intent was to entirely control the torsional cracking of the member and shift the mode of failure from sudden torsional failure to a more conventional flexural failure with a forewarning of collapse.

## DESIGN OF THE EXPERIMENT

The reinforced concrete members were designed in accordance with the American Concrete Institute (ACI) code and commentary (3,4). The relation between the test sections and the actual building framing is shown in Figure 1. The test members were modeled to represent a typical spandrel beam located between two adjacent columns and supporting a floor beam at each of the third points. In an actual building, a monolithically cast slab would complete the system. However, in order to better study the pattern of crack formation, the slab was omitted from the members in the testing program. The beams were specifically designed so that the mode of failure would be in torsion. For the experiment, the model was mounted so that it performed as a pinned connection with respect to flexure and normal shear and as fixed with respect to torsion.

The spandrel beams tested were 4x8 in (102x203 mm) in cross section and 9.5 ft (2.9 m) long. Four no. 6 bars of grade 60 steel were used as longitudinal reinforcement. The stirrups were 0.187 in (5 mm) of grade 40 steel. The steel plates, which

**Figure 1. Test specimen.**

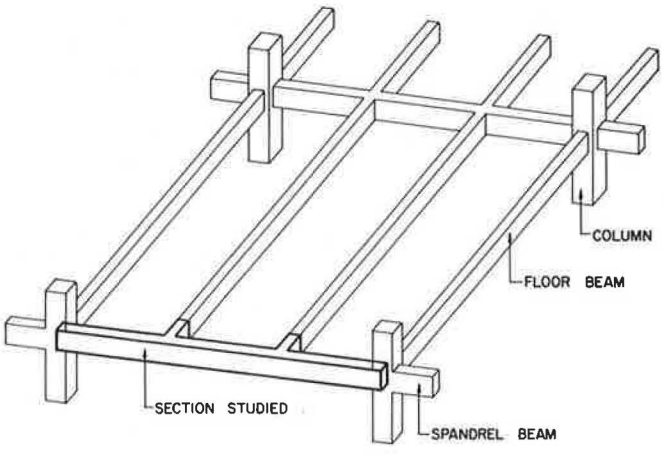

Figure 2. Testing arrangement.

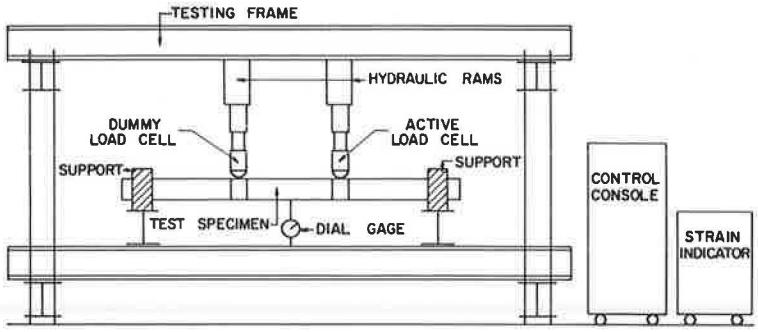


Figure 3. Strain-gage locations.

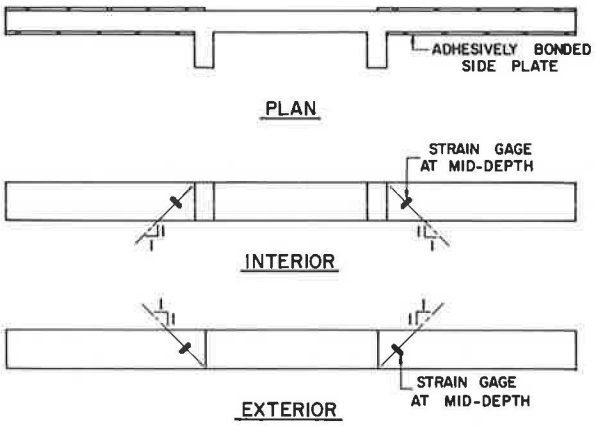


were used only in the outer thirds of the beam, were A-36 steel 0.187 in thick.

The design strength of the concrete was 5000 lbf/in² (36 000 kPa). However, the concrete actually used in the project had a 28-day strength of 8500 lbf/in² (61 000 kPa) and a slump of 2.5 in (64 mm).

In total, nine beams were tested to evaluate the performance of the proposed composite rehabilitation system. Set A consisted of three beams designed to fail in a combined normal and torsional shear failure in the exterior third of the spans. Set B consisted of the repair beams that initially failed as beam set A. Set C consisted of the control set. These were beams to which bonded plates were attached prior to any testing for observation of full composite action.

## TESTING PROCEDURE AND INSTRUMENTATION

The beams were mounted for testing in the loading frame as shown in Figure 2. Load was applied simultaneously to the two short cantilever stubs by an electronically controlled hydraulic ram system.

Since this experiment was the initial one of its kind, only an elementary amount of instrumentation was used. Three types of observations were made during the testing program:

1. The centerline deflection was monitored for all beams by using a dial gage incremented to the nearest 0.001 in (0.025 mm).
2. The crack patterns were carefully monitored for all beams to serve as a warning of impending failure.
3. Strain gages were used to evaluate the performance of the steel plates during the testing of beam sets B and C. Four strain gages were used on each beam. They were positioned and oriented on the beams in a direction perpendicular to the anticipated crack formation. The locations of gages are shown in Figure 3.

## LOADING

The load was applied in 200-lbf (0.89-kN) increments equally to each cantilever at a rate of 10 lbf/s (0.045 kN/s) for the first specimen in each beam set. For subsequent beams in each set, the load was applied in 400-lbf (1.78-kN) increments at a loading rate of 10 lbf/s. At each 400-lbf increment, the strain and deflection variations were allowed to stabilize for a 3-min period. During this time span, a close visual inspection of the beam was made for cracks that would indicate impending failure. Strain gage and deflection readings were made at both the beginning and the end of this period. This procedure was repeated until a load of 4000 lbf (17.8 kN) was being applied to the specimen. At that point, the procedure was changed so that 200-lbf increments were applied up to failure. Failure was determined as the load at which a torsionally induced concrete rupture occurred or a point at which deflections were visibly increasing without increasing the loading. For the protection of the technicians and the equipment, the dial gage was removed when centerline deflection approached 0.5 in (13 mm).

## RESULTS

The program showed that it is feasible to repair torsionally inadequate beams by using bonded side plates. However, the specific method of repair used in this program is not the complete answer.

Two positive effects and one negative effect were shown by the program. The failure load of the composite sections was 20 percent higher than that of the noncomposite members. In addition, excellent results were seen in the area of crack observation as a means of identifying the mode of failure. For all specimens in beam set A, the failure occurred in the classical torsional crack mode in the exterior thirds of the span. Although no new torsional cracks were observed on the top or bottom of the beams in the area of the bonded plates, the torsional stresses still remained to be accounted for. The bonded side plates forced a redistribution of stresses, which in turn forced the torsional stresses into the interior third of the span. Consequently, at a point at which no torsion failure was expected, a large torsional crack formed that led to a sudden failure of the specimens. This failure was sudden and explosive. It was not uncommon for pieces of the concrete to fly several feet from the specimen at failure. This is precisely the type of failure the investigators were trying to avoid.

**Figure 4. Load deflections.**

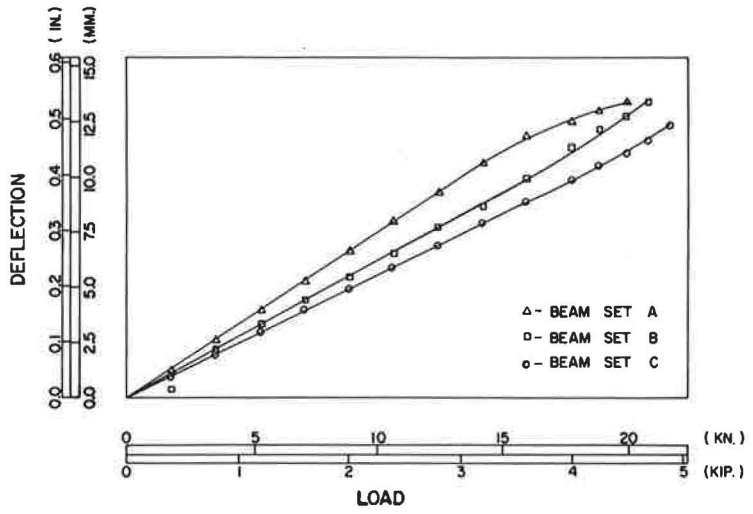


**Table 1. Test results.**

| Beam | Max Load (kips) | Mode of Failure |
|---|---|---|
| A1 | 8.80 | Combined normal and torsional shear |
| A2 | 8.80 | Combined normal and torsional shear |
| A3 | 7.20 | Combined normal and torsional shear |
| B1 | 10.10 | Torsionally induced shear cracking |
| B2 | 10.40 | Flexure in floor beam cantilever |
| B3 | 9.20 | Torsionally induced shear cracking |
| C1 | 9.20 | Torsionally induced shear cracking |
| C2 | 10.30 | Torsionally induced shear cracking |
| C3 | 10.00 | Torsionally induced shear cracking |

Note: 1 kip = 4.45 kN.

A preliminary judgment might be that the side plates had yielded. However, examination of the maximum strains in the plates showed that the stresses in the plates were well below yield. Consequently, thinner plates might be used.

A study of the deflections (see Figure 4) shows that the ultimate deflections of all of the beams were grouped quite closely. However, when the deflections at the ultimate load are compared, beam set A shows that the repaired beams not only restored the integrity of the failed specimens but also decreased deflections by 6 percent. At this same load, the control specimens had deflections 20 percent less than those of set A.

Table 1 gives the ultimate load and mode of failure of all the test specimens. The lower load for beam C1 is explained by the fact that the only adhesive failure between beam and plate occurred for this beam. It is worth noting that this was the first plate attached by the technicians.

## CONCLUSIONS AND RECOMMENDATIONS

As a result of the program described in this paper, it has been concluded that the use of adhesively bonded plates to rehabilitate torsionally inadequate beams is feasible. However, more analysis and testing are required in order to determine the plate configuration that will suppress torsional failure and force a yield failure in the tensile mode at a predicted load.

In a further testing program, the following steps should be taken:

1. A floor slab cast monolithically with the floor beams and spandrel beam should be included in the test.
2. The method of repair should be bonded plates on both sides of the spandrel beam for its entire length.
3. The plates should be of a smaller thickness to permit plate yielding.
4. A two-span model should be investigated in order to provide a better understanding of the interaction at the interface between column and spandrel beam.

## REFERENCES

1. C.J. Fleming and G.E.M. King. The Development of Structural Adhesives for Three Original Uses in South Africa. International Union of Testing and Research Laboratories for Materials and Structures (RILEM), Paris, Bull. 37, Dec. 1967.
2. C.A.K. Irwin. The Strengthening of Concrete Beams by Bonded Steel Plates. Department of the Environment, Transport and Road Research Laboratory, Crowthorne, Berkshire, England, TRRL Supplementary Rept. 160, 1975.
3. Building Code Requirements for Reinforced Concrete. ACI, Detroit, ACI 318-77, 1977.
4. Commentary on Building Code Requirements for Reinforced Concrete. ACI, Detroit, ACI 318-77 C, 1977.

*Publication of this paper sponsored by Committee on Adhesives, Bonding Agents, and Their Uses.*

# Development of a Construction Price Index for Major Public Transit Investment Planning

THOMAS DOOLEY

**A technique for indexing prices over time and between regions of the country is developed that is responsive to the labor, material, and equipment resource mix and to the different types of each of these resources that are used in typical transit construction projects. Currently available indices are reviewed, and their shortcomings are identified. A review of several actual projects and an analysis of recent trend data show the variations in resource mix among different types of transit projects. A framework is developed for a resource-price-oriented data base and indexing methodology. To illustrate the concept, the methodology is then applied to cut-and-cover tunnel construction. A national index and 20 city indices are computed and compared with currently available indices for general construction projects.**

During the system planning and corridor refinement processes for major public transit investments, data from projects completed at one location and time are often used in estimating the cost of implementing a new mode in a different place and at a different time and in projecting the cost of that investment into the future. This paper explores the issues involved in developing indices of transit capital cost that will be useful in this process. The best index currently available is identified. Recent projects are reviewed to identify the need for a more "relevant" transit index. A methodology is developed in which historical experience and current prices are used to produce a basis for a transit capital price index. In this paper, price refers to the resource--for example, wage rate in dollars per hour. Cost refers to the project cost, which is determined by resource prices and many other factors.

## CHARACTERISTICS OF PRICE INDICES

The major requirements for an index of regional and time trends in investment projects are as follows:

1. The index should be based on readily available data that are published frequently and have been published for a long time. This enables the user to update prices to the current year and identify trends for projecting future costs.
2. The index should cover a wide range of cities and be comparable between cities to permit regional adjustments for completed projects.
3. If the index is a composite of different quantities and their prices, the method of computing the measure should be available. This would enable the user to identify specific location prices not nationally available and to use these prices to relate national data to a specific project.
4. If the index is a composite of different quantities and their prices, the items in the index should reflect the type of labor, material, and equipment used in transit projects.
5. If the index consists of nonprice items, these should be explicitly identified and documented. Factors such as worker productivity are nonprice items.

## REVIEW OF TIME SERIES AND REGIONAL INDICES

Many construction price indices are available. Several indices that are published periodically are described in selected issues of the Engineering News Record (ENR). Several of these indices have both national and local data and would be available at local libraries or from construction contractors. Many of these indexing services also publish cost estimators for specific projects. ENR publishes a construction cost index (CCI) and a building cost index (BCI). These indices are based on fixed quantities of skilled or common labor and selected materials. These indices were started in 1913, and the quantities of the resources were determined in such a way that the cost of the package in 1913 was $100, based on average prices for 20 U.S. cities. The quantities have remained constant since then, and the BCI and CCI based on 1913 satisfy the first three characteristics of a transit price index cited above. ENR also publishes a BCI and a CCI for 20 cities in which each city's index was set to 100 in 1967. This index is good for determining the price changes within a city but not between cities, since the index in each city was normalized to 100 in 1967. Data given in Tables 1 and 2 show how the ENR-based 1913 indices are computed. The quantities of common labor or skilled labor and the materials (steel, lumber, and cement) were chosen to represent an implicit apportionment of resources for some "typical" project. The ENR 1913 base building construction index is recommended for regional comparisons as a preliminary cut at converting data from one city to another.

It is important to recognize that the ENR index does not necessarily represent the correct mix of resources, nor does it account for nonprice factors such as productivity or price factors such as the employer's cost burden for different skills. These will be discussed later.

The 1979 Dodge Guide (1), which is typical of cost-estimating manuals such as those of R.S. Means Company, Inc. (2), and Craftsman Book Company (3), provides cost factors for various public works projects. The Dodge Guide contains regional adjustment factors and labor, material, and equipment unit cost estimates for tunnel, track, power, and train-control capital projects. These unit cost estimates are not aggregate unit costs, such as those needed in system planning or corridor refinement. For example, the cut-and-cover tunnel costs in the Dodge Guide do not represent the total cost for a kilometer of tunneled rail rapid transit line. Costs for site preparation and the tunnel liner are not included. However, they do provide resource breakdowns. The Dodge Guide (1) states that, although the labor costs shown do not include the employer's labor costs (such as fringes), they do include some productivity (80 percent efficiency assumed) and work-rule variations (unfortunately, these are not documented). Labor and material adjustments are developed for major cities within each state. Since equipment is assumed to be contractor owned, no local rates are provided. The reader of the Dodge Guide must bear in mind that labor and material prices are set to a Boston base and thus cannot be directly related to a national-average-based figure such as the ENR. The use of Boston as a cost base and the fact that the Dodge Guide does not document the complete methodology used are drawbacks to these data. The Craftsman guide (3) also shows some typical employer burdens. Both the Dodge and Craftsman publications indicate that employer cost burdens

**Table 1. Computation of national and local ENR building construction indices.**

| Item | Description | Quantity | Unit Price ($) | | | Index Value ($) | | |
|---|---|---|---|---|---|---|---|---|
| | | | 20-City Avg[a] | Atlanta[b] | New York[b] | 20-City Avg | Atlanta | New York |
| Labor ($/h) | | | | | | | | |
| Common | Avg of heavy and building construction labor; union base rate and fringes | 200 h | 11.22 | 7.73 | 13.56 | 2244 | 1546 | 2712 |
| Skilled | Avg of bricklayers, structural ironworkers, and carpenters; union base rate and fringes | 68.38 h | 14.78 | 11.66 | 17.97 | 1010 | 797 | 1229 |
| Material | | | | | | | | |
| Structural steel ($/cwt) | Avg of 3 mills | 25 cwt | 18.12 | 18.12 | 18.12 | 453 | 453 | 453 |
| Lumber ($/1000 board ft) | Carload lots, avg of 2x4 pine and fir | 1088 ft | 341.20 | 290.44 | 337.50 | 371 | 316 | 367 |
| Cement ($/ton bulk) | Truckload lots, bulk | 1.128 tons | 56.31 | 48.82 | 50.30 | 63 | 55 | 56 |

Note: cwt = hundredweight.
[a]Price on January 3, 1980. [b]Price on January 10, 1980.

**Table 2. National and local building construction indices showing regional comparisons.**

| Item | Index | | | | | |
|---|---|---|---|---|---|---|
| | National ($) | Atlanta ($) | Atlanta/ National | New York ($) | New York/ National | New York/ Atlanta |
| Material (steel, lumber, and cement) | 887 | 824 | 0.93 | 876 | 0.99 | 1.06 |
| Construction cost (common labor and material) | 3131 | 2370 | 0.76 | 3588 | 1.15 | 1.51 |
| Building cost (skilled labor and material) | 1997 | 1621 | 0.81 | 2105 | 1.05 | 1.30 |

average 25 percent of the wage rate. The hourly wages in the Craftsman publication (3) are consistent with the values reported in the ENR (4). In summary, for system planning purposes the Dodge Guide data are useful for labor, material, and equipment resource breakdowns and as a check on the ENR values but should not be used as a regional or time-series index.

Indices published by various federal agencies have often been used as surrogates for a transit cost index. The Federal Highway Administration (FHWA) index--"Price Trends for Federal-Aid Highway Construction," published quarterly--is based on national average contract bid prices for a composite mile of Interstate highway, involving specific amounts of excavation, portland cement concrete and bituminous concrete surfacing and reinforcing, and structural steel and structural concrete. This index is useful for defining national trends in highway costs and excavation, structure, and surfacing costs. It is not published on a regional basis, contains only material prices, and contains nonprice factors involved in contract bidding. The U.S. Department of Commerce composite construction cost index (5) is another aggregate index. This index is a ratio of the estimate of total new construction put in place in current dollars to the corresponding estimate in 1972 dollars. This estimate does not use a constant quantity; hence, it measures the combined result of price changes as well as changes in the relative weights of different types of construction. This index does not seem particularly useful for application to transit planning. Although it is readily available and has been published for a long time, it does not have regional values nor does it contain specific quantities that would enable a local planner to relate national data to a specific project. There is no reason to suggest that the quantities of material, labor, and equipment for construction put in place are representative of transit construction. The Bureau of Labor Statistics monthly producer price indexes (PPIs) for relevant quantities could be used. For example, an aggregate finished-goods index such as the machinery and motive products index (PPI codes 11 and 14) has many of the same elements as transit hardware (vehicles, elevators, and power equipment). However, there is no transit hardware in this (or any other) PPI, and the PPIs have never been correlated with transit finished goods.

Time-series indices are used in transit investment planning to adjust costs from past years or other places to current time and place. Time-series indices are also used to forecast future-year prices. In the economic analysis of alternatives (present value), general inflation can be ignored; however, if the prices of a particular item are changing at a different rate than general inflation, this rate of real price inflation should be considered. If the appropriate index is deflated by the consumer price index (CPI) (assuming the CPI measures general price inflation), the resulting index can be used as a measure of real price inflation.

Figures 1 and 2 show the real price growth of the ENR BCI and the FHWA highway construction index and the 20-, 15-, 10-, and 5-year real rates of growth in these indices (CPI = 100). These rates of growth are summarized below:

| Period | Index (%) | |
|---|---|---|
| | ENR | FHWA |
| 1960-1980 | 1.07 | 2.37 |
| 1965-1980 | 1.08 | 2.76 |
| 1970-1980 | 0.87 | 2.94 |
| 1975-1980 | -1.81 | 1.26 |
| 1960-1980 | 1.75 | 2.66 |

The first four trends are calculated from the actual end points, whereas the last trend is calculated from the estimated end points (the $R^2$ of the fitted lines is 0.86). Construction prices and costs have been growing between 1.7 and 2.6 percent faster than the CPI over the past 20 years. The increasing volatility in the real indices over the past 10 years suggests that the factors that affect these indices need to be understood.

The use of real price index trends to forecast

Figure 1. Real FHWA road construction index.

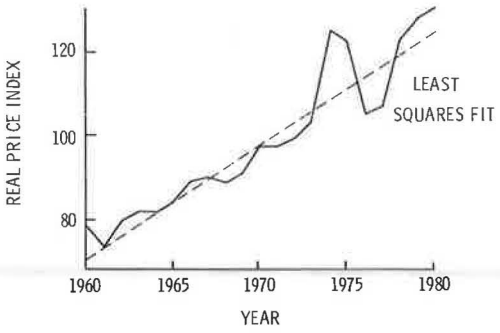


Figure 2. Real ENR building cost index.

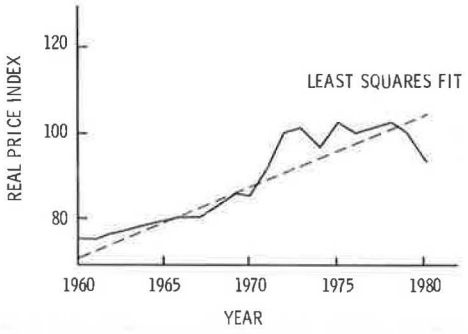


costs assumes that (a) input factors are accurate surrogates for costs and (b) the relation between the CPI and the real price index will remain constant over the forecast period. The CPI or gross national product (GNP) deflator or other general price index need not be forecast for an economic analysis. However, for financial analysis, actual dollar expenditures need to be forecast. A recent study by Data Resources Cost Forecasting Service, Inc., for FHWA (6) developed price indices for highway construction for use in forecasting costs. This study used input prices, market conditions, and general macroeconomic assumptions to forecast the percentage of actual dollar changes in highway costs.

## RESOURCE MIX

A review of the labor and material adjustments in the Dodge Guide (1) as well as those given in Table 1 indicates that the regional prices are different for these two resources while the equipment is assumed constant. Equipment is not included in the ENR indices. These resource price differences suggest that it is important to know the mix of resources for different types of transit projects. Table 3 gives the resource mix as a percentage of project expense for three different types of tunnel construction and the procurement and installation of track and power subsystems. The percentages were developed from the unit cost data given in the Dodge Guide (1). This review illustrates that for tunnel construction the labor cost varies between 35 and 67 percent of the total job cost, the material cost varies between 17 and 33 percent, and the equipment cost varies between 16 and 32 percent, depending on the construction method. Track-work cost is 96 percent materials and power costs are 42 percent labor and 46 percent materials.

Data given in Table 4 (4) show that the current national ENR construction index is 72 percent common labor cost and the current national ENR building

Table 3. Resource mix for three types of tunnel construction from Dodge Guide unit cost data.

| Project Type | Percent of Total Project Cost | | |
|---|---|---|---|
| | Labor | Material | Equipment |
| Cut-and-cover tunnel with slurry wall, 45 ft wide by 45 ft deep | 35 | 33 | 32 |
| Bored tunnel in clay with compressed air, 20-ft diameter with liner | 67 | 17 | 16 |
| Shield-driven tunnel without air, 20-ft diameter with liner | 35 | 28 | 37 |
| Track work (ballast, tires, rail) | 2 | 96 | 2 |
| Power (rail, cables, substations) | 42 | 46 | 12 |

Table 4. Resource mix: national ENR indices.

| Index | Item | Percent |
|---|---|---|
| CCI | Labor | |
| | Unskilled | 100 |
| | Percent of total index value | 72 |
| | Material | |
| | Steel | 51 |
| | Cement | 7 |
| | Wood | 42 |
| | Percent of total index value | 28 |
| BCI | Labor | |
| | Carpenters | 33 |
| | Metalworkers | 33 |
| | Bricklayers | 33 |
| | Percent of total index value | 56 |
| | Material | |
| | Steel | 51 |
| | Cement | 7 |
| | Wood | 42 |
| | Percent of total index value | 44 |

Table 5. Wage rates for 20 cities in 1979.

| Skill | Wage Rate ($/h) | | | | |
|---|---|---|---|---|---|
| | Lowest City | Fifth Lowest City | Median City | Fifth Highest City | Highest City |
| Common labor | | | | | |
| Construction | 7.18 | 7.96 | 10.42 | 12.07 | 13.68 |
| Building | 7.18 | 8.47 | 11.14 | 12.09 | 14.82 |
| Carpenter | 10.60 | 11.81 | 13.49 | 14.76 | 17.30 |
| Ironworker | 11.39 | 13.14 | 14.20 | 15.81 | 18.84 |
| Electrician | 12.65 | 13.44 | 15.22 | 16.05 | 20.70 |
| Hoist engineer | 10.67 | 11.57 | 14.34 | 15.10 | 16.61 |
| Crane operator | 10.67 | 11.73 | 14.63 | 15.37 | 18.60 |
| Truck driver | 7.93 | 9.64 | 10.69 | 12.15 | 14.58 |

index is 56 percent skilled labor cost. These data indicate that currently available indices are deficient in representing the resource mix used in transit construction. If all resources had the same price in every region or city, or if all prices were changing at the same rate, regional indices and resource-specific indices would be unnecessary. This is not the case. Table 5 (4) indicates that there is a wide variation in prices for different types of labor and, within each skill, a wide range between cities. Recall from Table 2 that the New York CCI was 151 percent of Atlanta's whereas the New York MCI was only 106 percent of Atlanta's. This undoubtedly reflects the high cost of unskilled labor in New York. Thus, it would be appropriate to develop an indexing methodology and transit price index that could capture the resource mix of typical transit projects.

SPECIFICATIONS OF RESOURCE TYPES WITHIN EACH RESOURCE CATEGORY

The use of comparative indices implies the selection of measurable items to develop the index. For example, for their construction index the ENR selected union-based heavy construction labor, mill prices for structural steel, 2x4 lumber delivered in carload lots, and bulk cement. Since a tunnel index must reflect the types of labor and materials that go into a tunnel, some research in this area is necessary. Data from actual projects, which suggest the type of labor and materials used and the relative proportion of each type, are summarized below:

1. Massachusetts Bay Transportation Authority (MBTA) Haymarket Extension, including tunnel, track, power, and signal work:

| Item | Percent of Total |
|---|---|
| Labor hours | |
| Unskilled | 18 |
| Carpenters | 11 |
| Metalworkers | 6 |
| Bricklayers | 2 |
| Electricians | 11 |
| Operators | 9 |
| Other | 43 |
| Material cost | |
| Steel | 14 |
| Cement | 15 |
| Wood | 3 |
| Electrical | 14 |
| Other | 54 |

2. MBTA Haymarket Extension, yards and shops:

| Type of Labor | Percent of Total Labor Hours |
|---|---|
| Unskilled | 32.5 |
| Carpenters | 8.1 |
| Metalworkers | 8.4 |
| Bricklayers | 1.4 |
| Electricians | 11.1 |
| Operators | 3.3 |
| Other | 35.2 |

3. Sixty-Third Street tunnel, New York:

| Type of Labor | Percent of Total Labor Hours |
|---|---|
| Unskilled | 15.9 |
| Carpenters | 23.8 |
| Electricians | 2.6 |
| Operators | 5.3 |
| Other | 52.4 |

4. Archer Avenue Extension, New York (fifth month of work):

| Type of Labor | Percent of Total Labor Hours |
|---|---|
| Unskilled | 20.5 |
| Carpenters | 11.7 |
| Operators | 33.8 |
| Other | 34.0 |

5. Second Avenue Extension between 97th and 105th Streets, New York:

| Type of Labor | Percent of Total Labor Hours | |
|---|---|---|
| | Excavation | Concreting |
| Unskilled | 36.6 | 75.5 |
| Carpenters | 14.5 | 10.0 |
| Metalworkers | 2.3 | |
| Bricklayers | | 1.2 |
| Operators | 9.2 | |
| Other | 37.4 | 13.3 |

6. Second Avenue Extension between 110th and 120th Streets, New York:

| Type of Labor | Percent of Total Labor Hours | |
|---|---|---|
| | Excavation | Concreting |
| Unskilled | 19.1 | 53.6 |
| Carpenters | 17.0 | 14.2 |
| Operators | 21.2 | 7.1 |
| Other | 42.7 | 25.1 |

The data on the MBTA Haymarket Extension are an extract from a Bureau of Labor Statistics survey of that transit construction project. The labor-skill breakdown in item 1 includes power, track, and signal as well as tunnel. These data indicate that the skilled to unskilled labor ratio is 80:20 and that carpenter, electrician, and equipment operator are the most significant skill areas. Item 1 also gives the percentage of total material cost for various materials used in the Haymarket Extension. Concrete, steel, and electrical products dominate. Item 2 gives a similar disaggregation of a yard and shop job. In this case, the skilled to unskilled ratio is 67:33, and carpenter, electrician, and metalworker are the most significant skill areas.

Item 3 gives the skill breakdown for the 63rd Street tunnel project in New York. In this case, the skilled to unskilled labor ratio is 80:20 and carpenter and miner are the dominant types of skills. Item 4 gives an example of a slurry-wall construction job. The skilled to unskilled labor ratio is again 80:20. Items 5 and 6 give excavation and concreting costs for two cut-and-cover jobs (no slurry wall). In the two jobs, the skilled to unskilled labor ratio is 70:30 for excavation and 35:65 for concreting. The concreting ratio is the only large deviation from the previous 80:20 pattern. From Table 4, it can be seen that the ENR overstates the labor contribution, particularly if the construction index is used. Within the skilled-labor area, carpenters are certainly an appropriate choice for inclusion in the transit cost index as are metalworkers and ironworkers. For transit projects, either electricians or operators should replace the wage rates for bricklayers used in the ENR. For material resources the ENR indices overstate the use of wood, and in the case of a complete project they understate the use of electrical material. The ENR BCI does not include equipment costs, which, according to the Dodge Guide (Table 3) are significant.

INDEXING METHODOLOGY

This section describes how to develop price indices for transit projects. Once developed, these indices can be used to relate transit project costs between different cities and different time periods. Costs can be forecast based on representative input prices.

To develop transit price indices, the following elements are necessary: (a) a data base hierarchy that relates input prices to unit or total costs, (b) a methodology for creating the index baseline, and (c) a set of time-series data on input factors. For system planning and corridor refinement studies, a major transit investment can be disaggregated into the following subsystems: guideway structure, stations, track, power, signal, vehicles, yards and shops, management, and land acquisition (each measured in dollars).

Total sytem cost can be defined as

$$SYSTEM = \sum_{I} SUBSYS(I) \quad (1)$$

where I is the index of subsystems, e.g., guideway.

The relative importance of the subsystem to the total system expense is a function of the unit cost and quantity of that subsystem. For subsystems such as guideway, the unit costs vary considerably depending on the type of construction, the elevation, and the development intensity of the site. Thus, subsystem-type indices may be developed for several types, as shown in the following example of a guideway subsystem. The guideway structure involves considerations of elevation and construction method, and the construction method in turn includes tunneling, which breaks down into the following construction methods (subsystem types): (a) cut-and-cover with or without slurry wall, (b) soft ground bore with or without air, (c) soft ground shield with or without air, and (d) hard rock bore, all measured in dollars per linear foot.

The subsystem cost would be defined as

$$SUBSYS(I) = \sum_{J} SUBTYPE(I,J) \times QUANT(I,J) \quad (2)$$

where J is the index of subsystem types, e.g., cut-and-cover tunnels, and QUANT (I,J) is the quantity of subsystem type, e.g., miles of cut-and-cover tunnels. The remainder of this section illustrates how an index would be developed by using the following subsystem type as an example: guideway tunnel, cut-and-cover construction, with slurry wall.

The unit cost resource mix for the subsystem type variable is defined as

$$SUBTYPE(I,J) = \sum_{K} RESOURCE(I,J,K) \quad (3)$$

where K is the resource, e.g., labor. For example, for a 45-ft-wide by 45-ft-deep tunnel, the resource cost per linear foot can be defined as follows (1):

RESOURCE (I,J,1) = labor = 701
RESOURCE (I,J,2) = materials = 656
RESOURCE (I,J,3) = equipment = 638

The resource type for each resource can then be defined as

$$RESOURCEL(I,J,K,L) = \text{fraction of RESOURCE (I,J,K) due to COMPONENT (L)} \quad (4)$$

where L is the type of resource K, e.g., carpenter.

For example, suppose that research on slurry-wall tunnel construction projects yields the resource-type mix shown below, where each fraction represents the relative contribution of each type to the total labor, material, or equipment expense:

| Resource | Type | Contribution |
|---|---|---|
| Labor | Heavy construction | RESOURCEL (I,J,1,1) = 0.4 |
| | Carpenter | RESOURCEL (I,J,1,2) = 0.2 |
| | Ironworker | RESOURCEL (I,J,1,3) = 0.2 |
| | Crane operator | RESOURCEL (I,J,1,4) = 0.2 |
| Material | Steel | RESOURCEL (I,J,2,1) = 0.333 |
| | Concrete | RESOURCEL (I,J,2,2) = 0.333 |
| | Wood | RESOURCEL (I,J,2,3) = 0.333 |
| Equipment | | RESOURCEL (I,J,3,1) = 1 |

Representative categories are used here and would be used in actual index computation for simplification. The representative categories should (a) be major input resources and (b) have available measurable items.

Given the percentage contribution of each type of labor, material, and equipment resource to the total of each resource category, the relative contribution of each resource type to the subsystem-type unit cost can be calculated as

$$COMPONENTX(I,J,K,L) = \%\text{ of COMPONENT (L) in SUBTYPE (I,J)} = [100 \times RESOURCE(I,J,K) \times RESOURCEL(I,J,K,L)]/SUBTYPE(I,J) = \text{contribution of COMPONENT (L) to SUBTYPE (I,J) price index} \quad (5)$$

To continue the example, the percentage of total index for each item is calculated as follows:

| Type of Resource | Percent of Total Index |
|---|---|
| Heavy construction labor | COMPONENTX (I,J,1,1) = (701/1995) x 0.4 = 14 |
| Carpenter, etc. | COMPONENTX (I,J,1,2-4) = (701/1995) x 0.2 = 7 |
| Steel, etc. | COMPONENTX (I,J,2,1-3) = (656/1995) x 0.333 = 11 |
| Equipment | COMPONENTX (I,J,3,1) = (638/1995) = 32 |

Equations 2-5 have been used to develop the relative contribution of each resource input to unit cost. The final item in the data base is the input price of each resource, which can be defined as

$$INDEX(C,T,K,L) = \text{price of COMPONENT (L) of resource (K) in city (C) at time (T)} \quad (6)$$

For example, the price of carpenter (L) labor (K) in Philadelphia (C) in January 1980 (T) would be defined as INDEX (C,T,K,L) = 15.00. January 1980 would be the base year for this index.

To compute the subtype baseline index (equal 100), the average value of each index price is computed as follows (assuming 20 cities with available data):

$$INDEX(T,K,L) = \sum_{C} INDEX(C,T,K,L)/20 \quad (7)$$

This is the 20-city average price from the data base of index items of this component.

The average prices of the index items in our example at T = January 1980, over 20 cities, are given below:

| Item | Unweighted Avg Price |
|---|---|
| Labor ($/h) | |
| Heavy construction | INDEX (T,1,1) = 11.07 |
| Carpenter | INDEX (T,1,2) = 14.83 |
| Ironworker | INDEX (T,1,3) = 14.83 |
| Crane operator | INDEX (T,1,4) = 14.83 |
| Material | |
| Steel ($/cwt) | INDEX (T,2,1) = 29.37 |
| Concrete ($/yd$^3$) | INDEX (T,2,2) = 40.38 |
| Wood ($/1000 board ft) | INDEX (T,2,3) = 357.1 |
| One equipment type, one price | INDEX (T,3,1) = 1 |

Given a set of baseline average prices, the quantity of each item in the baseline index can be computed as follows:

$$QINDEX(T,K,L) = COMPONENTX(I,J,K,L)/INDEX(T,K,L) \quad (8)$$

This is the quantity of the item in the baseline index. It is analogous to the 200 h of common labor in the ENR CCI and is simply the relative weight of COMPONENT (L) divided by the price at the time the index is started. In our example, the computations of the 20-city index baseline quantities are as follows (T = January 1980):

| Item | Baseline Quantity |
|---|---|
| Heavy construction (h) | QINDEX (T,1,1) = 14/11.07 = 1.26 |
| Carpenter, ironworker, crane operator (h) | QINDEX (T,1,2-4) = 21/14.83 = 1.42 |
| Steel (cwt) | QINDEX (T,2,1) = 11/29.37 = 0.37 |
| Concrete ($yd^3$) | QINDEX (T,2,2) = 11/40.38 = 0.27 |
| Wood (million board ft) | QINDEX (T,2,3) = 11/357.1 = 0.03 |
| Equipment | QINDEX (T,3,1) = 32/1 = 32 |

To compute the value of the subsystem index for a particular time and place, the baseline quantities are multiplied by the local prices at a given time, as follows:

$$\text{VINDEX}(C,T) = \sum_{KL} \text{INDEX}(C,T,K,L) \times \text{QINDEX}(T,K,L) \quad (9)$$

where C is the city of interest.

As an example, the component values of the index for cut-and-cover tunnel with slurry wall for Atlanta on January 1980 are computed below:

| Item | Atlanta Value | | QINDEX | | VINDEX Component |
|---|---|---|---|---|---|
| Heavy construction labor | 7.73 | x | 1.26 | = | 9.7 |
| Skilled labor | 11.51 | x | 1.42 | = | 16.3 |
| Steel | 28.40 | x | 0.37 | = | 10.5 |
| Concrete | 34.75 | x | 0.27 | = | 9.4 |
| Wood | 288 | x | 0.03 | = | 8.6 |
| Equipment | 1 | x | 0.32 | = | 32.0 |

The Atlanta price for heavy constuction labor, \$7.73/h, is multiplied by the baseline quantity of 1.26 h computed above to determine the contribution of heavy construction labor to the January 1980 total index for Atlanta: 86.5.

Column 1 in Table 6 gives the 20 cities in the index. Column 2 gives the results of applying the baseline index quantities developed in this paper for cut-and-cover tunnel with slurry wall and the prevailing January 1980 prices in 20 U.S. cities. The 20-city average value of the index is 100. Column 3 gives the ordering of the cities from lowest to highest index value. Column 4 gives the value of the index if equipment is excluded. Recall that equipment was 32 percent of the index but that no regional values were used. In column 2, each city's index included 32 for equipment. Column 4 is equal to column 2 minus 32 divided by 68. The use of a national value for equipment implies that contractors' costs for equipment are independent of location. Columns 5 and 6 give the rank order of cities and the index value of the ENR BCI normalized to January 1980. The difference between this index and the ENR is most dramatic for cities that have low material costs relative to labor (Cincinnati and Pittsburgh) or for cities that have high material costs relative to labor (Boston). This example has focused on one subsystem-type index. However, it is obvious that, once the subtype indices are developed, they can easily be combined for the project of interest, as follows.

**Table 6. Twenty-city index for cut-and-cover tunnel with slurry wall.**

| City | Including Equipment Component | Excluding Equipment Component | | ENR BCI | |
|---|---|---|---|---|---|
| | | Rank | Index | Rank | Index |
| Atlanta | 86.5 | 1 | 80.1 | 1 | 85.2 |
| Birmingham | 86.8 | 2 | 80.6 | 2 | 87.2 |
| New Orleans | 90.1 | 3 | 85.4 | 3 | 90.5 |
| Dallas | 92.4 | 4 | 88.8 | 4 | 90.6 |
| Baltimore | 94.7 | 5 | 92.2 | 6 | 96.0 |
| St. Louis | 96.6 | 6 | 95.0 | 7 | 97.3 |
| Denver | 97.4 | 7 | 96.2 | 5 | 94.5 |
| Minneapolis | 97.5 | 8 | 96.3 | 9 | 99.0 |
| Kansas City | 99.5 | 9 | 99.3 | 8 | 98.4 |
| Cincinnati | 99.5 | 10 | 99.3 | 14 | 103.7 |
| Pittsburgh | 100.0 | 11 | 100.0 | 16 | 104.0 |
| Chicago | 101.8 | 12 | 102.6 | 12 | 102.4 |
| Philadelphia | 102.0 | 13 | 102.9 | 15 | 104.0 |
| Seattle | 102.2 | 14 | 103.2 | 11 | 99.8 |
| Detroit | 103.1 | 15 | 104.6 | 17 | 107.7 |
| Cleveland | 105.1 | 16 | 107.5 | 13 | 102.6 |
| Boston | 107.4 | 17 | 110.9 | 10 | 99.2 |
| Los Angeles | 108.7 | 18 | 112.8 | 18 | 108.4 |
| New York | 108.8 | 19 | 112.9 | 19 | 111.6 |
| San Francisco | 113.3 | 20 | 119.6 | 20 | 117.4 |

First, compute the contribution of each COMPONENT (L) to the system cost as determined by its contribution to the subsystem-type index [COMPONENTX (I,J,K,L)] computed in Equation 5 and the subsystem, as follows:

$$\text{COMPONENTY}(I,J,K,L) = \text{COMPONENTX}(I,J,K,L) \times [\text{SUBTYPE}(I,J) \times \text{QUANT}(I,J) \div \text{SYSTEM}] \quad (10)$$

Then add up the contribution of the COMPONENT (L)'s to the system cost over all subsystem types and subsystems, as follows:

$$\text{COMPONENTZ}(K,L) = \sum_{IJ} \text{COMPONENTY}(I,J,K,L) \quad (11)$$

The average price, INDEX (T,K,L), is then computed as in Equation 7. The baseline quantity for each system component is then computed as follows:

$$\text{QINDEX}(T,K,L) = \text{COMPONENTZ}(K,L)/\text{INDEX}(T,K,L) \quad (12)$$

The value of the system index at any given place and time can then be computed as shown in Equation 9.

This section has focused on the use of an index for regional comparisons. Another aspect of this indexing methodology that is important but is not shown here is the development of time series from which projections of future prices can be made. Since the data base is based on measurable items, relevant time series can easily be developed.

Given the desirability and feasibility of developing such an index, the following additional steps are recommended:

1. Additional analysis of completed projects is necessary to determine the resource and resource-type mixes for different subsystems.
2. The components applicable to each resource type need to be defined.
3. Finally, a data base and equations are created on the computer so that index items for each resource type can be updated and the relations can be manipulated for different types of subsystems, locations, and times.

## SUMMARY AND EXTENSION TO NONPRICE FACTORS AFFECTING REGIONAL COSTS

The proposed transit price index will provide a reasonable way to

1. Provide transit professionals a means of tracking the resource costs most applicable to their work and
2. Provide planners, designers, and researchers a means by which to better compare costs of projects constructed at different times and places [currently used surrogates such as the ENR and producer indices

(formerly WPIs) suffer from inappropriate resource and resource-type mixes].

In addition to the price of the resource, many other factors affect the cost of a job. If one views cost as output x productivity x resource price x overhead, it can be seen that the price index will define one part of the cost picture. Productivity can be related to region-specific work rules and job specifications such as traffic control requirements, supply uncertainty, and weather. Overhead costs reflect market and institutional costs. Foster and others (7) identify market factors such as the bidding climate and institutional and support factors such as insurance, building permits, financing, real estate acquisition, geologic investigation, construction management, engineering design, and legal and community costs that affect the overhead rate on any job. Once the effects of price, time, and location (as represented by the transit price indices) have been determined, indices of productivity and overhead factors can be analyzed to understand costs.

ACKNOWLEDGMENT

The research for this paper was conducted as part of Transportation Systems Center work for the Office of Planning Assistance of the Urban Mass Transportation Administration to develop technical guidelines for system planning and corridor refinement studies. I wish to acknowledge the assistance of Don Ward and Mike Jacobs in the preparation of this paper. The ideas presented here are mine and do not represent official U.S. Department of Transportation policy.

REFERENCES

1. Dodge Building Cost Services. 1979 Dodge Guide for Estimating Public Works Construction Costs, 11th annual ed. McGraw-Hill Information Systems Co., New York, 1978.
2. Means Cost Guide. R.S. Means Company, Inc., Duxbury, MA, 1978.
3. National Construction Estimator, 27th annual ed. Craftsman Book Co., Solana Beach, CA, 1978.
4. Market Trends. Engineering News Record, March 22, 1979.
5. Construction Cost Indexes for 1915-78. U.S. Department of Commerce, Construction Review, Vol. 25, No. 12, Dec. 1979.
6. Data Resources Cost Forecasting Service, Inc. Forecasting Highway Construction Costs. FHWA, Rept. FHWA-DL80-005, Feb. 1981.
7. E.L. Foster and others. Economic Factors in Tunnel Construction. U.S. Department of Transportation, Rept. UMTA-MA-06-0025-79-10, Feb. 1979.

*Publication of this paper sponsored by Committee on Construction Management.*

# Nondestructive Monitoring of Chloride in Bridge Decks with a Mobile Neutron-Gamma Spectrometer

J.R. RHODES

**A mobile, self-contained instrument for rapid, nondestructive monitoring of chloride content at the reinforcing-bar level in portland cement concrete bridge decks has been developed to field prototype stage and tested on a range of concrete specimens and on five bridge decks in Texas. The instrument uses the technique of neutron-induced gamma-ray spectrometry with a 400-$\mu$g californium-252 sealed neutron source. Two measuring heads provide the capability for depth discrimination and enable chloride contents to be measured at the reinforcing-bar depth irrespective of surface washout, salt encrustation, the presence of overlays or membranes, and different depth distributions of chloride content. The sensitivity to chloride obtained depends on the required depth discrimination and speed of measurement but is normally sufficient to detect chloride concentrations below the corrosion threshold of approximately 300 mg/kg (~1.2 lb/yd$^3$).**

The chloride-induced deterioration of reinforced portland cement concrete (PCC) is one of the most important problems currently facing the highway industry (1). All PCC bridge decks to which deicing salts have been applied and all PCC structures exposed to sea salts are susceptible. As little as 300 mg/kg (~1.2 lb/yd$^3$) of chloride ion counteracts the passivity of the steel reinforcing and allows electrochemical corrosion to proceed rapidly. The onset of rapid corrosion can be very difficult to detect because the depth distribution of chloride concentration can vary due to factors such as surface washout or accumulation of salt and because the concrete surface may have been covered with a protective overlay or membrane.

In addition to membranes and asphalt overlays, other materials impermeable to chloride are being used both at repair sites and in new construction. Any test method should be capable of monitoring chloride content without interference from any of the materials used in bridge decks. The present test method is to remove pulverized core samples taken at various depth increments by means of a rotary hammer and to analyze them in the laboratory by using a wet chemistry-potentiometric technique. This method is time consuming, labor intensive, and traffic disrupting. Its destructive nature makes it unsuitable for sampling below impermeable membranes and requires refilling of the sample holes. Furthermore, because of the small sample size and the heterogeneity of concrete, more samples than might otherwise be needed have to be taken to yield a survey of acceptable accuracy (1).

The main objective of the project described here was to develop a field instrument and test procedure for rapid, in situ, nondestructive determination of chloride ion content in PCC bridge decks and other reinforced concrete members at the level of the outermost mat of reinforcing steel. A detailed feasibility study (2) resulted in the choice of neutron-induced gamma spectrometry as the preferred method of measurement. The unique advantage of neutron-gamma spectrometry is that the incident neutrons and emitted characteristic gamma rays have

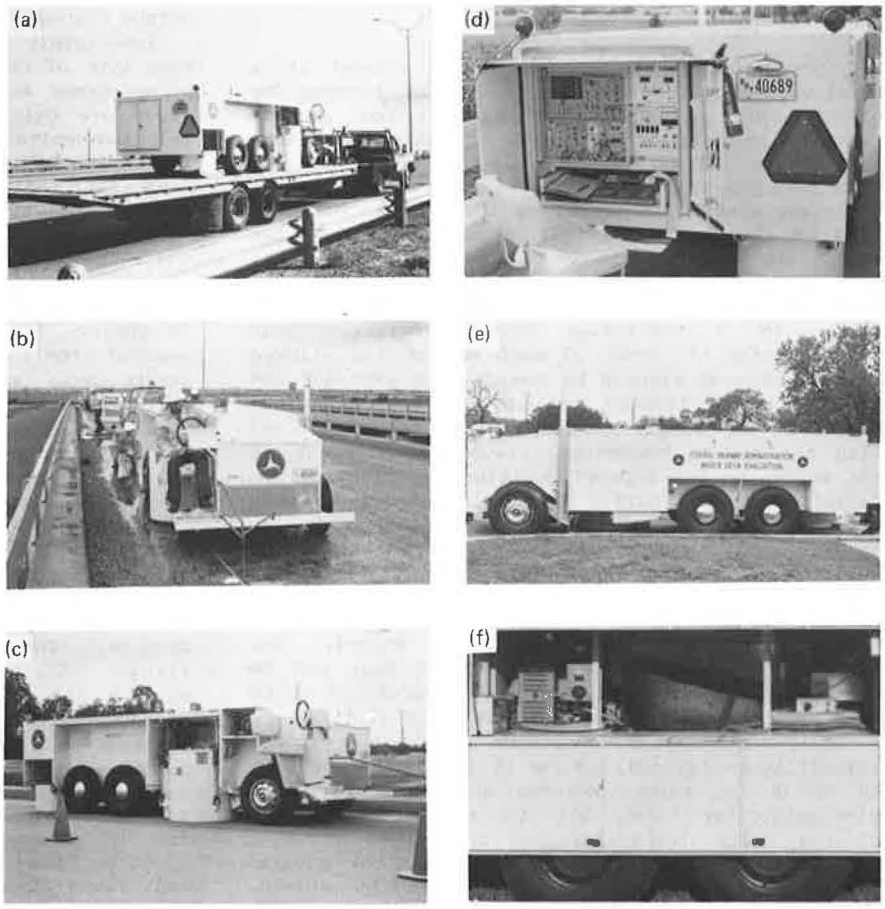


**Figure 1. Prototype bridge-deck analyzer: (a) on flatbed trailer, (b) being positioned, (c) measuring heads in position on road surface, (d) instrumentation panel at rear, (e) left-hand side of vehicle, and (f) support systems.**

ranges of several centimeters in solids, thus permitting representative analysis of coarse bulk materials and offering the possibility of nondestructive depth chloride determinations. A dual neutron-gamma measurement procedure was conceived and demonstrated experimentally to yield independent "surface" and "depth" chloride content determinations on PCC test specimens. Two measuring heads were designed, each of which has a different depth sensitivity. A prototype field instrument has been developed that incorporates the two measuring heads and provides all support systems necessary for semiautomatic, mobile field operation. In addition to real-time monitoring of bridge decks, the bridge-deck analyzer can be used for rapid chloride content determination of small [300-g (0.6-lb)] pulverized concrete samples and for multielement analysis of large [200- to 500-kg (440- to 1100-lb)] samples of coarse [minus 5-cm (minus 2-in)] bulk materials.

This paper describes the instrument and summarizes the results obtained in laboratory and preliminary field trials. Full details are reported elsewhere (3).

## DESCRIPTION OF INSTRUMENT

### General

The prototype bridge-deck analyzer shown in Figure 1 is a self-propelled vehicle that weighs 4300 kg (5 tons) and measures 1.44 m high by 5.64 m long by 1.98 m wide (4.75x18.5x6.5 ft). It is designed to be driven from one measurement spot to the next, but for analyses to be made the vehicle must be stationary and the measuring heads lowered hydraulically onto the surface of the material. The vehicle is moved long distances on a suitable transporter, such as a flatbed trailer, as shown in Figure 1a. Figure 1b shows the vehicle being positioned for a measurement. Note the fold-away pointer extended to aid accurate positioning. When extended, the pointer is 3.05 m (10 ft) in front of the axis of the forward (prompt-gamma) measuring head, which is itself 3.05 m in front of the axis of the rear (activation-gamma) measuring head. The pointer and the measuring-head axes are on the same straight line running fore and aft. Figure 1c shows both measuring heads lowered to the road surface for a dual neutron-gamma depth chloride measurement.

Figure 1d shows the instrumentation panel at the rear and the demountable operator's seat and "umbrella". Figure 1e shows the left-hand side of the vehicle. The forward cupboard has about 1 $m^3$ (35 $ft^3$) or storage space. The fold-down door gives access to the support systems (on-board power and temperature-controlled air and water), which are shown in Figure 1f.

### Nuclear Instrumentation

The nuclear instrumentation comprises (a) a prompt-gamma measuring head, which is also the irradiator for the activation-gamma measurement and the source storage chamber; (b) an activation-gamma measuring head; and (c) a gamma-ray spectrometer interfaced to a small computer with cassette tape storage and printer and to a data sequencer. During semiautomatic operation, six buttons with integral indicator lights on the data sequencer lead the operator through the measuring sequence and prevent acquisition of erroneous data, or improper source exposure, through various interlocks.

### Measuring Heads

The prompt-gamma measuring head is housed in a steel-walled cylinder 0.9 m (3 ft) in diameter by 0.9 m high that weighs 1080 kg (0.5 ton) and is filled with neutron and gamma-ray shielding material. The 400-μg californium-252 source (half-life 2.65 years) is encapsulated in a solid, welded, stainless steel cylinder, 1 cm (0.4 in) in diameter by 3 cm (1.2 in) long, that moves up and down the axis. The "home" position of the source is at the center, and the "exposed" position is 2.5 cm (1 in) from the base. The source movement mechanism is driven by a reversible stepper motor. Limit switches stop the motor at each end of the allowed travel and send signals to the "source exposed" and "source home" lighted buttons on the data sequencer. The sample contact switch is interlocked with the source mechanism, preventing movement of the source to the exposed position and lighting the "shield not down" button on the data sequencer when the prompt-gamma head is not in contact with the sample. Additional visual indication of the source position is provided in the form of the color of the source retraction chain visible to the operator: red for exposed and green for home. In addition, a Klaxon sounds when the source is moving. The neutron shield has a movable segment that can be raised by a hand crank to enable measurements to be made as close to roadside curbs as 31 cm (1 ft).

The prompt-gamma-ray detector is a sodium iodide scintillation crystal, 13 cm (5 in) in diameter by 10 cm (4 in) thick, mounted on a 13-cm-diameter photomultiplier tube, all in a light-tight enclosure. The temperature is controlled to ±1°C (±33.8°F). The whole subassembly is shock mounted inside the gamma-ray and thermal neutron shield. The source-detector geometry is optimized to provide maximum sensitivity to depth chloride for least cost in terms of signal-to-background ratio. The measurement cannot be made insensitive to surface chloride.

The activation-gamma measuring head comprises a temperature-controlled, shock-mounted detector assembly identical to that in the prompt-gamma head, all housed in a cylindrical steel-walled shield 0.61 m (2 ft) in diameter by 0.43 m (17 in) high that weighs 360 kg (800 lb). The activation measurements are optimized to provide maximum sensitivity to surface chloride and minimum response from depth chloride.

### Gamma-Ray Spectrometer

The gamma-ray spectrometer is housed in a custom-built NEMA 4 specification instrument cabinet that is air conditioned and temperature controlled to 24° ± 8°C (75° ± 14°F). The rack containing the multichannel analyzer (MCA) and electronic modules (the left-hand panel in Figure 1d) is covered by a plexiglas door, which prevents access during routine operation to every module except the data sequencer (top right in Figure 1d) and the electrical panel (bottom right). The electrical panel contains the switches and meters for the electrical supplies and detector temperature monitoring.

The spectrometer operates as follows. Gamma rays absorbed in the sodium iodide crystal produce light scintillations that are seen by the photomultiplier, converted into electrical charge pulses, and amplified by linear pulse amplifiers whose output pulses have voltages proportional to the original energies of the gamma rays. The MCA sorts the pulses into channels according to their voltages and accumulates each gamma-ray spectrum as a histogram of number of pulses per channel in a given measurement time versus channel number (i.e., gamma energy).

Immediately after absorbing a thermal neutron, each type of nuclide in the sample emits a group of prompt-gamma rays. The energies and number in the group are uniquely characteristic of the nuclide. Chlorine emits many prompt gammas in the energy range 3-9 MEV, and they are only partly resolved from all the other prompt gammas. In fact, a prompt-gamma spectrum is characterized by having a large number of gamma-ray peaks from a relatively small number of components in the sample.

Activation-gamma rays are emitted as a result of the decay of thermal-neutron-induced radioactivity. To observe these gamma rays, the sample is first removed from the source (or vice versa) to stop the prompt-gamma emission and eliminate the neutron background. Because the thermal neutron activation cross sections of Mn, Na, Al, and Cl are very high, their gammas predominate even at low concentrations of these elements. In contrast, H, C, O, Si, and Fe are not activated by thermal neutrons. The activation-gamma spectrum has fewer peaks than the prompt-gamma spectrum, but the problem of resolving the chlorine gammas remains.

Various methods of mathematical analysis have been used to deconvolute partly resolved gamma spectra. The method used here is least-squares fitting (LSF) of library spectra (4, p. 193). Gamma spectra are obtained for each and every uniquely characterized component of the material to be analyzed and are stored in a library (on a tape cassette in this case). Analysis then proceeds on the assumption that the "unknown" spectrum is a linear combination of the library spectra. The fraction of each library component in the unknown spectrum is assumed to be proportional to the concentration of that component in the material being analyzed. The values of these fractions are found by using the least-squares method to calculate the best fit of the library spectra to the unknown spectrum.

### Support Systems and Accessories

The instrument is propelled by a front-wheel-drive automobile engine complete with drivetrain, automatic transmission, and front suspension. The driver's station (Figures 1b and 1c) consists of a seat, steering wheel, instrument console, gear-shift lever, and brake and accelerator pedal. The driver's station is placed over the right-front wheel directly above the line that joins the centers of the two measuring heads and the pointer.

The power required for the electronic instrumentation, the heater and cooler for instrument air, and the heater and cooler for detector temperature control fluid is 110 V alternating current (ac). This is provided by a wall socket when available or by an on-board 4-KVA motor generator in the field. The pump for the detector temperature control fluid is powered by 12 V direct current (dc) so that fluid can be kept circulating at all times, particularly while the vehicle is being transported from site to site. The automotive car battery powers the pump as well as the rest of the 12-V dc system (ignition and lights). The battery is charged either from the 110-V ac system or by the automotive alternator.

Each measuring head is suspended from four hydraulic jacks and can be raised and lowered independently by using two levers in the hydraulic station directly behind the driver's seat. The hydraulic system is operated from a pump mounted above the automotive engine. A manually operated pump is also provided to obtain hydraulic pressure in the event of power failure. Sample holders in the form of dollies are provided for holding cali-

**Table 1. Definitions of calibration models.**

| Model | Description | $C_s$ | $C_d$ | Expected Precision (mg/kg) $\Delta C_s$ | $\Delta C_d$ |
|---|---|---|---|---|---|
| B | Uniform for first 1.3 cm exponential in range 1.3-7.6 cm; zero below 7.6 cm | Avg in 0- to 1.3-cm depth increment | Value at 5.1 cm below surface | 630 | 66 |
| D | Uniform chloride distribution | - | Avg in 0- to 15-cm depth increment | - | 38 |

Note: 1 cm = 0.39 in; 1 mg/kg = ~0.004 lb/yd$^3$.

bration standards, concrete test specimens, and bulk materials.

### Dual-Measurement Procedure

A dual measurement is required to determine chloride content at a given depth below the surface. Dual measurements are made along a straight line at premarked spots 3.05 m (10 ft) apart. The instrument is driven along the line until the extended pointer is over the second spot to be measured. The prompt-gamma measuring head is then over the first spot. This head is lowered, and the prompt-gamma measurement made. The head is then raised, the instrument is driven forward until the pointer is over the next spot, and both heads are lowered. The activation-gamma head then makes its measurement on the first spot while the prompt-gamma head is measuring and irradiating the second spot. The two readings for each spot are combined by applying them to a simultaneous linear equation to yield depth and surface chloride concentrations. The usual measurement time is 10 min with a 5- to 10-min delay period in between. Results are printed out about 5 min after the second measurement of each spot, and an average of 3 spots/h are measured.

### Single-Measurement Procedure

In the single-measurement mode, only the prompt-gamma head is used and the chloride concentrations obtained are weighted depth averages of the total chloride in the deck. The measurement spots need be neither on a straight line nor 3.05 m (10 ft) apart. At least 6 spots/h can be measured in this mode.

## EXPERIMENTAL RESULTS

Laboratory measurements were made on more than 100 test specimens to assess the effects on the chloride reading of changes in concrete composition, reinforcing bars, overlays and membranes, and chloride concentration gradients. The test specimens were mixed, cast, and cured by using standard procedures, and some of them were analyzed by using the standard method of sampling and wet chemistry. Field trials were conducted on five bridges in Texas that were chosen to yield experience on a range of bridge types, deck conditions, salting histories, and geographic locations.

### Laboratory Measurements on Specimens with Uniform Chloride Content

Some 122 prompt- and activation-gamma readings were made on test specimens that covered variations in chloride concentration [0-3000 mg/kg (0-12 lb/yd$^3$)] aggregate (eight widely varying types were tested), water/cement (w/c) ratio (0.45-0.65), free-water content (0-5 percent), reinforcing-bar pattern and depth, and presence of overlays and membranes. The overlays tested included polymer concrete, asphalt concrete, wax-bead-loaded PCC, and latex-modified PCC. In addition, typical asphaltic membranes were inserted between the asphalt concrete overlay and the PCC specimen.

The activation- and prompt-gamma methods each gave a linear response over the full range of chlorine content. No significant interferences were found due to variations in aggregate type or maximum particle size; w/c ratio or free-water content; reinforcing-bar presence, pattern, or depth; or, with one exception, the presence of overlays and membranes. Two polyvinyl chloride (PVC) materials, Dow Latex B overlay and Superseal 4000 membrane, gave very large signals when measured with a zero-chloride test specimen. This is to be expected since PVC is mainly chlorine.

### Nonuniform Chloride Content

Unknown chloride concentration distributions are handled by the dual-measurement procedure, which can, by solution of a pair of simultaneous equations, determine the chloride content at two specific depths below the surface of a bridge deck. One of these is the reinforcing-bar depth, which is usually 5.1 cm (2 in) but can be as little as 2 cm (0.75 in) for a worn deck and 10-15 cm (4-6 in) for an overlaid deck. The chloride content at the reinforcing-bar level is defined as the depth chloride ($C_d$); the second variable is the surface chloride ($C_s$). A calibration model must be defined that specifies the depth or depth increment for $C_s$ and $C_d$ and states the assumptions to be made about the chloride concentration distribution. There are an infinite number of such models, but the most useful ones can be chosen by taking into account our knowledge of real chloride concentration distributions and of the depth sensitivity profiles of each neutron-gamma measurement. The sensitivity of the prompt-gamma measurement falls off slowly from the surface down to about 20 cm (8 in), below which it is essentially zero. The sensitivity of the activation-gamma measurement falls off rapidly and is zero below about 4 cm (1.6 in) from the surface.

The chloride concentration distribution is only important in the sensitive ranges of the neutron-gamma measurements. In controlled experiments, Clear (5) obtained exponential distributions with varying gradients. The average gradient was a factor of two per 1.3-cm (0.5-in) depth increment. On real bridge decks, the first 5 mm (0.2 in) or so of a nonoverlaid deck can have any chloride content, independent of the distribution at greater depths, because of the possibility of surface washout or salt encrustation. Overlays present an additional thickness of 1-10 cm (0.5-4 in), which is usually chloride free.

Several calibration models were tested. The results for the two most promising models, B and D, are given here. Table 1 describes each model, defines $C_s$ and $C_d$, and gives the expected precisions ($\Delta C_s$ and $\Delta C_d$).

The instrument was calibrated for each model by measuring stacks of test specimens that had known chloride contents and concentration distributions that corresponded to the models as defined. The results were used to calculate the calibration coefficients, which are the coefficients of the pair of

simultaneous linear equations relating $C_s$ and $C_d$ with the responses, $I_1$ and $I_2$, of each measuring head.

The expected precisions were calculated by substituting the measured values, $\Delta I_1$ and $\Delta I_2$, of instrument repeatability into the pair of simultaneous linear equations relating $\Delta C_s$ and $\Delta C_d$ with $\Delta I_1$ and $\Delta I_2$. Repeated measurements of test specimens revealed that $\Delta I_1$ and $\Delta I_2$ are independent of any of the sample variables and are constant for a given source strength and measurement time sequence. The differences in $\Delta C_s$ and $\Delta C_d$ between models are the result of each model having a different set of coefficients. Better precision and sensitivity are traded for reduced depth "resolution".

## Laboratory Measurements of Nonuniform Chloride Content

Table 2 gives a selection of the results for the two models, obtained for measurements on 1.3-cm (0.5-in) thick test specimens stacked to simulate various chloride concentration distributions and concrete compositions. These include the average Clear exponential distribution with and without surface washout and salt encrustation as well as overlays, reinforcing bars, and different water contents. Model B is very successful at eliminating effects on $C_d$ due to high surface chloride concentrations (see samples 1, 3, 5, 8, 9, and 13). Model D, which requires only a single prompt-gamma measurement, is clearly a practical proposition for rapid screening. The model tends to overestimate the value of $C_d$, especially when the chloride is near the surface, but this can be corrected by a change in the calibration coefficient. The results for specimen stacks 10-14 illustrate the ability of each model to avoid "false positive" readings. Stack 10 yields results that are representative of all the non-PVC overlays and membranes tested. No model gave a $C_d$ reading more than about ±1 standard deviation different from zero. Stack 11 is representative of all of the different reinforcing-bar patterns and depths. No model gave an error in $C_d$ greater than ±2 standard deviations. Stack 12 is representative of all w/c ratios and free-moisture contents. Again, no error was greater than ±2 standard deviations. The effects of the PVC overlay and PVC membrane are shown in entries 13 and 14. Considering that the chlorine content of these materials is orders of magnitude greater than the range of interest for corrosion in bridge decks, the errors caused by them are small.

The effects of overlays 1.3-7.6 cm (0.5-3 in) thick are given in Table 3. The expected and measured values of $C_s$ and $C_d$ were recalculated for six specimen stacks after the surface and depth chloride concentrations were redefined as measured from the base of the overlay rather than the surface of the specimen. It is seen that model B tends to underestimate $C_d$ for large overlay thicknesses whereas model D shows good agreement for thick overlays. Prior knowledge of the approximate overlay thickness would eliminate these errors.

## Field Trials on Bridge Decks

Approximately 50 nondestructive neutron-gamma measurements were made on each of five bridges by using the dual- and single-measurement procedures described earlier. Conventional chloride determinations were made by sampling approximately one-third of the nondestructive measurement sites. The instrument operated reliably in moderate rainfall, but samples could not be taken in these conditions. The iron signal from steel beams was found to be much greater than that from reinforcing bars, but the data analysis procedures successfully handled this.

Analysis of the rotary hammer samples showed that in all but one case the assumption concerning exponential depth chloride distribution was supported. However, the exponents varied from -0.2x to -0.4x with an average value of approximately -0.3x (where x is depth in centimeters), which is at variance with the assumption of -0.6x on which the calibration for model B is based. The results for $C_d$ were corrected for this. In addition, the wet

**Table 2. Measurements on concrete specimens.**

| Description of Specimen Stack[a] | Chloride (mg/kg) | | | | | |
|---|---|---|---|---|---|---|
| | Model B | | | | Model D | |
| | Measured | | Expected | | | |
| | $C_s$ | $C_d$ | $C_s$ | $C_d$ | Measured | Expected |
| 5000, 450, 210, 100, 50, 20 mg/kg Cl; rest 0 | 5 090 | 109 | 5000 | 75 | 824 | 486 |
| 0, 450, 210, 100, 50, 20 mg/kg Cl; rest 0 | -1 104 | 234 | 0 | 75 | 249 | 69 |
| 5000, 1900, 900, 420, 210, 100 mg/kg Cl; rest 0 | 5 960 | 237 | 5000 | 315 | 1147 | 711 |
| 0, 1900, 900, 420, 210, 100 mg/kg Cl; rest 0 | 720 | 256 | 0 | 315 | 516 | 294 |
| 5000, 4000, 1900, 900, 420, 210 mg/kg Cl; rest 0 | 6 490 | 402 | 5000 | 660 | 1490 | 1036 |
| 0, 4000, 1900, 900, 420, 210 mg/kg Cl; rest 0 | -720 | 632 | 0 | 660 | 960 | 619 |
| 1900, 900, 420, 210, 100, 50 mg/kg Cl; rest 0 | 3 570 | 109 | 1900 | 155 | 633 | 298 |
| 4000, 1900, 900, 420, 210, 100 mg/kg Cl; rest 0 | 5 870 | 293 | 4000 | 315 | 1229 | 628 |
| 5000 mg/kg Cl; rest 0 | 5 120 | -2 | 5000 | 0 | 644 | 417 |
| 2.5-cm asphalt overlay; all 0 | -18 | -25 | 0 | 0 | -45 | 0 |
| Rebar at 4.5 cm, all 0 | -448 | -7 | 0 | 0 | -69 | 0 |
| All 0, any w/c or moisture | -29 | 5 | 0 | 0 | 5 | 0 |
| 2.5-cm PVC modifier overlay; rest 0 | 27 700 | 258 | High | 0 | 3924 | High |
| 0, 0, Superseal 4000 PVC membrane; rest 0 | -1 398 | 810 | High | 0 | 1170 | High |

Note: 1 mg/kg = ~0.004 lb/yd$^3$; 1 cm = 0.39 in.
[a]Chloride listed in successive 1.3-cm (0.5-in) depth increments from surface.

**Table 3. Effects of overlays.**

| Description of Specimen Stack[a] | Chloride (mg/kg) | | | | | |
|---|---|---|---|---|---|---|
| | Model B | | | | Model D | |
| | Measured | | Expected | | | |
| | $C_s$ | $C_d$ | $C_s$ | $C_d$ | Measured | Expected |
| 450, 210, 100, 50, 20 mg/kg Cl; rest 0[b] | -1104 | 110 | 450 | 35 | 249 | 69 |
| 1900, 900, 420, 210, 100 mg/kg Cl; rest 0[b] | 720 | 120 | 1900 | 155 | 516 | 294 |
| 420, 210, 100 mg/kg Cl; rest 0[c] | -110 | 19 | 420 | 0 | 163 | 61 |
| 450, 210, 100, 50, 20 mg/kg Cl; rest 0[d] | -1680 | 9 | 450 | 35 | 82 | 69 |
| 1900, 900, 420, 210, 100 mg/kg Cl; rest 0[d] | -2870 | 20 | 1900 | 155 | 317 | 294 |
| 4000, 1900, 900, 450, 210, 100 mg/kg Cl; rest 0[e] | -4580 | 8 | 4000 | 330 | 686 | 630 |

Note: 1 mg/kg = ~0.004 lb/yd$^3$.
[a]Chloride listed in successive 1.3-cm (0.5-in) depth increments from surface.
[b]All under 1.3-cm overlay.
[c]All under 3.8-cm (1.5-in) overlay.
[d]All under 5.1-cm (2-in) overlay.
[e]All under 7.6-cm (3-in) overlay.

**Table 4. Sample volumes and sampling errors.**

| Method | Effective Volume Sampled (cm$^3$) | Sampling Error[a] (%) |
|---|---|---|
| Neutron-gamma | 5000 | 0.6 |
| Core sample, 10 cm diameter x 2.5 cm deep | 210 | 8.4 |
| Rotary hammer sample, 3.8 cm diameter x 1.3 cm deep | 15 | 32 |

Note: 1 cm$^3$ = 0.061 in$^3$; 1 cm = 0.39 in.
[a]Coefficient of variation.

**Table 5. Comparison of average chloride contents for five bridge decks.**

| Bridge | Chloride (mg/kg) | | | |
|---|---|---|---|---|
| | Neutron-Gamma | | | |
| | Model B | | | |
| | $C_s$ | $C_d$ | Model D | Sampling Plus Wet Chemistry |
| 1 | 130 | 57 | 73±73 | 105±44 |
| 2 | 2090±1809 | 686±343 | 575±261 | 542±326 |
| 3 | 2401±1855 | 797±602 | 664±284 | 873±545 |
| 4 | 5339±2182 | 395±432 | 638±273 | 490±389 |
| 5 | 563±124 | 43±35 | 54±38 | 111±14 |

Note: 1 mg/kg = ~0.004 lb/yd$^3$.

chemistry results were corrected where necessary to a 5.1-cm (2-in) depth to allow comparison with the neutron-gamma measurements.

Chloride in PCC bridge decks does not penetrate the coarse aggregate but is distributed throughout the mortar. This causes the well-known "aggregate-induced distortion" (1), a local heterogeneity that is present even when the average chloride content is uniform on a large scale. Sampling errors caused by this can be very great when the sample size is similar to the volume of a coarse aggregate particle, as is the case with rotary hammer samples. Sampling errors can be reduced by making sample volumes so large that local fluctuations in coarse aggregate concentration become negligible. Table 4 gives the effective sample volumes of the neutron-gamma methods and the volumes of standard cores and rotary hammer samples. It can be seen that some 330 rotary hammer samples would be required to give the same sample volume as the neutron-gamma method. The corresponding sampling errors were calculated by using particulate sampling theory (6). The relative standard deviation of a single rotary hammer sample is 32 percent.

Comparisons of average chloride contents for the five bridges yielded by the conventional and neutron-gamma measurements are summarized in Table 5. These comparisons must of necessity be semi-quantitative because of the variability of the chloride distributions and the noncorrespondence between the volumes sampled by each method and the sites measured by each method. Even though the relative standard deviations vary from 13 to 109 percent, semiquantitative agreement between most of the mean values is quite good. The results for model D are especially interesting, since this model uses only one measuring head and can monitor with twice the sensitivity and at twice the rate of the dual method. Detailed results of the field trials are given elsewhere (3).

## CONCLUSIONS

The mobile bridge-deck analyzer shows promise of being able to evaluate bridge decks far more rapidly and economically than the conventional methods. Fewer measurements are required for equivalent quality of data. Each measurement is faster and decisions can be made to optimize measurement patterns on the basis of real-time results. Although the capital cost of the instrument is high, its operating costs are low and, with good planning, amortization can be spread over thousands of bridge decks. One technician-grade operator with one assistant (plus flagmen, as required by the location) could operate the instrument after suitable training.

## ACKNOWLEDGMENT

I wish to acknowledge the support of the 24 state highway agencies that sponsored this work and whose representatives directed it. I would also like to express appreciation for the encouragement and guidance of T.M. Mitchell of the Federal Highway Administration and for the work done by N.J. Carino of the National Bureau of Standards (formerly at the University of Texas) in preparing the concrete test specimens and J. Canfield of the Texas State Department of Highways and Public Transportation in helping to organize the field trials. Last but not

least, I wish to acknowledge the untiring efforts of my associates, J.A. Stout, J.S. Schindler, and R.D. Sieberg, in assembling and operating the instrument.

REFERENCES

1. Durability of Concrete Bridge Decks. TRB, Synthesis of Highway Practice 57, 1979.
2. J.R. Rhodes and others. In Situ Determination of the Chloride Content of Portland Cement Concrete in Bridge Decks: Feasibility Study. FHWA, Interim Rept. FHWA-RD-77-26, 1977.
3. J.R. Rhodes and others. In Situ Determination of the Chloride Content of Portland Cement Concrete Bridge Decks. FHWA, Final Rept. FHWA-RD-80-030, 1980.
4. L. Salmon. Analysis of Gamma Ray Scintillation Spectra by the Method of Least Squares. Nuclear Instruments and Methods, Vol. 14, 1961.
5. K.C. Clear. Time to Corrosion of Reinforcing Steel in Concrete Slabs: Volume 3--Performance After 830 Daily Salt Applications. FHWA, Interim Rept. FHWA-RD-76-70, 1976.
6. C.L. Grant and P.A. Pelton. Role of Homogeneity in Powder Sampling. ASTM, Philadelphia, Special Tech. Publ. 540, 1973, pp. 16-29.

*Publication of this paper sponsored by Committee on Instrumentation Principles and Applications.*

# Development of an Improved Automated Nuclear Backscatter Gage

RAYMOND A. FORSYTH, FRANK C. CHAMPION, AND JOSEPH B. HANNON

**The design, construction, and evaluation of a prototype automated vehicle-carried nuclear moisture-density backscatter gage are described. Gage development was based on research and analysis concerning several factors that affect gage performance. This research indicated that the prototype backscatter-gage measurements were approximately equivalent to measurements obtained by commercial transmission gages. The implication of this research finding is the possibility of a backscatter test method as a valid, reliable, and expedient procedure for determining in situ soil conditions. Field comparisons between the prototype gage and a commercial nuclear backscatter gage demonstrated a marked improvement in performance by the prototype gage. The prototype gage is installed in a motor vehicle together with a hydraulically operated mechanism that automatically positions the gage for testing. The vehicle gage unit, or Autoprobe, can determine in situ moisture and density values in 3 min. The Autoprobe is now ready for use by the California Department of Transportation for investigational and quality-control purposes.**

The work reported in this paper was the outgrowth of three separate, but interrelated, federally funded research projects that were carried out simultaneously. The first resulted in the development of nuclear gage standards for calibration and evaluation of gage performance (1). In the second project, various elements of nuclear gage performance were explored for the purpose of developing meaningful specifications for the purchase of nuclear gages (2). The objective of the third project, which is reported on here, was the development of a backscatter gage that would equal or exceed the performance of approved direct-transmission gages. The principal advantage of the backscatter mode of testing is that both the source and the detector remain at the surface, which eliminates the need for an access hole into the test material. The obvious benefit is a faster and simpler test, which allows more tests in a given time period.

Currently, the transmission mode is considered to be the most accurate and reliable method of nuclear density testing. The transmission technique, which requires insertion of the gamma source into the test material, has proved to be less affected by surface conditions and more sensitive to density changes. It also tests a larger volume of compacted materials due to gage configuration.

Previous analyses by California Department of Transportation (Caltrans) researchers of the factors that affect nuclear moisture-density gage measurements have been limited to investigations of the difficulties encountered under field conditions. Factors such as surface roughness, air gaps, and gage calibration methods were among the items investigated. The present project began with an evaluation of the basic commercial nuclear gage, including the characteristics of the backscatter and direct-transmission modes of operation. The paper describes the subsequent development of an optimized prototype backscatter gage. More detail is available in reports by Chan and others (3) and Champion and others (4).

## DEVELOPMENT OF PROTOTYPE GAGE

### General Considerations

During the development of the prototype backscatter gage, various interrelated gage features that have significant effect on gage performance were studied. These included the geometric relation between the radioactive source, the test material, and the radiation detector. The backscatter mode involves measurement of attenuated gamma-ray emissions deflected to and from the test medium surface. Thus, the distance separating the radioactive source and the radiation detector is a primary factor in gage performance. In the transmission mode, the radioactive source is lowered into the test medium while the detector remains at the surface.

Second, the detection of particular attenuated gamma-ray energies has a marked effect on gage performance. Each source has its own characteristic energy spectrum. Attenuation of the spectrum by the test medium produces a wider variation of low-energy gamma rays than originally emitted by the source. Detection of low energies is undesirable due to absorption effects of the test materials, which vary with the mineral composition of the soil. Consequently, this parameter was carefully examined to

reduce the error in chemical composition generated by various test materials.

An important consideration in gage design is proper shielding between the source and the detector. Inadequate shielding permits radiation that has been attenuated by materials other than the test material to activate the detector. This results in degraded gage performance, particularly for backscatter gages.

Last, detector and source collimation was examined for potential improvement of gage performance and reduction of gage error. Collimation restricts the direction and number of gamma-ray emissions entering the detector as well as the direction and number projected into the test material. Here the investigation was limited. Further work with various combinations and amounts of collimation could prove particularly beneficial in increasing gage accuracy.

## Detectors

### General

The detectors chosen for the prototype gage were of the scintillation type, which included a sodium iodide crystal for the detection of gamma photons for density determinations and a lithium-iodide detector for the detection of thermal neutrons for moisture measurement. In the past, the major disadvantage of scintillation detectors has been their sensitivity to temperature variations and to physical and thermal shock. Sensitivity to shock has been alleviated by providing a protective housing to enclose the crystal. The addition of a gain stabilizer to the system has eliminated the problem of sensitivity to temperature.

### Density Detector

For density determination, the attenuated gamma photon collides with the atoms of the crystal, causing an ionization event to occur that, in turn, causes a minute quantity of light to be emitted. The amount of light emitted is proportional to the energy yielded to the crystal and to the energy of the gamma photon. A photomultiplier tube is physically coupled to the crystal to detect the light-emitting event and produce an electrical pulse proportional to the amount of light emitted. The pulse is then proportionately amplified and fed to an analyzer that allows only pulses within a selected range of amplitude to pass. The advantage of this system is that it electronically allows precise energy discrimination of the detected count.

### Moisture Detector

The lithium-iodide crystal used for moisture determination produces a minute quantity of light when a thermal neutron is captured. The basic reaction is referred to as a neutron alpha reaction (3).

### Gain Stabilizer

The gain stabilizer functions by monitoring a peak in the detected energy spectrum of a cesium-137 microsource. The microsource is attached to the crystal. Any change in the system that would cause a change in the pulse amplitude will cause a shift of this peak as seen by a single-channel analyzer. The single-channel analyzer is incorporated in the gain stabilizer system, which detects this shift and instantaneously applies an electrical correction to the system amplification. This eliminates problems caused by the temperature sensitivity of the crystal or shifts caused by the system electronics.

## Density Source

Three commonly used radioisotopes (cesium-137, cobalt-60, and radium-226-beryllium) were evaluated. Several nuclear density gage properties were investigated to select the most appropriate gamma source for the prototype gage. The prime selection criterion was the gamma source that would provide the best sensitivity to density changes with the minimum chemical composition error. Radium was eliminated from consideration due to the low initial gamma-ray energy emissions, which are susceptible to photoelectric absorption, the primary cause of chemical composition error.

Cobalt and cesium possess comparable sensitivity and compositional qualities. In considering a suitable gamma source, it was recognized that using cobalt, as opposed to cesium, would require a gage of greater overall dimensions and weight due to lead shielding requirements. Our research has shown that the cobalt backscatter gage obtains 90 percent of its indicated density from a 135-mm (5.3-in) thick volume of test material beneath the gage. The cesium gage obtains the same percentage of indicated density from approximately 112 mm (4.4 in) of test material (3). Even though the depth of penetration and the volume of material tested are greater for the cobalt gage, the half-life is one-sixth that of cesium. The more frequent calibration schedule required would be a disadvantage with the cobalt gage. Therefore, cesium was selected as the density source.

Surface error (error induced by the surface texture of test material or minor air gaps) ranged from 0 to 0.05 g/cm$^3$ (0-3 lb/ft$^3$) of the true density for the cesium backscatter gage. The gage was elevated 1.30 mm (0.051 in) above the test surface to create a simulated air gap. The amount of surface error associated with the cobalt gage was not determined. Chemical composition error was found to be approximately 0.03 g/cm$^3$ (2 lb/ft$^3$) for both the cesium and cobalt gages under optimum configuration conditions. Cesium was selected as the preferable gamma source, although cobalt also proved to be excellent for density determination.

## Moisture Source

Two neutron sources, radium-beryllium and americium-beryllium, were tested in the laboratory to determine which was most suitable for use in a moisture-density gage. These experiments indicated that radium-beryllium would be less suitable as a neutron source, primarily because of the detrimental effects the low-energy gamma photons emitted by radium have on density determination.

## Shielding

The most important function of shielding is to keep gamma rays from reaching the gamma detectors without entering the sample material. Approximately 114 mm (4.5 in) of lead, placed directly between a cesium source and a gamma detector, will absorb at least 99.5 percent of all undesirable emissions directed toward the detector from within the gage. Cobalt requires approximately 50 percent more lead, 165 mm (6.5 in), to provide the same degree of protection. Lack of adequate shielding between gamma source and detector will produce a backscatter-mode gage that is insensitive to density (3).

Shielding the neutron detector from attenuated neutron energies created within the gage apparatus was not a major problem. The close physical proximity of the neutron source and detector precludes most fast neutron attenuation to thermal neutron

energies by the time the neutrons penetrate the detector. Because the moisture-gage neutron detector is relatively insensitive to high-energy neutrons, these neutrons pass through the detector unnoticed. Moisture-gage sensitivity is not impaired by fast neutron penetration.

## Source-Detector Separation

Source-detector separation directly affects both moisture- and density-gage sensitivities. Experiments conducted with the density gage indicate that gage sensitivity increases with increasing source-detector separation. Ultimate sensitivity, however, cannot be used because of other performance considerations. Count rates decline sharply, and error in chemical composition increases with increased source-detector separation. The optimal separation for 10 millicuries of cesium-137 is about 279 mm (11 in). The optimal separation for 3 millicuries of cobalt-60 is approximately 330 mm (13 in).

Moisture-gage sensitivity, as determined from experiments, increases with decreasing source-detector separation. Best sensitivity results were obtained when the detector was located directly adjacent to the neutron-source housing. Moisture-gage sensitivity (defined as the ratio of the relative change in count rate to the relative change in moisture content) varies considerably with separation distance. It was found that the neutron detectors exhibited a 50-400 percent increase in sensitivity when the original separation distance was reduced by one-half (3). The prototype moisture gage used a 64-mm (2.5-in) source-detector separation. This separation was a physical limitation based on detector and source housing diameters.

## Collimation

Source and detector collimations were explored to determine their potential benefit to backscatter gage performance. Prime emphasis was placed on gamma source and detector collimation. Laboratory experiments confirmed that specific amounts of collimation were beneficial to density-gage sensitivity. Excessive collimation proved to be detrimental. The laboratory apparatus, under adequate source-detector shielding conditions, revealed that source and detector collimation amounting to a collimation channel length of 25 mm (1 in) or less could improve density sensitivity by a maximum of approximately 4 percent. A 25-mm source and 13-mm (0.5-in) detector collimation produced this slight improvement in performance. The amount of collimation applied also depends on the collimator shape, source size, and count rate. Excessive collimation reduces the count rate to a point where it degrades density sensitivity and increases chemical composition error. The optimum collimation derived from the cesium backscatter gage was 17 mm (0.65 in) for the source and 6 mm (0.25 in) for the detector (3). The prototype gage developed in this research used a source and detector collimation of 19 mm (0.75 in) and 12.5 mm (0.50 in), respectively, to minimize test errors induced by surface texture and gage seating problems.

Collimator shape significantly influenced the reaction of the backscatter gage to the surface conditions of the test soil. A 5-mm (0.2-in) air gap between the bottom of the backscatter gage and the test surface simulated the error induced by an improperly seated gage. A modified wedge-shaped collimator reduced air-gap error by approximately 20 percent. Gage sensitivity appeared to be unaffected by the collimation shape, but a study of the test data revealed that source orientation and collimation height within the collimator govern sensitivity values.

Data obtained during the study clearly indicated a loss of moisture-gage sensitivity and count rate with increasing collimation of the moisture source and detector. Chemical composition error remained relatively unchanged with varied amounts of collimation.

## Gage Seating

In the past, proper seating of gages on nonuniform surfaces has presented problems for operators using the backscatter technique. Operators of portable gages have prepared the test surface by adding a thin layer of native materials to fill voids of the contact area. The native materials were first sieved through a 4.75-mm (no. 4) screen and then spread evenly over the surface and lightly compacted into place. This layer provided a level plane for gage seating. However, it introduced a number of variables that significantly influenced gage measurements. For example, the thickness of the layer and the degree of compaction depended solely on the judgment of the individual gage operator. Thus, preparation of each test site could result in wide variations in density values. Currently available backscatter gages are extremely sensitive to the condition of the surface of the test material, as shown in Figure 1. An overthick layer of sieved material would induce a reduction in measured density due to the difference in compactive effort. On the other hand, a deficient layer may result in an air gap beneath the source and detector. As gamma rays would migrate from the source to the detector by way of the air gap, the measured density would again indicate a lower value.

This investigation sought to enhance intimate contact of the gamma source collimator and detector with the test material through eliminating, or at least minimizing, the balance of the gage bottom area. Intuitively, it was reasoned that reduction of the contact area would reduce the probability of air gaps and, concomitantly, reduce the need for surface preparation.

## Prototype Backscatter Gage

The prototype backscatter gage developed as a result

**Figure 1. Cumulative percentage of total count versus sampling depth.**

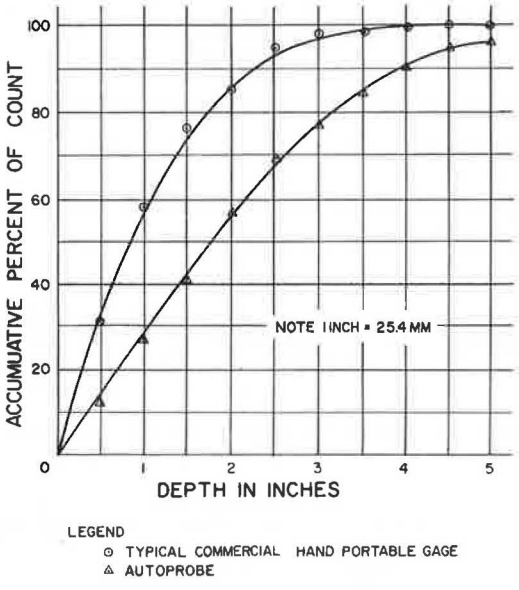

Figure 2. Electronic block diagram of Autoprobe.

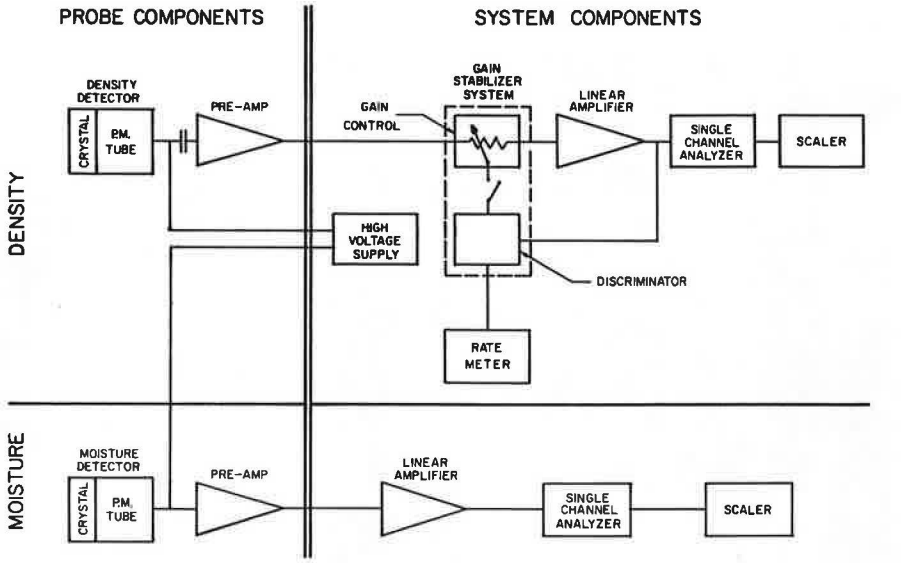


Figure 3. Cutaway view of Autoprobe.

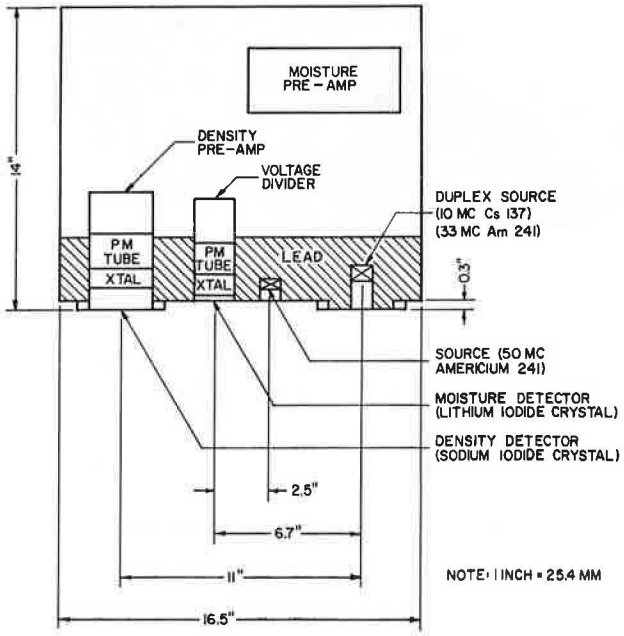


of this project has been designated as the "Autoprobe". Because it is an automated vehicular unit, it does not have the weight and size limitations of commercial portable gages. It is designed and constructed to allow the gage operator to (a) position it over the test site, (b) lower the gage to the test material, (c) seat the gage on the test surface, (d) record moisture and density readings, (e) retract the Autoprobe from the test site, and (f) move to another site, all without leaving the cab of the vehicle. This can all be accomplished in a period of less than 3 min.

An innovative feature of the Autoprobe, believed to be an improvement over the conventional commercial backscatter gage, is the reduced bottom surface area of the gage that contacts the material to be tested. Rather than being flat, as are most gages, the bottom of the Autoprobe has 8-mm (0.31-in) thick protrusions, 117 mm (4.6 in) in diameter, directly beneath the gamma detector and the gamma source. The advantage of the small contact areas is that surface irregularities such as small rocks, crowns, depressions, and bumps can be straddled and effective seating simplified. This reduces the amount of density-sensitive gamma rays streaming along the bottom of the gage to the detector. Such protrusions, or pads, have been used on early-model commercial gages.

The Autoprobe unit consists of an electronics system, located within the passenger compartment of the vehicle, and the probe, located outside the passenger compartment (see Figures 2 and 3). An automated hydraulic system is used to lower and raise the probe to and from the test surface, as shown in Figures 4 and 5. In this case, the vehicle modified to accommodate the Autoprobe is a pickup truck; other types of vehicles could be modified for this purpose. Specifications for the Autoprobe are summarized in Table 1.

## EVALUATION

### Preliminary Laboratory and Field Evaluation

Optimum backscatter-gage parameters established by this investigation were used in the construction of the Autoprobe. The unit was constructed so that the individual components could be modified to accommodate future improvements.

Several initial comparisons were made between the Autoprobe and a commercial gage that was a relatively new product of an established gage manufacturer. Initially, calibration curves were established for the Autoprobe and commercial transmission-backscatter gages in the laboratory by using three calcareous and three siliceous density standards fabricated by the Caltrans Laboratory. The count rate obtained from each density standard was divided by a standard count rate obtained from a density standard that accompanies the gage during field operations. The Autoprobe derives its standard count rate from a magnesium density standard. The commercial gage count is obtained on the gage storage container, which serves as a count-rate standard. Both count standards are used periodically during gage operations to verify or adjust gage performance.

A count ratio is calculated by dividing the density-measurement count rate by the standard count

Figure 4. Autoprobe seating assembly and restraining frame.


Figure 5. Testing of probe positioning with mechanism fully extended.


Table 1. Autoprobe specifications.

| Item | Specification |
|---|---|
| Duplex source[a] | 10-millicurie cesium-137 gamma source, 33-millicurie americium-241-beryllium neutron source |
| Duplex source collimation | 19 mm to center of source |
| Second neutron source | 50-millicurie americium-241-beryllium |
| Second neutron source collimation | 19 mm to center of source |
| Gamma detector | 76 x 51-mm sodium-iodide scintillation crystal with RCA 6342A photomultiplier tube and preamplifier |
| Gamma detector collimation | 13 mm to bottom of crystal |
| Separation between gamma source and detector | 279 mm center to center |
| Thermal neutron detector | 38 x 3-mm lithium-iodide scintillation crystall with RCA 6342A photomultiplier tube and preamplifier |
| Thermal neutron detector collimation | 9.5 mm to bottom of crystal |
| Separation between neutron source and detector | Duplex source: 170 mm center to center; 50-millicurie source: 64 mm center to center |
| Gamma discriminator setting | 0.12-0.55 MEV |
| Neutron discriminator setting | Undetermined |
| Moisture-density count period | 40 s |
| Lead shielding | Minimum of 127 mm between gamma source and detector |
| Gage bottom thickness | 1.6 mm stainless steel |
| Source and detector bottom protrusions | 7.9 mm |

[a]It is preferable to use separate neutron and density sources to enable selection of optimum conditions for density and moisture determination. The duplex cesium-137, americium-241-beryllium source was used because it was available and only for the gamma-ray emissions from the cesium-137 component, although the americium-241-beryllium component still contributes neutrons to the moisture determination.

rate. Thus, the relation between count ratio and gage-indicated density is established. The count ratio is used to minimize errors caused by electronic drift and gage source decay. A computer program was developed to calculate and tabulate a count ratio for each 0.003-g/cm³ (0.2-lb/ft³) change in density. The program ratios provide a density calibration over a range from 1.44 to 2.72 g/cm³ (90-170 lb/ft³). The tabulation, or computer output, is used by the gage operator to determine the gage-indicated density.

Four 1-min counts were obtained from the commercial gage on both unprepared and prepared test surfaces in both the backscatter and transmission modes. Four 40-s counts were obtained from the Autoprobe under unprepared and/or prepared conditions. Conversion of the gage-count rate to an indicated density was accomplished by determining the count ratio, as earlier defined, and then interpolating the corresponding density from the gage's computer ratio-density tabulation.

The performance of the commercially available nuclear density gage selected for this study was statistically compared with that of the Autoprobe with the assumption that the data collected from each gage conformed to a normal distribution. The commercial gage was operated in both the transmission and backscatter modes.

The mean density and standard deviation(s) were calculated for each gage. A graphical presentation provided an efficient means of evaluating and comparing gage performance.

Figure 6 shows the assumed normal distribution curves of the gage-indicated densities obtained from a silty-sand embankment material. The curves represent four individual test points at four different locations on the same project. The ordinate represents the percentage probability that the gage-indicated density will be a particular value. The area under the curve between ±1 standard deviation assumes that 68 percent of all transmission gage measurements will be within these limits. The density distributions of the Autoprobe and commercial backscatter gage were compared with the probability that their indicated density would be within the limits set by the transmission gage (±1 standard deviation). This comparison was made with the full realization that this conclusion is only valid if both gages see the same sample volume or the same density material when in reality that condition probably does not generally exist. The transmission test mode was chosen as the standard of comparison because it is the most widely accepted nuclear test mode for density determination. This analysis revealed that the Autoprobe has a significantly greater probability of indicating the transmission gage density than does the commercial backscatter gage. Surface preparation increased the probability and shifted the Autoprobe's mean indicated density toward the transmission value. The commercial backscatter gage did not respond in the same manner. A similar analysis was applied to each individual material tested in the field.

A review of the distribution curves for various other test materials indicated that the Autoprobe is not equivalent to the transmission gage in performance but did verify the backscatter-gage improvements built into the Autoprobe. The mean densities and standard deviations for these materials are summarized in Table 2. The Autoprobe appears to be less sensitive to irregularities in the test surface than the commercial gage and this is probably the primary factor in Autoprobe's improved performance.

Laboratory trials were conducted to determine how the protrusions would affect density-gage sensitivity, chemical composition error, and count-rate performance. The changes in protrusion-pad thickness and in the shape of the source collimator cavity resulted in both positive and negative differences in gage sensitivity, chemical composition effects, and error due to backscatter-gage seating or air gap. When the gage was properly seated on the standards (flush condition), these modifications reduced density-gage sensitivity by 3.5 percent. For the 5-mm (0.2-in) air-gap condition, they reduced density-gage sensitivity by 7.7 percent. Although the results were discouraging, the chemical composition error resulting from the modifications did not exceed 0.04 g/cm³ (2.5 lb/ft³) for both the flush and air-gap conditions. The chemical composition error increased by approximately 0.01 g/cm³ (0.5 lb/ft³) due to the air gap (3).

Comparison of the gage calibration curves before and after the source collimator and protrusion pads were modified indicates that the average error of the calibration line due to the air gap was reduced by approximately 27 percent, or 0.05 g/cm³ (3 lb/ft³). The value of the protrusions and modifications in the source collimator is therefore a priority selection between gage sensitivity and chemical composition on one hand and the errors caused by improper gage seating on the other. In view of the wide variation in field conditions, it was the opinion of the researchers that the loss of gage sensitivity was outweighed by the progress made toward ensuring a reduction of error when an air-gap condition is encountered.

Laboratory tests revealed that the average Autoprobe moisture-gage error is approximately 0.03 g/cm³ (1.9 lb/ft³) of water content due to varying quantities of neutron-capturing elements such as iron or boron or minerals such as bentonite and kaolinite. The commercial moisture gage tested under identical conditions produced an average 0.03-g/cm³ error.

The Autoprobe appears to be about 45 percent less sensitive to mineral absorbers than the commercial backscatter density gages under study. A primary advantage of the Autoprobe moisture gage is the count-rate sensitivity to changes in moisture content. Under normal operating conditions, the change in count rate for an 0.02-g/cm³ (1.2-lb/ft³) change in water content was found to be 121 percent

**Figure 6. Comparison of nuclear density gage measurement statistics.**

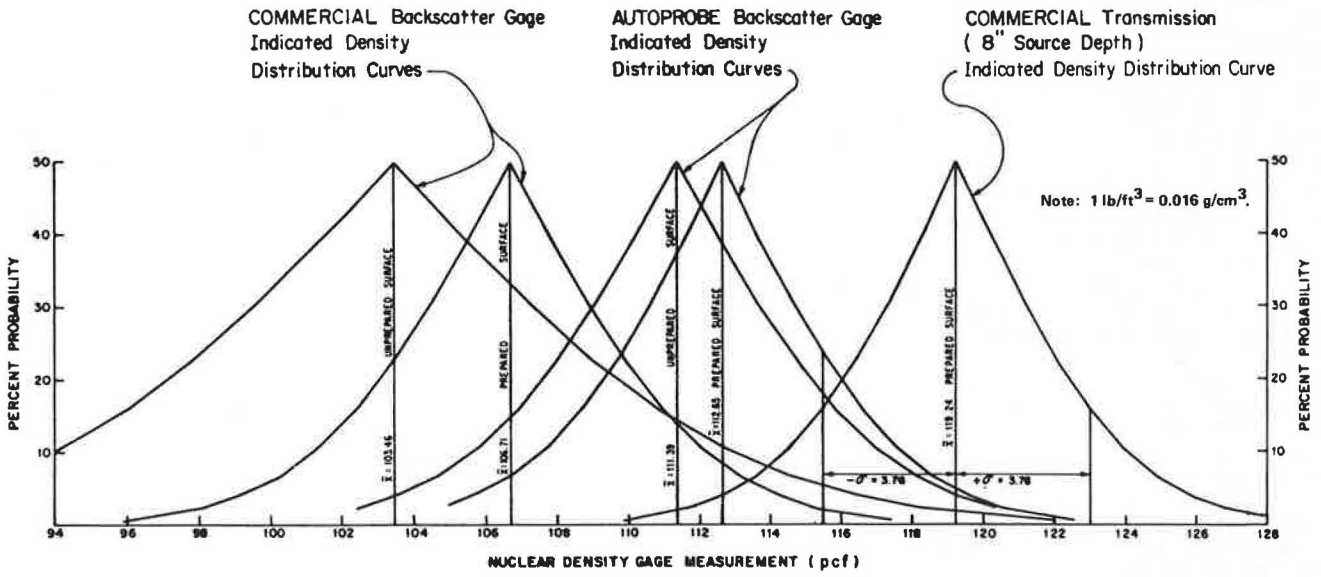

**Table 2. Mean density of gage measurements.**

| Material Tested | Backscatter Gage (lb/ft³) | | | | | | | | Transmission Gage (lb/ft³) | | | |
|---|---|---|---|---|---|---|---|---|---|---|---|---|
| | Commercial | | | | Autoprobe | | | | | | | |
| | Unprepared | | Prepared | | Unprepared | | Prepared | | $\bar{X}$ by Source Depth | | SD by Source Depth | |
| | $\bar{X}$ | SD | $\bar{X}$ | SD | $\bar{X}$ | SD | $\bar{X}$ | SD | 203 mm | 102 mm | 203 mm | 102 mm |
| Silty-sand gravel | - | - | 113.5 | 3.95 | 113.5 | 6.03 | 119.5 | 2.89 | 121.6 | 119.3 | 5.76 | 5.61 |
| Gravelly sand | - | - | 118.2 | 10.0 | 121.2 | 10.6 | 122.4 | 11.0 | 126.9 | 124.9 | 12.8 | 13.3 |
| Minus-0.6-mm sand | - | - | 115.0 | 0.55 | 115.5 | 1.29 | 117.3 | 1.15 | 113.9 | - | 1.02 | - |
| Silty sand | - | - | 103.8 | 5.35 | - | - | 109.8 | 4.00 | 114.0 | - | 3.08 | - |
| Silty sand | 103.5 | 7.39 | 106.7 | 4.29 | 111.4 | 4.48 | 112.7 | 3.95 | 119.2 | - | 3.76 | - |
| Fine silty sand | 106.0 | 3.87 | 106.0 | 3.33 | 105.0 | 1.51 | 112.3 | 3.53 | 110.1 | - | 4.32 | - |
| Fine sandy silt | 105.6 | 7.18 | 109.5 | 5.67 | 115.9 | 4.96 | 116.7 | 5.05 | 115.6 | - | 4.73 | - |
| Silt | 122.3 | 5.72 | 123.0 | 4.22 | 128.8 | 4.22 | 128.9 | 4.21 | 133.2 | - | 3.59 | - |
| Aggregate base | 132.1 | 2.93 | 138.5 | 1.95 | 134.2 | 5.00 | 140.9 | 2.07 | 138.6 | - | 1.58 | - |
| Aggregate base | 136.0 | 4.43 | 140.7 | 2.79 | 139.4 | 4.09 | 141.2 | 3.03 | 140.5 | - | 1.59 | - |
| Aggregate base | 132.8 | 12.65 | 137.8 | 7.65 | 137.4 | 3.77 | 139.2 | 3.55 | 138.8 | - | 2.45 | - |
| Minus-75-mm subbase | 104.6 | 6.13 | 106.4 | 2.28 | 107.6 | 4.32 | 115.9 | 2.84 | 109.3 | - | 2.69 | - |
| Gravel and cobbles with clay-silt binder | 105.2 | 11.2 | 116.9 | 3.80 | 112.7 | 11.5 | 121.2 | 6.7 | 127.9 | - | 3.70 | - |
| Cement-treated base | - | - | 129.2 | 3.35 | - | - | 134.9 | 2.71 | 136.4 | 136.8 | 2.87 | 2.64 |
| Silty clay | 97.0 | 4.65 | 102.3 | 3.94 | 106.3 | 3.63 | 107.6 | 2.51 | 113.7 | - | 1.70 | - |
| Silty clay | - | - | 112.8 | 2.37 | - | - | 116.2 | 1.56 | 119.9 | - | 0.87 | - |
| Gravelly clay | - | - | 117.3 | 1.37 | - | - | 120.6 | 1.12 | 121.7 | - | 1.89 | - |
| Alkali clay | - | - | 98.2 | 3.50 | - | - | 105.9 | 2.65 | 105.8 | 105.1 | 0.95 | 2.52 |
| Iron slag | - | - | 116.0 | 2.40 | 107.6 | 1.74 | 115.6 | 0.53 | - | 116.0 | - | 0.56 |
| Borate soil | - | - | 76.4 | 3.38 | - | | 87.1 | 2.51 | 99.5 | 89.3 | 1.88 | 2.42 |
| Asphalt concrete | - | - | 145.0 | 1.56 | - | | 145.5 | 1.12 | 149.5 core | | 0.75 core | |
| Concrete pavement | 143.9 | 2.30 | 144.8 | 3.18 | 148.4 | 0.64 | 149.3 | 1.01 | 149.7 core | | 0.90 core | |
| Concrete pavement | 141.4 | 4.22 | 141.4 | 2.41 | 144.5 | 0.88 | 145.5 | 0.70 | 149.7 core | | 0.90 core | |
| Concrete pavement | 142.1 | 0.97 | 142.7 | 1.76 | 145.1 | 0.41 | 146.0 | 0.72 | 149.7 core | | 0.90 core | |

Notes: 1 lb/ft³ = 0.016 g/cm³; 1 mm = 0.039 in.
Constants of backscatter-gage apparatus are (a) 50-mm (2-in) thick primary shielding (lead), (b) 38x38-mm (1.5x1.5-in) sodium-iodide scintillation detector, and (c) 10-millicurie cesium-137 gamma source.
Recorded count rate without 5-cm primary shielding.

greater than it was for the commercial moisture gage. With a 5-mm (0.2-in) air gap, the Autoprobe lost 7 percent of its count-rate sensitivity compared with a 25 percent loss for the commercial gage. This would suggest that the Autoprobe moisture gage would be less sensitive to irregularities in the test surface. The major factor contributing to this performance is the high efficiency of the lithium-iodide scintillation detector installed in the Autoprobe. The proportional counter detector found in most commercial backscatter gages possess only a fraction of this efficiency.

## Final Evaluation and Analysis

After the initial evaluation period, several modifications to the probe and the probe seating apparatus were required. When the modification program was completed, additional evaluations were conducted. The details of this final evaluation program were reported by Champion and others (4). The effectiveness of the modifications was again determined in the laboratory, where gage performance was evaluated by using the six master density standards and the two moisture standards maintained at the Caltrans Laboratory in Sacramento. Sensitivities to density, mineral composition, and air-gap error were determined from these calibrations and compared with values obtained prior to the gage modifications.

The Autoprobe and the probe positioning mechanism were field evaluated on numerous soil types. Major emphasis was placed on evaluating probe seating on various surface textures and slopes, such as those encountered in construction testing. These included the surface textures associated with sands, silts, clay, peat, aggregate base, portland cement concrete, and asphalt concrete. The probe positioning mechanism was tested for proper probe seating on slope angles up to 25 percent (see Figure 7).

Probe seating error was evaluated in the laboratory by using the laboratory standards. Calibrations were run with the probe seated flush on the standards and then were rerun after an air gap was introduced under the gage by using 1.3-mm (0.05-in) spacers. No significant change in air-gap sensitivity was noted between the before and after conditions.

As part of the field evaluation program, a gravelly silt subbase material was tested with the Autoprobe and also with a commercial gage. The commercial gage was used both in the backscatter and 203-mm (8-in) transmission modes. Table 3 gives the values of dry density obtained. It can be seen from examination of the data that the values obtained by the 203-mm transmission mode and the values obtained by the Autoprobe are nearly equal while those obtained by the backscatter mode are consistently lower.

This subbase material had been compacted and then left undisturbed for 3 h on a hot day prior to testing. This allowed considerable surface drying to occur. The commercial gage is extremely sensitive in the backscatter mode to surface material and surface seating, as shown by the data in Figure 6 and the table below, which reveal a large discrepancy between the test values for the Autoprobe and the commercial backscatter gage (1 mm = 0.039 in):

| Depth Increment (mm) | Cumulative Influence (%) | |
|---|---|---|
| | Autoprobe | Commercial Backscatter Gage |
| 13 | 12 | 31 |
| 26 | 27 | 58 |
| 38 | 41 | 76 |
| 51 | 57 | 85 |
| 64 | 69 | 94 |
| 77 | 77 | 97 |
| 90 | 84 | 98 |
| 102 | 90 | 99 |
| 115 | 94 | 100 |
| 128 | 96 | - |

**Figure 7. Testing on inclined embankment with probe in full inboard position.**

**Table 3. Dry density measurements: Autoprobe versus commercial gage.**

| | Dry Density ($g/cm^3$) | | |
|---|---|---|---|
| | | Commercial Gage | |
| Test Area | Autoprobe | 203-mm Transmission | Backscatter |
| A | 1.78 | 1.74 | 1.60 |
| B | 1.68 | 1.71 | 1.46 |
| C | 1.77 | 1.79 | 1.52 |
| D | 1.79 | 1.79 | 1.54 |
| $\bar{X}$ | 1.75 | 1.76 | 1.53 |

Note: 1 $g/cm^3$ = 62.4 $lb/ft^3$.

Transmission-mode testing displays a nearly equal influence of all layers of material tested. The table above illustrates the influence on the indicated density of 13-mm (0.5-in) incremental layers of material at increased depths below the gage and the sensitivity of the commercial backscatter gage to the surface material. This information was obtained by using magnesium plates 457x610x13 mm (18x24x0.5 in) thick, with a density of 1.80 $g/cm^3$ (112.0 $lb/ft^3$), and concrete. Density-count measurements taken on the concrete standard were compared with density-count measurements obtained by inserting the magnesium plates cumulatively, one at a time, under the gage and on top of the concrete standard.

## CONCLUSIONS

1. The Autoprobe nuclear moisture-density gage has been proved to provide significantly improved performance over the commercial backscatter gage.
2. The Autoprobe moisture gage is less sensitive to mineral absorbers than the commercial gage and is more sensitive to change in moisture content as indicated by count-rate sensitivity.
3. The Autoprobe is less sensitive to irregularities in the test surface and requires minimal surface preparation to provide improvement over the performance of commercial backscatter gage performance for both density and moisture determination.
4. The Autoprobe can be an effective tool for construction control testing or as a survey tool by the inspector to determine areas to test in the conventional manner.
5. The Autoprobe could be a valuable tool when a large volume of data is required for special investigations or research.
6. When used for conventional testing, the Autoprobe would prove effective in testing aggregate bases and subbases and relatively uniform basement soils composed of sands, silts, or clays.

## ACKNOWLEDGMENT

This paper presents an overview of the results of a federally financed research project. We wish to express our gratitude to the Federal Highway Administration for their financial support and encouragement. We also gratefully acknowledge the initiative and dedication of Ellsworth Chan, who worked on the initial phases of this study, and George Oki, for his contribution to the design and fabrication of the prototype gage.

## REFERENCES

1. T.W. Smith, E.C. Shirley, and R.E. Smith. Calibration Standards for Nuclear Gages (Density Standards). California Department of Transportation, Sacramento, Res. Rept. M&R 632908-1, Nov. 1969.
2. E.L. Chan, F.C. Champion, J.C. Chang, J.B. Hannon, and R.A. Forsyth. Improved Performance Criteria for Use in Nuclear Gage Specifications. California Department of Transportation, Sacramento, Final Rept. CA-DOT-TL-2108-1-75-21, May 1975.
3. E.L. Chan, F.C. Champion, D.R. Castanon, J.C. Chang, J.B. Hannon, and R.A. Forsyth. Improved Nuclear Gage Development: Phases 1 and 2. California Department of Transportation, Sacramento, Interim Rept. CA-DOT-TL-2857-1-76-45, Sept. 1976.
4. F.C. Champion, B.L. Lister, J.B. Hannon, and R.A. Forsyth. Improved Nuclear Gage Development: Final Report. California Department of Transportation, Sacramento, Rept. FHWA-CA-TL-78-35, Dec. 1978.

*Publication of this paper sponsored by Committee on Instrumentation Principles and Applications.*